THE ROLE OF THE IL-17 RECEPTOR-A20 AXIS IN TUMOR GROWTH AND TUMOR MICROENVIRONMENT

by

Chi Yan

Submitted in partial fulfilment of the requirements
for the degree of Doctor of Philosophy

at

Dalhousie University
Halifax, Nova Scotia
July 2017

Dedication Page

This thesis is dedicated to my lovely family
For my wonderful wife, Qianni
For my adorable daughter, Emma

巧笑倩兮缘堪爱，
福祉栾玥燕归来。

Table of Contents

LIST OF TABLES

LIST OF FIGURES

ABSTRACT

Constitutive activation of NF-κB and JNK is frequently seen in malignancies; however, the underlying mechanisms remain incompletely understood. During my PhD study, I discovered a previously unrecognized role of interleukin 17 receptors (IL-17RA and IL-17RC) in repressing aberrant activation of NF-κB and JNK in cancer cells. Using a shRNA knockdown (KD) approach, I first demonstrated that IL-17RA or IL-17RC KD in murine B16 melanoma and 4T1 carcinoma cells caused aberrant expression and activation of NF-κB and different JNK isoforms along with markedly diminished levels of the ubiquitin-editing enzyme A20. We also demonstrated that differential up-regulation of JNK1 and JNK2 isoforms in the two tumor cell lines was responsible for the reciprocal regulation of c-Jun activity and tumor-specific proliferation. I further demonstrated that A20 reconstitution in IL-17RKD clones reversed aberrant JNK1/JNK2 activities and tumor-specific proliferation, confirming a sophisticated role for the IL-17R-A20 axis in controlling tumor-specific proliferation. Notably, IL-17A stimulation resulted in selective up-regulation and down-regulation of different molecules in IL-17RKD clones compared to the parental control, highlighting parallel yin-yang activities associated with IL-17R-dependent signaling. Finally, immune profiling analysis revealed that the loss of IL-17R-A20 control in IL-17RAKD tumor cells favored the development of an immunosuppressive microenvironment *in vivo*. In order to validate these findings in human cancers, I conducted cross-cancer genome-wide analysis of somatic copy number alterations in IL-17R and A20 genes, and specifically examined its impact in colorectal cancer (CRC) development. Remarkably, CRC patients with concurrent copy number deletion in IL-17R and A20 had significantly reduced overall survival compared to their corresponding control patients. Accordingly, immunohistochemistry staining in CRC tissue arrays verified that high grade tumors had significantly reduced IL-17RA staining compared to low grade tumors. Collectively, my study reveals a critical role of IL-17R in maintaining baseline A20 production for controlling JNK isoform-dependent tumor-specific homeostatic proliferation and a novel role of the IL-17R-A20 axis in controlling tumor cell behavior. My work cautions the use of anti-IL-17R neutralization antibodies in cancer patients and sheds light onto the use of the IL-17R-A20 axis as prognostic and predictive markers in cancer patients, particularly in CRC patients.

LIST OF ABBREVIATIONS USED

3’-UTR	3’-untranslated region
ACK	Ammonium-chloride-potassium
ADCC	Antibody-dependent cell-mediated cytotoxicity
ATCC	American type culture collection
Ag	Antigen
AJCC	American Joint Committee on Cancer
Akt/PKB	Protein kinase B
ALL	Acute lymphoblastic leukemia
AML	Acute myeloid leukemia
Ampho-ΦNX	Amphotropic Phoenix cells
AP-1	Activation protein-1
APC	Antigen presenting cell
ARE	AU-rich element
ANOVA	Analysis of variance
BAFF	B-cell activating factor
BCA	Bicinchoninic acid
BCG	Bacillus Calmette-Guerin
Bcl-2	B-cell lymphoma 2
BM	Bone marrow
BMDC	Bone marrow derived dendritic cell
C/EBP	CCAAT/enhancer binding protein
CBAD	C/EBP-beta activation domain
CD	Cluster of differentiation
cDCs	Conventional dendritic cells
CDK	Cyclin-dependent kinase
CM	Complete medium
CNA	Copy number alteration
COX	Cyclooxygenase
CRC	Colorectal cancer
CRI	Cancer-related inflammation
CSF-1	Colony stimulating factor 1
CTL	Cytotoxic T lymphocytes
CTLA-4	Cytotoxic T-lymphocyte–associated antigen 4
DC	Dendritic cell
DNA	Deoxyribonucleic acid
ddPCR	Droplet digital polymerase chain reaction
DMEM	Dulbecco's modified Eagle's medium
DMSO	Dimethyl sulfoxide
EGFR	Epidermal growth factor receptor
ELISA	Enzyme-linked immunosorbent assay
EMSA	Electrophoretic mobility shift assay
ER	Estrogen receptor
ERK	Extracellular signal-regulated kinase
FACS	Fluorescence activated cell sorting

FBS	Fetal bovine serum
Flt3L	Fms-like tyrosine kinase 3 ligand
FN	Fibronectin
Foxp3	Forkhead box p3
FZD	Frizzled receptor
GAPDH	Glyceraldehyde 3-phosphate dehydrogenase
GEO	Genome Expression Omnibus
GITR	Glucocorticoid-induced tumor necrosis factor receptor
GM-CSF	Granulocyte-macrophage colony stimulating factor
GPR81	G protein-coupled receptor 81
GSK3β	Glycogen synthase kinase 3 beta
HBV	Hepatitis B virus
HCEC	Human colon epithelial cell
HCV	Hepatitis C virus
HEPES	2-[4-(2-hydroxyethyl)piperazin-1-yl]ethanesulfonic acid
Her2	Human epidermal growth factor receptor 2
HIF	Hypoxia inducible factor
HMEC	Human mammary epithelial cell
HPV	Human papillomavirus
HuR	Human antigen R
IBD	Inflammatory bowel disease
ICOS-L	Inducible co-stimulatory molecule-ligand
IDO	Indoleamine 2,3-dioxygenase
IFN-γ	Interferon gamma
Ig	Immunoglobulin
IHC	Immunohistochemistry
IKK	Inhibitor of nuclear factor-kappa B kinase
IL	Interleukin
IL-17RA	IL-17 receptor A
IL-17RC	IL-17 receptor C
imDC	Immature dendritic cells
iNOS	Inducible nitric oxide synthase
IRF4	Interferon regulatory factor 4
IWK	Izaak Walton Killam
JAK	Janus kinase
JNK	c-Jun N-terminal kinase
LPS	Lipopolysaccharide
Ly6	Lymphocyte antigen 6
MAPK	Mitogen-activated protein kinase
MCP	Monocyte chemoattractant protein
MCPIP	Monocyte chemoattractant protein 1-induced protein
MDSC	Myeloid-derived suppressor cell
MEF	Mouse embryonic fibroblast
MHC	Major histocompatibility complex
MIP	Macrophage inflammatory protein
mM	Millimolar

MMP	Matrix metallopeptidase
NCBI	National Center for Biotechnology Information
NF-κB	Nuclear factor-kappa B
NIK	Nuclear factor-kappa B-inducing kinase
NK	Natural killer
NO	Nitric oxide
Nrf2	Nuclear factor (erythroid-derived 2)-like 2
NSAID	Nonsteroidal anti-inflammatory drug
OD	Optical density
ORR	Objective response rate
PBS	Phosphate buffered saline
PBST	Phosphate buffered saline containing 0.01% Tween-20
PCR	Polymerase chain reaction
PD-1	Programmed cell death protein 1
pDCs	Plasmacytoid dendritic cell
PEI	Polyethyleneimine
PI	Propidium iodide
PI3K	Phosphatidyl-inositol-3-kinase
PR	Progesterone receptor
PTEN	Phosphatase and tensin homolog
qPCR	Quantitative polymerase chain reaction
RB	Retinoblastoma
RNA	Ribonucleic acid
ROR	Retinoid orphan nuclear receptor
ROS/RNS	Reactive oxygen/nitrogen species
RT	Room temperature
SAPK	Stress-activated protein kinase
SEFEX	Similar expression to fibroblast growth factor and IL-17R-extension
SEFIR	Similar expression to fibroblast growth factor and IL-17R
SF2	mRNA splicing regulatory factor 2
SHP2	Src homology 2 domain-containing tyrosine phosphatase 2
SNP	Single nucleotide polymorphism
STAT3	Signal transducer and activator of transcription 3
TAA	Tumor-associated antigen
TAB	Transforming growth factor beta-activated kinase 1-binding protein
TAK	Transforming growth factor beta-activated kinase
TAM	Tumor-associated macrophage
TCR	T cell receptor
TGF-β	Transforming growth factor beta
Th	T helper cell
TLR	Toll-like receptor
TME	Tumor microenvironment
TNF	Tumor necrosis factor
TNFAIP3	Tumor necrosis factor alpha-induced protein 3
TNM	Tumor, node, metastasis staging system
TPL	Tumor progression locus

TRAIL	Tumor necrosis factor-related apoptosis-inducing ligand
TRAF6	Tumor necrosis factor receptor associated factor-6
Treg	Regulatory T cell
TSA	Tumor-specific antigen
VEGF	Vascular endothelial growth factor
α-GalCer	Alpha-galactosylceramide
µl	Microliter
µm	Micrometer
µg	Microgram

ACKNOWLEDGEMENTS

This thesis would not have materialized if it was not for the sincere guidance and support from numerous people to whom I would like to thank from the bottom of my heart.

I would like to thank my committee, Dr. Brent Johnston, Dr. Craig McCormick and Dr. David Hoskin, as well as my former co-supervisor Dr. Scott Halperin, for their valuable collaboration, scientific rigor and feedback, which have served as an invaluable source of guidance over the years. I would like to extend my gratitude to my external examiner, Dr. Ann Richmond, for taking the time out of her busy schedule to read my thesis and offer her insight into my research. Foremost is to thank my thesis advisor Dr. Jun Wang who allowed me to enter the world of cancer. Her constant encouragement, excellent acumen, immense knowledge and constructive criticism helped to build my own perception of what it takes to flourish in science.

Special thanks to the Department of Microbiology and Immunology at Dalhousie University for providing me an opportunity to learn and pursue an excellent career in molecular oncology and immunology. I am humbled to have been able to work in the CCFV lab alongside some of the most remarkable students, staffs and colleagues over the years. Sincere thanks for creating a friendly and collaborative working environment. Also, thank you to all the friends in the Tupper building for your time and resources throughout my program.

This acknowledgment would remain incomplete without expressing my gratitude towards my family. I wish to acknowledge the enduring support of my parents for their unceasing care, love and blessings. I sincerely thank my grandparents. Although you may not see the value of a PhD, you have always stood by me throughout graduate school, supporting me in every way possible. I am so grateful for the family that I have gained during this time, my wife Qianni and my baby daughter Emma who have helped me put into perspective what is most important to me. Thank you for always there cheering me up through the good and bad times.

Last, but not least, I wish to acknowledge the Cancer Research Training Program and the IWK Health Centre for funding my graduate research through the years.

持身立世，谨引自勉：为天地立心，为生民立命，为往圣继绝学，为万世开太平。

CHAPTER 1 INTRODUCTION

Cancer is a wide array of diseases characterized by abnormal growth of mutated cells, which can invade nearby and distant tissues. It is among the leading causes of death worldwide with a mortality rate of more than 50% (1). As a major cellular component in solid tumors, cancer cells not only alter the cellular turnover process to favor proliferation and survival, they are also able to subvert host defense mechanisms and establish a counter-regulatory immunosuppressive microenvironment to promote tumor development and progression. The molecular and cellular mechanisms by which cancer cells facilitate tumor development are complex and not fully understood. In particular, tumor cells are highly heterogeneous, which represents a major challenge in cancer management as it may directly imprint aggression of the disease and response to the anti-cancer treatment. There is an urgent need for improved understanding of the heterogeneity of tumor cells and development of novel prognostic biomarkers in cancer medicine (2).

1.1 Cancer biology, cancer stage and grade

Cancer develops through complex multistep processes that include initiation, promotion, progression and metastasis. Tumor initiation usually begins in normal cells that have the accumulation of genomic alterations in tumor suppressor genes, oncogenes and/or deoxyribonucleic acid (DNA) repair genes, creating the potential for malignant transformation (3). Tumor suppressor genes play a critical role in controlling cell proliferation, division and survival. Mutations in tumor suppressor genes lead to the production of abnormal proteins that enable cells to grow in an uncontrolled manner (4). The most frequently mutated gene is *TP53*, which is mutated/lost in approximately 50% of human cancers (5). The protein p53, encoded by *TP53*, is a transcription factor, which exerts a tumor-suppressive role through transcriptional regulation of downstream target genes (6). Several examples of p53 targeted genes are the cyclin-dependent kinase inhibitor *p21* (CDKN1A) (7), proapoptotic B-cell lymphoma (*BCL*)-*2* family members Bcl-2-associated X (*BAX*) (8), p53 upregulated modulator of apoptosis (*PUMA*) (9), ferredoxin reductase (*FDXR*, encoding a mitochondrial flavoprotein required for electron transport in metabolism) (10), damage-regulated autophagy modulator 1 (*DRAM1*, encoding a lysosomal membrane protein required for the induction of autophagy) (11), as well as *Sestrins1* and *Sestrins2* [encoding proteins required for repressing messenger

ribonucleic acid (mRNA) translation] (12). Notably, *TP53* mutations are often detected in the inflamed, but non-dysplastic epithelium in patients with colitis, suggesting that chronic inflammation can directly cause genomic changes (13). Other examples of tumor suppressors include retinoblastoma protein (RB), phosphatase and tensin homolog (PTEN), cyclin-dependent kinase inhibitor CDKN2A (also known as p16) in melanoma, breast cancer proteins BRCA1 and BRCA2, as well as adenomatous polyposis coli in colorectal cancer (CRC) (14). In contrast to the tumor suppressor genes, oncogenes are generally mutated forms of normal cellular genes (proto-oncogenes) that are responsible for normal cellular proliferation, differentiation and apoptosis (15). They can be activated by structural alterations resulting from mutation or gene fusion, by juxtaposition to enhancer elements, or by amplification (16). The products of oncogenes can be classified into six broad groups: transcription factors, chromatin remodelers, growth factors, growth factor receptors, signal transducers, and apoptosis regulators (16). In melanoma, the most common oncogenic mutations are neuroblastoma RAS viral oncogene homolog (*NRas*) and v-raf murine sarcoma viral oncogene homolog B1 (*BRAF*) (60-70%) (17), whereas avian myelocytomatosis viral oncogene homolog (*Myc*) and epidermal growth factor receptor *(EGFR)2* are present in ~20% of breast cancer patients and *HRas* and *KRas* are found in 20-30% of CRC patients (16). Furthermore, oncogenic proteins can also be induced by viral infections, which contribute in approximately 15-20% of cancer cases worldwide (18, 19). Lastly, DNA damage occurs as a result of both endogenous (e.g., hydrolysis, oxidation and replication errors), as well as exogenous mechanisms (e.g., radiation and chemical agents in the environment) during the process of tumor development. Since DNA repair genes are involved in the process of fixing damaged DNA (20), alterations in these genes lead to the development of additional genetic mutations and epigenetic modifications in other genes, which may cause the cells to become cancerous.

While genetic mutations result in altered cellular proliferation that may initiate carcinogenesis, they also result in the generation of tumor-specific antigens (TSAs, or neoantigens) and tumor-associated antigens (TAAs), critical components for induction of anti-tumor immune responses known as immunosurveillance (21-23). Specifically, TSAs are derived from proteins that are specific to the tumor, such as mutated self-proteins or proteins from oncogenic pathogens (24). Thus, the immune responses against TSAs are

specific and potent, but usually restricted to a certain tumor (25). By contrast, TAAs are normal self-proteins that exhibit abnormal quantities or locations within the tumor cells (24). As a result, TAAs are less immunogenic than TSAs in general; however, these responses tend to have a broad spectrum activity to a variety of tumors (24). Finally, genetic mutations may trigger inflammatory responses that are required for inducing anti-tumor immune responses, but often times, are involved in mediating aberrant cancer-associated inflammation to promote tumor development. For instance, the *KRas* gene encodes a GTPase transductor protein, which is mutated in ~20% of all cancers (26), with the highest mutation rate >90% in pancreatic cancer (27). Of importance, *Kras* mutation alone in mice is insufficient to trigger the initiation of pancreatic neoplasia; however, chronic pancreatitis can provide an inflammatory environment that exhibits aberrant nuclear factor-kappa B (NF-κB) activation with enriched inflammatory infiltrates, necessary for Kras-induced pancreatic tumorigenesis (28). In recent years, somatic copy number alterations (CNA) have been recognized as one type of genetic alteration that has a critical role in tumorigenesis (29). Indeed, CNA are extremely common in lineage-specific and pan-cancer types (30, 31).

Tumor promotion involves the proliferation of genetically altered cells and progression involves an increase in the size of the tumor, the spreading of the tumor and the acquisition of additional genetic changes. While the promotion phase is usually asymptomatic, and tumor growth can be counter-balanced by immunosurveillance for a prolonged period of time, tumor progression exhibits increased tumor growth and invasiveness due to the outgrowth of less immunogenic tumor cells and/or induction of an immunosuppressive tumour microenvironment (TME) (32). Cancer metastasis and the associated cancer relapse are involved in over 90% of cancer deaths and are associated with the worst prognosis (1). Metastasis requires complex biological processes to enable primary tumor cells to migrate through the blood stream, or the lymphatic system, to where they can colonize and develop to form secondary metastatic loci (33).

Of note, the host immune system is a very active component participating in different stages of cancer by driving a process called immunoediting (see section 1.3.2), which dictates tumor fate through the avoidance of innate and adaptive immune mechanisms. It

is increasingly recognized that the immune system not only protects against cancer development, but also shapes the character of emerging tumors.

Clinically, pathological stages of cancers are defined via the TNM (tumor, node, metastasis) system according to the American Joint Committee on Cancer (AJCC) (e.g., CRC staging as shown in Table 1) (34). T represents the initial size of the primary tumor and whether it has invaded nearby tissue, whereas N shows the presence and extent of the tumor involvement in the draining lymph nodes, and M indicates the presence of distant metastatic tumors. The size and the spread status of cancers provide a general indication for prognosis and treatment (35). To further evaluate how abnormal or malignant a tumor is, histological grading has been applied (e.g., CRC grade as shown in Table 1). The grade of cancers is also a useful indicator in prognosis; however, it has been shown to be a stage-independent prognostic factor (36). In general, low-grade tumors have a better prognosis since they exhibit a lower growth rate and are less likely to spread compared to high-grade tumors (34, 37).

1.2 Hallmarks of cancer

Though different cancer types may present distinct clinical features, all cancers share characteristic hallmarks that are acquired through genetic mutations and/or developed along stages of cancer progression. Hanahan and Weinberg established that the first six hallmarks of cancers include [1] sustaining proliferative signaling, [2] evading growth suppression, [3] resisting cell death, [4] enabling replicative immortality, [5] promoting angiogenesis to acquire oxygen and nutrients from the blood stream, and [6] the activation of invasion and metastasis (38). These principles were further expanded in an update published in 2011 with four emerging hallmarks: [7] reprogramming of energy metabolism, [8] evading immunosurveillance and antitumoral immune responses, [9] promoting genome instability and mutations, as well as [10] fueling tumor-associated inflammation (39).

Tumor-associated inflammation contributes to multiple hallmarks of cancer by providing bioactive molecules and cellular components to the TME. In colitis-associated CRC (13), inflammatory conditions may be present before a malignant change occurs. Conversely, in other types of cancer, an oncogenic change induces an inflammatory microenvironment that promotes the development of the tumor. Regardless of its origin,

“smoldering” chronic inflammation in the TME has many tumor-promoting effects. It aids in the genetic instability, proliferation and survival of malignant cells, promotes angiogenesis and metastasis, subverts adaptive immune responses, and alters responses to hormones and chemotherapeutic agents (40-42).

The molecular pathways associated with tumor-associated inflammation are now being unraveled, resulting in the identification of new target molecules that could lead to improved diagnosis and treatment. In this regard, my PhD thesis characterizes a novel molecular mechanism controlled by the pro-inflammatory cytokine interleukin 17 receptors (IL-17RA and IL-17RC) on tumor cells in both directly regulating tumor growth and survival and indirectly shaping immune responses in the TME.

Table 1. Colorectal cancer stage and grade.

TNM stage groupings			
Stage 0	**Tis**	**N0**	**M0**
Stage I	**T1~T2**	**N0**	**M0**
Stage II	**T3~T4**	**N0**	**M0**
Stage III	**Any T**	**N1~N2**	**M0**
Stage IV	**Any T**	**Any N**	**M1**

T: tumour, N: node, M: metastasis.
Tis: carcinoma in situ: intraepithelial or invasion of lamina propria.
T1: tumour invades submucosa.
T2: tumour invades muscularis propria.
T3: tumour invades through the muscularis propria into the subserosa or into non-peritonealised perirectal tissues.
T4: tumour invades directly into other organs or structures and/or perforates visceral peritoneum.
N1: metastasis in 1-3 regional (peri-rectal) lymph nodes.
N2: metastasis in 4 or more regional lymph nodes.
M1: distant metastasis.

Histological grade

Grade 1	**Well-differentiated**	**Low Grade**
Grade 2	**Moderately differentiated**	
Grade 3	**Poorly differentiated**	**High Grade**
Grade 4	**Undifferentiated**	

Adapted from (34, 36).

1.3 The role of inflammation and the immune system in cancer

The term inflammation was first introduced by Aulus Cornelius Celus, referring to a local response characterized by redness, swelling, warmth, pain due to increased blood flow, capillary dilation, edema and leukocyte infiltration (43). Inflammation can be triggered by bacterial or viral infections, exposure to irritants (such as toxins) or trauma and is generally divided into acute and chronic inflammation based on the kinetics of the response. In 1863, Rudolf Virchow observed leukocyte infiltration into tumor sites, providing the first evidence to support the notion that cancer lesions are inflamed tissues (44). In general, acute inflammation in a cancer lesion is viewed as a good response, or at least benign, given that it stimulates immunosurveillance against cancers. By contrast, it is becoming increasingly recognized that chronic inflammatory conditions have pathological effects during cancer development (45) and it is widely accepted as the 10th hallmark of cancer (39, 40).

1.3.1 Chronic inflammation in cancer

Existing evidence indicates that around 25% of human cancer cases are related to chronic and unresolved inflammation caused by infection or physicochemical agents (46, 47). Chronic infection caused by various infectious agents, including viruses, bacteria and parasites, is an established risk factor of various cancers. For instance, *Helicobacter pylori* infection in humans induces chronic gastritis, which is associated with a more than 2-fold increase in the risk of stomach cancer (48, 49). While human papillomavirus (HPV) is a major cause of cervical cancer in women (50), chronic hepatitis triggered by hepatitis B virus (HBV) or hepatitis C virus (HCV) infection can lead to hepatocellular carcinoma (51). In addition, chronic parasitic infections with different strains of parasites infecting specific organs leads to various cancers, such as schistosomiasis induced cystitis and fibrosis, which are known to increase the risk of carcinoma of the bladder, liver, and rectum, as well as follicular lymphoma of the spleen (52). Furthermore, chronic inflammation caused by various environmental stimuli is also associated with an increased risk of cancer. For instance, there is a strong link between gastric acid-induced chronic reflux oesophagitis and the development of esophageal carcinomas (53). Lastly, chronic inflammatory diseases are also associated with increased risk of cancer. While

inflammatory bowel diseases may promote the development of CRC, obesity-associated inflammation is linked to postmenopausal breast, colon, and endometrial cancers (54, 55).

The concept of chronic inflammation in the promotion of cancer is also supported by the observation that nonsteroidal anti-inflammatory drugs (NSAIDs) are able to reduce the incidence and mortality of several cancers (56, 57). Multiple clinical trials have demonstrated a clear link between long-term aspirin (an inhibitor of cyclooxygenase [COX]1 and COX2) use and a reduction in the incidence and mortality for several cancer types, especially esophageal adenocarcinoma, CRC and stomach cancers, with an overall effect of 20% to 25% (58). Two large Danish cohort studies also showed a reduced risk for colorectal, stomach and ovarian cancer in non-aspirin NSAIDs users, but no clear differences in the risk estimates with breast cancer (59, 60). In addition, the long-term (>5 years), high-intensity use of COX2-specific non-aspirin NSAIDs was associated with a 30% to 45% reduction in CRC risk (61). However, not all chronic inflammatory conditions increase cancer risk and some of them, such as autoimmune disease-associated inflammation (e.g., rheumatoid arthritis or psoriasis), may even antagonize tumorigenesis (41, 62).

1.3.2 Inflammation in the context of immunosurveillance and immunoediting

The theory of cancer immunosurveillance explains the involvement of the immune system and beneficial inflammatory responses in cancer management; however, the fact that tumors develop in patients with a fully functional immune system suggests that it is only part of the story (32). In the last 2 decades, the concept of immunoediting has emerged, which has redefined the role of the immune system in cancer and more accurately describes the many facets of immune system–tumor interactions. The immunoediting process is very dynamic, which has three defined phases, namely, elimination, equilibrium and escape. Notably, inflammatory responses are an integral part of the immunoediting process.

The first elimination period involves the protective role of immunosurveillance wherein the immune system is able to find and eliminate most or all of the tumor cells before they grow to a clinically noticeable size. Inflammatory responses are indeed required for the generation of strong anti-tumor immunity. However, some tumor cells may manage to survive initial immune destruction and enter an equilibrium phase, in which the host immune system actively interacts with tumor cells and holds the tumor in a state of

functional dormancy (63, 64). Due to constant pressure from the immune system, some tumor cells undergo genetic and epigenetic changes, leading to generation of tumor variants that have a reduction or lack of expression of recognizable TSAs. These newly evolved tumor subclones possess poor immunogenicity due to antigen loss and are highly resistant to immune recognition and immune attack. While tumor cells continuously divide and grow, inflammatory cytokines and chemokines are produced and various cellular components of the innate and adaptive immune system are recruited into the TME in order to counteract tumor growth. However, tumor cells can evade anti-tumor immunity by facilitating immunosubversion mechanisms (see section 1.3.4) to avoid recognition and elimination. Tumor cells may evade immune recognition and killing through multiple mechanisms, such as loss of TSA, down-regulation of major histocompatibility complex (MHC) and/or co-stimulatory molecules, expression of molecules that allow resistance to host immunity, and/or induction of an immunosuppressive TME (64). The battle between the tumor and the immune system is a constant and dynamic process, which can last for months to decades. Although the molecular and cellular mechanisms underlying the immune-mediated tumor dormancy remain incompletely understood, the equilibrium phase is believed to reach a balance between immune stimulatory and immune inhibitory mechanisms, such as anti-tumor cytokines (e.g., IFN-γ) and pro-tumor cytokines (e.g., IL-10) (63). During the escape phase of cancer immunoediting, the immune system fails to control tumor growth and the tumor subclones progress causing clinically apparent disease. Notably, the entire cancer immunoediting process occurs in the TME, dynamically shaping the TME and being shaped in return by constituents of the TME.

1.3.3 Key constituents of the tumor microenvironment

An inflammatory tumor microenvironment has a complex tissue structure composed of noncellular and cellular elements. The noncellular components include soluble factors, signaling molecules, extracellular matrix, and mechanical (e.g., tumor vasculature and interstitial fluid pressure), as well as environmental (e.g., hypoxia and low pH) cues (65). The cellular component consists of tumor cells, stromal cells and tumor-infiltrating immune cells. Stromal cells are the cells that make up tumor-associated blood vessels (endothelial cells and pericytes) and the cells that contribute to structural integrity (fibroblasts). Based on the functional role of immune cells, tumor-infiltrating immune cells

can be divided into two distinct functional subtypes (Figure 1). While immune stimulatory cells are desirable for establishing immunosurveillance, immune suppressive cells are responsible for conducting immune subversion. Key examples of immununosurveillance cells include cytotoxic T lymphocytes (CTLs), type 1 tumor-associated macrophages (TAM1), natural killer cells (NK), immune stimulatory dendritic cells (DCs) and type 1 T helper cells (Th1). Examples of immunosuppressive cell subsets include T regulatory cells (Tregs), immature dendritic cells (imDC), myeloid-derived suppressor cells (MDSC), and type 2 macrophages (M2). In the following sections, I will discuss the role of several major cellular components and their associated molecules in inflammation, immune responses and cancer.

1.3.3.1 Dendritic cells

DCs are the most potent professional antigen presenting cells (APCs) that bridge innate and adaptive immunity via priming T cells for activation and expansion. Fms-like tyrosine kinase 3 ligand (Flt3L) and granulocyte-macrophage colony stimulating factor (GM-CSF) are major factors required for DC differentiation in the bone marrow (BM). Currently, conventional DCs (cDCs) and plasmacytoid DCs (pDCs) are the two major subsets of DC which are defined according to their phenotype, tissue distribution, specific transcriptional factors for DC fate development and functional properties (66). Of note, cDCs are the predominant population of DCs and exhibit strong phagocytosis and Ag presentation capacities. cDCs activate adaptive immune responses; however, they also can induce immune tolerance under specific conditions (66, 67). While pDCs represent a small population of DCs, they specialize in the generation and secretion of type I interferons and subsequently induce activation of CTLs and NK cells, which antagonize tumor development (66, 68-70). However, in certain TMEs, such as ovarian, head and neck, breast tumors and melanoma, pDCs also tend to be tolerogenic, which favor tumor progression and are often associated with poor prognosis (66, 70). Tolerogenic DCs, such as iDCs, can be induced by immunosuppressive IL-10 in the TME, stimulating autocrine IL-10 and the generation of Tregs (67). While mature DCs provide co-stimulatory molecules to promote division and survival in T cells, such as B7.1/B7.2 (CD80/CD86), inducible co-stimulatory molecule ligand (ICOS-L), tumor necrosis factor (TNF)-super family ligands, including CD40, 4-1BB (CD137), glucocorticoid-induced TNFR-related

protein (GITR), OX40 (CD134) and death receptor 3 (DR3), the tolerogenic DCs are characterised by a low expression of costimulatory and MHC molecules, low expression of IL-12 and high production of IL-10 and indolamine-2,3-dioxygenase (IDO) (67, 71, 72). Therefore, the function of DCs in cancer is context-dependent. The immunosuppressive TME can cause dysfunction of DCs, which is a main factor influencing the efficacy of DC-based therapies (66).

1.3.3.2 Monocytes and tumor-associated macrophages

Monocytes (~8% of circulating leukocytes) are derived from hematopoietic stem cells in the bone marrow and are an important cellular component of the innate immune system. The two best-characterized monocyte subsets in mice are circulating $Ly6C^{high}CCR2^{+}$ inflammatory monocytes and $Ly6C^{low}CCR2^{-}$ resident monocytes (73, 74). The human counterparts are also identified and phenotypically characterized by $CD14^{high}CD16^{-}$ and $CD14^{low}CD16^{+}$, respectively. In addition to circulating in the peripheral blood, monocytes may seed into tissue sites and differentiate into tissue macrophages (75). While some macrophages are seeded into developing tissues during the embryonic stage, others are recruited into the tissue sites in response to inflammatory stimuli and undergo *in situ* proliferation or *de novo* differentiation (76). It is well known that macrophages have evolutionarily conserved functions in tissue maintenance and host defense and are capable of immune modulation, phagocytosis and Ag-presentation, despite being weaker APC compared to DCs due to reduced co-stimulatory molecule levels (77). Notably, macrophages are heterogeneous and plastic and therefore may exhibit a wide spectrum of activation profiles, ranging from classically activated (M1 macrophages) to the alternatively activated (M2 macrophages) (74, 78).

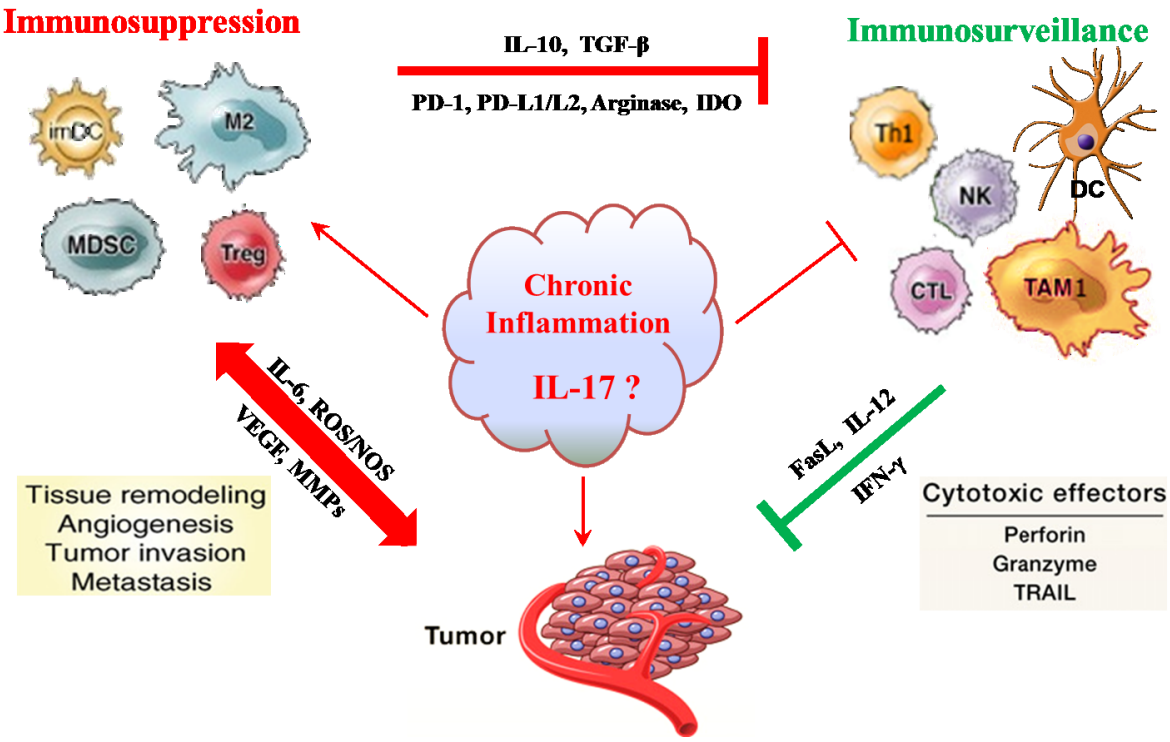

Figure 1. The key cellular components of tumor microenvironment (63, 79).

Tumor cells have long been recognized to be able to create a special microenvironment to subvert immunity and promote their own growth. The immunosurveillance immune effector cells, such as cytotoxic T lymphocyte (CTLs), tumor-associated macrophage M1 (TAM1) and natural killer cells (NK), with the help of dendritic cells (DCs) and type 1 T helper cells (Th1) are able to recognize and eliminate tumor cells. However, tumor cells can secrete cytokines that recruit suppressive cells, such as T regulatory cells (Tregs), immature myeloid cells, including immature dendritic cells (imDC) and myeloid-derived suppressor cells (MDSC), and M2 macrophages. The imDC can cause T-cell anergy due to a lack of co-stimulatory molecules. M2 macrophages and MDSCs inhibit T-cell responses through a variety of mechanisms, including nutrient sequestration via arginase, reactive oxygen/nitrogen species (ROS/RNS) generation, as well as interference with trafficking into the tumor site. Immunosuppressive cytokines and the up-regulation of immunosuppressive enzymes, like indolamine-2,3-dioxygenase (IDO) and arginase, which catabolize essential nutrients are required for effector cell activation and produce immunosuppressive catabolites. Furthermore, tumor cells promote the production of vascular endothelial growth factor (VEGF) and matrix metalloproteinases (MMPs) to favor angiogenesis, and up-regulate inhibitory molecules, such as PD-L1. As such, tumor-promoting immunosuppression dampens immunosurveillance, which otherwise inhibits tumor growth. Chronic inflammation plays a detrimental role and regulates all aspects of the TME. Nevertheless, the role of proinflammatory IL-17 in the TME is controversial.

TAMs are a major component of tumor infiltrating immune cells in solid tumors, which could represent up to 50% of the tumor mass (80). The increased number of TAMs at tumor sites is attributed to local expansion of tissue resident macrophages (embryonic or monocytic-derived) and/or the recruitment of circulating inflammatory monocytes (80, 81). One major population of TAMs is derived from circulating inflammatory monocytes, which are recruited and further expanded within tumor sites. CCL2 (or monocyte chemotactic protein-1, MCP-1) and colony stimulating factor 1 (CSF-1) signaling are shown to be critical for this process, which may function in an autocrine manner (81). Depending on the specific TME stimuli, including the profile of cytokines, chemokines and growth factors, TAMs are polarized into M1 or M2 phenotypes, which may positively or negatively regulate anti-tumor immune responses and the fate of tumor development and progression (76, 82, 83). The M1 subset is characterized as $CCR2^{high}CD14^{high}$ $CX3CR1^{-}CD16^{-}$ in humans and $CCR2^{high}CX3CR1^{-}$ and $Ly6C^{high}$ in mice, which have an anti-tumor or "killing" phenotype (78). The M1 TAMs are produced upon IFN-γ exposure, which stimulates inducible nitric oxide synthase (iNOS) and the production of nitric oxide (NO). The high level of NO may cooperate synergistically with proinflammatory and cytotoxic IFN-γ to kill the tumor cell.

By contrast, the M2 subset is defined as $CD14^{low}CD16^{mid\text{-}high}CCR2^{-}CX3CR1^{high}$ in humans and $Ly6C^{low}CCR2^{-}$ $CX3CR1^{high}$ in mice (84-87). While the M2 TAMs are induced primarily by IL-4 and IL-13, a tumor milieu enriched with IL-10, transforming growth factor (TGF)-β, endothelin-2 and VEGF also favors the differentiation of the M2 TAMs (88). In general, M2 macrophages produce a series of growth factors, cytokines, and extracellular matrix-modeling molecules and increase expression of arginase, which induce tumor cell proliferation, angiogenesis, and the tissue remodeling process ("healing" phenotype) (89). It has been shown that M2 macrophages are enriched in necrotic and hypoxic areas, which favor the production of hypoxia-inducible factor (HIF)-1α-dependent molecules (e.g., VEGF, CXCL12, and CXCR4) (90). The aberrant level of CXCL12 and its receptor CXCR4 in the TME promotes proliferation, migration and invasion of cancer cells (91). M2 macrophages produce a series of proangiogenic factors that sustain and promote tumor growth, such as VEGF, platelet-derived growth factor (PDGF), TGF-β, and members of the fibroblast growth factor family. Furthermore, M2 TAMs produce matrix

metalloproteinases MMP-7, MMP-2, MMP-9, MMP-1, which may promote tumor metastasis (82, 92). In addition, M2 TAMs can suppress T-cell-mediated anti-tumor immunity via promoting immunosubversion mechanisms (see section 1.3.4).

1.3.3.3 Neutrophils

Neutrophils are short-lived granulocytes, representing the most abundant subpopulation of leukocytes in the human blood. The production and turnover process of neutrophils is controlled by pro-inflammatory cytokine IL-17A-induced G-CSF production (93, 94). While neutrophils are mainly involved in the innate immune response against microbial infections (95-97), increased levels of neutrophils have been observed in several cancer types, such as melanoma, breast and colon cancer (90). Neutrophil recruitment is initiated by the induction of selectins and intercellular adhesion molecules (ICAM) on the surface of the endothelium that result from stimulation by inflammatory mediators, including histamine, cysteinyl leukotrienes, cytokines and chemokines (98, 99). In human tumors, neutrophil recruitment occurs mainly in response to IL-8 (or CXCL8), which is strongly induced by hypoxia (100, 101). After being recruited into the tissues, neutrophils are activated and able to generate reactive oxygen species (ROS) and release various pro-inflammatory proteins from intracellular granules, which include myeloperoxidase, lactoferrin, defensin, lysozyme, and proteases (e.g., elastase and gelatinase). These factors can cause tissue damage and cell lysis, as well as potential DNA damage (95). Like all other immune cells, neutrophils contribute to tumor outcome in a complex way. Similar to macrophages, neutrophils can also be polarized and display different phenotypes spreading from an antitumor (N1-like) to a pro-tumor (N2-like) phenotype (97, 102). Recent studies in experimental models have provided extensive support for the existence of pro-angiogenic (N2) or anti-tumor (N1) neutrophil phenotypes (102). The major player in the switch between the two phenotypes appears to be TGF-β, as increased levels of TGF-β stimulated polarization toward N2 neutrophils (102, 103). Neutrophils can produce a plethora of cytokines (including TNF-α, IL-1β, IL-12, IL-1Rα, and VEGF), chemokines (CXCL1, CXCL8, CXCL9, CCL3, and CCL4) and proteases (such as MMP9) (82). In addition, neutrophils can directly induce VEGF-dependent angiogenesis via CXCR2 binding chemokines (104, 105). More recently, neutrophils have also been reported to capture circulating cancer cells through the release of neutrophil-derived extracellular

traps, which favors the entry of metastatic cancer cells into tissues (106).

1.3.3.4 Myeloid-derived suppressor cells

MDSCs are a heterogeneous population of immature myeloid cells that share several common markers of monocytes, macrophages and neutrophils (107). As such, it may be difficult to distinguish among MDSCs, TAMs and tumor-infiltrating N2 neutrophils, since they possess similar immunosuppressive activities. Nevertheless, MDSCs often accumulate in cancer patients and produce arginase and IDO to suppress the immunosurveillance of several immune cell types, including M1 macrophages, NK cells, DCs and T cells (108, 109). Moreover, MDSCs can also induce the development and differentiation of suppressive immune cells, such as M2 macrophages and Tregs (110, 111). In mice, MDSCs are broadly characterized as $Gr1^{+}CD11b^{+}$. In particular, Gr1 is a myeloid differentiation marker, which contains two lymphocyte antigen 6 complexes (Ly6C and Ly6G), that are commonly used for the classification of two MDSC subsets in tumor-bearing mice: $CD11b^{+}Ly6C^{low}Ly6G^{+}$ granulocytic MDSCs (G-MDSCs), as well as $CD11b^{+}Ly6C^{high}Ly6G^{-}$ monocytic phenotype MDSCs (M-MDSCs) (112, 113).

1.3.3.5 NK and NKT cells

Natural killer (NK) cells are innate lymphocytes that recognize and kill virus infected cells and tumor cells through the expression of various activating and inhibitory receptors on the cell surface (114, 115). As an important component in immunosurveillance, NK cells exert direct cellular cytotoxicity without prior sensitization and secrete immunostimulatory cytokines, such as IFN-γ, for cancer elimination. According to the "missing-self" hypothesis, NK cells bearing killer-cell immunoglobulin-like receptors (KIRs) (or Ly49 receptors in mouse) preferentially target cells that have a reduction or lack of MHC-I expression, which is a common phenomenon in cancer cells (116). Furthermore, NK cells can make use of the fragment crystallizable (Fc) receptor to exert antibody-dependent cell-mediated cytotoxicity (ADCC) against antibody-coated tumor cells (116). Upon activation, NK cells exhibit elevated Fas-FasL interaction with target cells, along with the release of cytotoxic granules (perforin and various granzymes), leading to the apoptosis of target cells (117).

Natural killer T (NKT) cells are unique lymphocytes that have characteristics of both

NK cells and T lymphocytes. The differences in T cell receptor (TCR) rearrangements have allowed NKT cells to be separated into two categories, type I and type II (118). Type I NKT cells, or invariant or iNKT cells, are characterized by the expression of restricted invariant TCR encoded by Vα14Jα18 in mice and Vα24Jα18 in humans. These cells recognize the glycolipid Ag α-galactosylceramide (α-GalCer) in association with non-polymorphic CD1d molecules. Type I NKT cells are the predominant population of NKT cells and are usually associated with anti-tumor immunity (118, 119). In sharp contrast, CD1d-restricted type II NKT cells express a wide range of TCRs that recognize CD1d but do not recognize α-GalCer, which have the capacity to suppress the immunosurveillance response. Currently, much less is known about type II than type I NKT cells. However, in tumor immunity, the two NKT subsets (type I and type II) are reported to cross-regulate one another (120, 121).

1.3.3.6 T lymphocytes

T lymphocytes of the adaptive immune system have multi-faceted roles in cancer. In the three-signal model of Ag-specific T cell activation and expansion, binding of the TCR to Ag-loaded MHC (signal 1) on APCs is required for the activation of naive T cells. In order to generate and maintain an adaptive T cell response, full activation of a specific T cell lineage also requires simultaneous engagement of a co-stimulatory signal (signal 2), which is generated by the binding of CD28 on T cells to B7.1/B7.2 (CD80/CD86) on APCs, and an appropriate cytokine environment (signal 3) (122). However, T cell activation is also modulated by coinhibitory molecules, including molecules like cytotoxic T-lymphocyte–associated antigen (CTLA) 4 and programmed cell death protein (PD)-1 (123).

$CD4^+$ T helper cells (also known as Th cells) play critical roles during adaptive immune responses (124). Following activation, $CD4^+$ T cells can be differentiated into various Th subsets. Four $CD4^+$ Th cell lineages are generally recognized, namely, Th1, Th2, Th17 and Treg cells, although other Th lineages exist (125). The cytokine environment controls specific transcription factors that are required for Th cell differentiation. Th1 cells express the signature transcription factor T-bet and mainly produce IFN-γ, which is important for the activation of NK cells, M1 macrophage and CTLs in the clearance of intracellular pathogens and tumor cells. In comparison, Th2 cells produce IL-4, IL-5, IL-10 and IL-13, which cross-regulate Th1 responses and favor tissue

remodeling, angiogenesis and tumor promotion (126, 127). Th17 cell differentiation requires a combined stimulation of TGF-β, IL-6, IL-23, as well as IL-21 in mice (128) or IL-1β in humans (129). These cells express the IL-23 receptor (IL-23R) and are characterized by the secretion of high levels of the pro-inflammatory cytokines IL-17 (or IL-17A), IL-17F, as well as IL-21, IL-22 and the (130-132). In addition, Th17 cells also have unique expression of the transcription factor retinoid orphan nuclear receptor (RORγt in mouse, RORC in human), which is regulated by signal transducer and activator of transcription (STAT)3 and IFN regulatory factor 4 (IRF4) (133, 134). Overexpression of RORγt in CD4 T cells promotes Th17 differentiation and inhibits Th1 and Th2 lineage differentiation (133). Th17 cells play critical roles in autoimmunity and during immune responses against extracellular bacteria and fungi (135). However, the role of Th17 cells and their signature cytokine IL-17 in cancer is highly controversial (136) (see section 1.5.3). Furthermore, Tregs are another distinct T cell lineage endowed with regulatory properties that suppress a variety of innate and adaptive immune cells (137, 138). Tregs block antitumor immune responses via a number of contact-dependent and independent mechanisms (139).

$CD8^+$ CTLs play a critical role in immunity against intracellular infections and cancer (140). The cytolytic activity of CTLs is triggered by the recognition of Ag-bearing MHC-I on target cells. The direct interaction of CTLs with target cells is followed by efficient delivery and release of lytic granules or the engagement of Fas/FasL, resulting in the induction of apoptosis and shrinkage of the tumor lesion (141, 142). In addition to cytolytic function, CTLs also produce IFN-γ to indirectly inhibit tumor-induced angiogenesis (143). However, in the context of chronic Ag exposure in chronic inflammation-associated cancer, CTLs may become exhausted and exhibit reduced or defective proliferation, cytokine production and lytic functions (144). Gene profiling and phenotypical studies in mice and humans with chronic viral infections and cancer have shown that exhausted T cells upregulate co-inhibitory molecules, including PD-1, CTLA-4, T cell immunoglobulin, mucin-3 (Tim-3), lymphocyte activation gene 3 (LAG-3), and T cell immunoreceptor with Ig tyrosine-based inhibition motif domain (TIGIT) (71, 144). Notably, expression of multiple co-inhibitory molecules appears to correlate with more severe dysfunction of CTLs in cancer. For instance, it has been shown that the $PD\text{-}1^+TIM3^+$ CTLs produce less

IFN-γ, TNF, and IL-2, compared to PD-1^{+}TIM3^{-} CTLs in patients with advanced melanoma (145).

1.3.3.7 B lymphocytes

Besides T lymphocytes, B cells are another subset of adaptive immune cells and are responsible for humoral immunity. Naive B cells express both surface immunoglobulins(Ig) M and IgD. Once a B cell encounters a specific Ag that engages its membrane-bound antibody, it serves as an APC to present the Ag on its surface to a unique Th population called follicular T helper cells (Tfh) (146). The interaction with Tfh cells induces the activation of B cells, which undergo clonal expansion and develop into effector plasma cells and memory B cells (146). Plasma cells produce large amounts of Ag-specific antibodies and can undergo somatic hypermutaion and class switching to IgA, IgG, or IgE subtypes (146, 147).

The current understanding of B cells in the TME and tumorigenesis is quite limited and highly controversial. B cells do infiltrate into the TME (148, 149); however, they have been reported to induce both pro- and anti-tumor responses (150). In particular, B cells can exert antitumor effects via serving as potent APCs to enhance the activity of Th cells and CTLs. Secondly, the production of tumor-specific antibodies is important in mediating ADCC (151). Finally, B cells are reported to have a direct tumor killing effect via the secretion of granzyme B (152). However, B cells may skew macrophage differentiation into an M2-like, pro-angiogenic phenotype that favors tumor progression (153). Furthermore, B cells may stimulate Th2 cells and immunosuppressive Treg differentiation (154, 155). Furthermore, some regulatory B cells may produce the immunosuppressive cytokines TGF-β and IL-10 (156). Therefore, the balance of functionally distinct B cell subsets may determine whether B cells have pro- or anti-tumor functions.

In summary, both innate and adaptive components of the immune system contribute to an inflammatory TME (Figure 1). Specifically, the key features of tumor-associated inflammation include the infiltration and polarization of immune cells, predominantly immunosuppressive tumor-infiltrated M2 macrophages, MDSCs, Tregs and type 2 neutrophils; the presence of inflammatory cytokines and chemokines, such as TNF, IL-1, IL-6, as well as CCL2 and CXCL8; and lastly, the occurrence of tissue remodeling, metabolic alteration and angiogenesis under hypoxic conditions (157, 158). NK cells and

CTLs are critical immune cells engaged in tumor killing (via perforin, granzyme B and death ligand dependent mechanisms). Th1 cells confer anti-tumor immunity via IFN-γ production and provide important help to CTLs via activating DCs, a process called DC licensing (66). On the other hand, Th2 and Tregs suppress anti-tumor immune responses and are therefore pro-tumorigenic. In addition, different subsets of NKT cells and B cells are involved in both immunosurveillance and immunosuppression, which may positively or negatively regulate tumor development.

1.3.3.8 Stromal cells

The importance of stromal cells in tumorigenesis has been implicated in several animal xenograft models (159, 160). Emerging evidence suggests that stromal cells may respond to tumor cells and/or immune cells within the TME and promote tumorigenesis through the release of soluble mediators, including cytokines (e.g., IL-6 and TGF-β), chemokines (e.g., CXCL12), and growth factors (e.g., hepatocyte growth factor and fibroblast growth factor). For example, it has been shown that CXCL12 secreted by the tumor stromal cells attracts endothelial cell precursors to promote angiogenesis. Furthermore, stromal cell-derived extracellular matrix glycoprotein, tenascin C, promotes the stemness of cancer cells and the enhancement of the degrading capacity of the three-dimensional extracellular matrix, which support tumor cell metastasis (161-163). Therefore, existing evidence suggests that stromal cells play a critical role in shaping the specific TME and regulating tumor cell behavior (161, 162). However, it is relatively less understood how tumor cells may influence the property of stromal cells.

1.3.3.9 Tumor cells

While functionally distinct immune cells are recruited by inflammatory responses in TME, chronic inflammation may promote tumorigenesis by reeducating the TME through suppressing tumor extracellular matrix remodeling, innate and adaptive anti-tumor immunity; and/or by reinforcing angiogenesis and lymphangiogenesis; and/or by enhancing DNA damage and pro-proliferative and survival effects of the tumor cells (164-168). While immune cells and stromal cells are important cellular components in mediating chronic inflammation, malignant cells play a unique role in tumor-associated inflammation. Tumor cells are not only capable of producing different soluble mediators

to amplify inflammation, but also respond to various stimuli to modulate the immune responses, which can directly and/or indirectly influence the course of tumorigenesis (41). A variety of receptor-mediated signaling pathways may be utilized by cancer cells for self-evolving and adapting the TME, thereby modulating the process of tumor development. These signaling pathways may be involved in cell adhesion, inflammatory responses, hormone responses, growth and survival pathways, or they may be required for metabolic and stemness regulation (listed in Table 2). In particular, overexpression of IL-6 is found in many types of tumors and nearly all hallmarks of cancer are influenced by IL-6 during tumour development. The IL-6-triggered activation of primarily JAK/STAT3, but also Ras/Raf/MEK/MAPK and PI3K/AKT signalling pathways, stimulate tumor cell proliferation, survival, promote angiogenesis, invasiveness and metastasis and is also known to regulate cancer cell metabolism, as well as induce therapeutic resistance in cancer (41, 169).

Table 2. Selected receptor-mediated signaling pathways in tumor development

Gene altered	Biological function in cancer	Ref
EGFR	Activation of the CDK4/6-Cyclin D for cell cycle progression via RAS-RAF-MEK-ERK-AP1 and PI3K-AKT-mTOR signaling	(170)
Cadherin	Transmembrane Ca^{2+}-dependent adhesion receptors, suppress tumor growth and invasiveness	(171)
IL-6R	Promotes STAT3-dependent tumor cell proliferation, stemness, invasiveness and inflammation	(172)
TLR4	Promotes tumor growth, cell migration and invasion, as well as inducing tumor apoptosis and inflammation	(173)
TNFR1	Cytotoxicity, promotes cancer cell proliferation and metabolism, induces cancer-related inflammation	(174)
IL-1R1	Initiates and propagates inflammation, promotes cancer growth	(175)
ER/PR/Her2	Hormone and growth factor receptors, mediates tumorigenesis, cell growth, apoptosis and resistance to chemotherapy	(176-178)
GPR81	Lactate-specific cell-surface G-protein-coupled receptor, promotes lactate metabolism, cancer growth, survival and angiogenesis	(179)
Notch	Promotes self-renewal, differentiation and proliferation of stem-like population of cancer cells	(180)
FZDs	Wnt receptors, promote tumor cell growth, invasion, motility, stemness and metastasis	(181)

EGFR: epidermal growth factor receptor. CDK: cyclin-dependent kinase. TLR: Toll-like receptor. TNF: tumor necrosis factor. ER: estrogen receptor. PR: progesterone receptor. Her2: human epidermal growth factor receptor 2. GPR81: G protein-coupled receptor 81. FZD: Frizzled receptor.

1.3.4 Mechanisms of immunosubversion

1.3.4.1 Immune suppression

It has become clear over the last few decades that an immunosuppressive TME supports tumor cell proliferation, survival, metabolic reprogramming, angiogenesis and metastasis (Figure 1) (65). Immunosuppressive cells (e.g., Tregs and MDSCs) inhibit effector functions of tumor-infiltrating lymphocytes, such as T cells and NK cells, through either cell-cell interactions (182) or the release of soluble factors, such as IL-10, TGF-β and VEGF, that suppress the local immune responses in a paracrine fashion (183). The immunosuppressive cytokines may inhibit effector T cells indirectly through dendritic cells to attenuate the infiltration of T cells into the tumor bed (184) and/or directly by repressing the Ag presentation process for the activation of T cells (185).

A variety of immune cell-mediated suppressive mechanisms are described in the literature, many of which are known to be shaped by the soluble mediators and/or surface molecules expressed by tumor cells and/or stromal cells (62, 79, 183). For instance, granulocyte and granulocyte-macrophage colony-stimulating factors (G-CSF and GM-CSF, respectively), induced by proinflammatory cytokines (e.g., IL-1, IL-6 and IL-17) in the TME, promote the accumulation, expansion, and activation of MDSCs (107, 186, 187). In addition, tumor cells secrete high levels of tryptophan and L-arginine metabolizing enzymes, such as IDO and arginase, into the TME which lead to the depletion of these - building blocks that are essential for T cell proliferation (188). The metabolic disturbance, along with hypoxia and pH imbalance, in the TME result in further generation of ROS/RNS, which fuels chronic inflammation and the imbalance of immunosurveillance and immunosuppression.

Tumors also evade cell surface death receptor signals, such as Fas (189) and TNF-related apoptosis-inducing ligand (TRAIL) receptor (190), via down-regulation, mutation, or loss of expression. Furthermore, tumor cells can directly escape TCR recognition by HLA-loss and generating MHC class I processing-defective variants (191), the loss or down-regulation of HLA class I antigens (192), or by disabling other co-stimulatory signals of the antigen processing machinery (193). In addition, tumor cells may upregulate cell surface co-inhibitory ligands, such as PD-L1 (194), which mediate T-cell anergy (or immune exhaustion).

1.3.4.2 Immune exhaustion

The concept of immune exhaustion was first introduced to describe the stepwise and progressive loss of T-cell functions during chronic viral infections (195). Exhausted T cells express arrays of inhibitory molecules and distinctive patterns of cytokine receptors, transcription factors and effector molecules, which distinguish these cells from conventional effector, memory and anergic T cells (71, 144). PD-1, along with Tim-3 and Lag-3, are the most prominent coinhibitory receptors expressed by exhausted T cells. PD-1 is expressed by a variety of immune cells, including $CD4^+$ and $CD8^+$ T cells, B cells, monocytes, DCs and macrophages (196-199). PD-1 binds to two ligands: programmed cell death 1 ligand 1 (PD-L1, B7-H1, or CD274) and PD-L2 (B7-DC, or CD273). PD-L1 is broadly expressed on hematopoietic and non-hematopoietic tissues, whereas PD-L2 is only expressed on hematopoietic cells, such as DCs, macrophages, mast cells and B cells (200-203). The overexpression of (PD-L1 in mouse and human cancers supported a role for exhausted T cells in cancer (204, 205), which was later shown to render tumor cells less susceptible to the specific TCR-mediated lysis by cytotoxic T cells (194, 206).

T cell exhaustion is mediated by PD-1 forming negative costimulatory microclusters, which recruits the phosphatase SHP2 (Src homology 2 domain-containing tyrosine phosphatase 2) and TCRs, leading to the dephosphorylation of CD28 (207) and other TCR signaling molecules (205, 208). The exhausted T cells are incapable of further activation or division even when exposed to the antigen in pro-stimulatory conditions, which in turn induces anergy or apoptosis of these tumor-specific T cells (196). The expression of PD-1 by tumor-infiltrating lymphocytes (209), along with the constitutive or inducible expression of PD-L1/L2 in numerous tumor types (210, 211), have been correlated with invasiveness, metastasis and poor prognosis in cancer.

T-cell exhaustion is largely induced in the specific TME in cancer patients. Tumor cells, stromal cells and tumor-infiltrating immune cells (tumor-associated DC, Treg, TAM and MDSC) are major cellular components that regulate exhaustion by secreting soluble mediators and expressing specific ligands of inhibitory receptors. The induction of PD-L1 on cancer cells is mediated through multiple mechanisms, including cytokines and growth factors (primarily IFN-γ, but also type I IFNs, IL-4, IL-10 and VEGF) (196, 206, 212), the activation of oncogene pathways (e.g., EGFR) (213), the loss of tumor suppressor signals

(e.g., PTEN) (214) and other environmental cues (e.g., hypoxia) (215). Being a ligand to PD-1, PD-L2 also dampens the functional activity of effector T cells (216). However, the transcriptional regulation of PD-L2 is less well defined (206). Compared to PD-L1, PD-L2 can also be induced by some inflammatory cytokines, especially IL-4, along with other mediators (e.g., GM-CSF, IFN-γ and IFN-β) (200, 217, 218).

1.4 Key pro-inflammatory signaling pathways in cancer

1.4.1 Overview

During chronic inflammation, a wide array of intracellular signaling pathways, comprising cell surface receptors, kinases, and transcription factors, are often dysregulated, leading to malignant transformation, tumor development and metastasis (45, 219, 220). Inflammation activates a variety of protein kinases, including members of the Janus kinase (JAK), phosphatidyl-inositol-3-kinase (PI3K), and mitogen-activated protein kinase (MAPK) families to alter cellular proliferation. Besides protein kinases, inflammation also induces aberrant activation of transcription factors, such as STAT family members, hypoxia inducible factor-1α (HIF-1α), NF-κB and activation protein-1 (AP-1) downstream of the MAPK pathway, which have been implicated in tumor growth, angiogenesis, and metastasis (41, 219, 220). In the following sections, I will specifically discuss the signalling pathways that are highly relevant to my thesis.

1.4.2 NF-κB pathway

NF-κB consists of hetero- and homo-dimers of five different proteins (p50, p52, p65 or RelA, RelB, and c-Rel) sharing a conserved N-terminal region that can bind DNA (221). In most cases, NF-κB is trapped as an inactive form in the cytoplasm due to direct binding to inhibitor proteins of the IκB family, such as IκB-α. Upon activation by pro-inflammatory cytokines or stress stimuli [e.g., hypoxia, ROS and ultraviolet (UV)], activated NF-κB is liberated and translocated to the nucleus where it binds to the κB elements located in the proximal promoter region of genes of proinflammatory mediators, such as cytokines (222), iNOS (223), and COX2 (224). Specifically, the canonical (or classical) NF-κB pathway is triggered by IKKαβγ-induced IκBα degradation, leading to p50/RelA heterodimer nuclear localization and the gene expression of proinflammatory cytokines, chemokines, growth factors and MMPs. By contrast, the non-canonical (or alternative) pathway is largely

caused by activation of NF-κB-inducing kinase (NIK) mediated IκBα degradation, leading to p52/RelB heterodimer nuclear localization. This pathway differs from the canonical pathway in that only certain receptor signals (e.g., B-cell activating factor [BAFF], CD40) activate this pathway for adaptive immune responses and secondary lymphoid organ development (225). In the third pathway, IKK activation is not required. DNA damage (UV irradiation), certain chemotherapeutic drugs, or alternative reading frame (ARF) tumor suppressor inactivation results in the activation of this pathway and leads to p50 (or p52) homodimers entering the nucleus. The complex induces pro-apoptotic gene transcription and functions as a tumor suppressor (226). How this atypical pathway is regulated is largely unknown.

The canonical NF-κB is constitutively activated in many tumors (227, 228) and in chronic inflammatory conditions such as inflammatory bowel disease (IBD) and gastritis (229, 230). As a cancer-promoting factor, the classical NF-κB pathway represses apoptosis (231) and promotes angiogenesis (232), tumor metastasis (233), and cell cycle progression (234). To date, the molecular mechanisms underlying constitutive NF-κB activation in cancer are incompletely understood, although the stress conditions in TME (41, 230, 235), such as hypoxia, production of ROS/RNS and pro-inflammatory stimuli, are believed to play important roles in the process.

1.4.3 MAPK pathway

1.4.3.1 Overview

MAPKs are ubiquitously expressed and play an essential role in intracellular transduction of signals activated by a wide variety of extracellular stimuli, such as growth factors and stress (Figure 2) (236). Activation of the MAPK cascade consists of 3~5 tiers of protein kinases that are activated in a sequential, tight and specific fashion, in which one or more of each tier goes on to phosphorylate and activate components of the next tier. For instance, a MAP3K phosphorylates and activates a downstream dual-specificity MAP2K, which in turn stimulates MAPK activity through dual phosphorylation on threonine and tyrosine residues within a conserved tripeptide motif (Thr-X-Tyr) (237). The MAPK family proteins activate distinct cascades: extracellular signal-regulated kinase (ERK)1/2 pathway, p38-MAPK pathway, c-Jun N-terminal kinases (JNK)1/2/3 pathway, and ERK5 (also known as Big MAP kinase, or BMK1) pathway, according to their most downstream

kinase tier (238). The MAPK signaling cascades are highly conserved and mediate a plethora of critical cellular functions, including proliferation, differentiation, migration, apoptosis and inflammation (238, 239).

In 2002, the Cancer Genome Project conducted by the Sanger Institute identified hyper-activation of the MAPK pathway in over 90% of melanoma patients, which drew the world's attention to this pathway for potential targeted cancer therapies (240). Notably, the most frequently affected genes lay in the RAS-RAF-MEK (MAPK/ERK kinase)1/2-ERK1/2 cascade, with alterations on BRAF (40%–50%) and NRAS (15%–20%), which usually present as oncogenic gain-of-function mutations (240). In other solid and hematopoietic malignancies, KRAS or NRAS mutations have been found in about 55% of metastatic CRC [10-14]. While BRAF is mutated in about 20% of all cancers, lower rates of BRAF mutations have been observed in lung cancer (2-4%), whereas KRAS mutations remain the most frequent alteration (20-30%) in lung cancer (241). Furthermore, KRAS or NRAS mutations also occur in a significant number of acute myeloid leukemia (AML) and acute lymphoblastic leukemia (ALL) (20%-30%) (242-244). Of note, KRAS mutation in epithelial neoplastic cells directly induces the expression of proinflammatory cytokines and cytokine receptors, such as IL-17A and IL-17RA, highlighting the importance of inflammation in tumor development (245, 246).

The aberrant activation of JNK proteins has been reported in multiple cancer cell lines and tissue samples (247-250). In a mouse model of intestinal cancer, Apc^{Min} (Min, multiple intestinal neoplasia) mice bearing non-phosphorylatable mutant form of c-Jun developed smaller and fewer polyps, confirming the oncogenic function of c-Jun in tumorigenesis (251).

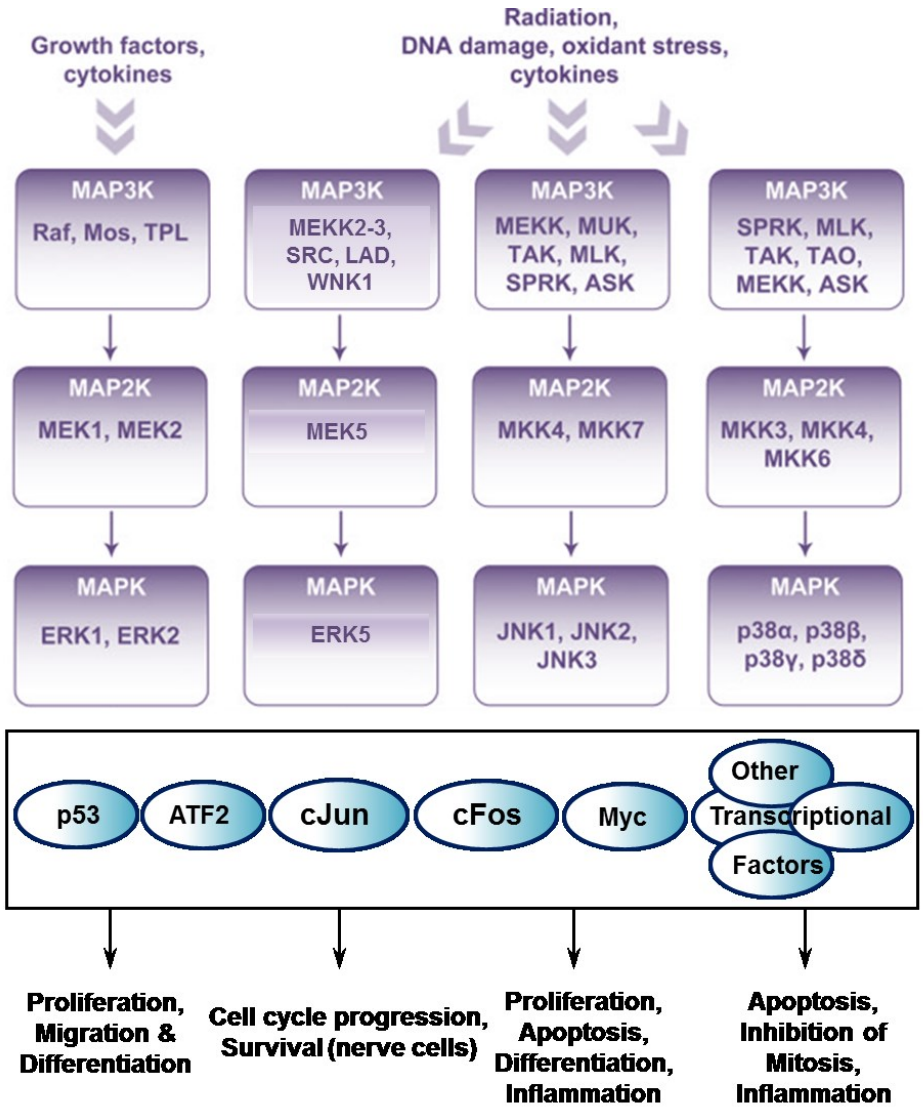

Figure 2. The four canonical MAPK signaling pathways. Modified from (237-239).

1.4.3.2 JNK pathway

The JNK branch of the MAPK pathway, also known as stress-activated protein kinases (SAPKs), are activated by a wide range of stimuli, including pro-inflammatory cytokines and stress signals, such as UV-irradiation and starvation, as well as some mitogenic signals such as lipopolysaccharide (LPS) (252, 253). These stimuli may recruit and phosphorylate the GTPase Ras-related C3 botulinum toxin substrate 1 (RAC1), which sequentially activates the p21-protein activated kinase family to phosphorylate and activate members of the MAP3K kinase tier. The MAP3K tier dual-phosphorylates MAP2K4 (MKK4) at Ser257 and Thr265, or MAP2K7 (MKK7) at Ser271 and Thr275, which in turn, activate the three members in the JNK family, including MAPK8 (JNK1), MAPK9 (JNK2), and MAPK10 (JNK3). While, MKK4 and MKK7 preferentially phosphorylate JNKs on tyrosine and threonine residues, respectively, mice with targeted deletions in either MKK4 or MKK7 genes exhibited early embryonic death, supporting an essential role for the JNK-MAPK signaling pathway in the regulation of developmental processes (254). MKK4 is also required for maintaining peripheral lymphoid homeostasis and therefore acts as a tumor suppressor (255). Dysregulation of the JNK cascade has been reported in cancer. For example, activating oncogenic RAC1 mutations have been found at a high frequency in melanoma (256). Furthermore, deletion and/or epigenetic silencing of MKK4 have been reported in breast, biliary, pancreatic, and prostate cancers (257, 258).

Upon stimulation, JNKs phosphorylate and activate a number of nuclear and non-nuclear proteins, including AP-1, p53, ATF2, STAT3 and nuclear factor of activated T-cells (NFAT), for signal transduction. In particular, AP-1 is a transcription factor that is formed by the dimerization of Jun proteins (c-Jun, JunB, JunD) with Fos proteins (c-Fos, FosB, Fra-1, Fra-2), to control cell proliferation, differentiation, cell death, inflammation and cell metabolism (252, 253). Oncogenic Ras-mediated cellular transformation has been shown to involve the induction of AP-1 activity and the accumulation of Cyclin D1, a signature protein downstream of c-Jun (259). Another important target is the tumor suppressor p53 whose expression as well as transcriptional function are regulated by AP-1 proteins (260). As such, the dysregulated expression of AP-1 is involved in tumorigenesis (261). Notably, the composition of AP-1 dimers and the relative abundance of individual AP-1 subunits, as well as the cell type and the cellular environment, are important factors

for determining cell fate (260, 262, 263). Specifically, the biological activity of c-Jun is controlled by post-translational phosphorylation of serine-63 and/or serine-73 residues, as well as the turnover level of c-Jun expression (264). While c-Jun is activated by JNK-mediated N-terminal phosphorylation, the phosphorylation of c-Jun at threonine-239 and serine-243 by glycogen synthase kinase 3 (GSK3) creates a high-affinity binding site for polyubiquitination and proteasomal degradation (265). Similar to the MKK4/7 deficient mice, embryonic lethality has also been reported at mid-gestation in c-Jun knockout (c-Jun$^{-/-}$) mice due to impaired hepatogenesis (266, 267). Furthermore, c-Jun$^{-/-}$ fibroblasts exhibit a severe defect in cell cycle progression, suggesting that the JNK/c-Jun pathway is a key mediator of cellular proliferation (Figure 3) (267).

The JNK pathway is also involved in apoptotic pathways, which include death receptor-initiated extrinsic pathways and intrinsic pathways involving mitochondria (Figure 3) (268). JNK is able to phosphorylate and inactivate the proapoptotic Bcl-2 family protein Bad, thereby suppressing IL-3 withdrawal-induced apoptosis in B cell lymphoma/leukemia (269). JNK activation is also involved in pro-apoptotic pathways. An important activator of the JNK apoptotic pathway is TNF-α, a pro-inflammatory cytokine that governs cell survival via promoting either cell proliferation or apoptosis (270). However, JNK activation alone can only potentiate apoptosis and is not sufficient to induce apoptosis. Furthermore, the activation of the NF-κB pathway inhibits TNF-α-induced JNK-dependent apoptosis (271). Nevertheless, this pro-survival role of NF-κB is not observed in JNK-dependent apoptosis triggered by IL-1 or UV. Therefore, JNK may mediate apoptosis in a stimulus- and cell type-dependent manner (272). In addition, JNK-induced apoptosis has been proposed to drive the surviving neighboring cells to proliferate in NF-κB-deficient *Drosophila* and animal models through a process named "Compensatory Growth" (Figure 3) (273-275), which adds even more complexity to the role of JNK in mediating cellular turnover.

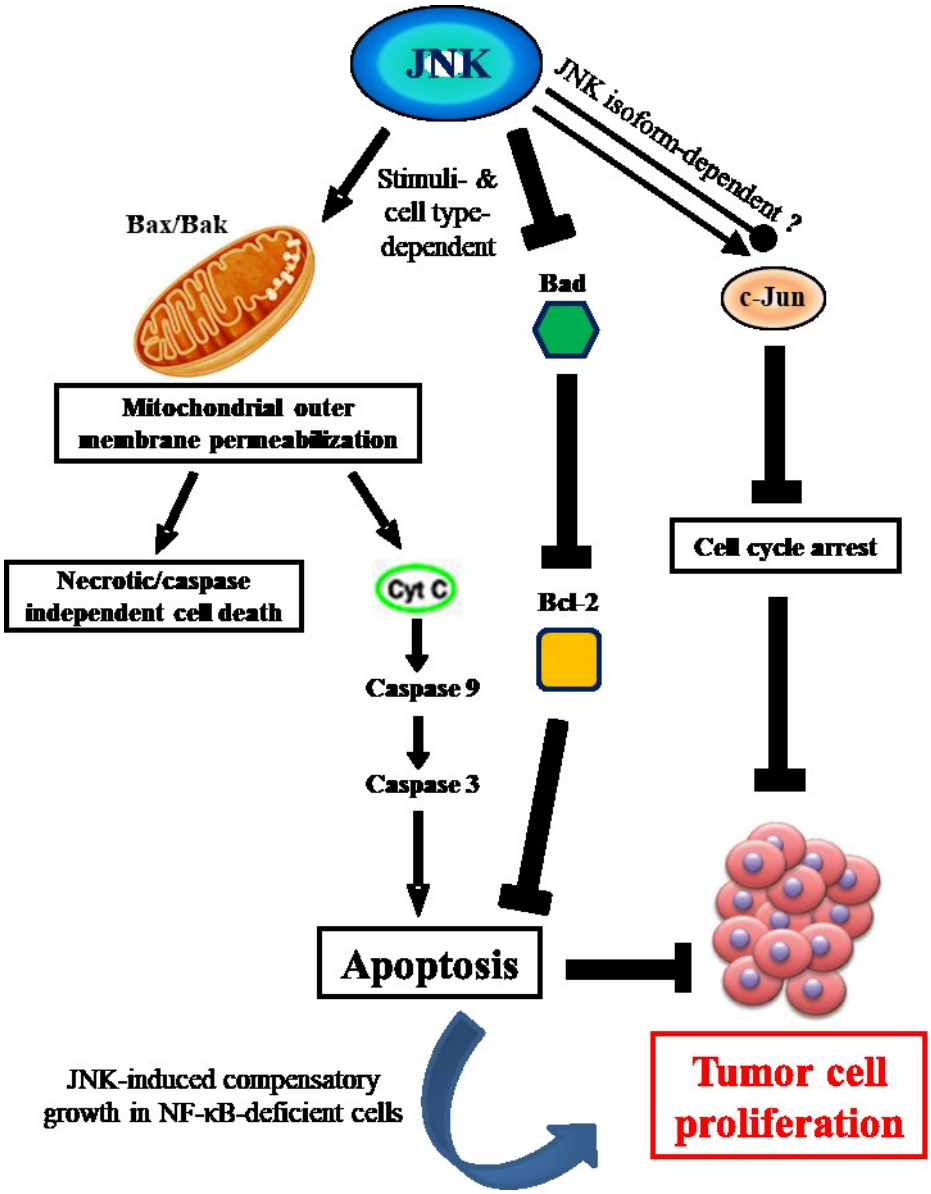

Figure 3. JNK signaling in the regulation of cellular apoptosis and proliferation (253, 268, 275).

1.4.3.3 Biology and function of JNK isoforms

The generation of mice deficient in one or more of the JNK isoforms, as well as shRNA targeted JNK isoform-specific knockdown on cell lines, have facilitated the functional analysis of the role of individual JNKs. While JNK1 and JNK2 are expressed broadly, JNK3 is expressed predominantly in the brain, testis, and heart (276). Consistently, in the adult mouse brain, JNK3, but not JNK1 or JNK2, was required for the kainic acid (kainate)-induced apoptosis of hippocampal neurons (277) and the loss of neurons following ischemic injury (278), clearly demonstrating that JNK3 plays a vital role in mediating stress-induced apoptotic responses of neurons.

While the two ubiquitously expressed JNK proteins—JNK1 and JNK2 are shown to have overlapping roles in various biological functions, such as promoting cytokine production, they are reported to have distinct roles in controlling c-Jun-dependent cellular proliferation (Figure 3) (253, 279, 280). Under homeostatic conditions, JNK2 mainly targets c-Jun for degradation, whereas following stimulation, JNK1 becomes dominant, phosphorylating and stabilizing c-Jun, leading to transcriptional activation (281). Consequently, JNK1 and JNK2 are shown to oppositely regulate the stability and activation of c-Jun-dependent proliferation in fibroblasts. Specifically, JNK1 promotes and JNK2 inhibits cell cycle progression, a phenotype that is directly correlated with c-Jun phosphorylation and AP-1 activity (279). The increased proliferation of $JNK2^{-/-}$ fibroblasts is primarily due to compensatory increases in JNK1/c-Jun expression and function (282). The opposing roles of JNK1 verses JNK2 in proliferation have also been reported in erythrocytes and keratinocytes (279). Furthermore, the epidermis isolated from $JNK2^{-/-}$ and $JNK1^{-/-}$ mice is hyperplastic and hypoplastic, respectively (280).

In addition to controlling cell proliferation, JNK1, but not JNK2, has been shown to promote UV- or TNF-α-induced apoptosis in skin cancer cells (283, 284). Conversely, JNK2 is shown to constitutively suppress JNK1-mediated apoptosis in multiple myeloma cells and promote cell survival (249). Notably, the loss of both JNK1 and JNK2 in murine embryonic fibroblasts protects them from apoptosis due to defective death signaling (285). Taken together, both JNK1 and JNK2 are involved in apoptosis in an antagonistic manner, it is likely that JNK1 exhibits a dominant role over JNK2 to promote apoptosis.

Furthermore, whether JNK1 and JNK2 act as oncogenes or tumor suppressor genes

has been examined using KO mice. In carcinogen-induced hepatocellular carcinoma and skin cancer models, increased and reduced tumor incidence were exhibited in $JNK1^{-/-}$ and $JNK2^{-/-}$ mice, respectively (247, 286, 287). Importantly $JNK1^{-/-}$ mice also develop spontaneous intestinal tumors, which further confirmed the tumor suppressor role of JNK in the cancer initiation process (288). However, how cancer cells utilize JNK isoform-dependent control in cancer development is largely unknown.

In current clinical applications, patients respond transiently to MAPK pathway inhibitors, such as BRAF and MEK inhibitors used in melanoma patients These drugs have toxic effects on non-cancer cells and generate drug-resistance leading to cancer relapse in more than 70% of patients (289). Thus, biomarker studies are needed to identify those tumors that are susceptible to MAPK inhibition and to provide support for potential combinational treatments. Given that current JNK inhibitors that have been developed for cancer therapy have several limitations, such as a lack of specificity and cellular toxicity (253), conditional genetic experiments of specific JNK isoforms in different cancer types are necessary to better define the molecular mechanisms of JNK function.

1.5 IL-17 and IL-17 receptor (IL-17R) family

1.5.1 Overview

IL-17A (IL-17) is recognized as one of the most potent cytokine stimuli in chronic inflammation (290, 291). IL-17A and IL-17 receptor A (IL-17RA) are the founding members of the IL-17/IL-17R family which consists of six structurally related ligands (IL-17A to IL-17F) and five receptors (IL-17RA to IL-17RE) (Figure 4) (129, 291-293). While the ligands are identified based on the rate of amino acid homology with IL-17A, members of the IL-17Rs are defined by the conservation of a SEFIR (similar expression to fibroblast growth factor and IL-17R) domain in the cytoplasmic tail (294). The extracellular domains of IL-17Rs contain two fibronectin (FN) III-like motifs, which mediate protein-protein interactions, such as pre-assembly of the IL-17R complex for dimerization and ligand binding (294-296). Notably, both IL-17RA and IL-17RC possess an extra ~100 residues beyond the conventional SEFIR domain. This non-conserved region is termed as the SEFIR-extension (SEFEX) domain and is required for IL-17RA and IL-17RC signaling functionality (297-299). Unique to IL-17RA, following the SEFIR/SEFEX domain in the cytoplasmic tail, there is an additional motif named CCAAT/enhancer binding protein

(C/EBP)-β activation domain (CBAD), whose function is associated with negative regulation of IL-17RA signaling (see section 1.6.2) (297, 300). Consistent with the unique structure of IL-17RA, it is located on chromosome 22, while all other family receptor subunits are encoded by a cluster on chromosome 3 (301, 302).

The IL-17 family ligands signal through multimeric receptor complexes, which are formed by the association of receptor subunits with one another (Figure 4) (291). IL-17RA is a common receptor subunit shared by the ligands IL-17A, IL-17F, IL-17C and IL-17E (IL-25). IL-17RC is an obligate co-receptor for IL-17RA and forms multimeric RA/RC complexes for IL-17A, IL-17F and IL-17A/F signaling (292). IL-17B signals through homodimeric IL-17RB, whereas IL-17C and IL-17E utilize receptor complexes of IL-17RA-RE and IL-17RA-RB, respectively (303). Currently, the receptors for IL-17D and IL-17RD remain unknown (291).

IL-17 receptor subunits are expressed in multiple tissues: IL-17RA is expressed ubiquitously, with a relatively higher level in hematopoietic immune cells (304, 305). By contrast, IL-17RC expression in hematopoietic cells is low, but high in non-hematopoietic structure cells of the prostate, liver, kidney, thyroid and joints (306, 307). IL-17RB is expressed in a variety of endocrine tissues, the kidney, pancreas, liver, intestine and on Th2 cells (308). IL-17RD is mainly expressed in the epithelial cells of breast, thyroid gland and prostate (309), as well as endothelial cells (310), whereas IL-17RE is found in the pancreas, brain and prostate (292). It is likely that different distributions of IL-17Rs are correlated with distinct biological functions of the IL-17 cytokine family members in various tissue compartments.

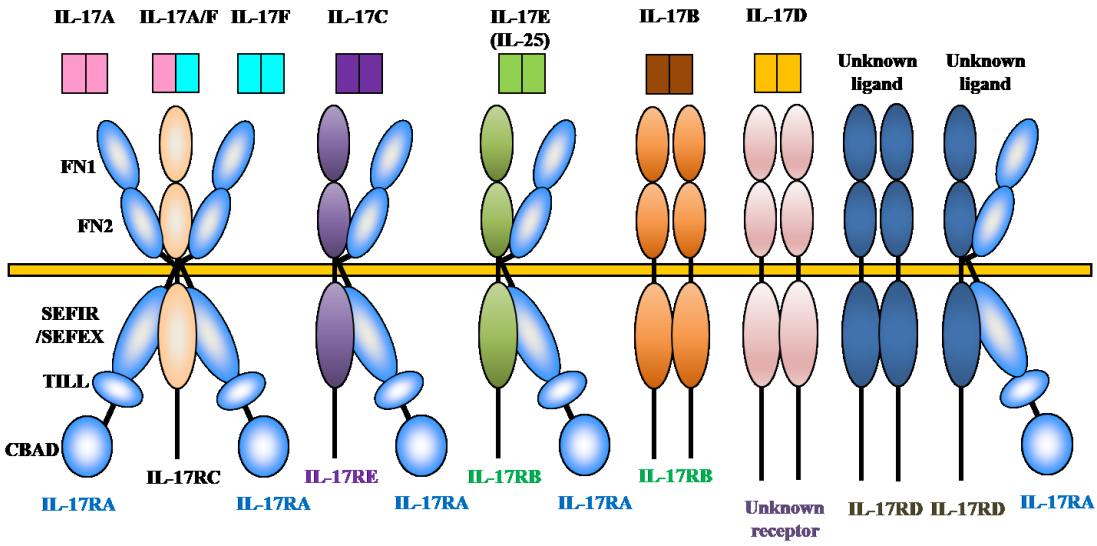

Figure 4. IL-17R family ligand-receptor structure (291, 303).

Some of the ligands or receptors are shown as unknown ligands and receptors. There are no known ligands for IL-17RD homodimers and IL-17RD/IL-17RA heterodimers. There is no known receptor for IL-17D. FN, fibronectin. SEFIR, similar expression to fibroblast growth factor and IL-17R. SEFEX, similar expression to fibroblast growth factor and IL-17R-extension. TILL, Toll/IL-1 receptor-like loop. CBAD, C/EBP-beta activation domain.

Among the IL-17 family ligands, pro-inflammatory IL-17A and IL-17F are the closest, share ~55% homology, and best understood family members (129). They are secreted as IL-17A and IL-17F homodimers, as well as IL-17A/F heterodimers. Both IL-17A and IL-17F induce activation of NF-κB and MAPK pathways in targeted cells, leading to the production of other pro-inflammatory cytokines, chemokines, and other molecules including growth factors and MMPs (291). While the homodimer of IL-17A is 10-30 fold more potent than IL-17F in activating proinflammatory responses, the heterodimer has an intermediate efficacy (301, 311). Notably, in the context of cytokine-driven inflammation, which is enriched for proinflammatory mediators, such as TNF, there is a clear synergy between IL-17F and TNF, reaching a comparable potency to the effect that is induced by the combination of TNF and IL-17A (312, 313). IL-17A and IL-17F fuel inflammation through the production of a variety of inflammatory cytokines (e.g., IL-6), chemokines (e.g., IL-8 and CXCL1), and growth factors (e.g., GM-CSF and G-CSF), which facilitate leukocyte differentiation and recruitment, particularly neutrophils and monocytes, into the inflammatory sites (291-293, 314). IL-17A also stimulates IL-12 production by DCs thereby, bridging innate and adaptive immunity (315). In addition, IL-17A-induced CCL20 favors the migration of Th17 cells and immature dendritic cells which interact with local mesenchymal cells, leading to a massive secretion of IL-17A at the site in an autocrine fashion (294, 295). Besides the potent proinflammatory role of IL-17A in neutrophil differentiation, migration and activation, it also contributes to the induction of angiogenesis by promoting VEGF production (316), plays roles in maintaining gut barrier function and host defense against extracellular pathogens (317-319). IL-17A also plays important roles in the pathogenesis of auto-immune and inflammatory diseases, with increased concentrations documented in psoriasis, rheumatoid arthritis, inflammatory bowel disease, allergic asthma and cancers (136, 298, 320-322). After its first description in 1993-1995, IL-17A/IL-17RA signaling has been recognized as a target in chronic inflammation due to its role in the pathogenesis of numerous autoimmune and inflammatory diseases, as well as cancers (316, 323-325). However, while promising outcomes were observed in certain diseases such as psoriasis and psoriatic arthritis, clinical trials of secukinumab (anti-IL-17A) and brodalumab (anti-IL-17RA) in Crohn's disease were terminated early due to worsening of disease in the treatment group (326, 327), highlighting the need to further

investigate this axis in a tissue microenvironment specific manner.

Compared to IL-17A and IL-17F, the functions of IL-17B, IL-17C, IL-17D and IL-17E in cellular turnover and immune responses are less well defined. IL-17B promotes tumorigenesis via the induction of NF-κB dependent anti-apoptotic protein Bcl-2 (B-cell lymphoma 2) expression and heightens inflammation through augmented neutrophil accumulation and granulopoiesis (308). As such, elevated IL-17B expression often correlates to poor prognosis in breast cancer patients (303). Similarly, IL-17C exhibits an autocrine ability to induce Bcl-2 and Bcl-xL expression in epithelial cells, which in turn, promotes cell survival and tumorigenesis (328). Furthermore, as an IL-17RA ligand, IL-17C also induces the production of proinflammatory cytokines, chemokines and antimicrobial peptides (329, 330). IL-17D was reported to promote pro-inflammatory gene expression in endothelial cells and exhibits a mild inhibitory effect on myeloid progenitor cell proliferation *in vitro* (331). More recently, the expression of IL-17D has been reported to be triggered by oxidative stress through the transcription factor nuclear factor (erythroid-derived 2)-like 2 (Nrf2), which offers protection to the host by recruiting NK cells to suppress tumor growth (310) and viral infection (332). IL-17E is the most distant homolog with IL-17A of 17% homology. IL-17E is produced by epithelial cells, eosinophils, basophils, mast cells, monocytes, macrophages and T cells (292, 293). In sharp contrast to other IL-17 family ligands, IL-17E presents distinct functional behavior, stimulating lymphocytes to produce Th2-related cytokines, such as IL-4 and IL-13. To this end, IL-17E inhibits Th1-mediated anti-tumor responses and plays roles in allergic inflammation and host defense against parasites (333-335). Recently, a pro-apoptotic role of IL-17E has also been identified in breast cancer cells (336), suggesting the role of IL-17E in cancer may be context-dependent.

1.5.2 IL-17A, IL-17F and IL-17RA/RC axis

A wide range of cell types, including type 17 $CD4^+$ T helper cells (Th17), γδ T cells, and innate lymphoid cells (337-339), as well as tissue structure cells like Paneth cells of the intestinal epithelium (340), are capable of producing IL-17A. The expression, signaling and biological function of IL-17F often overlap with IL-17A, however, minor differences lay in their relative distributions in various organs and cell types, as well as their receptor binding affinities (291, 293).

In humans, IL-17RA has an extremely low affinity to IL-17F, but can bind to IL-17A with a higher affinity than IL-17RC; whereas IL-17RC binds with higher affinity to IL-17F than to IL-17A (307). Therefore, cells with high IL-17RC expression could be highly responsive to IL-17F, whereas cells with low IL-17RC expression but high IL-17RA expression might respond better to IL-17A. The situation is somewhat different in mice, in which IL-17RA binds both IL-17A and IL-17F equally, whereas IL-17RC binds strongly only to IL-17F (292). Although human IL-17A and IL-17F homodimers can bind independently to IL-17RA and IL-17RC, both chains are reported to be required for IL-17A and IL-17F biological functions such as ligand-induced chemokine production (292, 341).

Notably, more than 20 spliced variants of human IL-17RA have been reported in NCBI databases (AceView) and at least 90 splice isoforms of IL-17RC are identified in human prostate cancer lines (292, 301). Similarly, mouse IL-17RA and IL-17RC are found to have at least 3 and 6 splice variants according to NCBI databases, respectively (292, 301). While full-length IL-17RA and RC are required for intracellular signal transduction leading to chemokine production (292, 341), the biological role of truncated splicing variants of IL-17RA and IL-17RC is unknown.

1.5.3 IL-17A functional paradox in cancer

IL-17A is a pleiotrophic inflammatory cytokine that has multi-faceted roles in cancer (136, 316). Clinical studies have detected IL-17A-producing cells in a variety of human cancer samples with elevated frequencies of tumor-infiltrating Th17 cells in ovarian, melanoma, breast and colon cancers (136, 342). Consistently, there is an increased IL-17A level in blood from patients with gastric (343) or lung cancers (344). Notably, phenotypic analyses suggested that tumor-infiltrating Th17 cells do not express CCR2, CCR5 or CCR7, which limit their capacity to home to the draining lymph nodes (345). This feature may explain the accumulation of Th17 cells in the TME, where CCL20 and CXCL12 are expressed at high levels (346). Furthermore, Th17 can secret CCL20 in an autocrine manner (347), which could enhance their recruitment to the tumor site.

An increased level of IL-17A in cancer patients is associated with poor prognosis in some studies, but improved prognosis in other reports (136, 316). To deal with this controversy, the role of IL-17A in tumorigenesis has been postulated to depend on multiple

factors including the specific tumor type and the cellular sources of IL-17A (136, 291, 316, 345). Various molecular and cellular mechanisms are reported to mediate the pro-tumor and/or anti-tumor functions of IL-17A. IL-17A can control cancer development via promoting inflammatory responses (324, 348), or inducing the production of VEGF and MMPs to favor angiogenesis, tumor invasion, and establishment of metastatic foci at secondary sites (349-352), or by facilitating tumor growth via enhancement of the IL-6-STAT3 signaling pathway (353). IL-17 may also promote an immune-suppressive TME by inducing the production and recruitment of MDSCs and Tregs (345, 354). In sharp contrast, the anti-tumor effect of IL-17 is attributed to increased immune responses by effector T cells and NK cells (355, 356). Finally, IL-17A may directly influence tumor growth, survival and neoplastic transformation in a cell type-dependent manner (Table 3). Notably, while IL-17A is reported to induce neoplastic transformation and proliferation with suppression of apoptosis in some tumor cell lines *in vitro*, it fails to do so in many other tumor cell lines (355, 357), and some primary cell types (358-360). This phenomenon suggests that the role of IL-17A signaling in tumor cell proliferation and survival is tightly regulated. However, the molecular mechanisms underlying the tumor-specific control of cellular turnover are largely understudied.

Table 3. Examples of IL-17/IL-17R signaling impacts on cellular turnover.

Gene	Model	Biological function	Ref
IL-17	Human cervical cancer cell lines	No direct effect on *in vitro* cellular proliferation	(357)
IL-17	P815 & J558L cells	No direct effect on *in vitro* cellular proliferation	(355)
IL-17	HIEC	Inhibits p38-MAPK-dependent proliferation without altering survival	(358)
IL-17RC	KO mouse	Promotes the formation and growth of prostate adenocarcinoma	(361, 362)
IL-17RC	Human prostate cancer cell lines	Anti-apoptotic in androgen-independent prostate cancer cell lines	(363)
IL-17RA	KD in 4T1 cells	Promotes tumor proliferation with inhibition of apoptosis in pooled shRNA-transfected clones	(364)
IL-17	Human ASMC	Promotes ERK1/2-MAPK-dependent proliferation	(365)
IL-17	Human & mouse prostatic cell lines	No direct effect on *in vitro* cellular proliferation	(359)
IL-17	JB6 Cl41 & MCF7 cells	Induces TPL2-depedent neoplastic transformation	(366)
IL-17	Human FLS	Promotes the STAT3-dependent survival and proliferation	(367)
IL-17	Mouse NSC	Inhibits proliferation and differentiation without inducing cytotoxicity or apoptosis	(360)
IL-17	AGS & SGC7901 cells	Promotes cell proliferation and monolayer wound healing with inhibition of apoptosis	(368)
IL-17	Human MM cells	Induces cell proliferation and migration with inhibition of cellular apoptosis and adhesion	(369)
IL-17	Mouse keratinocytes	Promotes TRAF4-ERK5-dependent keratinocyte proliferation and tumor formation	(370)
IL-17	T47D, IJG-1731 BT-20, MCF7cells	Induces proliferation and survival of tumor cells	(371)
IL-17	Human B-ALL	Promotes proliferation and resistance to daunorubicin-induced cell death	(372)

P815: mouse mastocytoma cell line. J558L: mouse B myeloma cell line. HIEC: human intestinal epithelial cell. KO: knockout. KD: knockdown. 4T1: mouse breast carcinoma cell line. ASMC: airway smooth muscle cell. JB6 Cl41: mouse epidermal cell line. MCF7, T47D, BT-20: human breast carcinoma cell line. FLS: fibroblast-like synoviocyte. NSC: neural stem cell. AGS & SGC7901: human gastric cancer cell lines. MM: multiple myeloma. IJG-1731: primary breast cancer biopsy cells. B-ALL: B-cell acute lymphoblastic leukemia.

1.5.4 IL-17A signaling pathways

1.5.4.1 Gene transcription

The downstream signaling cascades from IL-17RA and IL-17RC have been studied mostly using primary fibroblast cells (291-293) (Figure 5). The binding of IL-17A, or its close family member IL-17F, to the IL-17RA-RC complex recruits the intracellular adaptor protein Act1, which is required for the activation of signaling pathways triggered by all known IL-17 family ligands (293, 373). As a lysine-63 (K63) E3 ubiquitin ligase, Act1 recruits and activates TNF receptor associated factor-6 (TRAF6) via ubiquitination. Upon ligand binding, IL-17R recruits a unique adaptor protein known as Act1 through a SEFIR-SEFIR interaction, Notably, TRAF6 is also a K63 E3 ligase, which recruits and facilitates transforming growth factor β-activated kinase (TAK)1-TAB (TAK1-binding protein) 2/3-dependent phosphorylation and activation of the inhibitor of nuclear factor-κB kinase (IKK) complex, including IKKα, IKKβ and IKKγ (or NF-kappa-B essential modulator, NEMO). Subsequently, the activated IKK phosphorylates the IκB subunit (e.g., IκBα), leading to its proteasomal degradation and the release of canonical NF-κB for rapid nuclear translocation and consequent gene transcription (291-293, 374). The molecular mechanism of how TAK1 is activated by ubiquitinated TRAF6 during IL-17 signaling is unclear; however, a lysine at position 63 is both necessary and sufficient for ubiquitin to activate TAK1, likely through the K63-linked polyubiquitination by TRAF6 (375).

Besides the canonical NF-κB pathway, IL-17RA/RC-Act1-TRAF6 signaling also induces selective activation of MAPK (ERK, p38 and/or JNK) pathways in different target cells, which leads to the activation of AP1 transcription factors (376-379). In particular, activated TAK1 can phosphorylate MAP2Ks (such as MKK6) (375), or activate IKK-dependent release and activation of the serine/threonine kinase, tumor progression locus (TPL) 2 (366), which leads to pro-inflammatory gene transcription. More recently, IL-17R-Act1-TRAF4-MEKK3-MEK5-ERK5 signaling has been reported to promote IL-17-induced gene transcription resulting in keratinocyte proliferation and tumorigenesis (370).

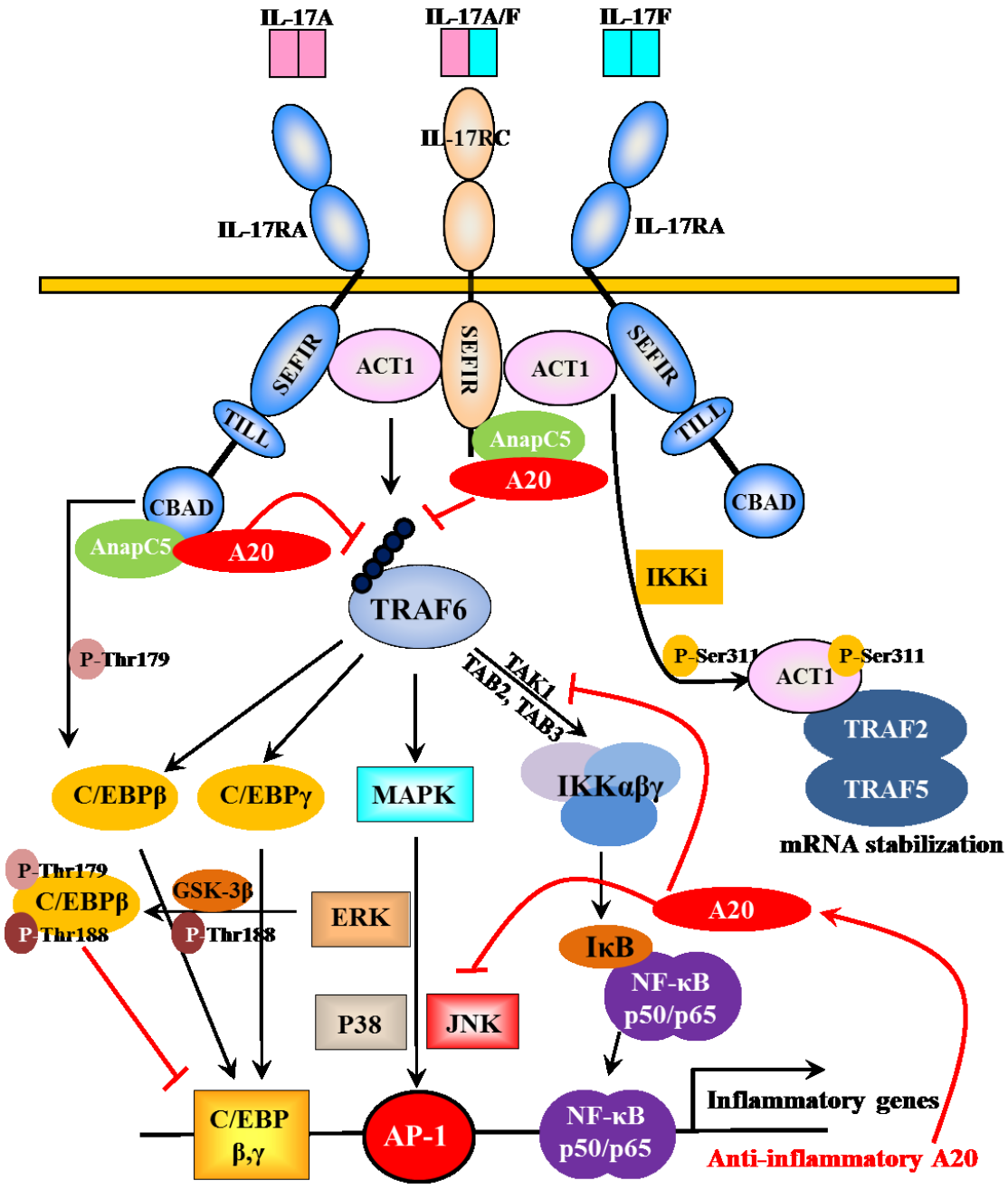

Figure 5. Schematic of IL-17/IL-17R signaling (291).

In addition, a microarray screen for IL-17A-induced genes identified that the activation of the *IL-6* promoter has an absolute requirement for the transcription factors C/EBP-β/ δ following IL-17A and TNF-α stimulation (380). Further studies suggested that C/EBP-β and C/EBP-δ are indispensable for transcription from several gene promoters (e.g., *IL-6*), even with an intact NF-κB site (381, 382). Furthermore, as stated above, both IL-17A and IL-17F have synergistic effect with TNF in the transcriptional induction of proinflammatory cytokine genes, such as the *IL-6* and *CXCL1*, and the overexpression of either C/EBP-β or C/EBP-δ can replace the contribution of IL-17A in this additive signal (380). Nevertheless, C/EBP-β and C/EBP-δ seem to function redundantly, as reconstitution of cells lacking both C/EBP-β and C/EBP-δ with either transcription factor can restore IL-17A-dependent induction of IL-6 expression (380).

IL-17A also induces cytokine production through the PI3K/Akt pathway in epithelial cells and fibroblasts (383, 384). However, more comprehensive and solid biochemical data are needed to validate and illustrate how the PI3K/Akt pathway is involved in this process.

1.5.4.2 mRNA stability

Besides promoting gene transcription, a unique Act1-dependent, TRAF6-independent arm of the IL-17RA/RC signaling pathway has been shown to control the stabilization of mRNA transcripts encoding proinflammatory molecules (e.g., *CXCL1*) in both human (385) and mouse primary epithelial cell lines (386) (Figure 5). Around 8% of transcripts encoding proinflammatory cytokines and chemokines exhibit short half-lives due to AU-rich elements (AREs) located within their 3'-untranslated regions (3'-UTR) (387). These AREs can be recognized and bound by ARE-binding proteins for AU-mediated mRNA degradation (388). Therefore, the regulation of mRNA stability is an important mechanism to control the magnitude of inflammatory gene expression. For this function, after stimulation with IL-17A, inducible IκB kinase IKKε (also known as IKKi) forms a complex with Act1, which leads to the phosphorylation of Act1 and a conformational shift that favors the recruitment of TRAF2 and TRAF5, rather than TRAF6 (385, 388, 389). The Act1-TRAF2/5 complex further recruits the ubiquitously expressed RNA-binding protein human antigen R (HuR), which competes with an mRNA decay factor, the mRNA splicing regulatory factor 2 (SF2), for binding with the 3'-UTR, preventing the degradation of mRNAs (e.g., *CXCL1*). As a modest activator of the pro-inflammatory NF-κB pathway

(390), it has been noted that mRNA stabilization is the primary function of IL-17 in promoting inflammation, alone and in synergy with other stimuli (386). For instance, TNF-α-induced mRNA transcripts are intrinsically unstable, while IL-17 synergizes with the TNF-α-induced production of pro-inflammatory mediators IL-8 and IL-6 by maintaining the stability of the respective mRNAs (391).

1.6 Regulators of IL-17A signaling

1.6.1 Positive regulators

The inhibitor of NF-κB (IκB)-ζ, encoded by the *NFKBIZ* gene downstream of the non-canonical NF-κB signaling, is an autocrine transcription factor that facilitates IL-17-induced canonical NF-κB-dependent gene transcription (392-396). IκB-ζ also directly promotes IL-17 production in Th17 cells, which in turn, forms a positive feedback loop (397). In addition, IκB-ζ also suppresses the expression of miR-23b, an inhibitor of IL-17 signaling (see section 1.6.2) (398).

The IL-17R family member IL-17RD exhibits dual roles in mediating IL-17A/IL-17RA-dependent signaling. On one hand, IL-17RD facilitates the activation of IL-17A-induced p38-MAPK signaling and the expression of the neutrophil chemokine macrophage inflammatory protein (MIP)-2 (399). The loss of IL-17A-induced MIP-2 expression in IL-17RD-deficient mice is associated with dampened IL-17A-induced neutrophil infiltration in the lungs and the peritoneum, whereas exogenous MIP-2 administration restores neutrophilia in these mice. Currently, the molecular mechanism responsible for IL-17RD promotion of IL-17A-induced p38-MAPK signaling is unclear. On the other hand, IL-17RD is able to negatively regulate IL-17-induced expression of NF-κB-dependent pro-inflammatory genes, such as *IL-6* and *CXCL1* (see section 1.6.2) (399).

Among the six C/EBP family members, IL-17 only induces C/EBP-β and C/EBP-δ (373, 380). While C/EBPβ can be inducibly phosphorylated and lead to the inhibition of IL-17-dependent pro-inflammatory gene induction (see section 1.6.2) (400, 401), C/EBP-δ has not been reported to be involved in post-translational modifications. As a positive mediator of IL-17A-dependent transcription, the *C/EBP-δ* gene is subject to autoregulation, as its own enhancer contains a functional C/EBP binding element (402).

1.6.2 Negative regulators

IL-17RA signaling is tightly controlled by several negative regulators of the signaling cascade. At the receptor level, IL-17RD interacts with both IL-17RA and Act1 basally via a SEFIR-SEFIR interaction, sequestering them from binding TRAF6, which in turn prevents the Act1-dependent ubiquitination and activation of TRAF6 and thus negatively regulates IL-17A-induced activation of NF-κB and the expression of pro-inflammatory genes such as *IL-6* and *CXCL1* (373). In general, the dual functions of IL-17RD in IL-17A/IL-17R-dependent immunomodulation highlight the complexity of this signaling axis.

There are two mechanisms underlying an inhibitory effect of C/EBP-β in IL-17A/IL-17RA signaling, which are both mediated by the CBAD domain of IL-17RA (400, 401). Firstly, C/EBP-β protein exists in multiple isoforms (403), while IL-17 preferentially induces the full-length C/EBP-β isoform (known as LAP) (400, 403), one of the alternatively generated C/EBP-β isoforms contains only the DNA-binding domain, which in turn, is potentially a transcriptional repressor (380, 403). Secondly, it has been shown that IL-17R signalling activates ERK to phosphorylate Thr188 of C/EBPβ, which is required for sequential Thr179 phosphorylation of C/EBPβ by GSK3β. The dual phosphorylation of C/EBPβ results in inactivation, inhibiting IL-17-mediated downstream gene transcription via a negative feedback loop (401).

TRAFs, such as TRAF3 and TRAF4, act to disrupt downstream signaling complex formation after ligand binding (404, 405). Thus, TRAFs don't affect the cytokine production downstream of IL-17 signaling (e.g., IL-6 and CXCL1) under homeostatic conditions (without exogenous ligand stimulation). In particular, TRAF3 inducibly binds to the CBAD motif in IL-17RA and thus competes with Act1 to interact with IL-17RA (404), while TRAF4 competes with TRAF6 for Act1 binding (405).

The micro-RNA, miR-23b, inhibits IL-1β-, TNF-α- or IL-17A-induced NF-κB activation via targeting the activities of TAB2/3 and IKK-α (398). Furthermore, IL-17A can down-regulate miR-23b expression, which in turn, promotes IL-17A signaling in an autocrine fashion (398). In contrast to miR-23b, the other mico-RNA inhibitor of IL-17A signaling miR-30a, targets Act1 expression, which inhibits both IL-17A-induced NF-κB and MAPK pathways (406).

More recently, the endoribonuclease monocyte chemoattractant protein-1-induced

protein (MCPIP)-1, also known as regnase-1, was reported to negatively regulate not only the IL-17A-induced mRNA stability of proinflammatory cytokines such as *IL-6*, but also the mRNAs of *IL-17RA* and *IL-17RC* (396). Notably, MCPIP1 expression can be induced by IL-17A, which acts as a negative feedback inhibitor. Furthermore, the RNA binding proteins roquin-1 and roquin-2 were shown to down-regulate mRNA of *IL-6* (407). Indeed, roquins inhibit IL-6 production downstream of IL-17 signaling, which has a synergistic effect with MCPIP1 (396).

Deubiquitinating enzymes like USP25 and A20 regulate the ubiquitination status of TRAFs and place a brake on the signaling cascade (408-411). Upon ligand binding, USP25 deubiquitinates Act1-mediated K63-linked ubiquitination of TRAF5 and TRAF6, thereby turning off IL-17 signaling via inhibiting mRNA transcription as well as stability (408). Notably, A20 deubiquitinates TRAF6 and restricts the activation of NF-κB and MAPK pathways (409-411).

1.6.2.1 Biology of A20

A20, a widely expressed and inducible cytoplasmic protein encoded by the gene TNFα-induced protein 3 (*TNFAIP3*), was first reported as a negative regulator of the NF-κB pathway and has a vital role in controlling inflammation and apoptosis (412, 413). Although initially described as a negative feedback inhibitor of TNFα-induced signaling, A20 also inhibits Toll-like receptor (TLR), IL-1R, and Nod-like receptor pathways in addition to the IL-17R pathway (414-416). Notably, A20 is a NF-κB transcription dependent gene, which can be induced by multiple pro-inflammatory stimuli, such as TNF, IL-1β, bacterial LPS and IL-17A (409, 412).

Functionally, A20 is essential for the development and function of a variety of immune cells such as dendritic cells, B cells, T cells and macrophages (417). A20-deficient mice exhibit multi-organ inflammation and perinatal lethality due to uncontrolled NF-κB activity triggered by homeostatic TLR signaling (418, 419). More recently, genome-wide association studies revealed the association between single nucleotide polymorphisms (SNPs) at the *TNFAIP3/A20* gene locus and multiple autoimmune and inflammatory diseases in humans, such as Crohn's disease and rheumatoid arthritis (420, 421).

1.6.2.2 Molecular mechanisms of A20

Biochemically, A20 is a ubiquitin-editing enzyme that exhibits de-ubiquitinating, E3 ligase, and ubiquitin-binding activities (Figure 5). The N-terminal ovarian tumor domain of A20 is responsible for its de-ubiquitinating activity whereas the seven zinc fingers at the C-terminus mediate E3 ubiquitin ligase and ubiquitin-binding activities (416). While activation of NF-κB is controlled by both K48- and K63-polyubiquitination of upstream signaling proteins, A20 turns off NF-κB by modulating both types of ubiquitination (409, 413, 422). For example, A20 controls TNF-induced and IL-17A-induced NF-κB activation by removing Lys63-linked ubiquitin chains from TRAF6. In addition, A20 catalyzes Lys48-linked poly-ubiquitynation of RIP1 via its E3 activity, which in turn triggers proteasome-mediated degradation of RIP1. A20 also inhibits IRF-3-dependent gene transcription (413, 415), TNF-induced apoptosis and IL-17A-induced IL-6 production via inhibition of the JNK pathway (409, 423). Furthermore, A20 inhibits Wnt signaling and reduced A20 expression is associated with human CRC development (424, 425). Given a vital role of A20 in controlling inflammation, it is conceivable that steady-state levels of A20 dictate the overall magnitude of inflammatory signals. While many pro-inflammatory stimuli can induce A20 production during inflammatory responses (412, 413, 415), it is less clear how A20 is maintained under steady-state conditions.

1.6.2.3 The role of A20 in cancer

The role of A20 in tumorigenesis has been studied; however, contradictory results were reported. For example, a tumor suppressor role for A20 in hematopoietic malignancies was generally accepted following the discovery that A20 is frequently inactivated due to somatic mutations and/or deletions in various lymphoid malignancies (426-429). Nevertheless, A20 is often overexpressed in leukemia, facilitating leukemic pathogenesis, cell proliferation and chemotherapy resistance (430-432). A functional paradox for A20 in solid tumors has also been suggested. On one side, A20 prevents hepatocellular carcinoma and colon cancer tumorigenesis (425, 433). On the other side, A20 over-expression is found in some other solid tumors, such as head and neck cancer, squamous cell carcinoma and aggressive breast cancer subtypes lacking either estrogen or progesterone receptors and is associated with a poor survival rate and chemo-resistance (434-436). Given that cancer arises and develops in the context of an *in vivo* tumor-specific

microenvironment, which orchestrates molecular and cellular events taking place in the course of tumor progression, these data support the notion that the role of A20 in the carcinogenesis of various cancers may depend on TME-specific A20 responses (162, 437). However, the intrinsic sources that maintain A20 levels in human neoplasms under steady state conditions are poorly understood.

1.7 Hypotheses and objectives

Given that IL-17RA and IL-17RC are differentially expressed by hematopoietic and non-hematopoietic cells (129), the ratio of IL-17RA/IL-17RC is postulated to control IL-17A-induced cytokine responses in a cell-type-dependent manner (129). However, the mechanism(s) by which IL-17R may regulate cell-type-dependent proliferation remains elusive. My first hypothesis is that tumor cells may rely on IL-17A signaling to directly control cellular proliferation in a cell-type-specific manner. Since intensive studies suggested that IL-17A-induced signals exhibited both pro-tumor and anti-tumor effects, **the primary objective of this study was to define how tumor cells utilize IL-17A/IL-17R signals to mediate tumor-specific growth**.

The increased levels of IL-17A and IL-17A-producing cells within the TME of different types of cancer suggest an important role for this cytokine signal in tumor progression. Previous research in Dr. Wang's laboratory has developed a novel adenovirus-mediated transgene delivery system to over-express IL-17A or IL-17F, or deliver an IL-17RA antagonist (a soluble decoy fusion protein containing the extracellular domain of IL-17RA and Fc) to the tumor cells to understand the impact of IL-17A and IL-17F on tumor growth. Using a mouse B16 melanoma model, preliminary results indicated that over-expression of the IL-17RA antagonist at the tumor site inhibited tumor growth in C57BL/6 mice. Analysis of tumor-infiltrating leukocytes showed that the IL-17RA antagonist led to increases in $CD4^+$ and $CD8^+$ T cell populations and NK cells compared to other treatment groups. Conversely, over-expression of IL-17A resulted in reduced $CD4^+$, $CD8^+$ and NK cell infiltration into tumors. These results led us to hypothesize that tumor cell intrinsic IL-17A also plays an active role in shaping the immunosuppressive TME. **The 2nd objective of my PhD research is to dissect the contribution of IL-17A/IL-17R signaling the regulation of the TME**.

CHAPTER 2 MATERIALS AND METHODS

2.1 Cells and Cell lines

All human tumor cell lines including human breast cancer cell lines (MCF7, SKBR3, MDA-MB231 and MDA-MB468), colon cancer cell lines (HT29 and CaCo2), prostate cancer cell line PC3, ovarian cancer cell lines (OVCA429 and SKOV3), as well as lung carcinoma epithelial cell line A549 were originally purchased from the American Type Culture Collection (ATCC) (Manassas, VA USA). Mouse B16 melanoma cells were provided by Dr. Brent Johnston (Dalhousie University, Nova Scotia) and 4T1 mouse mammary carcinoma cells were obtained from Dr. Tim Lee (Dalhousie University). All tumor cell lines were maintained in complete Dulbecco's modified Eagle's medium (DMEM) with 10% fetal bovine serum (FBS), 10 mM 2-[4-(2-hydroxyethyl)piperazin-1-yl]ethanesulfonic acid (HEPES), 100 U/ml penicillin/streptomycin, and 2 mM of L-glutamine (Life Technologies, Waltham, MA USA). Primary human mammary epithelial cells (HMECs) (Lonza, CC-2551) were provided by Dr. David Hoskin (Dalhousie University). Primary human colon epithelial cells (HCECs) from ATCC (CRL-1831) were maintained in DMEM:F12 medium supplemented with 10% FBS, 30 ng/ml epidermal growth factor, 0.005 mg/ml insulin, 0.005 mg/ml transferrin, 100 ng/ml hydrocortisone (all purchased from Sigma-Aldrich, Oakville, Ontario Canada) and 10 mM HEPES. Amphotropic Phoenix cells (Ampho-ΦNX) were obtained from Dr. Craig McCormick (Dalhousie University) and cultured in complete MEM F11 medium. McCoy cells were obtained from ATCC. The cells were grown in McCoy medium (minimum essential medium; Earle’s salts, L-glutamine, non-essential amino acids (Invitrogen, Waltham, MA USA), 2.2 g sodium bicarbonate, 5% FBS (Sigma Aldrich), gentamicin (10 µg/ml) (Invitrogen) and fungizone (2 µg/ml) (Invitrogen).

To isolate the mouse embryonic fibroblasts (MEFs), T175 flasks were coated with 0.2% bovine gelatin (Sigma Aldrich) in sterile distilled water for 2 hrs. Pregnant mice were euthanized 2 weeks post-coitum. The uterine horns containing the embryos were removed, rinsed in 70% ethanol, then submerged in 5% bovine serum Roswell Park Memorial Institute (RPMI) medium. Using sterile technique, individual embryos were removed from the yolk sac in a Petri dish and the head and red organs were removed and discarded. The embryos were mechanically disrupted with glass slides until the pieces could be pipetted.

A mixture of 0.05% trypsin/ ethylenediaminetetraacetic acid (EDTA, Wisent Bio Products, ST-BRUNO, Quebec Canada), 10 µg/ml DNase I (Sigma Aldrich), and 300 µg/ml collagenase II (Sigma Aldrich) (1 ml/embryo) was added to the suspension and then pipetted into a tube. The sample was incubated at 37°C for 20 min with gentle vortexing every 5 min. The reaction was stopped with at least one volume of complete DMEM and then pelleted (525 g, 10 min at 4°C). The supernatant was carefully aspirated with a pipette and the pellet was resuspended in complete DMEM. The cell suspension was plated onto the 0.2% bovine gelatin-coated flasks (3-4 embryos per flask) and then incubated at 37°C until confluent. Cells were then detached, filtered through a 70 µm cell strainer, and passaged for experiments.

Bone marrow derived dendritic cells (BMDCs) were generated from the femurs and tibia of naïve mice. Bone marrow was flushed with 5% bovine serum RPMI into Petri dishes containing 5-10 ml of 5% bovine serum RPMI. Samples were centrifuged at 525×g for 10 min at 4°C. The pellet was resuspended and red blood cells were lysed by incubation in 1 x Ammonium-chloride-potassium (ACK) buffer for 5 min at room temperature (RT) followed by addition of 5-10 ml 5% bovine serum RPMI. Samples were centrifuged for 10 min and resuspended in 10 ml complete RPMI medium and 20 ng/ml (200 U/ml) recombinant mouse GM-CSF (R&D Systems, Burlington, Ontario). The concentration of cells in single-cell suspensions was determined by trypan blue-dye exclusion method using a hematocytometer. On day 0, 3 x 10^6 bone marrow cells were seeded in100-mm tissue culture dishes in 10 ml complete RPMI and incubated at 37°C, 5% CO_2. Cells were fed by adding an additional 10 ml complete RPMI at day 3. On day 6, loosely adherent cells were collected by gently pipetting the suspension media and used as the source of DCs.

2.2 Mice

C57BL/6 male and BALB/c female mice were purchased from Charles River Laboratories (Senneville, QC) and were normally used between 8 to 12 weeks of age. Mice were housed at the Izaak Walton Killam (IWK) Health Centre animal facility under pathogen-free conditions. All animal procedures were approved by the Dalhousie University Committee on Laboratory Animals.

2.3 Construction and use of retroviral vectors and DNA plasmids

Recombinant lentiviruses encoding shRNA sequences that target four different regions of mouse IL-17RA (OB320663, OB215726, OB15280 and OB3035) or IL-17RC (OB495966, OB495968, OB495970 and OB6972) were cloned into a pSMP vector (Open Biosystems) and confirmed by sequencing (GENEWIZ, Inc., South Plainfield, NJ USA). Approximately 0.8 x 10^6 Ampho-ΦNX cells per well were plated in 6-well plates to grow overnight. The Ampho-ΦNX cells are ready for transfection at approximately 80% confluency which occurs 16 hrs after culture. Approximately 0.5 µg of plasmid DNA encoding different shRNA constructs were mixed with 10 ul of 1 mg/ml polyethyleneimine (PEI) (40,000 MW, Polysciences Inc.) in 100 ul DMEM medium. The mixed constructs were vortexed 1 second intervals for 15 seconds and incubated at RT for 15 mins. During the incubation, Ampho-ΦNX cells were gently washed with pre-warmed phosphate buffered saline (PBS) and then transfected with the mixed constructs allowing virus production for 3 days. The virus-containing culture supernatants were collected and used to transduce B16 and 4T1 tumor cells. At one day before the transduction, tumor cells were seeded into 6-well plates (0.25 x 10^6 per well), which normally reached about 40-50% confluency after 16 hrs culture and used for transduction. On the day of transduction, 2 ml of virus-containing culture supernatants were briefly centrifuged at 1000×g for 5 min to remove the cellular debris and the supernatants were subsequently incubated with cells in the presence of 8 µg/ml polybrene (Sigma Aldrich) for 2 hrs at RT and spun at 800×g. After spinning, cells in the 6-well plates were directly transferred to a 37°C incubator overnight. Subsequently, culture supernatants were removed and cells were grown with complete DMEM medium for an additional 24 hrs. Stable transfectants were selected by treating cells with 4 µg/ml puromycin (Bio Basic Inc.) for 7 days or until all non-transfected tumor cells died. Selected cells were subjected to a limiting-dilution-assay to obtain single-cell-derived subclones (438). Ten subclones of each of the 8 shRNA constructs (e.g., IL-17RA1.1 to IL-17RA1.10), as well as the pSMP control cells, were expanded for further characterization and analyses. For the B16 cells, IL-17RAKD3.1, IL-17RCKD4.5 and pSMP.5 were the best clones. For the 4T1 cells, IL-17RAKD4.6, IL-17RCKD4.8 and pSMP.4 were the best clones.

For reconstituting mouse IL-17RA, the full-length coding sequence of mouse IL-

17RA (NM_008359) was cloned into retroviral vector pBMN-IRES-Hygro, which was provided by Dr. Craig McCormick (Dalhousie University). The best stable RAKD subclone of B16 cells (B16-RAKD3.1) and B16-pSMP.5 transfectants were selected by 400 μg/ml hygromycin B (Life Technologies). Unlike the B16-RAKD3.1 clone that was generated by targeting 3'end un-translated region of IL-17RA, the viral vector used in the representative 4T1-RAKD4.6 clone targeted the coding sequence of IL-17RA, which would prevent the reconstitution of IL-17RA. Thus, the reconstitution was not performed in 4T1 cells.

In some experiments, GIPZ lentiviral shRNAs (Thermo Scientific, Waltham, MA USA) targeting JNK1 (V2LMM49133) and JNK2 (V3LMM472591, V3LMM515242 and V3LMM515241), were used to knockdown JNK1 or JNK2 in IL-17RCKD tumor cells. The lentivirus vector GIPZ has a green fluorescent protein (GFP) expression cassette, therefore, the cell transfection rate was observed directly under a fluorescent microscopy, which could reach up to 80%. At day 3 post-transfection, tumor cells were starved in serum-free medium for 14 hrs and then rescued with complete medium (CM) for 1 hr. Whole-cell extracts were harvested and the level of JNK1 or JNK2 protein was examined using Western blotting.

In some experiments, A20 reconstitution was conducted using plasmids encoding murine A20 or a deletion-mutant, which were purchased from the plasmid repository at BCCM/LMBP (Belgian Coordinated Collections of Micro-organisms and Laboratory of Molecular Biology–Plasmid collection). Lipofectamine 3000 Reagent (Life Technologies) was used for plasmid DNA transfection in tumor cells following the manufacturer's instructions.

2.4 Gene expression analysis

2.4.1 RNA extraction, reverse transcription-PCR and quantitative real-time PCR (qPCR)

Total RNAs were extracted from 3 x 10^6 tumor cells using RNeasy columns (QIAGEN) and first strand cDNA was generated through reverse transcription-PCR using a QuantiTect Reverse Transcription kit (QIAGEN) following the manufacturer's instructions. PCR reactions were performed with gene-specific primers using PCR Master Mix (Promega) in an Eppendorf Mastercycler PCR machine. Primers were designed against the mRNA sequence of each gene of interest using Primer Premier Version 5

(PREMIER Biosoft, Palo Alto, CA USA). The properties of primers used in this study are listed in Table 4. The standard PCR cycling program in a 20 µl reaction volume was initially heated for 3 min at 95°C, processed through 30 cycles of sequential temperatures of 95°C (30 sec), 56°C (30 to 90 sec), 72°C (30 sec) and finally incubated for 10 min at 72°C, using an Eppendorf Mastercycler PCR machine. Pooled complementary DNA (cDNA) samples were used as template to assess the optimal annealing temperature of the individual primer pairs. The standard PCR cycling program was modified by replacing the annealing temperature step with a thermal gradient between 52°C and 64°C for 1 min extension time. Samples were stored at 4°C, prior to electrophoresis at 110 V on 0.8% agarose gels containing ethidium bromide.

For qPCR, cDNA was amplified in RT² SYBR® Green ROX qPCR Mastermix (QIAGEN) following the manufacturer's instructions using a 7900 HT Fast Real-Time PCR System (Applied Biosystems, Foster City, USA). Each amplification was performed with no-cDNA control wells and positive control wells containing XpressRef™ Mouse Universal Total RNA (QIAGEN). The following thermal profile was used: 10 min at 95°C for HotStart DNA Taq Polymerase activation, followed by 40 amplification cycles of 15 sec at 95°C and 1 min 60°C (annealing-extension step). Dissociation curve analysis was performed after each run. All PCR components are denatured 1 min at 95°C, followed by complete annealing 2 mins at 65°C, followed by a gradual increase in temperature up to 95°C. Fluorescence intensity is monitored during this final temperature increase, resulting in the generation of a dissociation curve (or melting curve). A single peak in the dissociation curve of each primer pairs verifies the PCR specificity. GAPDH and β-actin were used as internal normalization controls for qPCR. The data were analyzed using the SDS software 2.2.2 from Applied Biosystems. In some assays, cells were treated with recombinant mouse IL-17A, IL-17F and IL-17E which were purchased from R&D Systems and reconstituted in sterile 4 mM HCl at a concentration of 100 µg/ml. Recombinant mouse IL-17C (eBioscience) was stored and used according to the manufacturer's protocol.

Table 4. Primers used in this study.

Gene*	Sequence (5'→3')	TM (°C)	Length
mIL-17RA sense PCR	TTGCATGTTGAGTGGACCCTGCA	61.5	698bp
mIL-17RA antisense PCR	AGGCCATACACCCACAGGGGA	62.9	
mIL-17RA sense qPCR	AGGGCTGCGGCATGTGAT	60.4	140bp
mIL-17RA antisense qPCR	GCCTCCCGAGTTCTCCTGTTA	58.5	
mIL-17RC sense	AGATGCCTGTGTCCTGGTTC	57.1	243bp
mIL-17RC antisense	CGCAATCTGTCTTCTGTGGA	54.9	
mIL-17RC isoform sense	GTGGGTTCTGCGGTATTT	52.8	598bp
mIL-17RC isoform antisense	CATTCACAGTGGCGTTCTT	53.7	
mIL-17RD sense	GGCATAAGGAAAACAGTAACATAGCA	55.5	118bp
mIL-17 RD antisense	AACCAAGAAGCCCAGGAAACA	57.1	
mIL-17A sense	CTCAGACTACCTCAACCGTTCCA	58.1	131bp
mIL-17A antisense	CCAGCTTTCCCTCCGCATT	58.1	
mIL-17F sense	ACTGTTGATGTTGGGACTTGCC	57.9	160bp
mIL-17F antisense	AGAAATGCCCTGGTTTTGGTT	55.4	
mIL-17C sense	AGGACCCTGCGGTGCTACTC	61.5	129bp
mIL-17C antisense	GCCCGTGGCCTCCAAACT	61.2	
mIL-17E sense	CCAGCAAAGAGCAAGAACCCC	58.8	179bp
mIL-17E antisense	CCGATTCAAGTCCCTGTCCAAC	57.9	
mA20 sense	AATCGGCTGCTTCCTATGACTC	60.3	236bp
mA20 antisense	CTTCCTCGTCCTCACGGCTA	60.2	
mJNK1 sense	GGAGGTAATGGATTTGGAGGA	58.1	119bp
mJNK1 antisense	ACAGACGGCGAAGACGATG	59.0	
mJNK2 sense	ACACGAATAGATGTTGAAGTGTCG	58.9	203bp
mJNK2 antisense	TTGGCAGGTTCTCCTGGTTA	58.0	
mGAPDH sense	CGATGCCCCCATGTTTGTGAT	58.2	249bp
mGAPDH antisense	GCAGGGATGATGTTCTG	55.8	
hIL-17 RA sense	TCCTGCCCAGAAATGCCA	60.1	84bp
hIL-17 RA antisense	GGAGATGCCCGTGATGAACC	62.2	
hIL-17 RC sense	GGACGATGACTTGGGAGCG	60.9	99bp
hIL-17 RC antisense	GCAGCGGCAAAGAGTAGGC	60.9	
hβ-actin sense	AGCGGGAAATCGTGCGTG	58.8	309bp
hβ-actin antisense	CAGGGTACATGGTGGTGCC	58.4	

* m: mouse, h: human, TM: melting temperature.

2.4.2 PCR microarray

For RT² Profiler™ PCR array of mouse chemokines & receptors (QIAGEN, PAMM-022A), cDNAs were generated from approximately 3 x 10^6 B16 tumor cells treated with 200 ng/ml recombinant IL-17A (R&D Systems) stimulation for 16hrs, or tumors isolated from C57BL/6 mice at day 12 post-inoculation. The same thermal profile described for qPCR was used in this experiment. RT² Profiler PCR Array Data Analysis version 3.5 (QIAGEN) was used for processing the raw data and auto-selecting the best housekeeping gene for normalization. This microarray pannel is customized with 84 inflammation-related genes and 5 housekeeping genes. Among the 5 housekeeping genes [β-actin, β2-microglobulin, glyceraldehyde-3-phosphate dehydrogenase (GAPDH), β-glucuronidase and heat shock protein 90 α (cytosolic) class B member 1], GAPDH was the most stable and was selected for normalization. Representative gene expression profiles were validated by qPCR. All the gene expression data were normalized to the level of GAPDH.

2.4.3 Droplet digital PCR (ddPCR)

ddPCR reactions were prepared using BioRad QX200 ddPCR EvaGreen Supermix (Bio-Rad, Mississauga, Ontario) following the manufacturer's instructions. Twenty microliters of each reaction mix were converted into droplets with 65 µl of Droplet Oil (Bio-Rad) in the QX200 droplet generator (Bio-Rad). Droplet-partitioned samples were then transferred to a 96-well plate, sealed and cycled in a C1000 deep well Thermocycler (Bio-Rad) under the following cycling protocol: 95°C for 5 min (DNA Taq polymerase activation), followed by 50 cycles of 95°C for 30 sec (denaturation), 60°C for 1 min (annealing) and 72°C for 1 min (elongation), followed by post-cycling steps of 4°C for 5 min hold, 90°C for 5 min (enzyme inactivation) and an infinite 10°C hold. The cycled plate was then transferred and read in the 6-carboxyfluorescein (FAM) and high-energy X-ray (HEX) channels using the QX200 Droplet reader (Bio-Rad) using "QuantaSoft" software (Bio-Rad) either the same day or the following day.

2.5 Cell proliferation assays

2.5.1 MTT assay

Tumor cells were plated in quadruplicate in a 96-well plate at a density of 5,000 cells per well. Cells were incubated at 37°C for a maximum of 72 hrs with or without serum

starvation to cell cycle synchronization. At the end of the assay, cells were incubated with 0.5 mg/ml MTT for 2 hrs and the purple formazan products were dissolved in 100 µl of dimethyl sulfoxide (DMSO). The plates were read on a plate reader (BioTek Synergy HT) at 570 nm with a reference reading at 630 nm. Optical density values collected 6 hrs post-seeding were used to calculate the fold-change in proliferation at different time points. In some assays, the cells were treated with different chemical inhibitors (Table 5) or DMSO vehicle. The inhibitors SB203580, FR180204, 420116 and SP600125 were purchased from EMD Millipore. KIN001-102 and BMS-345541 were purchased from Sigma Aldrich. All inhibitors were reconstituted in DMSO.

2.5.2 Ki67 staining

The proliferation rates of primary and tumor cells were determined based on expression of nuclear antigen Ki67. Cells were plated in 100 mm tissue culture dish at a density of 0.75 x 10^6 cells per dish, cultured in serum-free DMEM medium for 12 hrs and transferred into complete DMEM for 1-12 hrs. Cells were harvested and washed with 1 x PBS in 96-well plate. Meanwhile, the fixable viability dye eFluor506 (eBioscience) was thawed for 10 – 15 mins at RT. Cells were then resuspended in 100 ul 1 x PBS containing 1:1000 dilution of eFluor506 and incubated at 4°C for 30 mins in the dark. After staining, cells were washed once with fluorescence activated cell sorting (FACS) wash buffer (1% bovine serum in 1 x PBS). Following washing, 200 µl of Foxp3 Fixation/Permeabilization working solution (eBiosicience) were added to each well and cells were fully resuspended by pipetting. Cells were then incubated in the dark for 30 mins at RT. Samples were centrifuged at 400 x g for 5 mins at RT, then the supernatant was discarded. Wells were washed twice with 200 µl 1 x Permeabilization Buffer (eBiosicience, 10x concentrate diluted in dH_2O). After washing, cells were blocked with 2% normal rat serum in 100 µl 1 x Permeabilization Buffer per sample for 15 mins at RT. After removing the supernatant, cell pellets were mixed with 50 µl 1:300 Ki67 PerCP-eFluor® 710 (eBiosicience, clone: SolA15), diluted in 1 x Permeabilization Buffer, and incubated in the dark for 30 mins at RT. The wash was repeated twice with 200 µl of 1 x Permeabilization Buffer and cells were resuspended in 200 µl of FACS wash buffer. Data were collected using a BD LSR Fortessa flow cytometer.

Table 5. Chemical inhibitors used in this study and their properties.

Inhibitor	Target pathway	Mode of action
KIN001-102	AKT	Isozyme selective Akt1/2 kinase inhibitor
BMS-345541	NF-κB	Highly selective I kappa B kinase (IKK) allosteric site inhibitor
SB203580	p38 MAPK	Competitive inhibition of ATP binding site of p38 MAPK
FR180204	ERK1/2 MAPK	ATP-competitive inhibition to ERK1/2
420116	JNK MAPK	(L)-form peptide with inhibition to JNK phosphorylation
SP600125	JNK/c-Jun MAPK	Competitive inhibition to JNK and c-Jun phosphorylation

Note: The inhibitors SB203580, FR180204, 420116 and SP600125 were purchased from EMD Millipore. KIN001-102 and BMS-345541 were purchased from Sigma.

2.5.3 Growth curve assay

In the growth curve assay, 0.25 x 10^6 cells were seeded in a 60 mm dish. Cells were allowed to grow at 37°C. At different time points, cells were trypsinized and diluted 1:1 with 0.4% trypan blue stain. Ten microliters of the cell-stain mixture was then loaded onto a hemacytometer and viable cells were counted.

2.5.4 Cell cycle analysis

To conduct cell cycle analysis, 0.25 x 10^6 tumor cells were synchronized in serum-free DMEM for 24 hrs and then cultured in complete DMEM medium in 6-well flat-bottom tissue culture plates for 24 or 48 hrs. Cells were harvest by trypsinization, washed, and resuspended in 0.5 ml ice-cold 1 x PBS. With gentle vortexing, 4.5 ml ice-cold 70% ethanol was added to fix the cells (final volume of 5 ml). The cells were further fixed by storing at -20°C for at least 24 hrs. Cells were then thawed, washed in 1 x PBS and (depending on cell number) resuspended in 0.5-1.5 ml of the cell cycle solution, which consists of 0.02 mg/ml propidium iodide (PI), 0.1% v/v Triton X-100, and 0.2 mg/ml DNase-free RNase A in 1 x PBS. Cells were incubated at RT for 30 mins. Data were collected with FACSCalibur on low flow (around 40 to 80 events per second) and DNA content in PI-stained cells was analyzed using ModFitLT V2.0 software (BD Biosciences).

2.6 Cytokine ELISA

The concentrations of cytokines and chemokines in culture supernatants were determined using enzyme-linked immunosorbent assay (ELISA) kits (eBioscience). The optimal concentration of each antibody was specified by the manufacturer.

Wells in 96-well flat-bottom ELISA plates (Greiner Bio-One, Monroe, NC USA) were coated with 50 µl of the specific capture antibody for against cytokine or chemokine of interest. The capture antibodies were all initially diluted in Coating Buffer (eBioscience). The plates were sealed and incubated overnight at 4°C. To wash the plates, 200 µl of 0.01% Tween-20/PBS (PBST) buffer was added to each well and then dumped out and patted dry on paper towel. Alternatively, an automatic plate washer was used for this process (BioTek, ELx405). After 5 washes, blocking buffer (100 µl) (Assay Diluent) (PBS containing 1% BSA) was added to each well and the plates were incubated for 2 hrs at RT. The plates were then washed 5 times as described above. The cytokine standards were prepared in a

1:2 serial dilution in Assay Diluent starting at 2,000 pg/ml. Eight dilutions were performed to generate a standard curve. Samples were diluted in Assay Diluent if the concentration of the cytokine being measured exceeded the upper limit of quantitation of the standard curve. Standards and samples were added to wells (50 µl each) and plates were incubated overnight at 4°C. After the incubation, the plates were washed 5 times with 200 ul/well of PBST. Following the washes, 50 µl of biotinylated detection antibody diluted in Assay Diluent was added to each well and the plates were incubated for 2 hrs at RT. Plates were washed 5 times and 50 µl of streptavidin-horse radish peroxidase (eBioscience) diluted in Assay Diluent was added to each well and incubated for 20 mins in the dark at RT. After seven washes with 200 µl/well PBST, 50 µl of 1x 3,3',5,5'-Tetramethylbenzidine substrate solution (eBioscience) was added to each well. Assays were monitored for color change and the reaction was stopped with 50 µl of 0.2M H_2SO_4. Within 30 mins, plates were read at 450 nm using a BioTek Synergy HT plate reader and the data was analyzed using Gen5 software (BioTek).

2.7 Western blotting

Approximately 2.5 x 10^6 cells in 100 mm tissue culture dishes were washed twice with ice-cold 1 x PBS. Cells were then scraped into 1 ml ice-cold 1 x PBS and pelleted 500 x g for 3 mins at 4°C. The cell pellet was resuspended with 100~200 µl whole cell extraction buffer (20 mM HEPES [pH 7.4], 100 mM potassium chloride, 10 mM β-glycerophosphate, 50 mM sodium fluoride, 0.2% Triton X-100, 1 mM sodium orthovanadate, 1 mM phenylmethylsulfonyl fluoride, 2 mM dithiothreitol, and protease inhibitor cocktail [Sigma Aldrich]). Lysates were stored on ice for 15 mins with brief vortexing and spun at 12,000 x g for 3 mins. Supernatants were collected and protein concentrations were determined using the bicinchoninic acid (BCA) assay (Thermo Scientific) following the manufacturer's instructions. Sodium dodecyl sulfate (SDS) sample buffer was added to an aliquot of each extract and then boiled for 10 min. Protein samples (25 µg) were electrophoresed on SDS-polyacrylamide gel electrophoresis (PAGE) gels using the buffer system of Laemmli (439) (Mini PROTEAN electrophoresis system, Bio-Rad; 200 V, ~ 45 mins).

Polyacrylamide gels were transferred onto nitrocellulose membranes (Bio-Rad) with a wet transfer apparatus (Mini Trans-Blot, Bio-Rad) at 200 mA for 1 hr. All blots were

blocked in 1 x PBS with 5% BSA and 0.1% Tween at RT for 1 h. The blots were then probed with various primary antibodies as listed in Table 6. All primary antibodies were diluted in PBS/0.1% Tween-20 containing 5% BSA. After overnight incubation at 4°C, unbound antibodies were removed by washing 4 x 1 min with 1 x PBS with 0.1% Tween. Secondary antibodies conjugated with horseradish peroxidase were added for 1 hr at RT. The membranes were then washed 4 x 1 min with 1 x PBS with 0.1% Tween and 2 x 1 min with 1 x PBS. Quantitative western blots were developed using ECL Advanced Technology (GE Healthcare, Chicago, IL USA) and the reactivity was detected and visualized by chemiluminescence. The intensity of bands of interest was analyzed using ImageJ software (NIH).

2.8 Electrophoretic mobility shift assay (EMSA)

Nuclear protein extracts were prepared using a nuclear extract kit (Active Motif) per the manufacturer's protocol. All preparation procedures were carried out at 4°C. Total protein concentration was determined using the bicinchoninic acid (BCA) assay (Thermo Scientific) following manufacturer's instructions. EMSA was performed using a double-stranded oligonucleotide probe specific for the NF-κB consensus sequence on the IL-6 promoter, 5′-AGTTGAGGGGACTTTCCCAGGC-3′ (Promega) (440). The oligonucleotides were labeled with ^{32}P adenosine triphosphate (Perkin Elmer) using T4 kinase (Life Technologies) and purified using a Sephadex G-25M column (GE Healthcare). Ten micrograms of nuclear protein were added to 10 µl of binding buffer supplemented with 1 µg of poly-(dI-dC) (GE Healthcare) and incubated at RT for 15 mins before mixing with the labeled oligonucleotides. The reaction mixture was incubated at RT for 30 mins and subjected to electrophoresis on a 6% polyacrylamide gel in Tris–boric acid–EDTA buffer. Gels were vacuum-dried and subjected to autoradiography.

Table 6. List of antibodies used in western blotting and immunohistochemistry.

Antibody name	Company (CAT#)	Dilution
Anti-Akt	Cell Signaling (9272)	1:1000 (WB)
Anti-phospho-Akt (Ser473)	Cell Signaling (9271)	1:1000 (WB)
Anti-phospho-Akt (Thr308)	Cell Signaling (9275)	1:1000 (WB)
Anti-IκB-α	Cell Signaling (9242)	1:1000 (WB)
Anti-phospho-IκB-α (Ser32/36)	Cell Signaling (9246)	1:1000 (WB)
Anti-SAPK/JNK	Cell Signaling (9252)	1:1000 (WB)
Anti-JNK1	Santa Cruz Biotech. (sc-1648)	1:200 (WB)
Anti-JNK2	Santa Cruz Biotech. (sc-827)	1:200 (WB)
Anti-phospho-SAPK/JNK (Thr183/185)	Cell Signaling (4668)	1:1000 (WB), 1:50 (IHC)
Anti-c-Jun	Cell Signaling (9165)	1:1000 (WB)
Anti-phospho-c-Jun(Ser63)	Cell Signaling (2361)	1:1000 (WB)
Anti-phospho-c-Jun(Ser73)	Cell Signaling (3270)	1:1000 (WB)
Anti-A20/TNFAIP3	Cell Signaling (5630)	1:1000 (WB), 1:50 (IHC)
Anti-caspase-3	Cell Signaling (9662)	1:1000 (WB)
Anti-cleaved caspase-3	Cell Signaling (9664)	1:1000 (WB and IHC)
Anti-GAPDH	Cell Signaling (5174)	1:2000 (WB)
Anti-Ki67 (SolA15)-FITC	eBioscience (11-5698)	1:50 (IHC)

WB: western blotting. IHC: immunohistochemistry.

2.9 Flow cytometry

2.9.1 Extracellular staining

To determine the cell surface expression of IL-17RA and IL-17RC on stable transfected tumor cell lines, cells were analyzed by flow cytometry. Transduced tumor cells were washed with FACS wash buffer (1 x PBS supplemented with 1% BS), then to avoid non-specific Fc-mediated binding, each pellet was blocked using 50 µl of FACS wash buffer containing 10% rat serum, and incubated for 20 min at 4°C. After washing, cell pellets were resuspended in 50 µl of FACS wash buffer containing anti-mouse fluorescent conjugated monoclonal antibodies targeting either IL-17RA (PAJ-17R, eBioscience) or IL-17RC (FAB-2270A, R&D Systems) at recommended dilutions, and incubated for 20 min at 4°C. After staining, cells were washed and fixed with 200 µl/tube of fixation buffer (1% formalin in 1 x PBS), and transferred into flow cytometry mini-tubes.

To identify different cell types within a heterogeneous population based on surface antigens, instead of single color staining, washed cell pellets were resuspended in 50 µl of FACS wash buffer containing a cocktail of fluorescent conjugated antibodies that bind specific surface markers at appropriate dilutions and colors (Table 7). The same washing and fixation procedures were conducted as outlined above. All FACS data were acquired on a Becton Dickinson FACSCalibur then analyzed using FCS Express 4 Flow Research Edition (De Novo, Los Angeles, CA USA).

2.9.2 Intracellular staining

Intracellular staining identifies cells based on markers inside the cells. Cells were washed, resuspended in FACS wash buffer at a concentration of 1-2 x 10^6 cells/ml, and triplicate 100 µl samples were seeded in separate wells on a 96-well tissue culture plate. One hundred µl of complete RPMI supplemented with 1 ng/ml of phorbol myristate acetate (PMA), 1x Brefeldin A, and 1 µg/ml of Ionomycin was added to each well (final volume/well is 200 µl) and incubated for 4-5 hrs at 37°C. After incubation, 2 µl of 1 mM EDTA was added to each well and incubated for 5-10 mins at RT. Cells were then transferred to a V-bottom 96 well plate and washed with FACS wash buffer. For blocking, each well was supplemented with 20 µl of wash buffer containing 10% rat serum, incubated for 20 mins at 4°C, and washed. Extracellular staining was performed as above without the fixation step. After extracellular staining and wash, 100 µl of intracellular fixation buffer

was added to each well, followed by incubation in the dark for 20 mins at RT. Without washing, 100 µl of 1x permeabilization buffer was added to the mixture, which was centrifuged for 10 min (750 x g, 4°C). Washing was repeated using 200 µl of permeabilization buffer. Pellets were then resuspended in 50 µl of permeabilization buffer containing a cocktail of fluorescent conjugated antibodies against specific intracellular cytokines (IFN-γ, IL-17A, IL-4) at appropriate dilutions and colors (Table 7). Following incubation for 20 mins at 4°C, cells were washed using 100 µl of 1x permeabilization buffer, washed three times with wash buffer, mixed with 200 µl per tube of fixation buffer, and transferred into flow cytometry mini-tubes. Data were acquired on a Becton Dickinson FACSAria and analyzed using FCS Express 4 Flow Research Edition (De Novo).

2.9.3 Apoptosis assay

Apoptosis in cells was assessed using a PI/Annexin V-fluorescein isothiocyanate (FITC) Apoptosis Detection Kit (eBioscience) per the manufacturer's protocol. B16 and 4T1 cultures were serum starved for 14 hrs and rescued with complete DMEM medium for 1 hr. The cells were then washed with ice-cold 1 x PBS and resuspended in 1 x binding buffer. Aliquots of 2 x 10^5 cells were mixed with 5 µl Annexin V-FITC and 10 µl PI for 10 mins at RT in the dark. Fluorescence was detected within 4 hrs using flow cytometry. Flow cytometric analysis was performed on cells that were undergoing apoptosis (Annexin V^+) (441).

Table 7. List of antibodies used in flow cytometry.

Antibody	Conjugate	Clone	Company (CAT#)	Dilution
α-IL-17RA	PE	PAJ-17R	eBioscience (12-7182-80)	1:150
Rat IgG2a Isotype Ctrl	PE	eBR2a	eBioscience (12-4321-83)	1:150
α-IL-17RC	APC	Polyclonal	R&D Systems (FAB2270A)	15ul/test
Goat IgG Isotype Ctrl	APC	Polyclonal	R&D Systems (IC108A)	15ul/test
α-Ki-67	PerCP-eFluor710	SolA15	eBioscience (46-5698-80)	1:300
α-CD4	Fitc	RM4-5	eBioscience (11-0042-82)	1:200
α-CD3e	PerCP-Cy5.5	145-2C11	eBioscience (45-0031-82)	1:100
α-CD8α	PE-Cy7	53-6.7	eBioscience (25-0081-82)	1:400
α-MHCII	APC-eFluor780	M5/114.15.2	eBioscience (47-5321-82)	1:800
α-NKp46	eFluor660	29A1.4	eBioscience (50-3351-82)	1:100
α-CD8α	PE	53-6.7	eBioscience (12-0081-85)	1:100
α-CD19	PE-Cy7	eBio1D3	eBioscience (25-0193-82)	1:500
α-CD45	Fitc	30-F11	eBioscience (11-0451-85)	1:200
α-CD11c	APC	N418	eBioscience (17-0114-82)	1:100
α-F4/80	PE	BM8	eBioscience (12-4801-82)	1:200
α-Ly-6C	PerCP-Cy5.5	HK1.4	eBioscience (45-5932-82)	1:300
α-CD11b	Fitc	M1/70	eBioscience (11-0112-85)	1:200
α-Ly-6G	PE	1A8	BD Biosciences (551461)	1:200
α-Gr1(Ly-6G)	Biotin	RB6-8C5	eBioscience (13-5931-85)	1:400
α-CD80	Biotin	16-10A1	eBioscience (13-0801-82)	1:600
α-CD86	Biotin	GL1	eBioscience (13-0862-82)	1:600
α-CD40	Biotin	1C10	eBioscience (13-0401-82)	1:600
α-ICOS-L	Biotin	HK5.3	eBioscience (13-5985-82)	1:50
α-PD-L1	Biotin	1-111A	eBioscience (13-9971-82)	1:100
α-PD-L2	Biotin	TY25	eBioscience (13-5986-81)	1:100
α-MHCI	Biotin	28-14-8	eBioscience (13-5999-82)	1:100
α-IL-4	PE	11B11	eBioscience (12-7041-81)	1:100
Rat IgG1 Isotype Ctrl	PE	R3-34	BD Biosciences (554685)	1:100
α-IFN-γ	Alexa647	XMG1.2	eBioscience (RM90021)	1:100
α-IL-17	Alexa647	eBio17B7	eBioscience (51-7177-82)	1:100
Rat IgG1 Isotype Ctrl	Alexa647	43414	BD Biosciences (IC005R)	1:100

2.10 *In vivo* models

For the B16 melanoma model, 1 x 10^6 B16-pSMP, B16-RAKD or B16-RCKD cells suspended in 100 µl of supplement-free DMEM were injected subcutaneously into the hind leg of C57BL/6 male mice. Tumor growth was monitored and the volume was measured using an engineer's caliper. Mice were sacrificed at days 8, 12 or 19 and the tumors were collected and weighed. For the 4T1 mammary carcinoma model, 1 x 10^6 of 4T1-pSMP, 4T1-RAKD or 4T1-RCKD cells were injected subcutaneously in the fourth mammary fat pad of female BALB/c mice. The tumor volume was determined at days 6, 12 and 18 post-inoculation. Mice were sacrificed using an overdose of CO_2 and lung metastases were quantified using a colony assay (see section 2.10.2). All tumor volumes were measured by an engineer's caliper and calculated as $V = (W^2 \times L)/2$ (442). Tumor weight was determined after tumor resection on the day of the sacrifice.

2.10.1 Isolation of immune cells from organs of tumor-bearing mice

2.10.1.1 Tumor

At the time points indicated for each experimental model, tumors were resected from mice and weighed. Each tumor was minced in 2.5 ml of HBSS buffer using sharp scissors, then incubated for 20 mins at 37°C with an additional 2.5 ml of HBSS containing collagenase II enzyme (Bioshop, Burlington, ON) (final concentration of 150 µg/ml) to digest connective tissues. The tissue digest was filtered through a 70 µm cell strainer and the cells were washed twice using 5% bovine serum RPMI. Cells were counted and resuspended at a predetermined cellularity for immune profiling by flow cytometry analysis.

2.10.1.2 Lymph node

The inguinal draining lymph node was removed aseptically into 1 ml of HBSS. Lymphocytes were isolated by mashing the lymph node tissue with frosted slides. Cells were suspended in complete RPMI, filtered through a 70 µm cell strainer and counted. Cells were resuspended in a predetermined cellularity for immune profiling by flow cytometry analysis.

2.10.1.3 Blood samples

Blood was collected from the tail (50 µl per mouse) into a 75 µl micro-hematocrit

capillary tube containing 25 µl of 0.1 M EDTA. After collection, samples were diluted in a 1:3 ratio with PBS and centrifuged (300 x g, for 10 mins, at 4°C). The red blood cells within the pellet were lysed by mixing samples with 2 ml of ACK buffer. Following 5-7 mins of incubation, the reaction was stopped using 6 ml of 5% bovine serum RPMI. The cells were then washed with 5% bovine serum RPMI, pelleted (300 x g, for 10 mins, at 4°C), and resuspended in 1 ml of complete RPMI. Total cell number was determined by hemocytometer counting and leukocytes were suspended at a predetermined cellularity for immune profiling by flow cytometry analysis.

2.10.2 Quantification of lung metastases by colony assay

To recover 4T1 tumor cells that metastasized to the lung, a combination of mechanical and enzymatic digestion was performed to release cells from lung connective tissues. Lungs were removed after sacrifice, and swirled in HBSS to remove remaining blood. After mincing with scissors, lungs were digested in 5 ml of HBSS containing 1 mg/ml collagenase IV and 10 units of elastase. The tissue was digested for 75 min at 4°C on a rotating wheel. Lung cells were then filtered through 70 µm cell strainers and washed twice with RPMI containing 10% FBS. Single-cell suspensions were then re-suspended in complete RPMI supplemented with 60 µM 6-thioguanine to select for 4T1 cells that are resistant to this drug. Cells were seeded into 100 mm tissue culture plates and incubated at 37°C for 10-14 days until tumor colonies were visible. The colonies were then fixed with methanol for 5 mins and washed with distilled water. The fixed colonies were stained with 5 ml of 0.03% methylene blue stain and colonies that turned blue were counted. Data were expressed as total number of metastatic colonies per lung.

2.11 Immunohistochemistry (IHC) staining and Image J densitometry

For IHC staining of mouse tumor samples, 5 µm-sections were dewaxed and hydrated through graded ethanol, cooked in 10 mM citrate buffer at pH 6.0 in a pressure cooker/antigen retriever at 125°C for 30 mins (2100-Retriever, Electron Microscopy Sciences), then transferred into water to cool for 10 mins. After 5 mins of treatment in 3% H_2O_2, the slides were blocked with 10% normal goat serum (NGS) for 1 hr. The slides were dried and incubated with the primary antibody overnight at 4°C. The slides were washed three times and then incubated with the secondary antibody for 1 hr. Following

this, the slides were washed and dried, and then incubated with ABC solution (Vector Laboratories, Brockville, Ontario) at RT for 1 hr followed by the addition of DAB solution (Vector Laboratories) for 2 mins. The DAB solution was washed away and slides were counterstained with Mayer's Haematoxylin for 2 mins followed by rinsing with tap water 2–3 times. The slides were then immersed in Scott's solution for 2 mins, dehydrated and mounted with a coverslip.

For IHC staining of human tissue arrays, duplicate slides of a human melanoma tissue array ME481a (48 cases/48 cores), a human breast cancer and adjacent normal tissue array BC081120 (110 cases/110 cores), a human lung disease spectrum tissue array (99 cases/100 cores), and four sets of human colon tissue arrays, specifically COC1021 (102 cases/102 cores), CO952 (30 cases/95 cores), BC05023 (18 cases/54 cores) and T055 (6 cases/24 cores), were purchased from US Biomax Inc. (Rockville, MD USA). Each set of tissue array was immunostained with either polyclonal goat anti-hIL-17RA antibody (Abcam, ab133416) or goat IgG isotype control antibody (Sigma Aldrich) per my established protocol as stated above. Images of each sample at 50x, 100x and 1000x magnifications were captured using LEICA Application Suite (version 2.5.0 R1) on a LEICA DM2500 microscopy with LEICA DFC490 camera. The imaging conditions (e.g., exposure, saturation, gamma, gain, focus and light power, etc.) were optimized and used consistently for all samples for each set of the tissue array. Images captured at 50x magnification were subjected to densitometry analysis using ImageJ software with the minimum threshold (0–255) adjusted for each image to exclude background. The threshold values were used consistently between regions stained with anti-hIL-17RA and isotype control. The percent positive staining area and mean fluorescent intensity for each image were recorded and the value of isotype control sample was subtracted for the calculation.

2.12 Analysis of publicly available datasets

I searched the National Center for Biotechnology Information (NCBI)'s Genome Expression Omnibus (GEO) database for relevant studies published on or before May 31st, 2016. The search terms included "Cancer" and "TNFAIP3". I then set five criteria to manually screen the 564 datasets identified in GEO-NCBI, including: (1) original papers containing independent data which have been published in a peer-reviewed journal, (2) basal level expression of A20 with no pre-treatments, (3) the sample size is above 20, (4)

the Affymetrix Human Genome U133 Plus 2.0 Array was used, which includes all genes of interest, (5) samples are from human patients or cell lines. After applying the five filters, a total of 34 datasets covering approximately 2185 samples from 12 types of solid cancers were identified and downloaded. Similarly, 30 datasets covering around 2083 solid malignancy samples were identified in Oncomine. All data obtained from Oncomine, but not GEO-NCBI, were pre-normalized and converted into Log2 values. Thus, to avoid biases resulting from artificially pooling unnormalized datasets, only the raw data retrieved from Oncomine were used to do the pooled analyses for specific cancer types. To analyze the effect of IL-17RA and A20 expression on prognosis of CRC patients, I downloaded the raw data for mRNA expression, copy number alteration and survival rate of TCGA Colorectal Adenocarcinoma dataset (633 patients) from cBioportal for Cancer Genomics (www.cbioportal.org) (443, 444) and Kaplan-Meier survival curves for CRC patients were generated using GraphPad Prism5 software.

2.13 Statistical analysis

Data were expressed as means ± the standard error of the mean. Statistical analyses were done using GraphPad Prism version 5.0 software program for Windows. Correlations between groups were analyzed by Pearson's and Spearman's correlation coefficient. For normally distributed data, the two-tailed unpaired Student t test was used to determine the significance of the differences between two groups. For comparison of multiple groups, analysis of variance (ANOVA) was performed followed by post-hoc multiple comparisons of means. Dunnett's post-hoc test was used for one-way ANOVA and Bonferroni's post-hoc analysis was used for two-way ANOVA. For data does not have a normal distribution, nonparametric Mann Whitney test was used to determine the significance of the differences between two groups. Nonparametric Kruskal-Wallis test was performed for comparison of multiple groups, followed by Dunn's post-hoc multiple comparisons of means. P values $\leq$ 0.05 were considered statistically significant. The following symbols were used to denote statistical significance: * $P < 0.05$, ** $P < 0.01$, *** $P < 0.001$.

CHAPTER 3 RESULTS

3.1 A novel role for IL-17R in repressing JNK1/JNK2 isoform-dependent tumor cell proliferation via the ubiquitin-editing enzyme A20

Parts of this chapter were included in the article "IL-17RC is critically required to maintain baseline A20 production to repress JNK isoform-dependent tumor-specific proliferation" Oncotarget. 2017;8:43153-68. https://doi.org/10.18632/oncotarget.17820 (445).

3.1.1 IL-17RC silencing in cancer cells directly alters tumor growth in a cell type dependent manner *in vitro* and *in vivo*

To examine the role of IL-17A/IL-17R in controlling cancer cell proliferation, I selected two well-characterized tumor cell lines B16 melanoma and 4T1 mammary carcinoma. IL-17RCKD clones were generated using several retroviral shRNA constructs cloned into the pSMP vector. Notably, all four shRNA constructs used were able to significantly reduce IL-17RC expression at mRNA and protein levels (Figure 6a/b). Representative clones that had >80% IL-17RC reduction and marginal change in IL-17RA expression were selected for further characterization. Compared to the pSMP control cells, the representative RCKD4.5 clone, produced significantly less CXCL1 upon IL-17A and IL-17F stimulation (Figure 6c), demonstrating a functional impairment of the IL-17A/F-induced signal transmission. Of interest, I noticed that B16-RCKD4.5 cells grew significantly slower than B16-pSMP control cells as measured by direct cell counting (Figure 6d) and MTT proliferation assay under normal culture condition and after serum starvation (Figure 6e). Correlation analysis revealed that cell proliferation was significantly and positively correlated with the level of IL-17RC expression in B16-RCKD clones (Figure 6f). When tumor cell clones were subcutaneously inoculated into C57BL/6 mice, the resulting B16-RCKD4.5 tumors were significantly smaller by volume and by weight compared to B16-pSMP tumors (Figure 6g). Together, my data suggest a positive role of IL-17RC in supporting the proliferation of B16 melanoma cells *in vitro* and *in vivo*.

Figure 6. Specific knockdown of IL-17RC expression in B16 melanoma cells attenuates tumor growth *in vitro* and *in vivo*.

B16 cells were transduced with retroviral vectors containing shRNAs against IL-17RC or scrambled sequences. IL-17RC expression by different B16 knockdown sub-clones was determined by qPCR, PCR (a) and flow cytometry (b). The threshold of gene expression for selecting the best knockdown is shown as a red line. (c) CXCL1 production upon IL-17A and IL-17F stimulation was assessed in culture supernatants by ELISA. Cell growth was measured by (d) direct cell counting and (e) MTT assay with or without serum starvation. (f) Proliferation of different KD strains was correlated with IL-17RC expression using Pearson and Spearman correlation analysis. (g) Weight and volume of B16-IL-17RCKD and B16-pSMP control tumors were determined in C57BL/6 mice after inoculation with 1 x 10^6 cells. All values are means ± SEM of 3 independent experiments for *in vitro* studies (a-f), or means ± SEM of n = 5-15 mice per group at each time point for *in vivo* studies (g). Statistical analyses were compared with the pSMP control; *$p < 0.05$; **$p < 0.01$; ***$p < 0.001$.

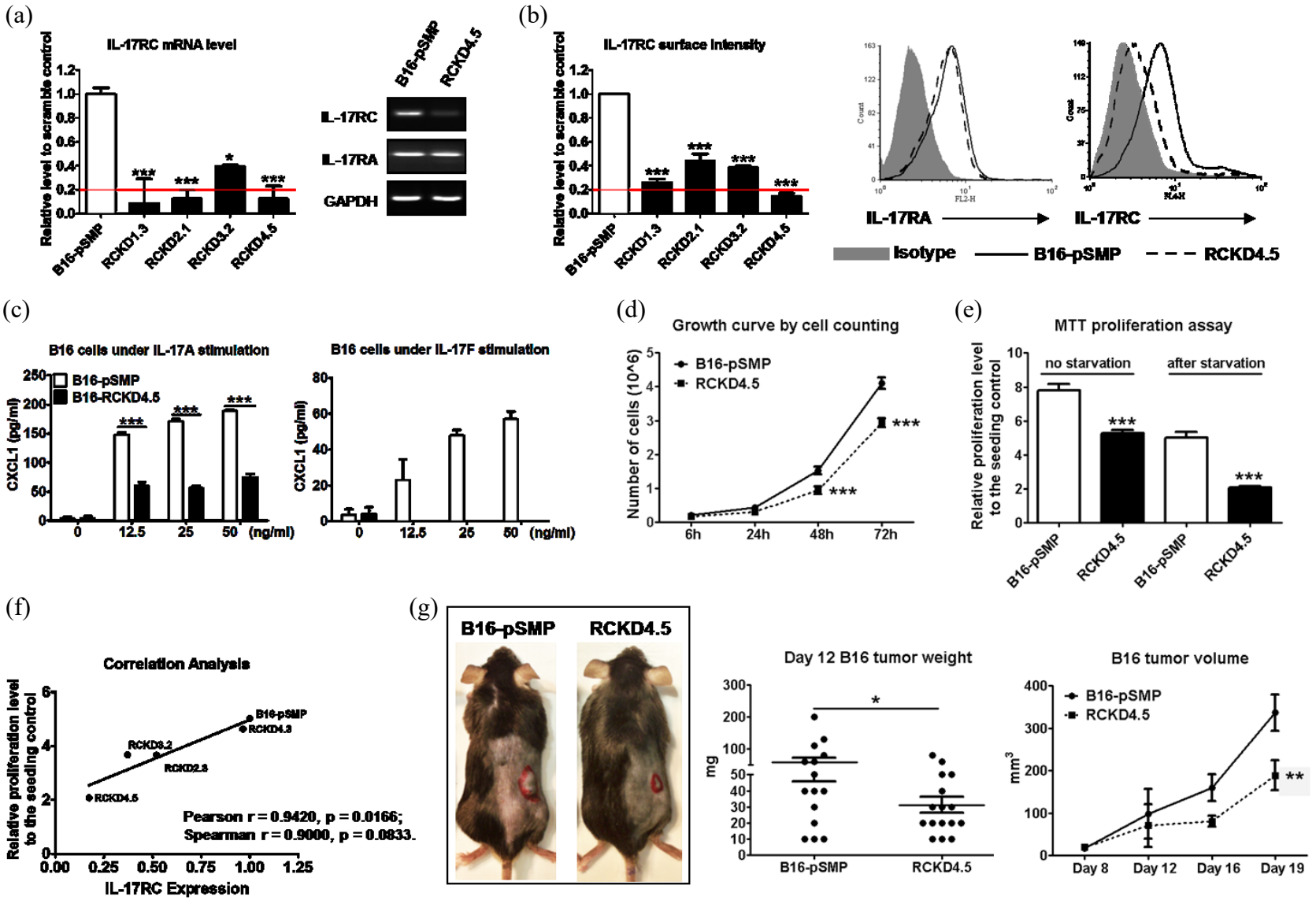
(a)
IL-17RC mRNA level
Relative level to scramble control
B16-pSMP
RCKD1.3
RCKD2.1
RCKD3.2
RCKD4.5
IL-17RC
IL-17RA
GAPDH
(b)
IL-17RC surface intensity
IL-17RA
IL-17RC
Isotype
B16-pSMP
RCKD4.5
(c)
B16 cells under IL-17A stimulation
B16-pSMP
B16-RCKD4.5
CXCL1 (pg/ml)
(ng/ml)
B16 cells under IL-17F stimulation
(d)
Growth curve by cell counting
Number of cells (10^6)
6h
24h
48h
72h
(e)
MTT proliferation assay
no starvation
after starvation
Relative proliferation level to the seeding control
(f)
Correlation Analysis
Relative proliferation level to the seeding control
IL-17RC Expression
Pearson r = 0.9420, p = 0.0166;
Spearman r = 0.9000, p = 0.0833.
(g)
Day 12 B16 tumor weight
mg
B16 tumor volume
mm3
Day 8
Day 12
Day 16
Day 19

Figure 6.

RCKD clones with reduced IL-17RC at mRNA and protein levels were also generated using 4T1 cells (Figure 7a-c). Surprisingly, the loss of IL-17RC expression in 4T1 cells directly promoted tumor cell growth in culture. As shown in Figure 7d, the representative 4T1-RCKD4.8 clone displayed a 1.5- to 2-fold increase in proliferation rate *in vitro* compared to the 4T1-pSMP control. Furthermore, primary 4T1-RCKD tumors grown in BALB/c mice were approximately 2.5-fold larger than 4T1-pSMP tumors at day 18 post-inoculation (Figure 7e), and generated significantly more lung metastases (Figure 7f). Therefore, in sharp contrast to its role in B16 melanoma, IL-17RC is a negative regulator of 4T1 homeostatic proliferation and invasiveness *in vitro* and *in vivo*.

To investigate whether IL-17RC-controlled tumor growth was associated with altered apoptosis, flow cytometric analyses were conducted to measure the rates of serum starvation induced apoptosis in RCKD clones and pSMP controls. Notably, RCKD reduced the frequency of annexin V-positive B16 cells, but markedly increased the apoptosis of 4T1 cells (Figure 8a). I also measured caspase-3 activity via western blotting to verify the results (Figure 8b). Consistent with the flow cytometric analyses of annexin V staining, the levels of total and cleaved caspase-3 were reduced in B16-RCKD cells compared to B16-pSMP controls; in sharp contrast, the amount of cleaved caspase-3 was dramatically increased in 4T1-RCKD cells; however, the total caspase-3 level was comparable among 4T1-RCKD cells and 4T1-pSMP control cells. Similar to the *in vitro* observations, the level of cleaved caspase-3 was significantly increased in 4T1-RCKD tumor sections compared to their pSMP counterparts (Figure 8c). Therefore, my data suggest that IL-17RC has divergent roles in controlling homeostatic proliferation and stress-induced apoptosis in different tumor types. Notably, despite its impact on stress-induced apoptosis, IL-17RC-controlled homeostatic proliferation appears to ultimately dictate the invasiveness of the tumor cells *in vitro* and *in vivo*.

Figure 7. Specific knockdown of IL-17RC expression in 4T1 cells promotes tumor proliferation and tumor invasiveness *in vitro* and *in vivo*.

4T1 cells were transduced with retroviral vectors containing shRNAs against IL-17RC or scrambled sequences. (a-b) IL-17RA and RC mRNA and surface protein expression from a representative IL-17RCKD clone (RCKD4.8) and pSMP control of 4T1 cells were examined by RT-PCR and flow cytometry. The threshold of gene expression for selecting the knockdown clones is shown as a red line. (c) CXCL1 production upon IL-17A stimulation was determined by ELISA. (d) Cell growth was measured by direct cell counting and MTT assay with serum starvation treatment. (e,f) Tumor volume, weight and lung metastasis of 4T1-IL-17RCKD and 4T1-pSMP control tumors in BALB/c mice. All values are presented as the mean ± SEM of 3-5 independent experiments for *in vitro* studies (a-d), or the mean ± SEM of 5-10 mice per group at each time point for *in vivo* studies (e, f). *$p \leq 0.05$; **$p \leq 0.01$; ***$p \leq 0.001$; statistical analysis was compared with the pSMP control.

Figure 7.

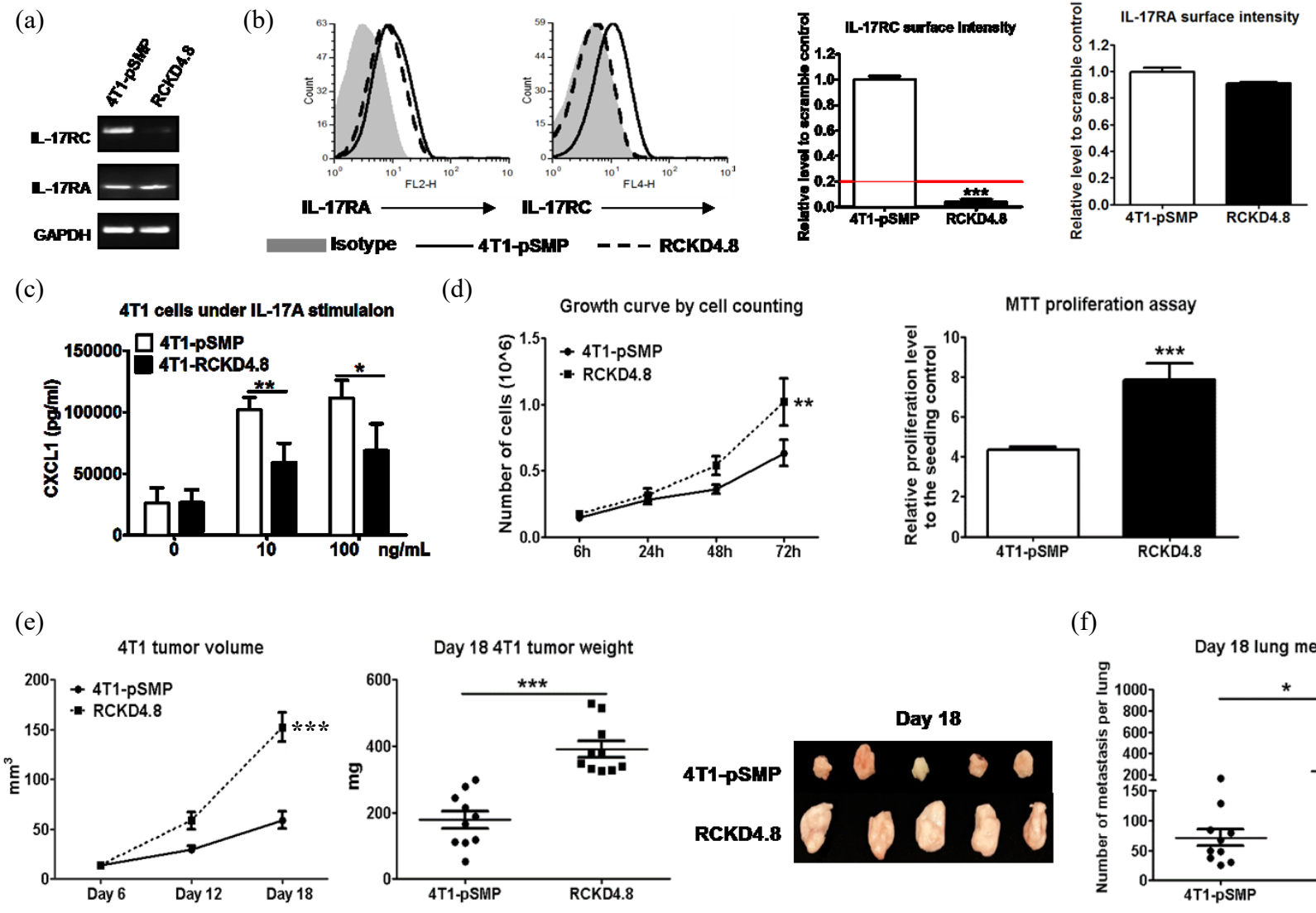
(a)
4T1-pSMP
RCKD4.8
IL-17RC
IL-17RA
GAPDH
(b)
Count
FL2-H
FL4-H
IL-17RA
IL-17RC
Isotype
4T1-pSMP
RCKD4.8
IL-17RC surface intensity
Relative level to scramble control
***
4T1-pSMP
RCKD4.8
IL-17RA surface intensity
Relative level to scramble control
4T1-pSMP
RCKD4.8
(c)
4T1 cells under IL-17A stimulaion
4T1-pSMP
4T1-RCKD4.8
CXCL1 (pg/ml)
**
*
0
10
100
ng/mL
(d)
Growth curve by cell counting
4T1-pSMP
RCKD4.8
Number of cells (10^6)
**
6h
24h
48h
72h
MTT proliferation assay
Relative proliferation level to the seeding control
***
4T1-pSMP
RCKD4.8
(e)
4T1 tumor volume
4T1-pSMP
RCKD4.8
mm3
***
Day 6
Day 12
Day 18
Day 18 4T1 tumor weight
mg
***
4T1-pSMP
RCKD4.8
Day 18
4T1-pSMP
RCKD4.8
(f)
Day 18 lung metastasis
Number of metastasis per lung
*
4T1-pSMP
RCKD4.8

Figure 8. IL-17RC silencing alters tumor cell apoptosis *in vitro* and *in vivo* in a tumor-dependent manner.

(a) Quantified results of Annexin V^+ cell percentage in B16 and 4T1 culture after serum starvation for 14 hrs and recovery in CM for 1 hr. (b) RCKD and pSMP control subclones of B16 and 4T1 cells were serum starved for 14 hrs and recovered in CM for different periods of time as indicated. Whole-cell extracts were harvested and immunoblotted with the indicated antibodies to detect pro- and cleaved-caspase-3. GAPDH was used as a loading control. (c) Representative images and quantitative assessment of cleaved-caspase-3 protein level observed in day 18 4T1 tumors by immunohistochemistry. Values are means ± SEM of 4-6 replicates in two independent experiments (a,c). Statistical analyses were compared with the pSMP control; *$p < 0.05$; **$p < 0.01$; ***$p < 0.001$.

Figure 8.

(a)

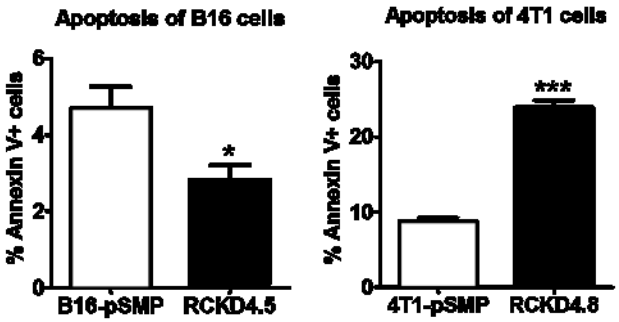
Apoptosis of B16 cells
% Annexin V+ cells
6
4
2
0
*
B16-pSMP
RCKD4.5
Apoptosis of 4T1 cells
% Annexin V+ cells
30
20
10
0
***
4T1-pSMP
RCKD4.8

(b)

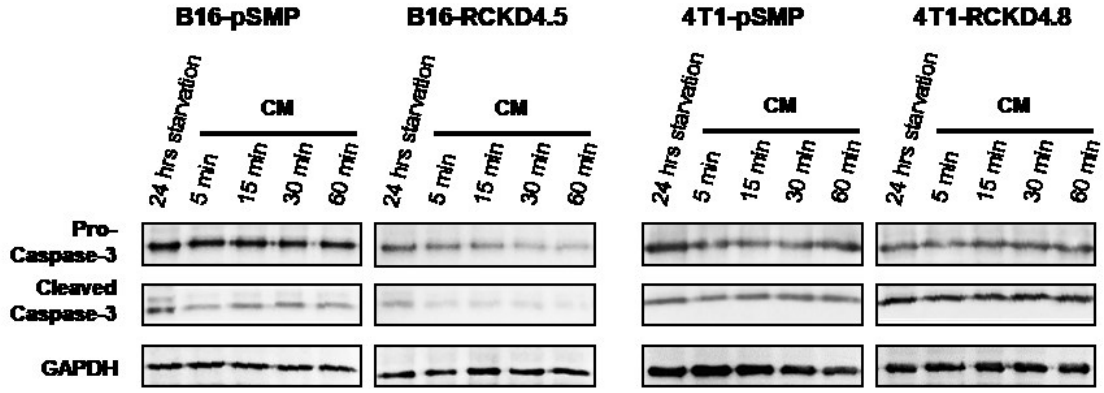
B16-pSMP
B16-RCKD4.5
4T1-pSMP
4T1-RCKD4.8
24 hrs starvation
CM
5 min
15 min
30 min
60 min
Pro-Caspase-3
Cleaved Caspase-3
GAPDH

(c)

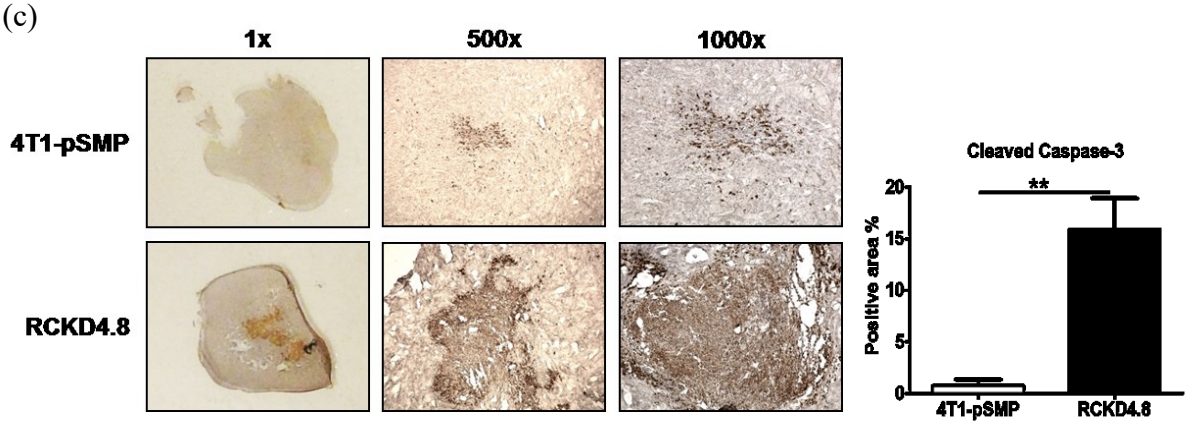
1x
500x
1000x
4T1-pSMP
RCKD4.8
Cleaved Caspase-3
**
Positive area %
20
15
10
5
0
4T1-pSMP
RCKD4.8

3.1.2 IL-17RC silencing induces acquired-activation of distinct JNK isoforms in different tumor cells, which differentially regulates c-Jun-dependent homeostatic proliferation

To identify the specific signaling pathway(s) responsible for the altered homeostatic proliferation of B16 and 4T1 RCKD clones, well-characterized pharmacologic inhibitors were used to block NF-κB, PI3K-AKT and MAPK pathways in cell culture. Notably, the homeostatic proliferation of IL-17RCKD clones and pSMP controls of both B16 and 4T1 cells was significantly inhibited by KIN001-102 and BMS-34554 (Figure 9a/b), specific inhibitors for AKT and IKK, respectively, suggesting that AKT and NF-κB pathways provide survival signals for both B16 and 4T1 cells under steady-state conditions. However, B16 and 4T1 clones exhibited similar sensitivities to AKT and IKK inhibitors, indicating that IL-17RC-controlled cell proliferation is not mediated by AKT or NF-κB signals. Of interest, 4T1 and B16 clones displayed distinct sensitivities to inhibitors targeting the JNK/c-Jun pathway (Figure 9c/d), while they responded to the ERK and p38 inhibitors similarly (APPENDIX A). Specifically, L-form JNK inhibitor was able to inhibit proliferation of B16-pSMP cells, but not 4T1-pSMP cells; however, IL-17RC silencing resulted in reduced sensitivities to L-form JNK inhibitor in B16-RCKD cells, but markedly enhanced sensitivity of 4T1-RCKD cells (Figure 9c). Furthermore, the 4T1-RCKD clone was sensitive to the SP600125 JNK/c-Jun inhibitor, which exhibited no activity against 4T1-pSMP cells, but similar inhibition in B16-pSMP and B16-RCKD clones (Figure 9d). This highlights a role for IL-17RC in suppressing homeostatic JNK/c-Jun activation in 4T1 but not B16 cells.

To verify this finding, I examined total JNK/c-Jun and phospho-JNK/cJun levels by western blotting. As demonstrated in Figure 9e-h, phospho-JNK and phospho-c-Jun, as well as total JNK and c-Jun levels, were markedly increased in 4T1-RCKD cells compared to 4T1-pSMP control cells. Surprisingly, JNK phosphorylation, but not total protein level, was significantly increased in B16-RCKD cells. However, phospho-c-Jun and total c-Jun levels were significantly reduced in B16-RCKD clones compared to B16-pSMP clones (Figure 9g-h). In agreement with differential activation patterns of c-Jun in the two cell lines, the expression of cyclin D1, one of the c-Jun target genes, was also markedly reduced in B16-RCKD clone, but evidently increased in 4T1-RCKD cells, compared to their corresponding pSMP controls (Figure 9g). Collectively, my data demonstrate that IL-17RC

silencing results in acquired JNK-activities in B16 and 4T1 cells but distinct c-Jun activities, at both production/stability and functional activity levels, in the two tumor cell lines.

Given that the IL-17RC silencing induced consistent JNK-activation with distinct c-Jun activities and inverse proliferation patterns in the two tumor models, I questioned whether IL-17RC silencing induced activation of different JNK isoforms in B16 and 4T1 cell lines. Indeed, IL-17RC silencing in B16 cells significantly increased mRNA and protein levels of JNK2 (Figure 10a-c). Conversely, IL-17RC silencing in 4T1 cells induced marked upregulation of JNK1 (Figure 10a-c). To further verify whether the distinct c-Jun activities and proliferation profiles observed in RCKD clones of B16 and 4T1 cells were due to differential expression/activation of JNK1 and JNK2 isoforms, I used another retroviral vector pGIPz to deliver shRNAs targeting endogenous *Jnk1* or *Jnk2* in B16-RCKD and 4T1-RCKD cells (Figure 10d/e). While both JNK1 and JNK2 shRNAs displayed specific targeting effects in both B16-RCKD and 4T1-RCKD clones (Figure 10d/e), the JNK1 shRNA increased *Jnk2* mRNA and JNK2 protein in 4T1 cells (Figure 10d/e), indicating a potential role of JNK1 in repressing JNK2 expression under steady-state conditions. Importantly, the level of phospho-JNK in B16-RCKD and 4T1-RCKD clones was markedly attenuated by JNK2 and JNK1 shRNA, respectively (Figure 10e), reinforcing the notion that IL-17RC silencing induces differential acquired-activation of distinct JNK isoforms in the two tumor cell lines. Despite differential expression/activation of JNK isoforms in B16 and 4T1 cells, JNK1 shRNA was able to completely remove total and phospho-c-Jun signals, demonstrating a critical role of JNK1 in maintaining baseline c-Jun activities. Conversely, JNK2 shRNA enhanced total and phospho-c-Jun (S73) levels in B16-RCKD and, possibly, 4T1-RCKD cells, indicating a potential role of JNK2 in suppressing baseline c-Jun activities (Figure 10e). Importantly, JNK1 silencing consistently attenuated the proliferation of both B16-RCKD and 4T1-RCKD cells, whereas JNK2 silencing increased the proliferation of both cell lines (Figure 10f). Notably, the apoptosis rates were not significantly affected by JNK1/JNK2 silencing in both cell lines (Figure 10g). Taken together, my data suggest that IL-17RC silencing induces tumor-specific expression and activation of JNK1 and JNK2 isoforms, which have opposing roles in controlling downstream c-Jun activity and c-Jun-dependent homeostatic proliferation.

Figure 9. IL-17RC silencing results in acquired-JNK activation but distinct c-Jun activities in B16 and 4T1 cells.

(a-d) IL-17RCKD and pSMP clones of B16 melanoma and 4T1 mammary cancer cells were treated with DMSO or one of the inhibitors indicated for 48 hrs. Cell proliferation was then measured by MTT assay. *$p \leq 0.05$; **$p \leq 0.01$; ***$p \leq 0.001$; statistical analysis was compared with the DMSO control. ##$p \leq 0.01$; ###$p \leq 0.001$; statistical analysis was compared with the pSMP control line. All values are means ± SEM of 4-6 replicates in two independent experiments. (e-h) Whole-cell extracts were harvested and immunoblotted to detect total or phosphorylated proteins as indicated. GAPDH was used as a loading control. Scanning densitometry of relative phospho (p)-JNK, total JNK, p-cJun and total cJun protein levels at 30 mins post CM recovery were performed.

(a)

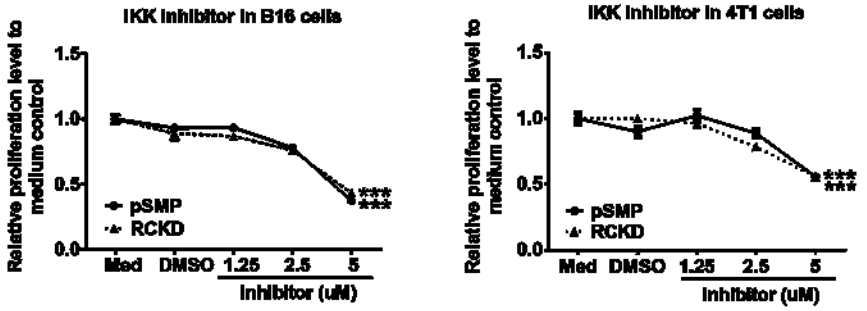

(b)

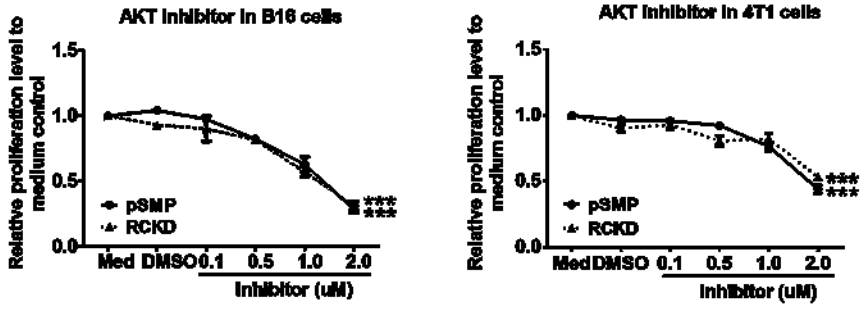

(c)

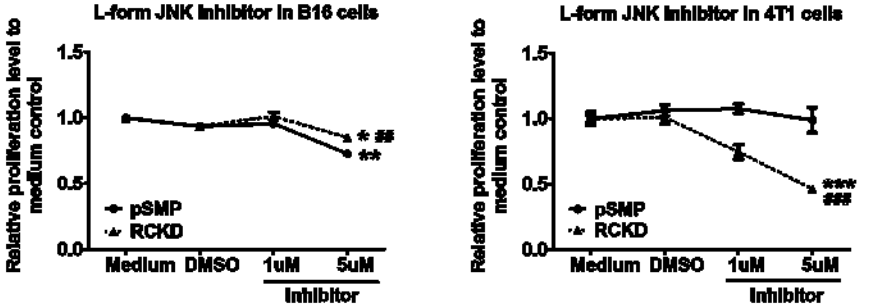

Figure 9. Continued.

(d)

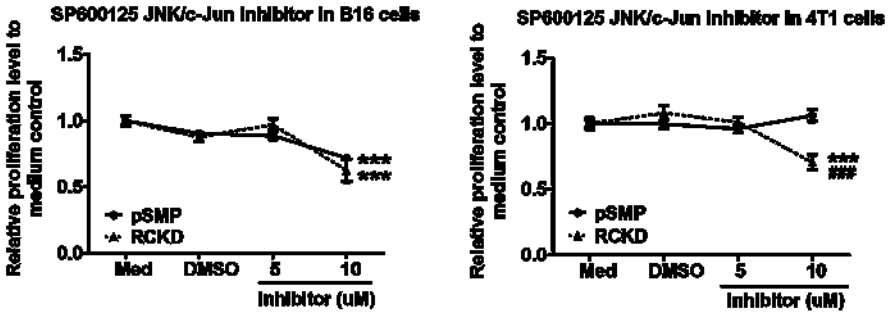

(e)

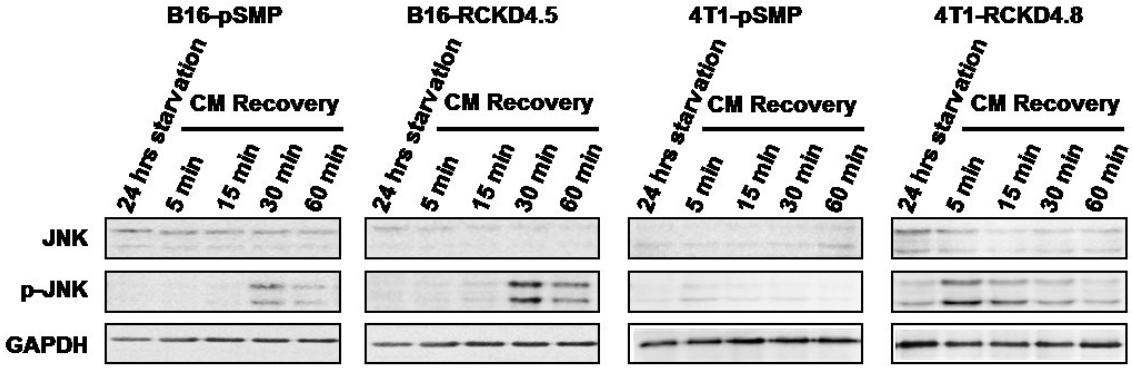

(f)

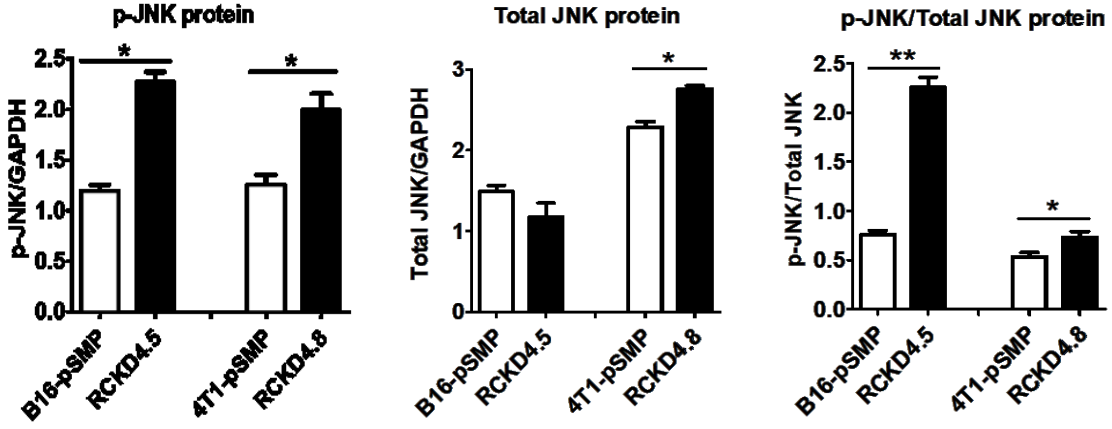

Figure 9. Continued.

(g)

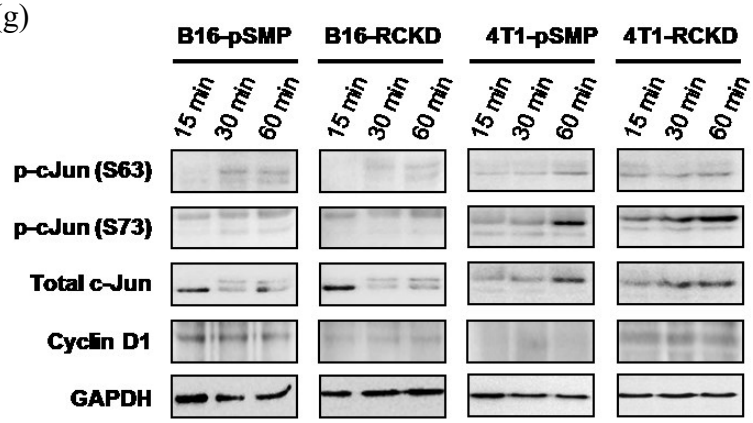

(h)

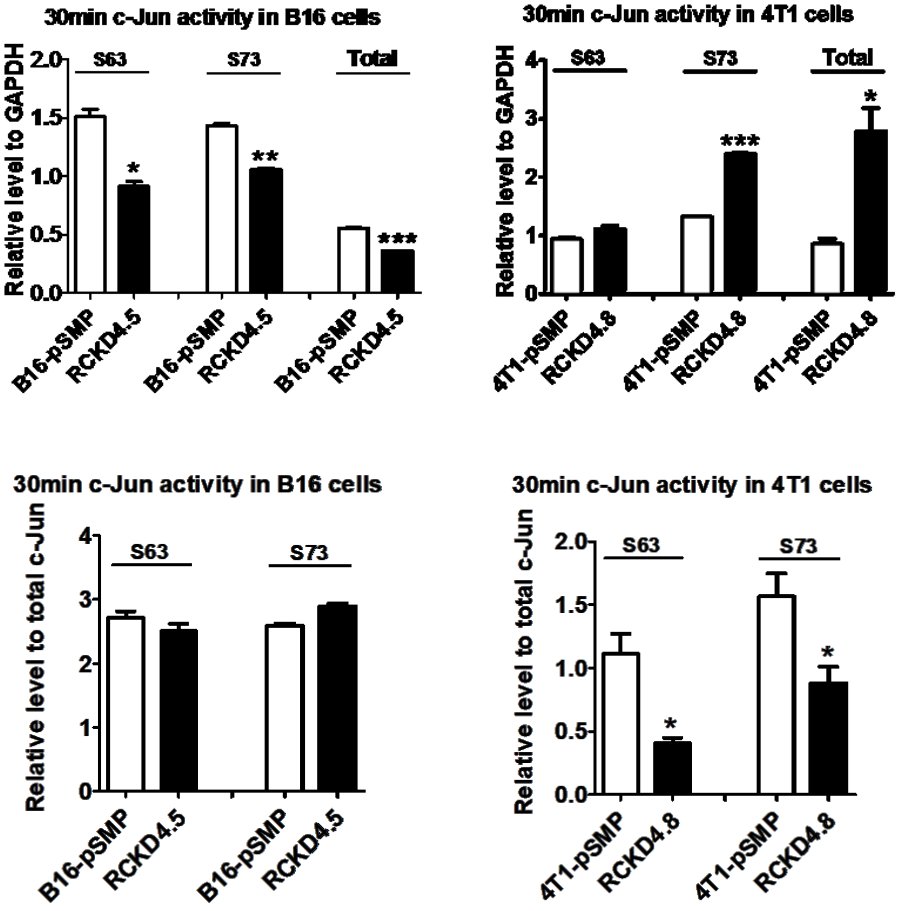

Figure 10. IL-17RC silencing induces acquired activation of different JNK isoforms in different tumor cells, which differentially regulate c-Jun activities and homeostatic cell proliferation.

(a) JNK1 and JNK2 mRNA levels were determined by qRT-PCR in pSMP and RCKD subclones of B16 and 4T1 tumor cells. (b) Whole-cell extracts were harvested and immunoblotted to detect total JNK1 and JNK2 protein. GAPDH was used as a loading control. (c) Scanning densitometry of relative JNK1 and JNK2 protein levels at 30 mins post CM recovery were performed. (d-g) RCKD subclones of B16 and 4T1 cells were transiently transfected with JNK1 and JNK2 shRNA. (d) JNK1 and JNK2 mRNA levels were determined by qRT-PCR 3 days after transfection. (e) Day 3 transfected cells were serum starved for 14 hrs and rescued with CM for 1 hr. Whole-cell extracts were harvested and immunoblotted to detect total or phosphorylated proteins. GAPDH was used as a loading control. (f) Day 3 transfected cells were seeded and cultured for an additional 3 days. Cells were then collected for flow cytometric analysis of their proliferation rate. For each sample, 20,000 events were collected and the time of collection was recorded. PI was used to exclude the dead cells. The PI^- live cell count for each sample was divided by the respective time of collection to quantify the cell proliferation rate. (g) Quantified results of Annexin V^+ cell frequency in B16 and 4T1 cultures. Values are means ± SEM of 4-6 replicates in two independent experiments. Statistical analyses were compared with the vector control cells; *$p < 0.05$; **$p < 0.01$; ***$p < 0.001$.

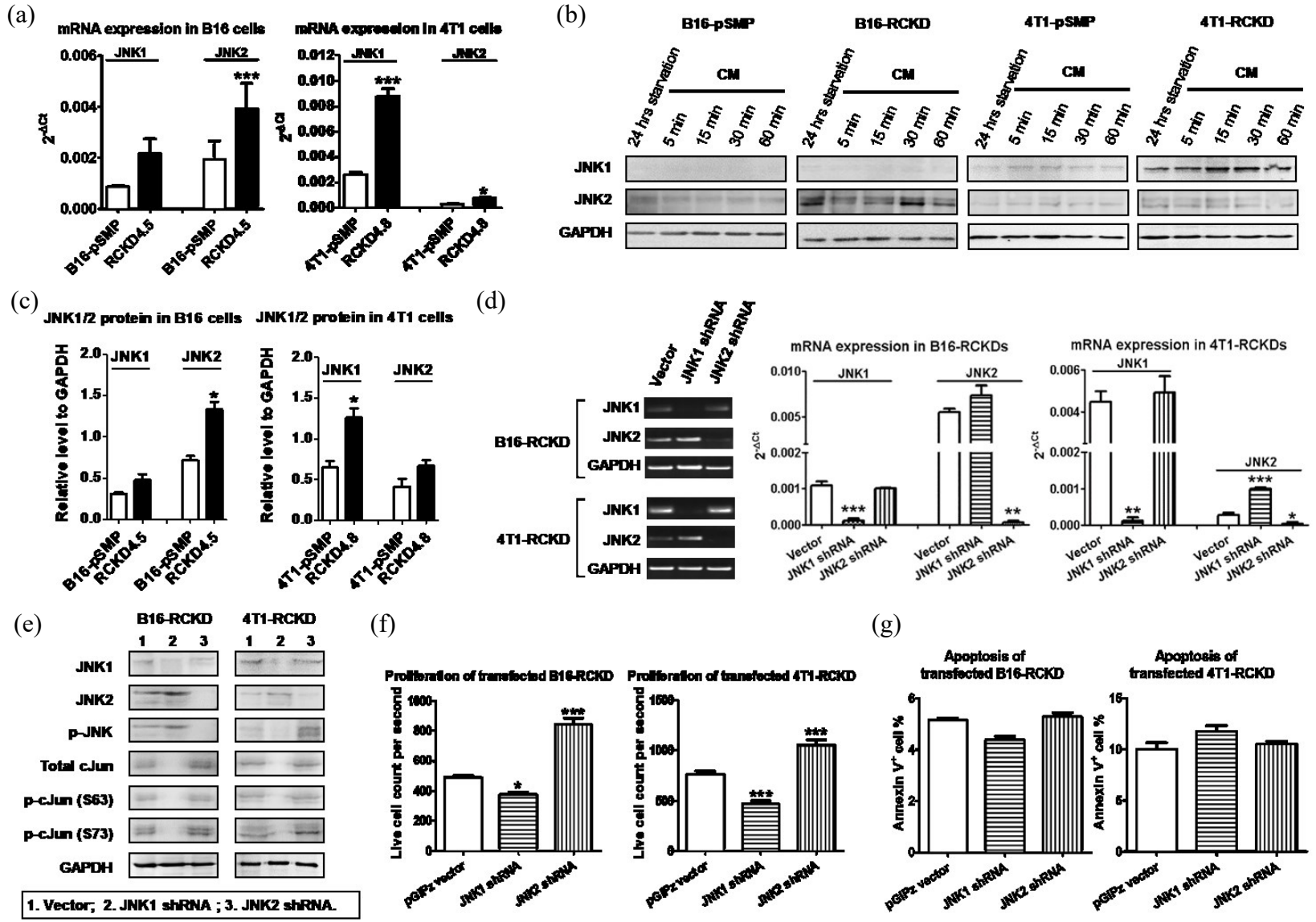
(a)
mRNA expression in B16 cells
mRNA expression in 4T1 cells
JNK1
JNK2
B16-pSMP
RCKD4.5
4T1-pSMP
RCKD4.8
(b)
B16-pSMP
B16-RCKD
4T1-pSMP
4T1-RCKD
24 hrs starvation
CM
5 min
15 min
30 min
60 min
JNK1
JNK2
GAPDH
(c)
JNK1/2 protein in B16 cells
JNK1/2 protein in 4T1 cells
Relative level to GAPDH
(d)
Vector
JNK1 shRNA
JNK2 shRNA
B16-RCKD
4T1-RCKD
mRNA expression in B16-RCKDs
mRNA expression in 4T1-RCKDs
(e)
1 2 3
p-JNK
Total cJun
p-cJun (S63)
p-cJun (S73)
1. Vector; 2. JNK1 shRNA ; 3. JNK2 shRNA.
(f)
Proliferation of transfected B16-RCKD
Proliferation of transfected 4T1-RCKD
Live cell count per second
pGIPz vector
(g)
Apoptosis of transfected B16-RCKD
Apoptosis of transfected 4T1-RCKD
Annexin V+ cell %

Figure 10.

3.1.3 IL-17RC is required for maintaining basal A20 level that restrains homeostatic activation of JNK and NF-κB pathways

Having demonstrated a role for IL-17RC in restraining activation of JNKs in both B16 and 4T1 tumors, I questioned whether this observation was due to the loss of a critical negative control. By comparing the published information regarding baseline versus IL-17-induced signaling, I found that most of the negative regulators require ligand binding to actively interfere with IL-17A signaling. While several of these inhibitors are IL-17A-dependent transcripts, A20 seems to be the only IL-17A-dependent autocrine regulator identified under homeostatic conditions, which forms an intrinsic negative feedback loop to block IL-17A signaling (409) (Figure 5). Given the critical role of A20 in negatively regulating multiple pathways, I examined A20 expression in RCKD and pSMP clones of B16 and 4T1 cells. As demonstrated in Fig. 11, A20 mRNA levels in RCKD clones of both B16 and 4T1 tumors were consistently reduced by four different IL-17RC-targeting shRNA constructs (Figure 11a). Notably, the basal level of A20 in B16-pSMP cells was significantly lower than that in 4T1-pSMP cells. In agreement with the mRNA profile, A20 protein levels were also consistently reduced in RCKD clones compared to pSMP cells under regular CM conditions or after 24 hrs of serum starvation (Figure 11b), highlighting a critical role of IL-17RC in maintaining basal production of A20. In accordance with a role of A20 in negatively regulating the NF-κB pathway (413), NF-κB activity, as measured by the phospho-IκB-α level and EMSA assays, demonstrated that the nuclear translocation of NF-κB was markedly and persistently elevated in RCKD clones compared to pSMP counterparts (Figure 11b/c).

To further verify that IL-17RC-controlled A20 was responsible for acquired-JNK activation in RCKD clones, I transfected RCKD clones with a plasmid carrying full length A20 or the empty plasmid vector and examined the intracellular signaling molecule profile by western blot. While the A20 plasmid effectively restored A20 levels in RCKD clones, A20 reconstitution also reduced the level of phopho-IκBα, total and phospho-JNK1 and JNK2 at 72 hrs post-transfection in both B16-RCKD and 4T1-RCKD cells (Figure 11d/e), confirming that acquired homeostatic activation of both NF-κB and JNK pathways in RCKD clones was due to reduced A20 production. Since the ZnF4-5 domain of A20 is critical for K48-mediated ASK1 degradation that inhibits TNF-induced JNK-c-Jun

activation (423), I used a ΔZnF4-5 mutant (~65kDa) plasmid to determine whether A20 may also utilize this mechanism in controlling homeostatic JNK activation. Notably, the ΔZnF4-5 mutant exhibited clear functional impairment in reducing JNK phosphorylation compared to WT A20 counterparts in both B16-RCKD and 4T1-RCKD clones, suggesting that A20 inhibits homeostatic JNK activation mainly through the ZnF4-5 domain. In comparison, the ΔZnF4-5 mutant exhibited less consistent functional alterations in controlling homeostatic NF-κB activity compared to WT A20 (Figure 11d).

3.1.4 The IL-17RC-A20 axis is required to selectively repress cytokine production downstream of NF-κB and JNK/c-Jun pathways

Having demonstrated that NF-κB and JNK pathways are up-regulated in RCKD cells, I hypothesized that, in addition to controlling homeostatic proliferation, the IL-17RC-A20 axis may also control secretion of pro-inflammatory cytokines downstream of NF-κB and JNK pathways under steady state conditions and upon cytokine stimulation. To this end, I cultured 4T1-pSMP control and 4T1-RCKD cells in the presence or absence of recombinant IL-17A and measured the levels of GM-CSF and IL-6 in the culture supernatants as representative cytokines downstream of NF-κB and JNK pathways. Given an impaired CXCL1 production by RCKD cells upon IL-17A stimulation observed in my initial characterization experiments (Figure 7c), I also measured CXCL1 as a control. Notably, the levels of IL-6 and GM-CSF, but not CXCL1, showed a clear trend toward enhanced basal production in 4T1-RCKD cells compared to the pSMP control cells. Despite a very low level of IL-17RC expression on the surface of RCKD cells, 4T1-RCKD cells actually produced significantly more IL-6 and GM-CSF, but not CXCL1, upon IL-17A stimulation (Figure 12a). A similar experiment was conducted using mouse embryonic fibroblasts (MEFs) isolated from C57BL/6 mice and A20-knockout (A20KO) mice. As shown in Figure 12b, A20KO MEFs produced significantly more IL-6 and a trend toward higher GM-CSF compared to WT counterparts. In comparison, a marked reduction of CXCL1 was observed in A20KO MEFs under steady-state condition while they produced similar amounts upon IL-17A stimulation. Collectively, my data suggests that, in addition to controlling tumor-specific proliferation, the IL-17RC-A20 axis has a regulatory role in selectively repressing production of pro-inflammatory cytokines including IL-6 and GM-CSF, but not CXCL1.

Figure 11. IL-17RC is required to maintain basal production of A20 and repress homeostatic activities of JNK1 and JNK2.

(a) A20 mRNA level determined by qRT-PCR in pSMP and RCKD subclones of B16 and 4T1 tumor cells. (b) Whole-cell extracts were harvested and immunoblotted to detect total or phosphorylated proteins as indicated. GAPDH was used as a loading control. (c) Nuclear proteins were extracted from RCKD and pSMP cells of B16 and 4T1 cells and subjected to EMSA using ^{32}P-labeled NF-κB DNA probes. (d) RCKD cells were transfected with plasmid vector, plasmids expressing A20 or A20 with a mutant ΔZnF4-5 domain. After 72 hrs, whole-cell extracts were harvested and immunoblotted to detect phosphorylated or total proteins as indicated. GAPDH was used as the loading control. (e) Scanning densitometry of relative protein levels was performed. Values are means ± SEM of at least two independent experiments. Statistical analyses were compared with the respective vector control cells (white bar). *$p < 0.05$; **$p < 0.01$; ***$p < 0.001$.

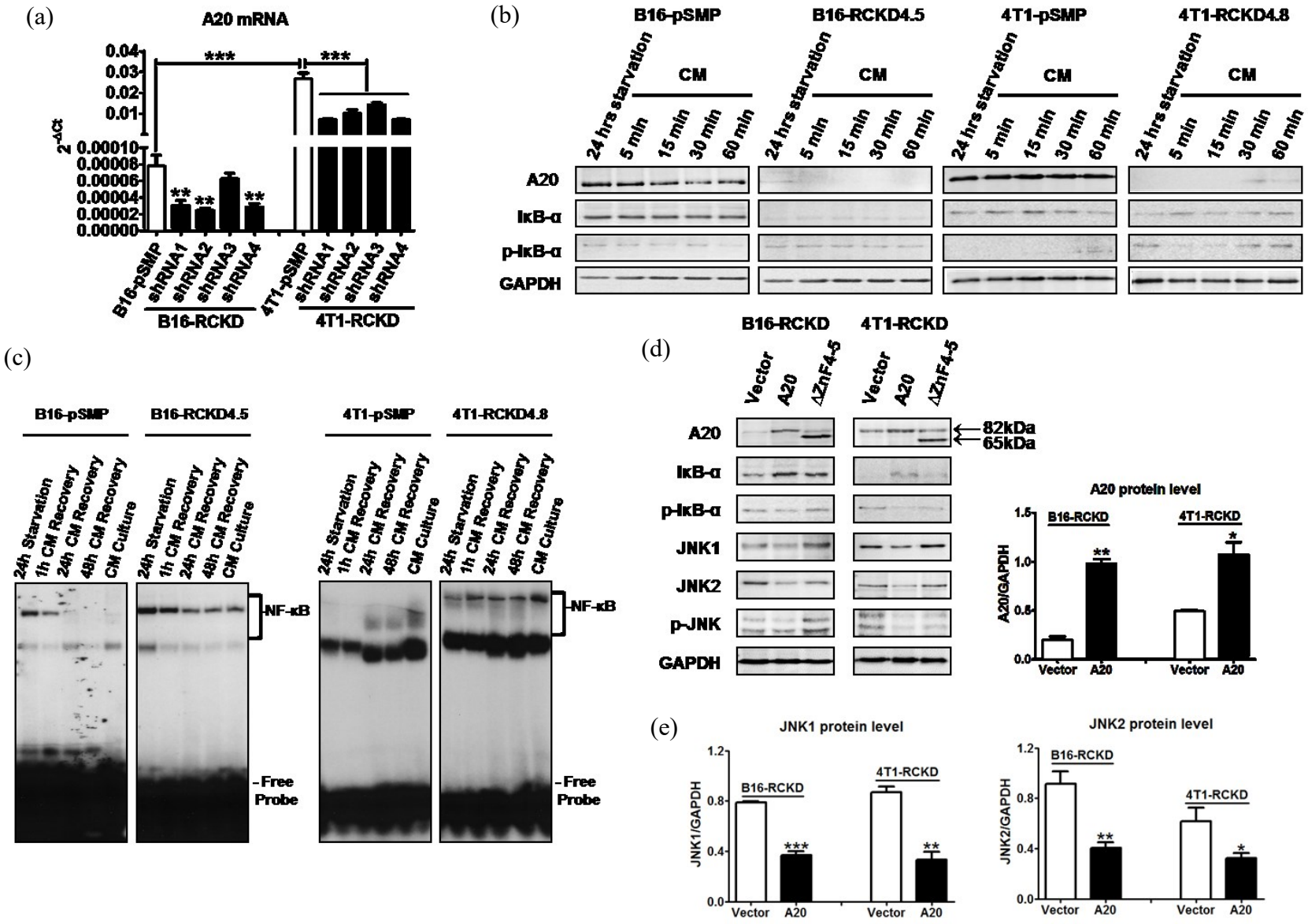
(a)
A20 mRNA
0.04
0.03
0.02
0.01
0.00010
0.00008
0.00006
0.00004
0.00002
0.00000
***
***
**
**
**
B16-pSMP
shRNA1
shRNA2
shRNA3
shRNA4
4T1-pSMP
shRNA1
shRNA2
shRNA3
shRNA4
B16-RCKD
4T1-RCKD
(b)
B16-pSMP
B16-RCKD4.5
4T1-pSMP
4T1-RCKD4.8
24 hrs starvation
CM
5 min
15 min
30 min
60 min
A20
IκB-α
p-IκB-α
GAPDH
(c)
B16-pSMP
B16-RCKD4.5
4T1-pSMP
4T1-RCKD4.8
24h Starvation
1h CM Recovery
24h CM Recovery
48h CM Recovery
CM Culture
NF-κB
Free Probe
(d)
B16-RCKD
4T1-RCKD
Vector
A20
ΔZnF4-5
A20
IκB-α
p-IκB-α
JNK1
JNK2
p-JNK
GAPDH
82kDa
65kDa
A20 protein level
A20/GAPDH
1.5
1.0
0.5
0.0
B16-RCKD
4T1-RCKD
**
*
Vector
A20
(e)
JNK1 protein level
JNK1/GAPDH
1.2
0.8
0.4
0.0
***
**
JNK2 protein level
JNK2/GAPDH
**
*

Figure 11.

(a)

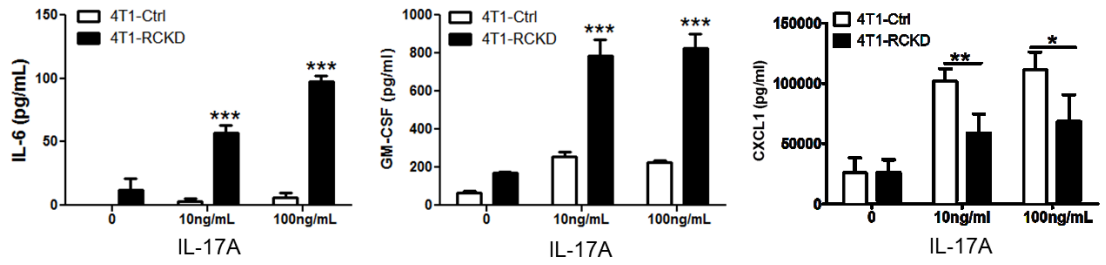

(b)

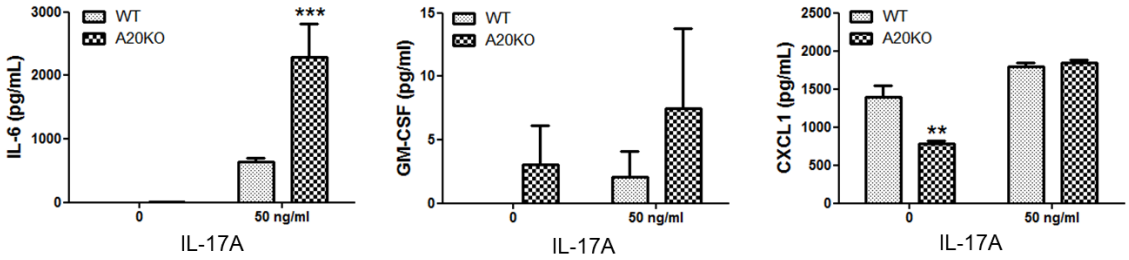

Figure 12. The IL-17RC-A20 axis selectively represses cytokine production downstream of NF-κB and JNK/c-Jun pathways.

(a) IL-17RCKD and scramble control 4T1 cell lines were cultured or stimulated with recombinant IL-17A as indicated. Cytokine ELISAs were performed using the day-three culture supernatants. (b) WT and A20KO MEFs were stimulated with or without 50 ng/ml recombinant IL-17A. Cytokine ELISAs were performed using the day-three culture supernatant. Values are means ± SEM of 3-5 replicates in at least two independent experiments. Statistical analyses were compared with the pSMP vector control in panel a, or WT cells in panel b. **p < 0.01; ***p < 0.001.

3.1.5 IL-17RA silencing in B16 melanoma and 4T1 mammary carcinoma cells enhances tumor cell growth *in vitro* and *in vivo*

Since both IL-17RC and IL-17RA are obligate receptors for IL-17A signaling, I created IL-17RAKD clones of B16 melanoma cells to examine the role of IL-17RA in controlling cancer cell behavior. Using 4 retroviral shRNA constructs, a total of 38 single clones were selected, expanded and characterized for IL-17RA/RC levels by RT-PCR and flow cytometry. A representative clone B16-RAKD3.1, which exhibited a 90% reduction in IL-17RA and no change in IL-17RC expression was selected (Figure 13a/b). As expected (292, 293), IL-17A and IL-17F stimulation induced significantly less CXCL1 production from B16-RAKD3.1 cells compared to the B16-pSMP control, demonstrating a functional impairment in IL-17A/F-induced signal transmission (Figure 13c). In contrast to B16-RCKD cells, B16-RAKD clones exhibited significantly enhanced proliferation compared to the B16-pSMP control. This observation was consistent among all clones regardless of where the shRNA target sequences were located and whether the cells were cultured directly in CM or after serum starved (Figure 13d). The observation was further verified by Ki67 staining (Figure 13f) and direct cell counting (Figure 13g). The correlation analysis revealed that cell proliferation was significantly and inversely correlated with the IL-17RA level in B16-RAKD clones (Figure 13e), highlighting a critical role for IL-17RA-mediated signals in negatively controlling homeostatic proliferation of B16 melanoma cells *in vitro*.

I also generated RAKD clones from 4T1 mammary carcinoma cells and observed the same phenotype and growth patterns as B16-RAKDs. The representative 4T1-RAKD4.6 clone, which had an approximately 80% reduction in IL-17RA but intact IL-17RC, displayed significantly elevated proliferation compared to the 4T1-pSMP control (Figure 14). Notably, while RCKDs in both of my cancer cell line models exhibited altered apoptotic rates, RAKD clones exhibited comparable levels of apoptosis to the corresponding pSMP controls (Figure 15).

Figure 13. Knockdown of IL-17RA expression in B16 melanoma cells promotes tumor growth *in vitro*.

B16 cells were transduced with retroviral vectors containing shRNAs targeting different regions of IL-17RA or the pSMP control vector. (a, b) IL-17RA and IL-17RC expression measured by flow cytometry and qRT-PCR on representative clones. (c) CXCL1 production determined by ELISA following IL-17A or IL-17F stimulation. (d) Growth of IL-17RAKD and pSMP clones under normal and serum-starved condition measured by MTT assay. (e) Correlation analysis between growth rate and IL-17RA expression. (f) Cells were starved with serum medium for 12 hrs and then cell proliferation, as measured by Ki67 staining, was assessed by flow cytometry 1 hr and 12 hrs after addition of complete medium. (g) Cell growth measured by direct cell counting. All values are means ± SEM of 3 independent experiments. *$p < 0.05$; **$p < 0.01$; ***$p < 0.001$; compared with the pSMP control.

Figure 13.

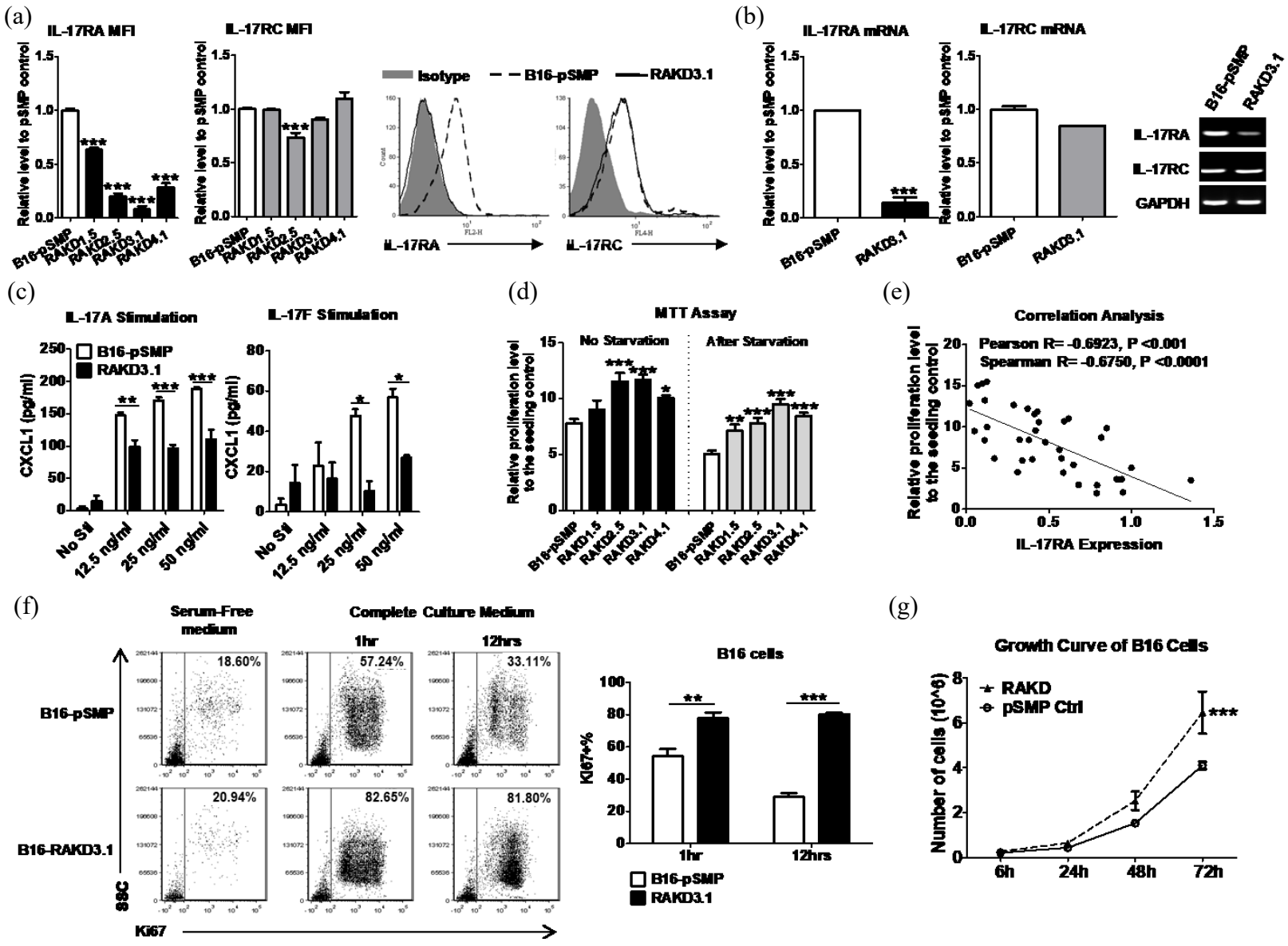
(a)
IL-17RA MFI
IL-17RC MFI
Relative level to pSMP control
B16-pSMP
RAKD1.5
RAKD2.5
RAKD3.1
RAKD4.1
Isotype
B16-pSMP
RAKD3.1
IL-17RA
IL-17RC
(b)
IL-17RA mRNA
IL-17RC mRNA
B16-pSMP
RAKD3.1
IL-17RA
IL-17RC
GAPDH
(c)
IL-17A Stimulation
IL-17F Stimulation
CXCL1 (pg/ml)
B16-pSMP
RAKD3.1
No Stl
12.5 ng/ml
25 ng/ml
50 ng/ml
(d)
MTT Assay
No Starvation
After Starvation
Relative proliferation level to the seeding control
(e)
Correlation Analysis
Pearson R= -0.6923, P <0.001
Spearman R= -0.6750, P <0.0001
IL-17RA Expression
(f)
Serum-Free medium
Complete Culture Medium
1hr
12hrs
B16-pSMP
B16-RAKD3.1
18.60%
57.24%
33.11%
20.94%
82.65%
81.80%
SSC
Ki67
B16 cells
Ki67+%
(g)
Growth Curve of B16 Cells
RAKD
pSMP Ctrl
Number of cells (10^6)
6h
24h
48h
72h

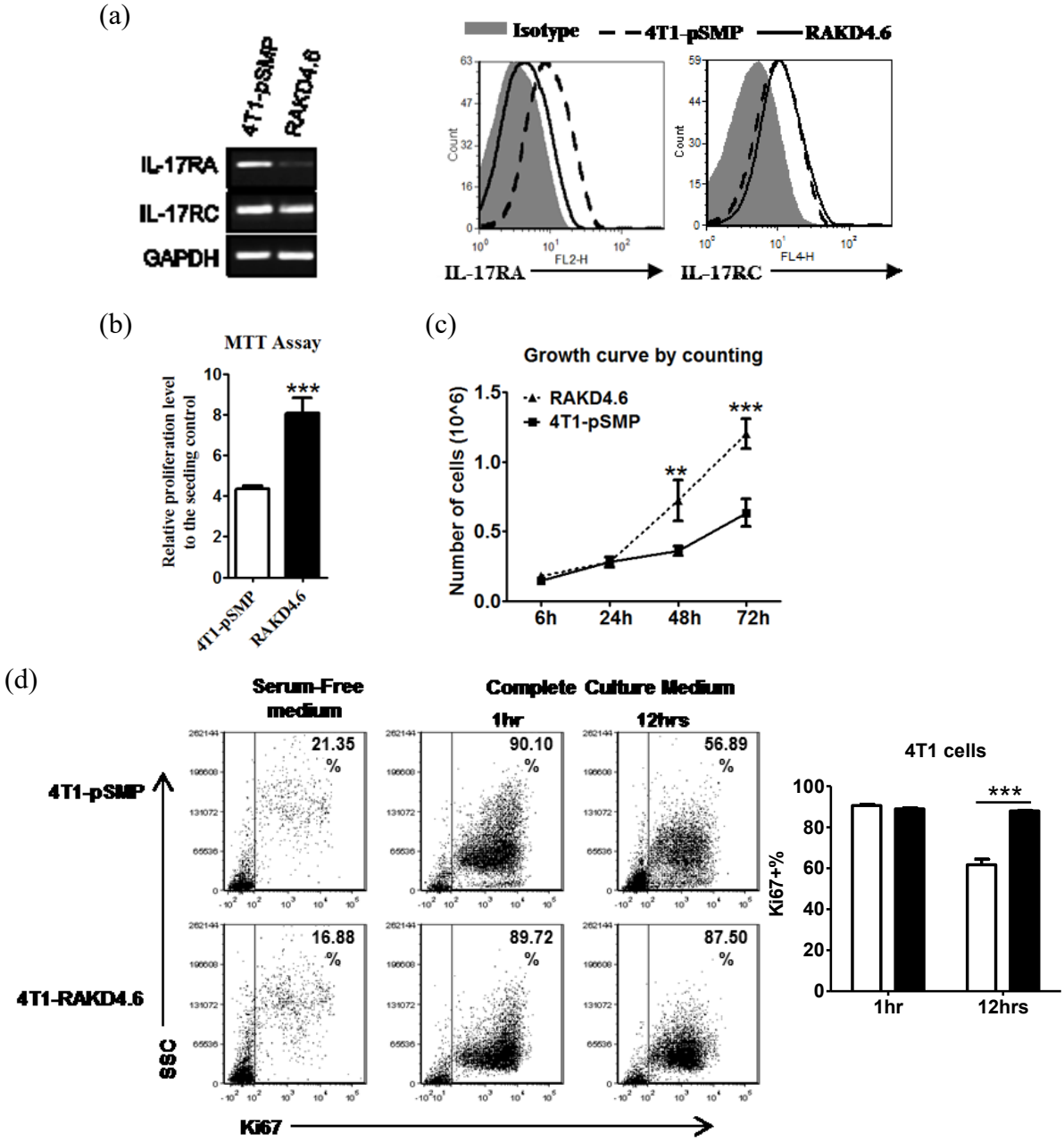

Figure 14. Characterization of IL-17RA knockdown clones of 4T1 cells *in vitro*.

(a) IL-17RA and IL-17RC expression in representative 4T1 clones measured by RT-PCR and flow cytometry. (b) Cell growth measured by MTT assay. (c) Cell growth measured by direct cell counting. (d) Cells were starved with serum-free medium for 12 hrs and then cell proliferation, as measured by Ki67 staining, was assessed by flow cytometry 1 hr and 12 hrs after addition of complete medium. All values are means ± SEM of 3 independent experiments. *p < 0.05; **p < 0.01; ***p < 0.001; compared with the pSMP control.

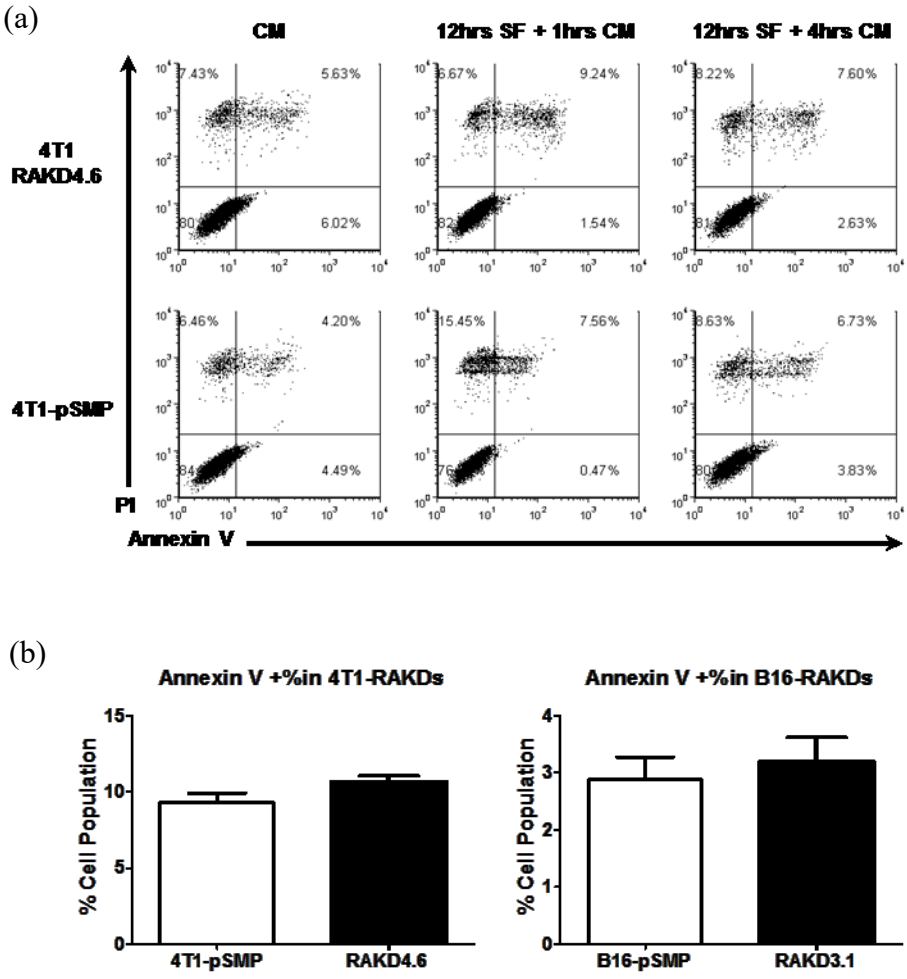

Figure 15. Flow cytometric analysis of PI-Annexin-V to quantify IL-17RA-associated apoptosis in B16 and 4T1 cells.

(a) Dot plots of 4T1-RAKD and control cells in complete DMEM medium with 10% FBS, or serum starved for 12hrs and rescued with CM for 1hr or 4hrs. The results shown are representative of three independent experiments. (b) Quantification of Annexin V^+ B16 and 4T1 clones in culture after serum starvation for 12hrs and rescue with complete medium for 1hr. Values are means ± SEM of 3 independent experiments.

Subsequently, I subcutaneously inoculated B16 tumor cells into C57BL/6 mice and monitored the kinetics of tumor growth for a period of 19 days. Consistent with *in vitro* data, B16-RAKD3.1 cells grew into significantly larger tumors by volume and/or weight at days 12, 16 and 19 post-inoculation, compared to the control B16-pSMP cells (Figure 16a), indicating that in contrast to IL-17RC signaling in B16 cells, IL-17RA-mediated signaling has a significant role in restraining tumor progression *in vivo*. In comparison, 4T1-RAKD4.6 cells grew into significantly larger primary tumors compared to 4T1-pSMP cells (approximately 2.5-fold larger at day 18 post-tumor inoculation), and generated significantly more lung metastases compared to the control cells (Figure 16b). The slightly higher growth rate of 4T1-RAKD tumors compared to the 4T1-RCKD tumors may be the result of the increased apoptotic rate in 4T1-RCKD tumor cells (Figure 8). Together, in contrast to the role of IL-17RC in controlling tumor-specific proliferation, my data demonstrate that the reduction or loss of IL-17RA expression in tumor cells uniformly enhances cell proliferation and invasiveness of tumor cells *in vitro* and *in vivo*.

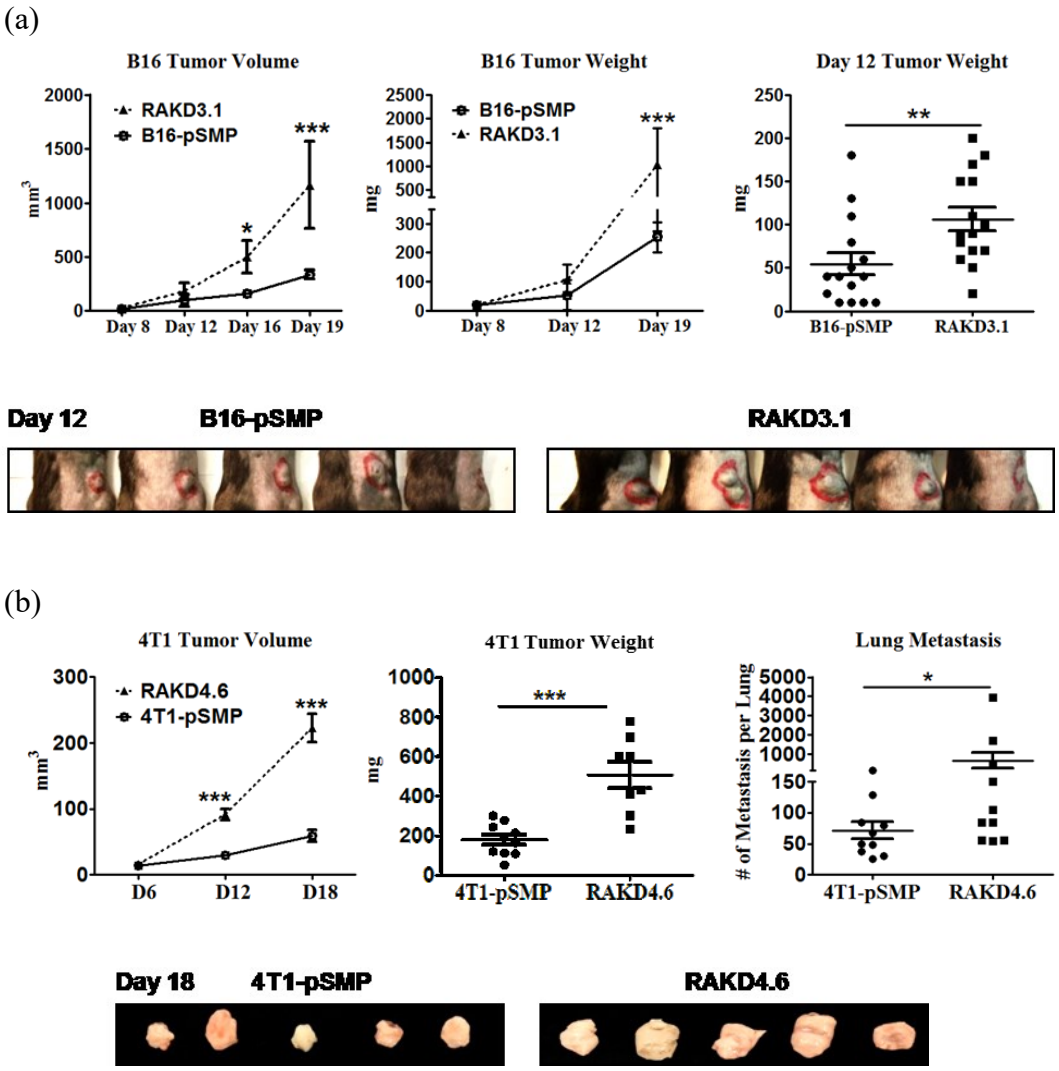

Figure 16. Knockdown of IL-17RA expression promotes tumor growth *in vivo*.

(a) Tumor volume and weight following inoculation of B16-IL-17RAKD and B16-pSMP control cells into C57BL/6 mice. (b) Tumor volume, weight and lung metastasis following inoculation of 4T1-IL-17RAKD and 4T1-pSPM control cells in BALB/c mice. All values are means ± SEM of 3 independent experiments. n = 5-10 mice per group for each time point.

3.1.6 Baseline IL-17RA level restrains tumor cell proliferation by inhibiting homeostatic JNK/c-Jun activation

Once again, I utilized pharmacologic inhibitors to identify the specific signaling pathway(s) which may be responsible for the hyper-proliferation of 4T1-RAKDs and B16-RAKDs and further examined the NF-κB, MAPK and PI3K-AKT pathways in cultured cells with or without exogenous IL-17A (Figure 17a). The homeostatic proliferation of B16-pSMP and 4T1-pSMP control lines was significantly reduced in the presence of AKT and IKK inhibitors, but not MAPK inhibitors; however, the effects of AKT and IKK inhibitors were either completely (B16-pSMP) or partially (4T1-pSMP) reversed by stimulation with exogenous IL-17A. These results indicate that AKT and NF-κB activities induced by endogenous IL-17A act as modest pro-proliferation signals in pSMP clones. Interestingly, the IKK inhibitor was also suppressive in both B16-RAKD and 4T1-RAKD clones, and the level of suppression was not affected by exogenous IL-17A (Figure 17a), indicating that the NF-κB activity in RAKDs is primarily induced by IL-17RA-independent signaling. The AKT inhibitor was suppressive in B16-RAKD, but not 4T1-RAKD, and the level and pattern of suppression were not affected by exogenous IL-17A, suggesting that AKT is activated by IL-17RA-dependent and IL-17RA-independent signaling pathways, depending on the cell type, and not responsible for hyper-proliferation of RAKD clones. Remarkably, consistent with the hyper-proliferative 4T1-RCKD clone, both B16-RAKD and 4T1-RAKD clones also displayed obvious sensitivities to JNK and c-Jun inhibitors, which were not observed in control pSMP counterparts (Figure 17a).

Cell cycle analysis was conducted to understand the involvement of the JNK pathway in the hyper-proliferation of RAKD clones. Compared to B16-pSMP control cells, a significantly higher frequency of B16-RAKD3.1 cells accumulated in the G1 phase after serum-starvation and progressed into S phase upon recovery in complete medium (Figure 17b), indicating that the hyper-proliferation of RAKD clones is primarily due to enhanced G1-to-S phase transition. Notably, inhibiting the JNK/c-Jun pathway with SP600125 effectively eliminated the differences between B16-RAKD3.1 and B16-pSMP cells entering S phase (Figure 17c). Together, though distinct proliferation patterns have been observed in IL-17R KDs, my data demonstrated that IL-17R silencing uniformly induced

the activation of JNK signaling and JNK-mediated G1-to-S phase cell cycle control in both cancer cell lines.

3.1.7 Baseline IL-17RA level is required for maintaining the basal production of A20 that controls aberrant activation of JNK and hyper-proliferation

I next determined whether JNK activation induced by IL-17RA silencing was due to impaired basal production and/or function of the endogenous IL-17A-induced regulatory signaling molecule A20. Though some results from IL-17RCKD clones were presented in previous sections, I purposely included them herein as internal controls to provide a direct comparison between IL-17RA verses IL-17RC signals. A20 mRNA levels were consistently upregulated by IL-17A and IL-17F, but not IL-17C or IL-17E, in both B16 and 4T1 cells (Figure 18a). Furthermore, A20 mRNA levels were reduced in both RAKD and RCKD clones compared to pSMP counterparts in B16 and 4T1 cells, highlighting the importance of IL-17RA/RC in maintaining A20 homeostasis (Figure 18b). In comparison, C/EBPβ had irregular expression patterns among different clones of B16 and 4T1 cells, suggesting that IL-17RA/IL-17RC selectively control A20 but not C/EBPβ. In agreement with the mRNA profile, A20 protein levels were consistently reduced in KD clones under serum-starvation and regular culture conditions (Figure 18c/d), indicating that baseline IL-17R is essential for basal production of A20. Notably, RAKDs exhibited a trend toward greater A20 mRNA loss compared to RCKDs; however, this is not reflected by A20 protein level, suggesting that A20 expression may also be controlled at post-transcriptional levels by other IL-17R-independent signals. Unlike A20 expression, basal levels of phospho-JNK in RAKD and RCKD clones of 4T1 and B16 cells were significantly increased compared to pSMP counterparts (Figure 18c/e). B16-RAKD and B16-RCKD cells displayed quicker kinetics and enhanced intensities of JNK phosphorylation upon CM recovery compared to the B16-pSMP clone. In comparison, 4T1-RAKD and 4T1-RCKD had constitutive JNK phosphorylation compared to the 4T1-pSMP control. Indeed, the 4T1-pSMP clone had negligible phospho-JNK levels in all samples (Figure 18c/e). To examine whether the JNK isoform-dependent proliferation may also explain hyper-proliferation of B16-RAKDs, I blotted for both JNK isoforms. Surprisingly, JNK1 and JNK2 were both upregulated in RAKDs compared to their respective B16 and 4T1 pSMP clones (Figure 18c). Given the hyper-proliferation phenotype of RAKDs, these data support the notion that the IL-17R-

silencing induced pro-proliferative JNK1 activity is dominant compared to the anti-proliferative JNK2.

In accordance with a role of A20 in negatively regulating the NF-κB pathway, the NF-κB activity as measured by phospho-IκB-α and EMSA assays indicated that the NF-κB nuclear translocation was markedly and persistently elevated in RCKD clones, but only marginally increased in RAKD clones compared to pSMP counterparts (Figure 18f/g).

In order to validate the role of IL-17R/A20 axis in controlling JNK-dependent proliferation *in vivo*, I immunoblotted 4T1 tumor sections for Ki67, A20 and phosphor-JNK staining (Figure 19). Both 4T1-RAKD and 4T1-RCKD tumors exhibited around 3-fold higher $Ki67^{+}$ expression intensity and percentage area staining, than the 4T1-pSMP control tumors. Consistent with my *in vitro* results, the hyper-proliferative nature of IL-17R-KD tumors was associated with markedly reduced A20 expression and enhanced activation of JNK. Together, the profile of intracellular signaling molecules provides solid evidence that the baseline IL-17A/IL-17R signal is essential for maintaining basal levels of A20, which actively restrains baseline JNK activation in RAKD and RCKD clones, as well as the NF-κB activity in RCKD clones.

I also examined whether the IL-17R-A20 axis may control the proliferation of primary cells. Bone marrow-derived dendritic cells (BMDC) and mouse embryonic fibroblasts (MEF) from an IL-17RA- or IL-17RC-deficient mice all displayed significantly reduced A20 levels compared to their wild type (WT) counterparts (Figure 20). BMDC from IL-$17RA^{-/-}$, IL-$17RC^{-/-}$, and WT mice exhibited different proliferation capacities with the order of IL-$17RA^{-/-}$>IL-$17RC^{-/-}$>WT (Figure 20b). MEF proliferation assays indicated that MEF from IL-$17RA^{-/-}$ and IL-$17RC^{-/-}$ mice had significantly higher rates of proliferation compared to WT MEF upon CM recovery (approximately 40% in RAKO, 20% in RCKO and 8% in WT) while serum starvation stopped MEF proliferation (approximately 0.9% $Ki67^{+}$) (Figure 20c/d). These results demonstrate that baseline IL-17R level is required for basal production of A20 in primary cells and controlling homeostatic proliferation of primary hematopoietic and non-hematopoietic cells.

Figure 17. Baseline IL-17RA level restrains tumor cell proliferation via inhibiting homeostatic JNK/c-Jun activation.

(a) IL-17RAKD and pSMP control lines of B16 melanoma and 4T1 breast cancer cells were cultured with or without IL-17A (50 ng/ml) stimulation. Cells were treated with DMSO or one of the inhibitors (2 μM AKT inhibitor, 5 μM IKK inhibitor, 10 μM ERK inhibitor, 10 μM p38 inhibitor, 5 μM L-form JNK inhibitor or 10 μM JNK/c-Jun inhibitor) for 48 hrs. Cell proliferation was measured by MTT assay. The absorbance value in each treatment condition was normalized relative to the MTT value in the seeding control. (b/c) Cell cycle analysis in B16-pSMP and B16-RAKD3.1 cells. (b) Cells were synchronized for 24 hrs in serum-free medium or cultured in complete medium for an additional 48 hrs prior to PI staining and analysis of DNA content. (c) To assay the role of JNK/c-Jun, B16-RAKD3.1 cells were starved in serum-free medium for 24 hrs and recovered in complete medium, DMSO-containing medium or SP600125-containing medium for 48 hrs. Values are means ± SEM of 3 independent experiments. *$p < 0.05$; **$p < 0.01$; ***$p < 0.001$; compared with the respective control (white bar) using one-way or two-way ANOVA.

Figure 17.

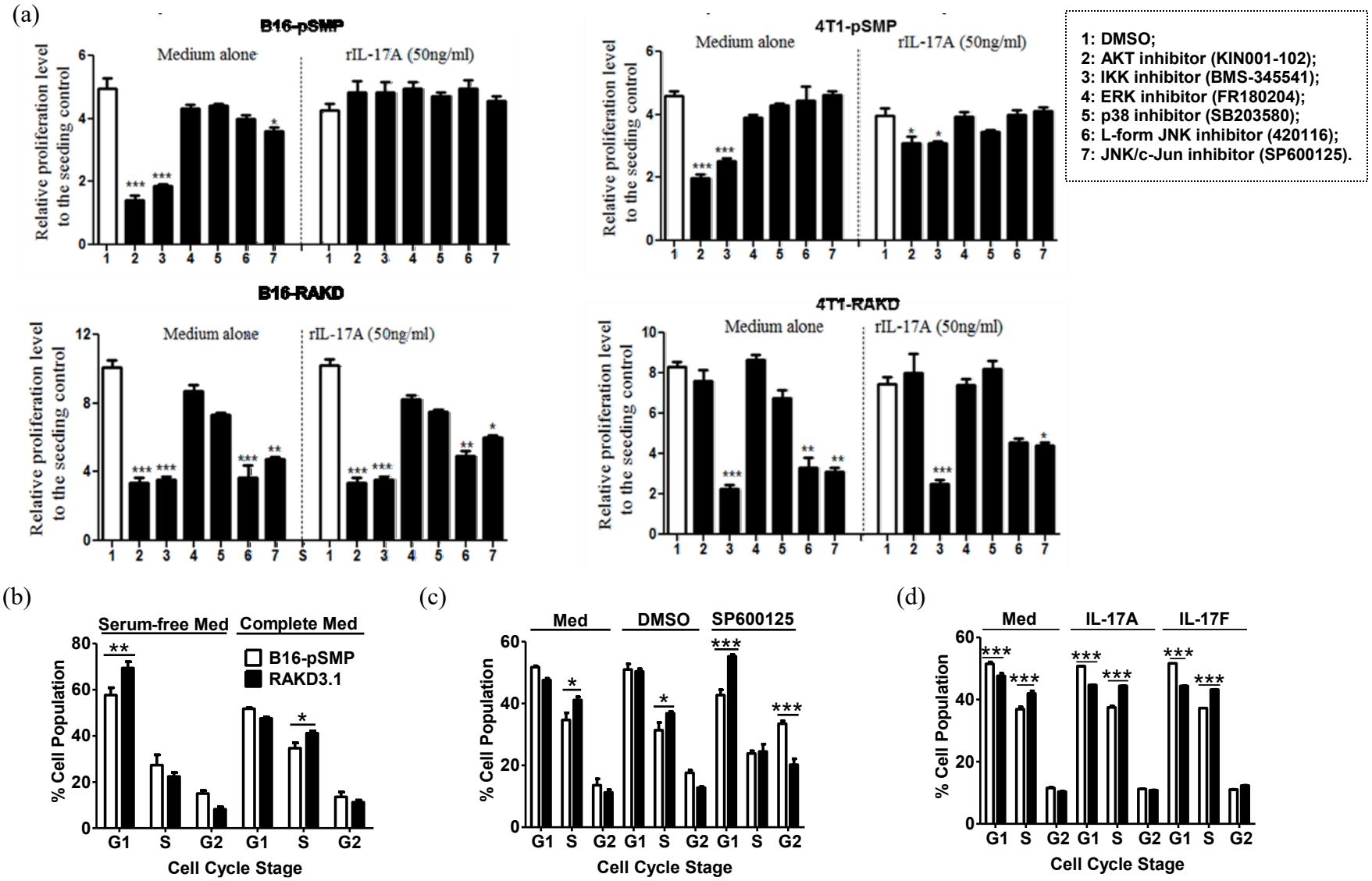
(a)
B16-pSMP
4T1-pSMP
B16-RAKD
4T1-RAKD
Medium alone
rIL-17A (50ng/ml)
Relative proliferation level to the seeding control
1: DMSO;
2: AKT inhibitor (KIN001-102);
3: IKK inhibitor (BMS-345541);
4: ERK inhibitor (FR180204);
5: p38 inhibitor (SB203580);
6: L-form JNK inhibitor (420116);
7: JNK/c-Jun inhibitor (SP600125).
(b)
Serum-free Med
Complete Med
B16-pSMP
RAKD3.1
% Cell Population
G1 S G2 G1 S G2
Cell Cycle Stage
(c)
Med
DMSO
SP600125
% Cell Population
G1 S G2 G1 S G2 G1 S G2
Cell Cycle Stage
(d)
Med
IL-17A
IL-17F
% Cell Population
G1 S G2 G1 S G2 G1 S G2
Cell Cycle Stage

Figure 18. IL-17RA/RC silencing leads to reduced A20 production and enhanced activation of JNK and NF-κB pathways.

(a) B16 melanoma and 4T1 mammary carcinoma cells were starved with serum-free DMEM for 14 hrs and allowed to recover in complete DMEM medium with or without exogenous 200 ng/ml IL-17 ligands for 30 mins. Gene expression was determined by qRT-PCR with 6 replicates from 2 independent experiments. Values were compared with the respective CM treated group (black bar). (b) A20 and C/EBPβ mRNA levels were determined by qRT-PCR in pSMP, RAKD and RCKD subclones of 4T1 and B16 tumor cells. (c) Whole-cell extracts were harvested from serum starved and recovered cells and immunoblotted to detect total or phosphorylated proteins as indicated. GAPDH was used as a loading control. (d, e) Scanning densitometry of relative A20 and p-JNK protein levels at 60 min post CM recovery were performed. (f, g) Nuclear proteins were extracted from RAKD, RCKD and control cells of B16 and 4T1 cells and subjected to EMSA using ^{32}P-labeled NF-κB DNA probes. Values are means ± SEM of 3 independent experiments. *$p < 0.05$; **$p < 0.01$; ***, $p < 0.001$; compared with the respective control cell line (black bar) using one-way ANOVA.

Figure 18.

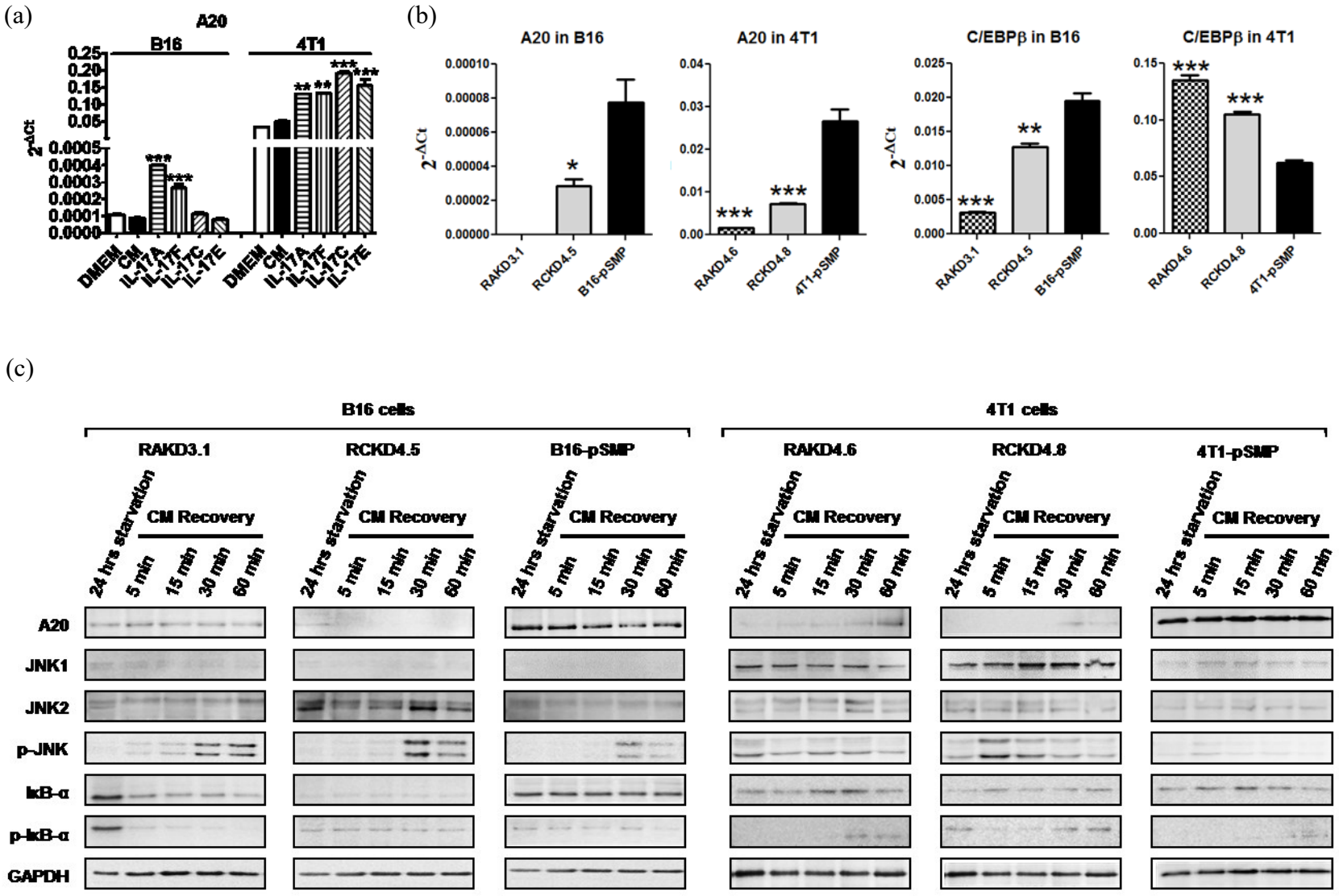
(a)
A20
B16
4T1
2^-ΔCt
DMEM
CM
IL-17A
IL-17F
IL-17C
IL-17E
(b)
A20 in B16
A20 in 4T1
C/EBPβ in B16
C/EBPβ in 4T1
RAKD3.1
RCKD4.5
B16-pSMP
RAKD4.6
RCKD4.8
4T1-pSMP
(c)
B16 cells
4T1 cells
24 hrs starvation
CM Recovery
5 min
15 min
30 min
60 min
A20
JNK1
JNK2
p-JNK
IκB-α
p-IκB-α
GAPDH

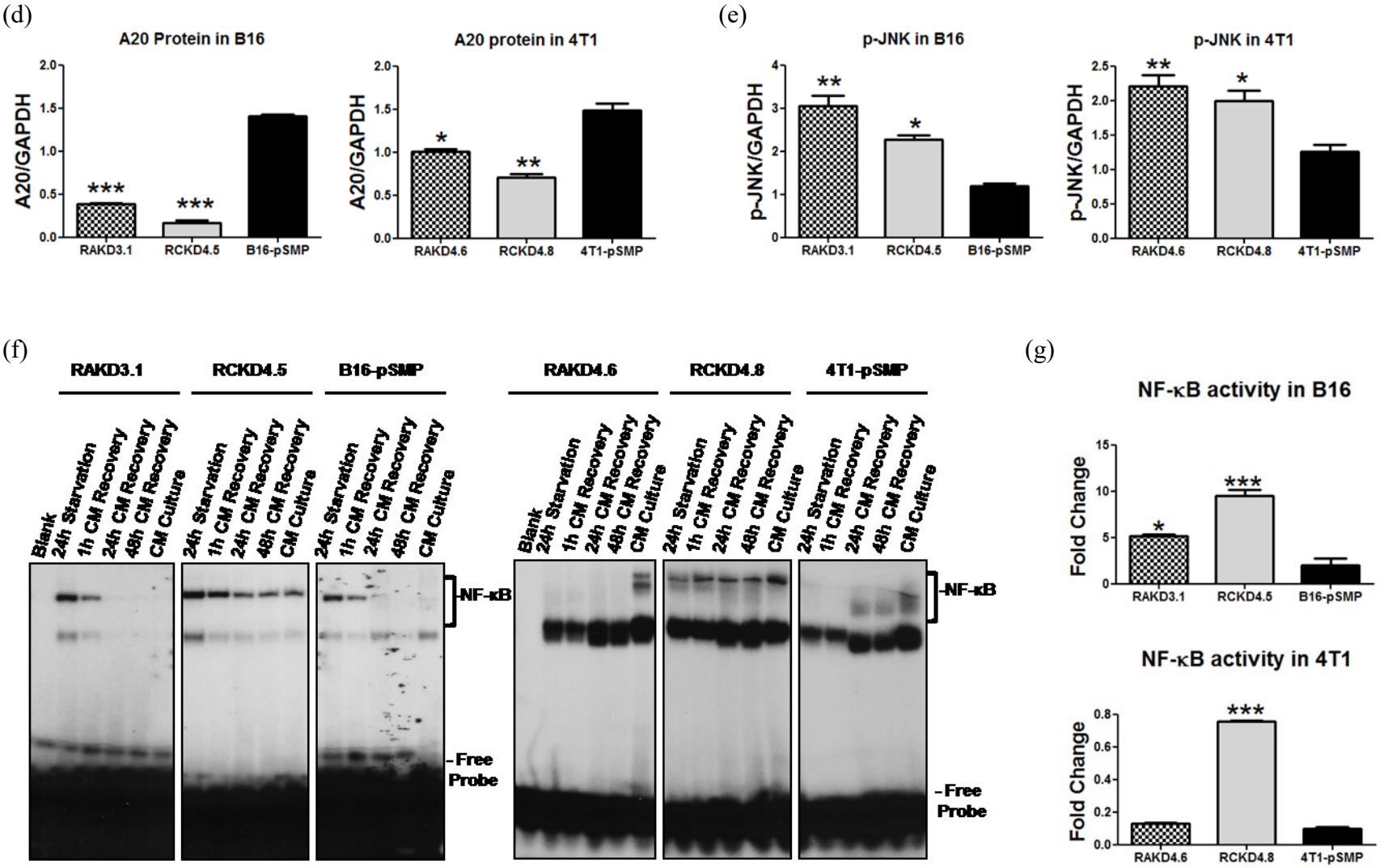

Figure 18. Continued.

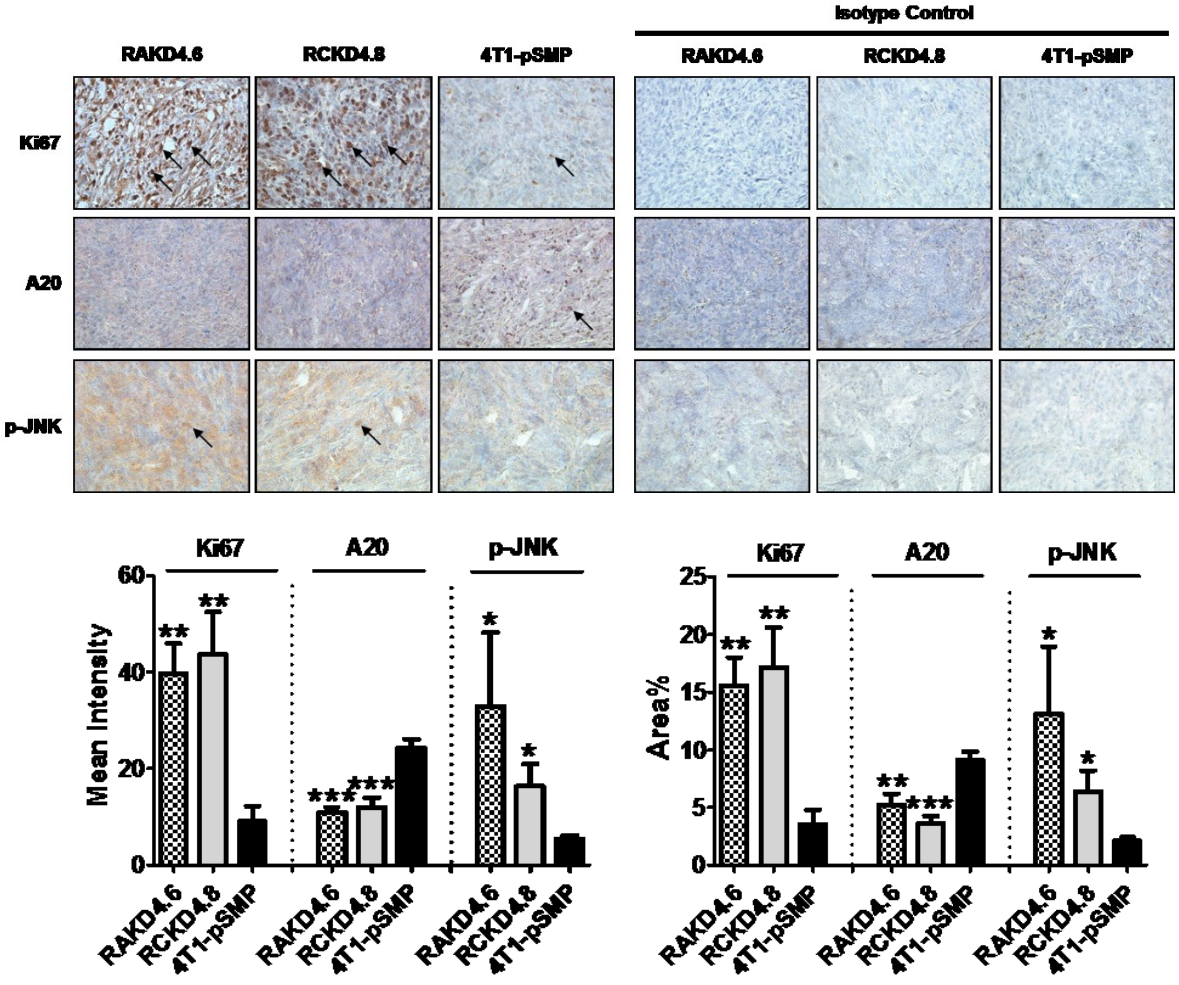

Figure 19. IL-17RA/RC silencing leads to reduced A20 production and enhanced activation of JNK *in vivo*.

Mice were inoculated with 1 x 10^6 4T1 mammary carcinoma cells. On day 18, tumors were harvested and prepared for immunohistochemistry. Sections were stained with antibodies against Ki67, A20 and phosphorylated JNK. Staining was developed using ABC and DAB solutions (Vector Laboratories, Brockville, Ontario). Slides were counterstained with Mayer's Haematoxylin and staining intensity was determined. Original magnification was 400x. Values are means ± SEM of 3 independent experiments. *$p < 0.05$; **$p < 0.01$; ***, $p < 0.001$; compared with the respective control cell line (black bar) using one-way Kruskal-Wallis test.

Figure 20. BMDC and MEF with IL-17RA or IL-17RC deficiency show reduced basal expression of A20 and increased proliferation.

(a) A20 mRNA levels in GM-CSF-induced BMDCs and MEF cells from WT, IL-17RAKO and IL-17RCKO mice. (b) BMDCs were labeled by Cell Proliferation Dye eFluor® 670 staining and the cell proliferation was measured at 4 days post culturing in GM-CSF-containing medium. (c) MEF cells were starved in serum-free medium for 12 hrs and the cell proliferation via Ki67 staining was measured at 1 hr after addition of complete medium. Data are presented as mean ± SEM of 3 independent experiments. *$p < 0.05$; **$p < 0.01$; ***$p < 0.001$; compared with the WT control using one-way ANOVA.

Figure 20. (a)

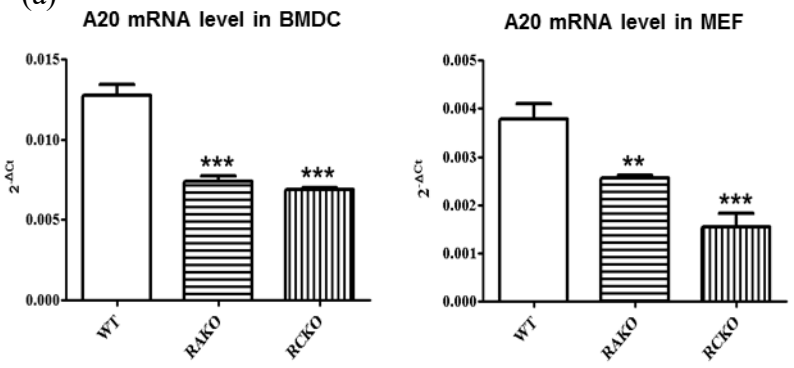

(b)

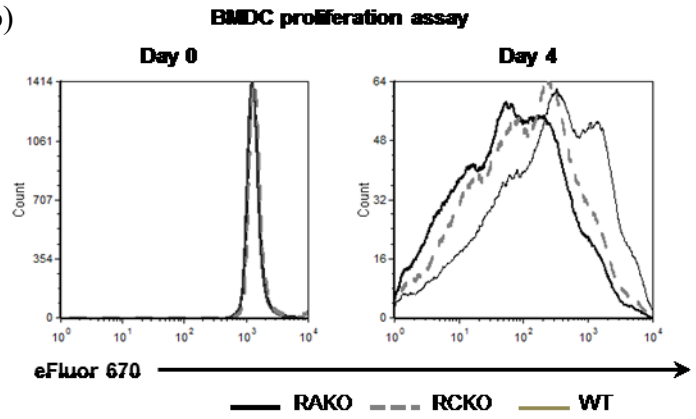

(c)

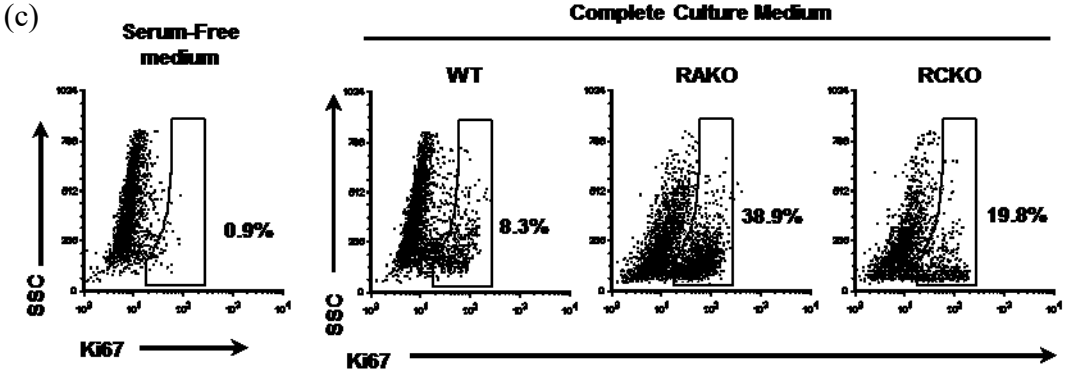

(d)

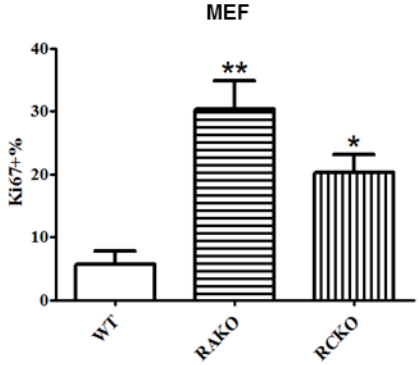

3.1.8 Reconstitution of IL-17RA in RAKD clones restores parental proliferation, A20 expression and JNK activity

Given the opposing proliferation phenotypes in IL-17RAKD and IL-17RCKD B16 cells, I conducted reconstitution experiments to rule out the possibility of off-target effects. To this end, I transduced B16-RAKD3.1 and B16-pSMP cells with a viral vector expressing full-length of IL-17RA (pBMN-RA) in order to restore or over-express IL-17RA. The pBMN vector (pBMN-Ctrl) lacking a transgene sequence was used as a negative control. As anticipated, pBMN-RA, but not pBMN-Ctrl, restored IL-17RA expression in B16-RAKD3.1 cells to an extent that was comparable to B16-pSMP cells transduced with the pBMN-Ctrl vector (Figure 21a), suggesting a complete reconstitution of IL-17RA in B16-RAKD cells. The pBMN-RA transduction in B16-pSMP doubled the mRNA expression of IL-17RA; however, it was not able to further increase surface IL-17RA expression (Figure 21b), indicating a tight post-transcriptional regulation of IL-17RA under steady-state conditions. Importantly, IL-17RA reconstitution successfully attenuated hyper-proliferation of B16-RAKD clones and restored the proliferation profile back to the parental level (Figure 21c). Furthermore, IL-17RA reconstitution effectively eliminated IL-17RA-silencing-induced sensitivities to L-form JNK inhibitor and reduced the responsiveness to SP600125 JNK/c-Jun inhibitor in MTT proliferation assays (Figure 21d). Notably, IL-17RA reconstitution restored the basal mRNA expression and protein levels of A20 to the levels observed in pSMP control cells (Figure 21e/f). Associated with these observations, the aberrant activation of JNK/c-Jun was attenuated to the pSMP control level (Figure 21f). While these observations allow us to rule out a possible off-target effect of my technology, the complex phenotype of IL-17RAKD and IL-17RCKD suggests that JNK isoform expression is controlled via complex mechanisms.

Figure 21. Reconstitution of IL-17RA in RAKDs is able to restore the parental rate of proliferation and associated A20 expression and JNK/c-Jun activity.

IL-17RA was reconstituted into B16-RAKD and pSMP control cells with a viral vector expressing full-length of IL-17RA (pBMN-RA). (a, b) The IL-17RA and IL-17RC levels in different subclones of B16 cells were detected by qRT-PCR and flow cytometry. (c, d) The proliferation of different subclones and their responsiveness to JNK inhibitors was measured via MTT assay. The data was normalized to the MTT response of the respective seeding controls. The % of proliferation inhibition was calculated relative to the respective DMSO control. (e, f) A20 mRNA levels in different subclones were determined by qRT-PCR and western blot. (f) Whole-cell extracts were harvested and immunoblotted to detect phosphorylated or total proteins of A20, JNK, c-Jun and GAPDH. Values are means ± SEM of 3 independent experiments. *$p < 0.05$; **$p < 0.01$; ***$p < 0.001$. Statistical analyses were compared using one-way ANOVA.

Figure 21.

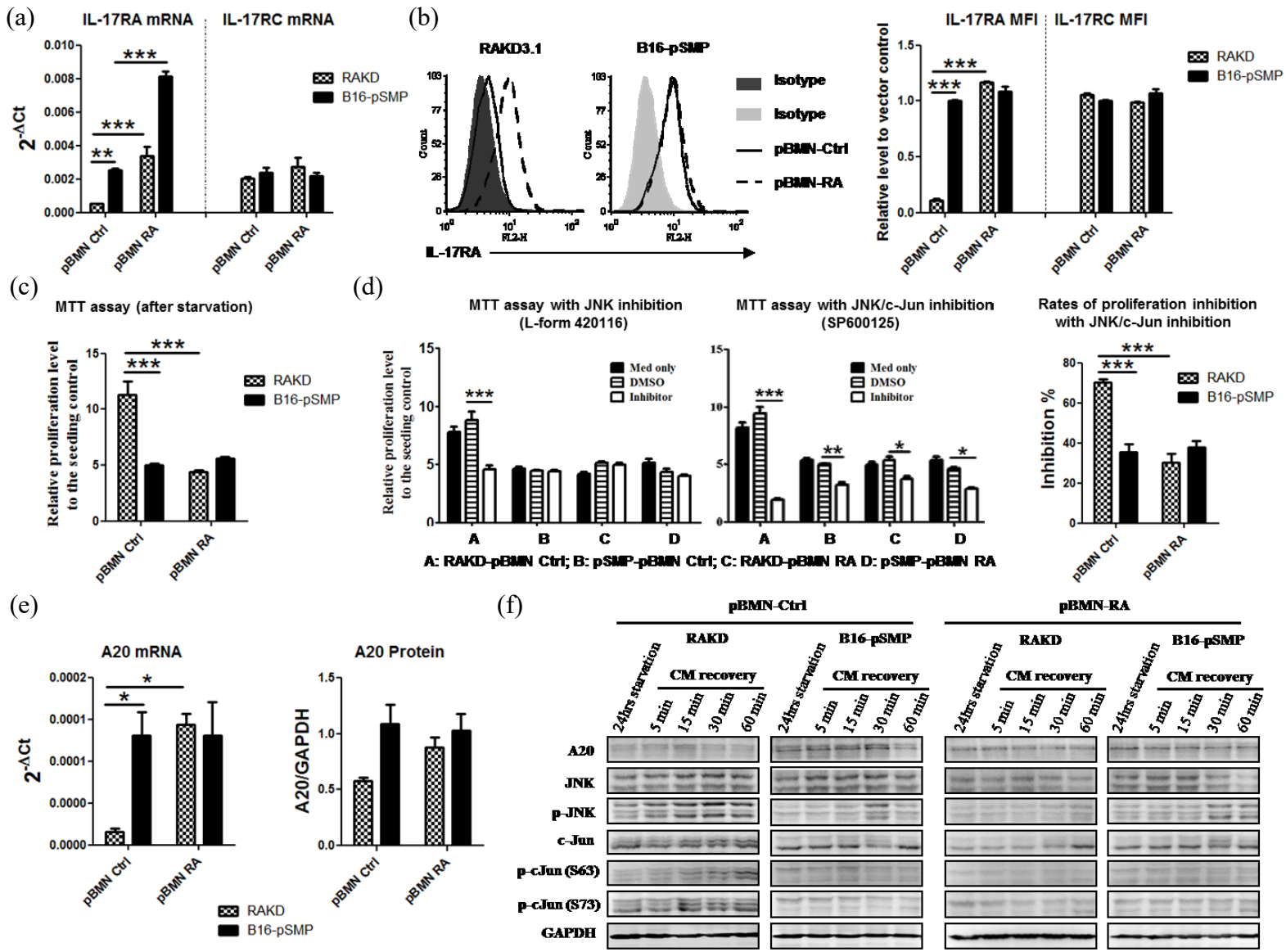
(a)
IL-17RA mRNA
IL-17RC mRNA
2^-ΔCt
RAKD
B16-pSMP
pBMN Ctrl
pBMN RA
(b)
RAKD3.1
B16-pSMP
Isotype
Isotype
pBMN-Ctrl
pBMN-RA
IL-17RA
IL-17RA MFI
IL-17RC MFI
Relative level to vector control
(c)
MTT assay (after starvation)
Relative proliferation level to the seeding control
(d)
MTT assay with JNK inhibition (L-form 420116)
MTT assay with JNK/c-Jun inhibition (SP600125)
Rates of proliferation inhibition with JNK/c-Jun inhibition
Med only
DMSO
Inhibitor
Inhibition %
A: RAKD-pBMN Ctrl; B: pSMP-pBMN Ctrl; C: RAKD-pBMN RA D: pSMP-pBMN RA
(e)
A20 mRNA
A20 Protein
A20/GAPDH
(f)
pBMN-Ctrl
pBMN-RA
RAKD
B16-pSMP
24hrs starvation
CM recovery
5 min
15 min
30 min
60 min
A20
JNK
p-JNK
c-Jun
p-cJun (S63)
p-cJun (S73)
GAPDH

Given that A20 is the key molecule required for controlling JNK activation in IL-17RC signaling (Figure 11d), I verified this in IL-17RA signaling. I transfected RAKD and pSMP control cells with the plasmid carrying full length A20 or the empty plasmid vector alone (Figure 22a/b). Notably, in both B16 and 4T1 models, A20 transfection in RAKD cells effectively restored A20 protein levels. In addition, the JNK/c-Jun activity at 48 and 72 hrs post-transfection were markedly reduced, as indicated by reduced phosphorylation of JNK and c-Jun. Along with the restored A20 expression, the cellular proliferation of RAKD cells was restrained to the normal level observed in the pSMP control. Together with the RCKD results, the A20 reconstitution experiments in RAKDs further demonstrate that the IL-17R-A20 axis is required for restraining homeostatic proliferation via inhibiting aberrant JNK/c-Jun activation.

3.2 Loss of IL-17RA expression in cancer cells promotes an immunosuppressive TME

3.2.1 IL-17RA silencing in B16 melanoma cells induces an immunosuppressive TME

Having demonstrated a role for IL-17R signaling in mediating cancer cell proliferation *in vitro* and *in vivo*, I next questioned how tumor cells may ultilize IL-17R signaling in shaping the TME. Using the B16 melanoma model, I first isolated and examined the tumor-draining lymph nodes (DLNs), the primary site for inducing anti-tumor immune responses. To my surprise, IL-17RA silencing in B16 melanoma cells induced comparable immune induction in DLNs compared to the pSMP control despite increased tumor size (Figure 23a), suggesting an active immunosuppression may be associated with the IL-17RAKD tumors. Indeed, while the overall cell density did not differ among the groups, the density of tumor-infiltrating $CD4^+$ Th cells, $CD8^+$ Tc cells, and NK cells was markedly reduced in RAKD tumors, and to a lesser extent, in RCKD tumors compared to the controls (Figure 23b). Notably, the frequency of $MHCII^+CD19^+$ B cells in the DLNs, as well as their density in the TILs, were both decreased significantly in the RAKD, but not RCKD tumors, compared to the pSMP controls. Together, the general resemblance with minor differences in the immune profile, suggested that IL-17RA and IL-17RC signaling in tumor cells may ultilize both common and differential mechanisms to restrain the suppressive TME.

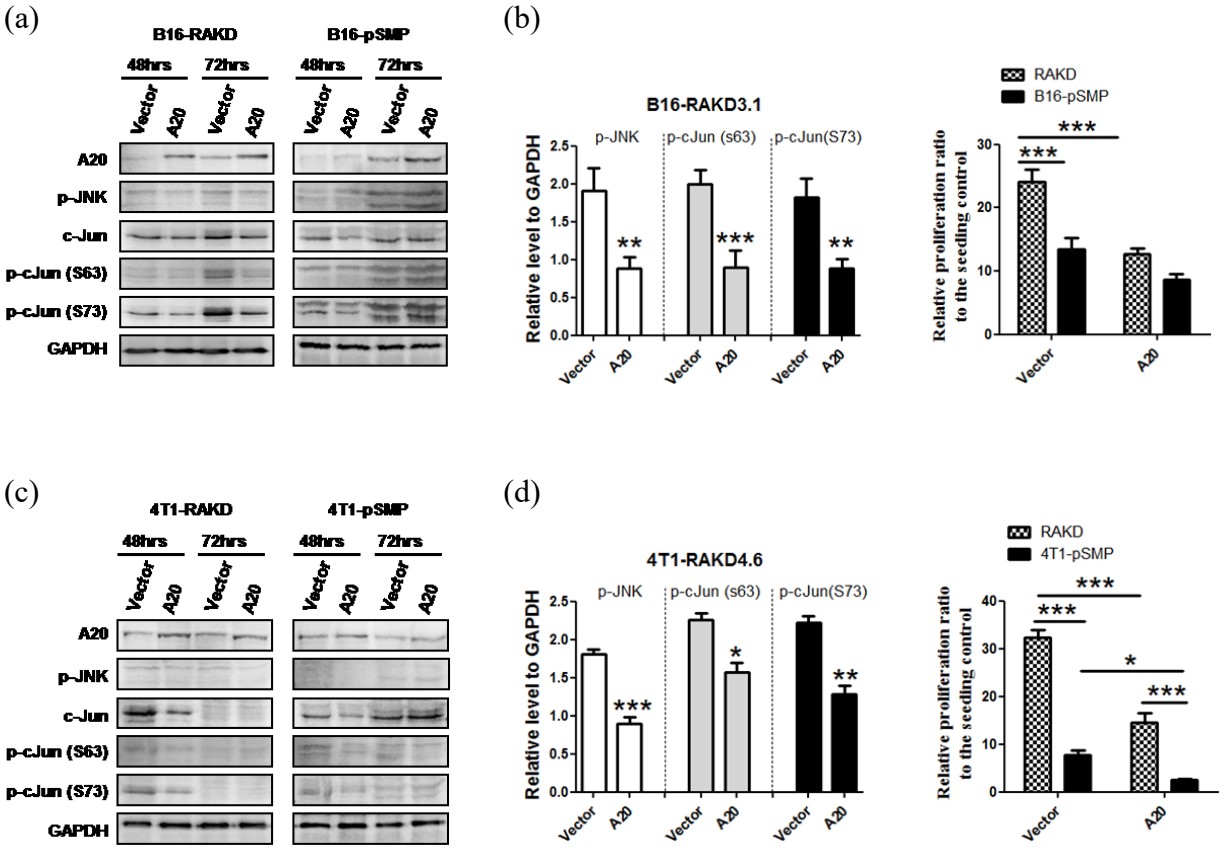

Figure 22. Reconstitution of A20 in RAKD clones is able to restore the normal rate of proliferation and associated JNK/c-Jun activity.

(a/c) IL-17RAKD and pSMP control of B16 and 4T1 cells were transfected with plasmids containing A20 or a control vector for 48hrs and 72hrs. Whole-cell extracts were harvested and sequentially immunoblotted with the indicated antibodies to detect phosphorylated and total levels of A20, JNK, c-Jun and GAPDH proteins. (b/d) The proliferation rate of different subclones was measured by MTT assay 72 hrs after transfection. The data was normalized to the respective seeding control. Values are means ± SEM of 3 independent experiments. *p < 0.05; **p < 0.01; ***p < 0.001.

Figure 23. IL-17RA silencing in B16 melanoma cells promotes an immunosuppressive TME

Mice were inoculated subcutaneously in the hind flank with 1 x 10^6 B16 melanoma cells. (a) DLNs and (b) tumors were collected 12 days post-innoculation. Total $CD45^+$ leukocytesand the frequency in DLNs or density in tumors of $CD4^+$ Th cells, $CD8^+$ Tc cells, $CD19^+$ B cells and $NKp46^+$ NK cells were obtained by flow cytometric analysis. Data are presented as the mean ± SEM. *$p<0.05$ versus pSMP control as determined by Kruskal-Wallis test with Dunn's post-hoc analysis.

Figure 23.

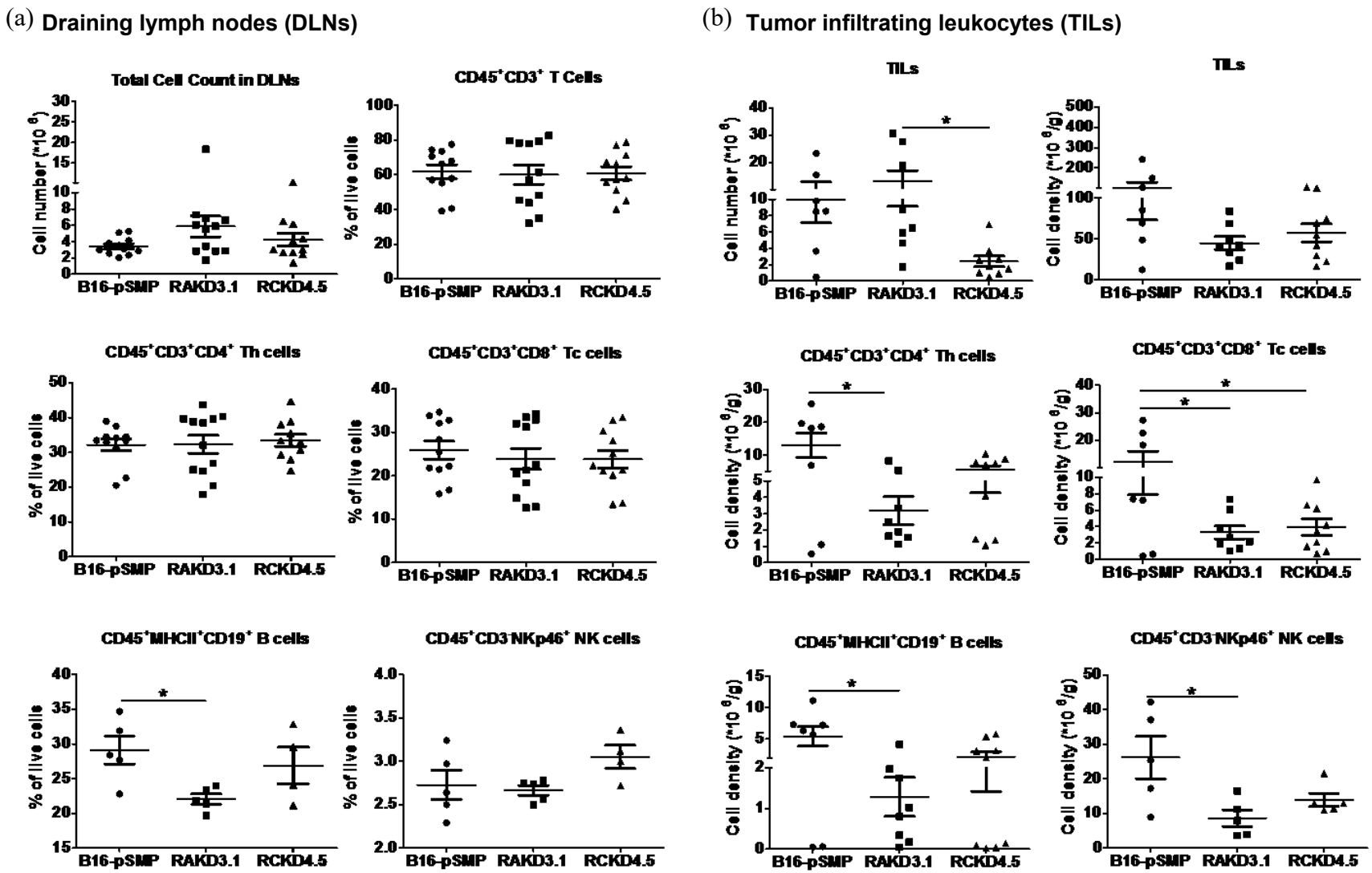
(a) Draining lymph nodes (DLNs)
(b) Tumor infiltrating leukocytes (TILs)
Total Cell Count in DLNs
Cell number (*10^6)
CD45+CD3+ T Cells
% of live cells
TILs
Cell number (*10^6)
TILs
Cell density (*10^6/g)
CD45+CD3+CD4+ Th cells
% of live cells
CD45+CD3+CD8+ Tc cells
% of live cells
CD45+CD3+CD4+ Th cells
Cell density (*10^6/g)
CD45+CD3+CD8+ Tc cells
Cell density (*10^6/g)
CD45+MHCII+CD19+ B cells
% of live cells
CD45+CD3-NKp46+ NK cells
% of live cells
CD45+MHCII+CD19+ B cells
Cell density (*10^6/g)
CD45+CD3-NKp46+ NK cells
Cell density (*10^6/g)
B16-pSMP
RAKD3.1
RCKD4.5

3.2.2 Loss of baseline IL-17RA expression in B16 melanoma cells induces pro-inflammatory cytokine production *in vitro* and *in vivo*

Given that cells with an attenuated IL-17R/A20 signaling are sensitive to IL-17A stimulation and exhibited elevated production of proinflammatory cytokines *in vitro*, including IL-6 and GM-CSF, but not CXCL1 (Figure 12), I questioned what other proinflammaory cytokines and chemokines are subject to this regulatory mechanism. To this end, I screened 84 inflammation-related genes along with 5 housekeeping genes, using the RT² Profiler™ PCR Array (QIAGEN). I first screened the gene expression profiles *in vitro* using B16-pSMP and B16-IL-17R KD cells following 16hrs treatment with 200 ng/ml IL-17A (Figure 24a). I found three genes, CXCR5, IL-6 and the angiogenesis factor thymidine phosphorylase (Tymp) (446), were highly up-regulated in both RAKD and RCKD compared to pSMP control, suggesting that these genes are restrained by IL-17R expression. Furthermore, the expression levels of CXCL1, CCL25 and CCBP2 (or ACKR2, atypical chemokine receptor 2) were reduced in both RAKD and RCKD clones, indicating these genes may be induced by the IL-17 signal to favor inflammatory repsonses. Together, these two clusters of gene alteration may result from the IL-17/IL-17R-induced signal and the IL-17R/A20-repressed signal. To validate whether the IL-17R/A20 controling mechanism may also apply for *in vivo* settings, I performed a micro-array on bulk tumor samples collected at day 12 post-innoculation with B16-RAKD and B16-RCKD clones (Figure 24a/b). Several ligands and receptors were upregulated or downregulated > 2-fold in the IL-17R KD samples compared to the pSMP controls. To validate the microarray data and examine the dynamics of gene expression profiles of the *in vivo* tumor samples, I further collected tumor samples at day 8, 12, 19 post-innoculation and performed qRT-PCR using the pre-validated primers (Bio-Rad) targeting 16 different genes. As shown in Fig. 24a/b, consistent with the observation of *in vitro* samples, proinflammatory cytokines IL-6, as well as IL-1β, were highly upregulated within the *in vivo* IL-17RAKD tumors, and to a lesser extent, the IL-17RCKD tumors compared to the pSMP controls. In addition, Tymp exhibited significant upregulation in both IL-17RA and IL-17RC KD tumors, confirming the impact of IL-17R-downregulation in the production of pro-inflammatory cytokines and pro-tumor molecules. In addition to the genes which exhibited similar alteration pattern *in vitro* and *in vivo*, I found serval gene profiles were altered only in *in*

vivo tumors, highlighting the role of TME in shaping the functional role of the IL-17/IL-17R/A20 axis in tumor development. For instance, the anti-tumor cytokine of the type 1 response, IFNγ, was severely downregulated only in early cancer development at day 8 post-innoculation of both IL-17R KD tumors (Figure 24a/b). Furthermore, there was a 3-fold increase of Mill1, CXCL14 and CXCL10 in the IL-17RAKD tumors, but not IL-17RCKD tumors, suggesting the differential impact of IL-17RA and IL-17RC signaling in regulating the TME.

Given the inflammatory and immunosuppressive TME observed in the IL-17R KD tumors, especially in the IL-17RAKD tumors, I further examined the immune profile in the DLNs (Figure 24c). Surprisingly, there was a 2- to 3-fold increase of IFNγ-producing APCs and $CD8^+$ Tc cells in the IL-17RAKD DLNs compared to the pSMP controls, which suggests that the IL-17RKD-induced immune dysfuntion is restricted within the TME. Of note, no alteration of type 2 (e.g., IL-4) and type 17 (e.g., IL-17) immune responses was detected.

Figure 24. Loss of baseline IL-17RA in B16 melanoma cells selectively induces pro-inflammatory cytokine production *in vitro* and *in vivo*.

(a) Total RNA was extracted from either approximately 3 x 10^6 B16 cells treated with 200 ng/ml IL-17A stimulation for 16 hrs, or *in vivo* B16 tumors that were isolated from mice at day 8, 12 and 19 post-inoculation. RNA was reverse-transcribed into cDNA. Target genes amplified by a QIAGEN RT² Profiler™ PCR array of mouse chemokines & receptors,Gene expression levels were confirmed by qPCR using pre-validated primers (Bio-Rad). All the gene expression results were normalized to the level of the housekeeping gene GAPDH. The relative level of gene expression compared to the control group is shown. (b) List of chemokine and chemokine receptor genes differentially regulated by IL-17RA and IL-17RC signals. (c) Intracellular cytokine staining for IFNγ was performed on lymphoctytes isolated from DLNs on day 8, 12 and 19 post-innoculation with tumor cells. *$p < 0.05$; **$p < 0.01$; ***$p < 0.001$. Statistical analyses were compared using Kruskal-Wallis test.

Figure 24.

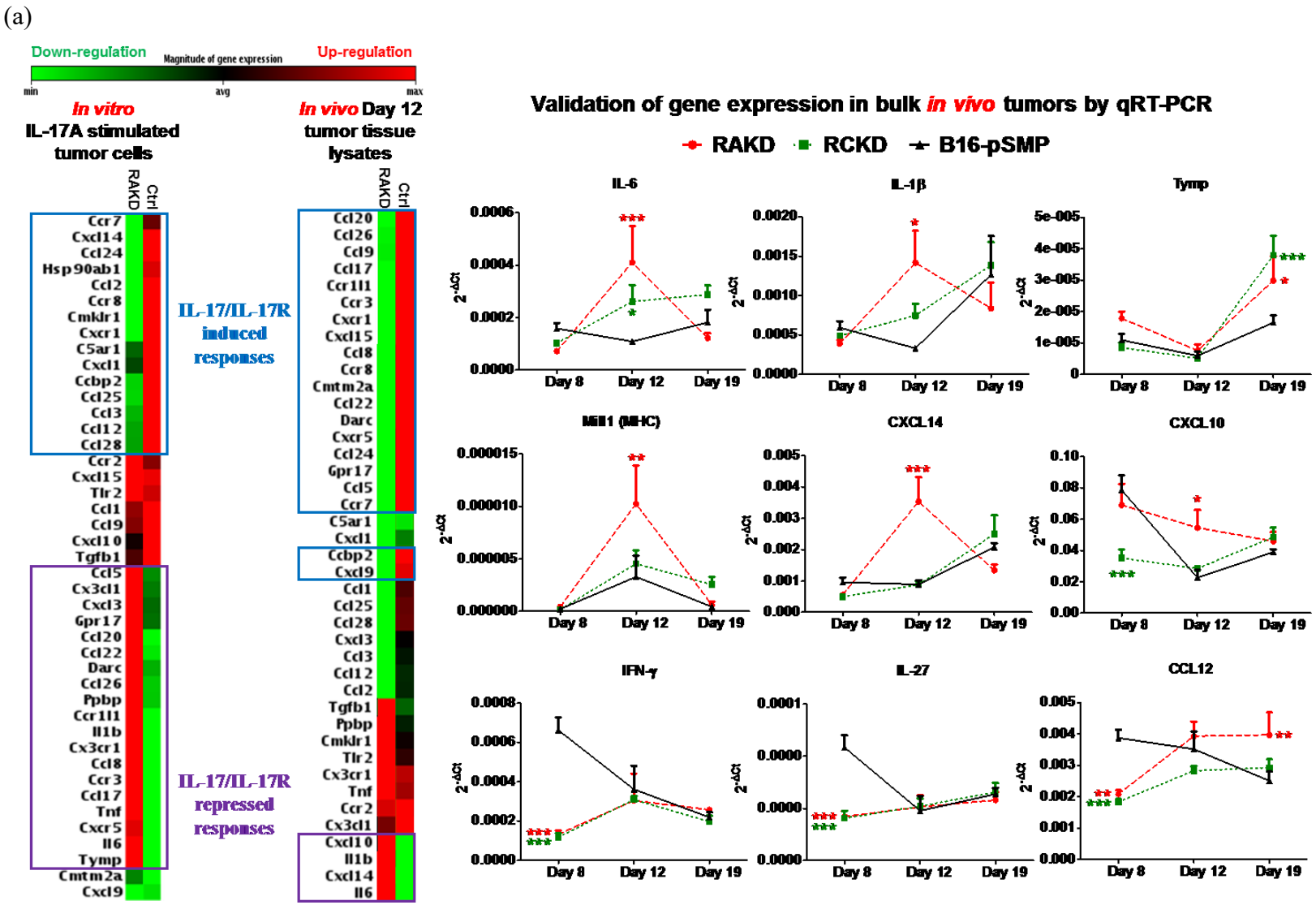
(a)
Down-regulation
Magnitude of gene expression
Up-regulation
min
avg
max
In vitro
IL-17A stimulated tumor cells
In vivo Day 12 tumor tissue lysates
RAKD
Ctrl
Ccr7
Cxcl14
Ccl24
Hsp90ab1
Ccl2
Ccr8
Cmklr1
Cxcr1
C5ar1
Cxcl1
Ccbp2
Ccl25
Ccl3
Ccl12
Ccl28
Ccr2
Cxcl15
Tlr2
Ccl1
Ccl9
Cxcl10
Tgfb1
Ccl5
Cx3cl1
Cxcl3
Gpr17
Ccl20
Ccl22
Darc
Ccl26
Ppbp
Ccr1l1
Il1b
Cx3cr1
Ccl8
Ccr3
Ccl17
Tnf
Cxcr5
Il6
Tymp
Cmtm2a
Cxcl9
IL-17/IL-17R induced responses
IL-17/IL-17R repressed responses
Ccl20
Ccl26
Ccl9
Ccl17
Ccr1l1
Ccr3
Cxcr1
Cxcl15
Ccl8
Ccr8
Cmtm2a
Ccl22
Darc
Cxcr5
Ccl24
Gpr17
Ccl5
Ccr7
C5ar1
Cxcl1
Ccbp2
Cxcl9
Ccl1
Ccl25
Ccl28
Cxcl3
Ccl3
Ccl12
Ccl2
Tgfb1
Ppbp
Cmklr1
Tlr2
Cx3cr1
Tnf
Ccr2
Cx3cl1
Cxcl10
Il1b
Cxcl14
Il6
Validation of gene expression in bulk in vivo tumors by qRT-PCR
RAKD
RCKD
B16-pSMP
IL-6
IL-1β
Tymp
Mll1 (MHC)
CXCL14
CXCL10
IFN-γ
IL-27
CCL12
2-ΔCt
Day 8
Day 12
Day 19

Figure 24. Continued.

(b)

Array ID	Gene name	*In vitro*		*In vivo*		Biological function
		RAKD	RCKD	RAKD	RCKD	
F02	**Darc**	**3.83**	0.49	0.56	0.7	Non-specific receptor for many chemokines such as IL-8, GRO, RANTES, MCP-1 and TARC.
A11	**Ccl24**	**0.22**	0.89	**0.19**	0.63	Chemotactic for resting T-lymphocytes, and eosinophils. Lower for neutrophils. Binds to CCR3.
D07	**Cxcl1**	0.52	**0.25**	0.86	1.42	Chemotactic for neutrophils. Pro-inflammation and exerts its effects on endothelial cells in an autocrine fashion.
B01	**Ccl26**	**9.3**	**0.09**	**0.34**	**0.33**	Chemotactic for eosinophils and basophils. Binds to CCR3.
A01	**C5ar1**	0.92	0.89	0.88	**3.34**	Receptor for the chemotactic and inflammatory peptide anaphylatoxin C5a.
G10	**Tymp**	1.21	1.18	**0.13**	**0.22**	Thymidine Phosphorylase, this gene encodes an angiogenic factor.
A05	**Ccl12**	0.57	**0.48**	**0.4**	1.82	Specifically attracts eosinophils, monocytes and lymphocytes.
D08	**Cxcl10**	0.59	**0.11**	1.5	1.49	Chemotactic for monocytes and T-lymphocytes. Binds to CXCR3.
D12	**Cxcl14**	0.82	0.94	**2.59**	1.12	Potent chemoattractant for neutrophils, and weaker for dendritic cells.
F08	**IL-1b**	1.58	1.08	**2.35**	1.63	Pro-inflammation, thymocyte proliferation, B-cell maturation and proliferation, and fibroblast growth factor activity.
F07	**IL-6**	1.67	1.61	**2.57**	1.4	Pro-inflammation, B-cell maturation and proliferation.
N/A	**IL-27**	N/A	N/A	N/A	N/A	Promotes Th1 cell commitment and IFNγ production. Inhibits Th2 and Th17 differentiation.
N/A	**IFNγ**	N/A	N/A	N/A	N/A	Potent activator of macrophages and NK cells with antiviral and antitumor effects.
N/A	**Mill1**	N/A	N/A	N/A	N/A	MHC class I-likegly glycoprotein encoded outside the MHC, associated with β2-microglobulin.
N/A	**Itgax**	N/A	N/A	N/A	N/A	Also known as Integrin, αX (complement component 3 receptor 4 subunit), or CD11c
H3	**GAPDH**	1	1	1	1	Has glyceraldehyde-3-phosphate dehydrogenase and nitrosylase activities in glycolysis and nuclear functions

(c)

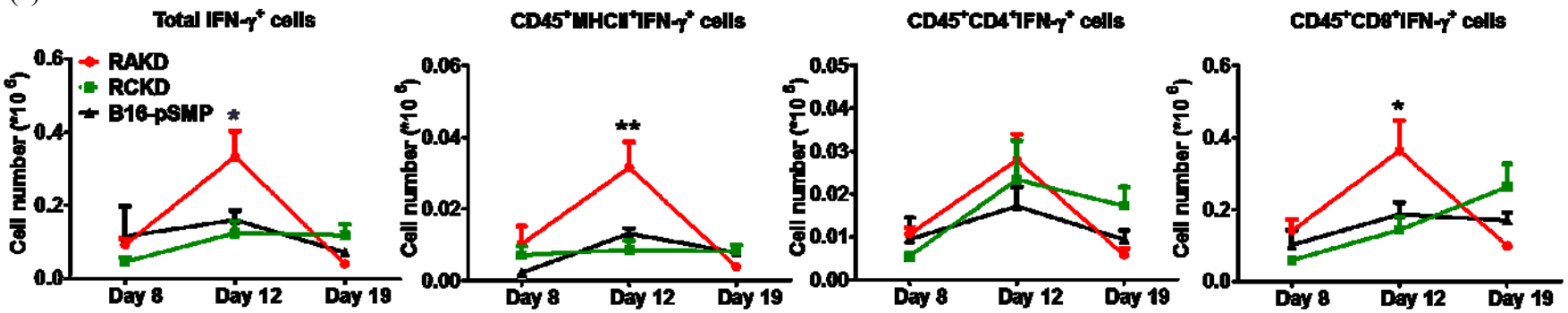

3.2.3 The inflamed TME of B16-RAKD tumors converts host-derived $CD45^-$ cells into $MHCII^+PD\text{-}L1^+$ immunosuppressive cells

Given the broad reduction of different effector cell subsets, I hypothesized that the immunosuppression may be triggered in IL-17RAKD tumors by coinhibitory signals on the APCs within the TME. To this end, I further gated the TILs by their expression levels of CD45 and MHCII (Figure 25a). As expected, the $CD45^+$ immune cells exhibited small cell size on the FSC, while the $CD45^-$ populations that consist of structual cells and tumor cells have relatively larger sizes and higher cellular complexities as indicated by SSC. Surprisingly, there was no significant difference in the frequency of $CD45^+MHCII^+$ APCs among groups. However, the B16-RAKD tumors exhibited a significantly increased frequency of $CD45^-MHCII^+$ cells in the TME. I further examined the origin of these $CD45^-MHCII^+$ cells by innoculating the B16-RAKD cells into wild-type and GFP-knockin mice. Notably, the enriched $CD45^-MHCII^+$ cells were also GFP^+ (Figure 25b), suggesting that these cells were host-derived cells rather than tumor cells. Subsequently, I further screened the co-stimulatory/inhibitory signals on the $CD45^-MHCII^+$ cells, including CD80, CD86, CD40, PD-L1, PD-L2 and Icos-L. Remarkably, $CD45^-MHCII^+$ cells in the TME of B16-RAKD tumors, but not B16-RCKD or the B16-pSMP tumors, markedly increased co-inhibitory PD-L1 expression (Figure 25c), which is consistent with an immunosuppressive profile. All other co-stimulatory/inhibitory signals were not altered in B16-RAKD tumors compared to the controls.

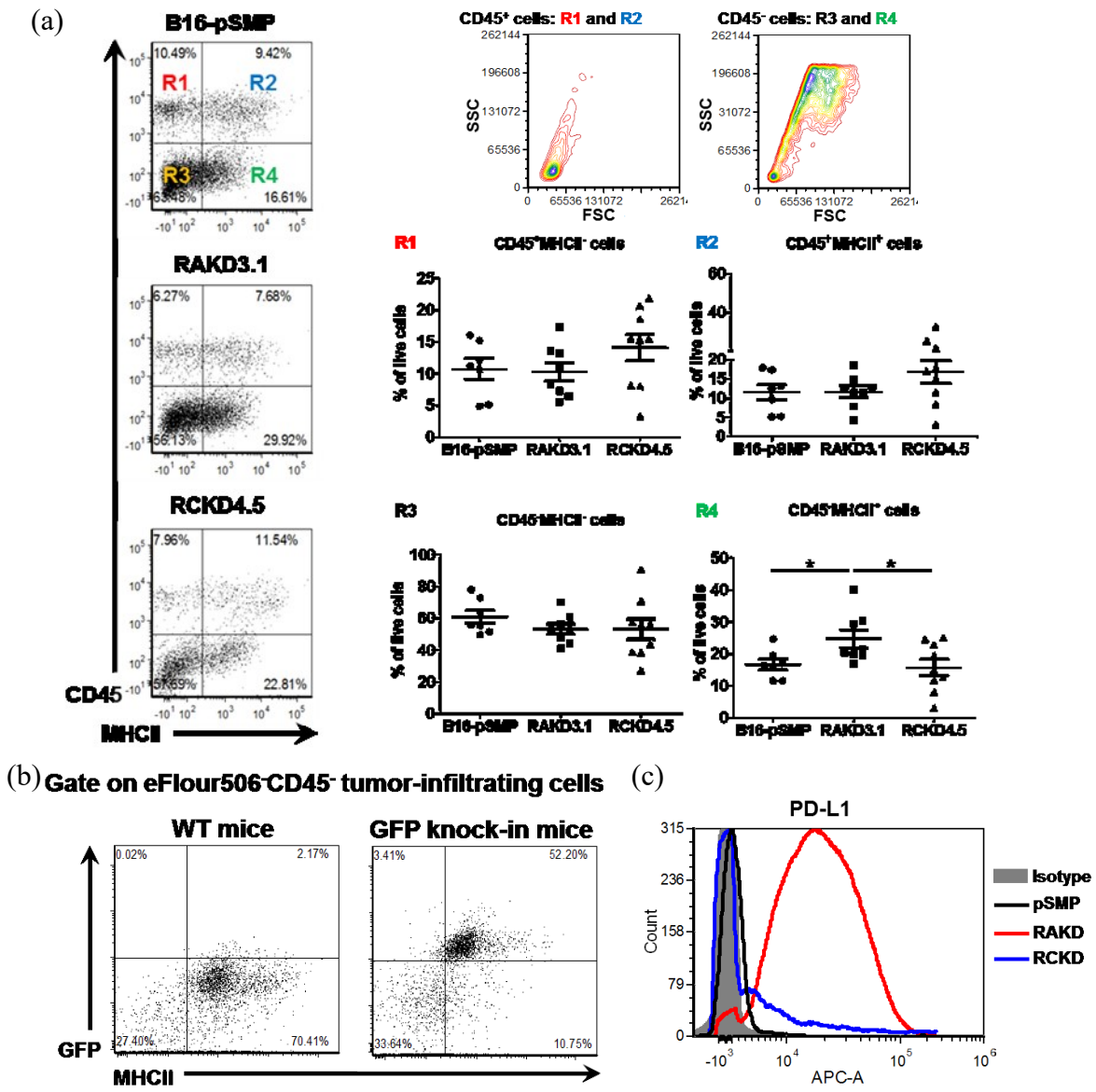

Figure 25. B16-RAKD tumors are enriched with host-derived CD45$^-$MHCII$^+$PD-L1$^+$ cells

Mice were inoculated subcutaneously in the hind flank with B16 melanoma cells. Tumor-derived cells were collected 12 days after tumor cell inoculation. (a) The gating strategy and frequencies of CD45$^{+/-}$MHCII$^{+/-}$ cells were shown. (b) B16-RAKD cells (1 x 10^6) were innoculated subcutaneously into the wild-type and GFP-knockin C57BL/6 mice. On day 12 TILs were harvested and analyzed by flow cytometry. Live CD45$^-$ cells were gated via the Fixable Viability Dye eFluor™ 506 (eFluor506$^-$) to identify whether CD45$^-$MHCII$^+$ cells were derived from the tumor cells or the host recipient and (c) the expression of PD-L1 was examined.

3.2.4 B16-RAKD tumors are enriched with PD-L1/PD-L2$^+$ M2 macrophages

Given that there was no alteration in the frequency of CD45$^+$MHCII$^+$ cells in IL-17R KD tumors comprared to the pSMP controls (Figure 25a), I further assessed the different APC subpopulations, including CD11c$^+$ DCs, F4/80$^+$ macrophages, and CD19$^+$ B cells. As shown in Figure 26, all three APC subpopulations exhibited comparable frequencies among different groups, suggesting that the quantity of APCs is dispensable for the immunosuppression observed in the IL-17R KD tumors. Nevertheless, CD45$^+$MHCII$^+$ APCs in the B16-RAKD tumors, but not B16-RCKD tumors, had markedly increased the expression of PD-L1 and PD-L2. The tumor-infiltrated APCs showed comparable expression levels of both CD80 and CD86 in B16-RAKD and B16-RCKD tumors, while no detectable expression of Icos-L and CD40 was observed. Further sub-population analyses on the APCs suggeted that the elevated PD-L1/L2 expression was due to enriched M2 polarization, but not DCs or B cells. Consistent with the severe immunosuppression in the B16-RAKD, and to a lesser extent in B16-RCKD tumors, the PD-L1/PD-L2 expression levels on tumor-infiltrating macrophages were B16-RAKD > B16-RCKD > B16-pSMP. Taken together, these data suggested that the loss of IL-17RA and IL-17RC in tumor cells triggers an immunosuppresive TME phenotype through both common (pro-inflammatory cytokine production and the quality of tumor-infiltrating macrophages), as well as distinct mechanisms (CD45$^-$MHCII$^+$PD-L1$^+$ host-derived cells uniquely enriched in B16-RAKD tumors).

Figure 26. Enriched PD-L1/L2^{+} M2 polarization in the TME of B16-RAKD tumors. Mice were inoculated subcutaneously in the hind flank with 1 x 10^{6} B16 melanoma cells. TILs were collected 12 days after tumor cell inoculation. Live CD45^{+}MHCII^{+} APCs were gated via the Fixable Viability Dye eFluor™ 506 (eFluor506^{-}). The gating strategy and frequencies of CD19^{+} B cells, F4/80^{+} macrophages and CD11c^{+} DCs are shown. The expression of CD80, CD86, CD40, PD-L1, PD-L2 and Icos-L was analyzed by flow cytometry.

Figure 26.

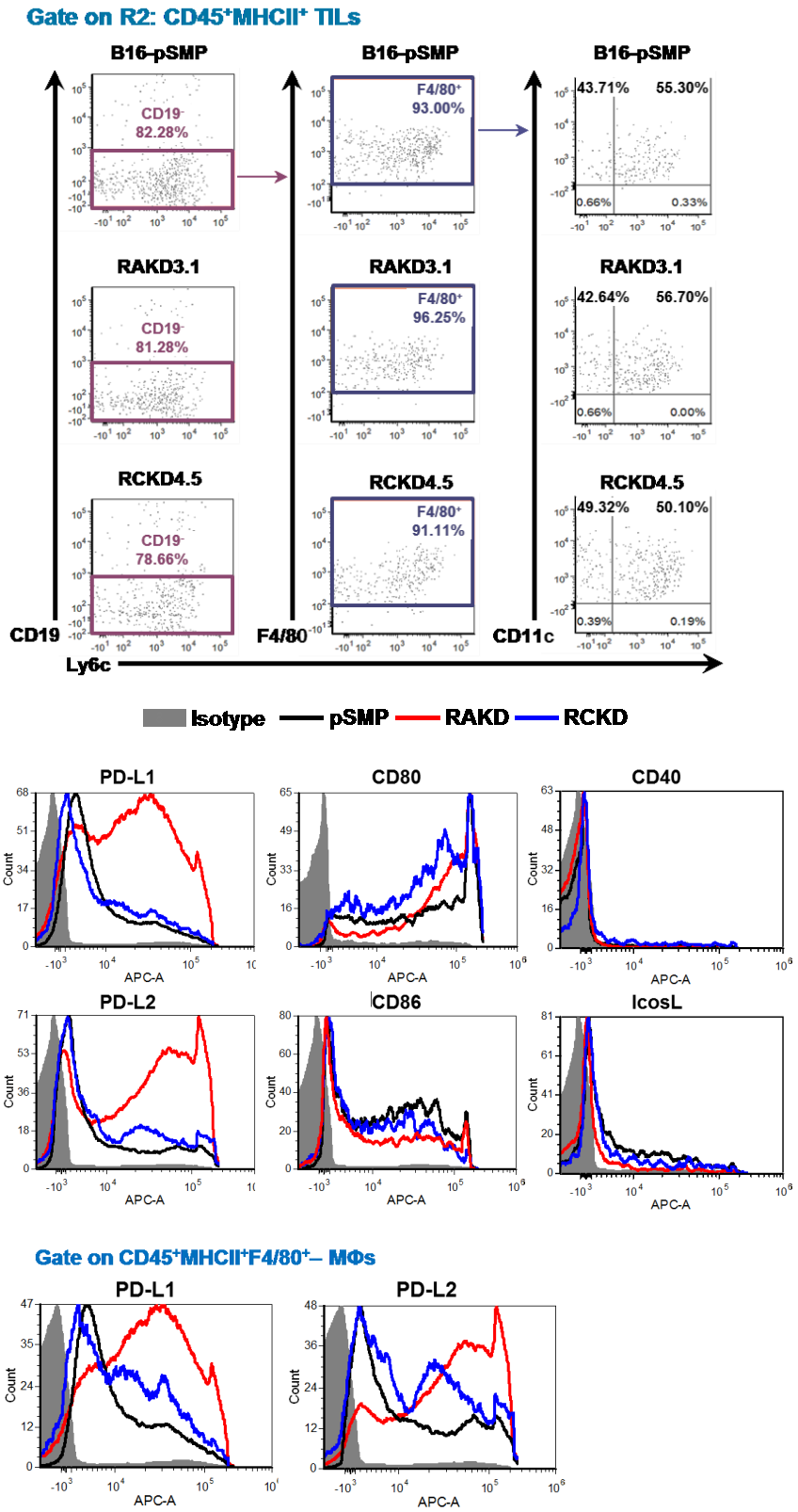
Gate on R2: CD45+MHCII+ TILs
B16-pSMP
RAKD3.1
RCKD4.5
CD19-
82.28%
81.28%
78.66%
F4/80+
93.00%
96.25%
91.11%
43.71%
55.30%
0.66%
0.33%
42.64%
56.70%
0.66%
0.00%
49.32%
50.10%
0.39%
0.19%
CD19
F4/80
CD11c
Ly6c
Isotype
pSMP
RAKD
RCKD
PD-L1
CD80
CD40
PD-L2
CD86
IcosL
Count
APC-A
Gate on CD45+MHCII+F4/80+– MΦs
PD-L1
PD-L2

3.2.5 Loss of baseline IL-17RA expression in 4T1 breast carcinoma cells promotes $Gr1^+CD11b^+$ cells and immunosuppression in blood cells

To validate the immunosuppressive phenotype of IL-17RAKD tumors deserved in the B16 melanoma model, I innoculated 4T1 subclones into BALB/c mice and blood samples were collected from mice at different time points post-innoculation. Peripheral leukocytes were analyzed by flow cytometry. I found that $CD11b^+Gr1^+$ myeloid cells accounted for approximately 14% of peripheral leukocytes in naïve mice. Upon 4T1 cell inoculation, $CD11b^+Gr1^+$ cells progressively increased to 50-60% by day 6 and remained at this level at day 18 (Figure 27). Notably, IL-17RA KD 4T1 cells significantly increased the frequency of $CD11b^+Gr1^+$ myeloid cells in the blood to 80% at day 18 post-innoculation. Conversely, the frequency of circulating lymphocytes (T cells, B cells, and NK cells) was markedly reduced compared to the pSMP control group. Since myeloid cells are a heterogeneous population of granulocytic and monocytic cells, I further analyzed subpopulations in my model. I found that the main subpopulation induced by 4T1 tumors were granulocytic cells ($CD11b^+Ly6C^{low}Ly6G^+$), but not monocytic cells ($CD11b^+Ly6C^+Ly6G^{-/low}$), which increased in frequency and absolute cell number. Given that both IL-17RAKD and IL-17RCKD tumors exhibited increased tumor growth in the 4T1 model, I expected a similar immunosuppressive phenotype within 4T1-RCKD tumors. However, in sharp contrast, the IL-17RC KD in 4T1 cells significantly reduced the frequency of $CD11b^+Gr1^+$ cells in blood as early as six days following tumor injection, suggesting that the IL-17RC signal may meditate immunosuppression through distinct mechanism(s). To confirm the causal link between the increased $CD11b^+Gr1^+$ cells and the decreased effector cells (e.g., T cells), a suppression assay using co-cultured cell populations is needed. Furthermore, although the IL-17A-induced immunosuppressive TME of 4T1 tumors has been reported in previous work in our lab using adenovirus to overexpress IL-17A (187), further studies will be required to validate and explore the IL-17RA versus IL-17RC signals in shaping the immunosuppression in 4T1 tumors.

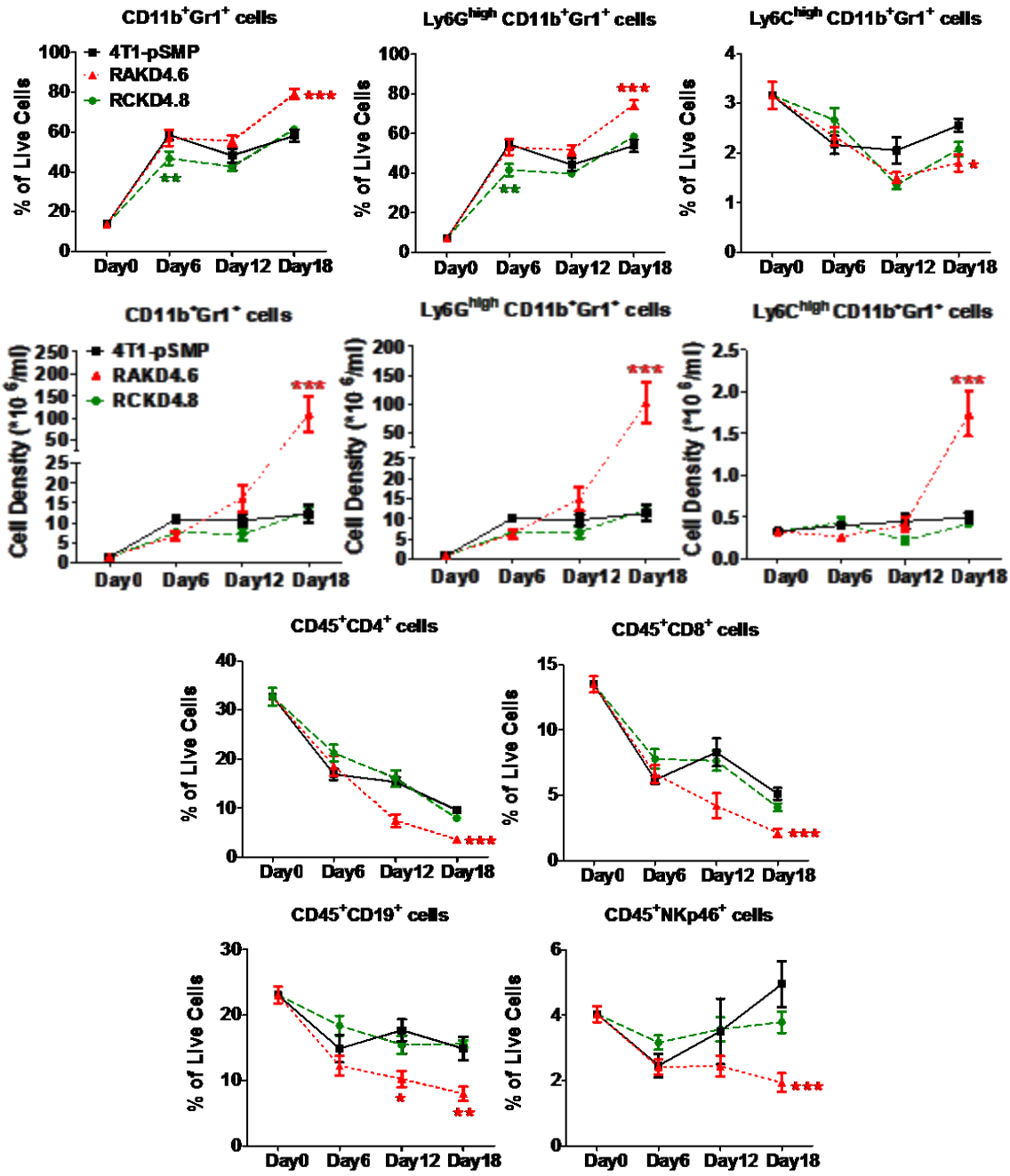

Figure 27. IL-17RAKD 4T1 cells preferentially induce the expansion of granulocytic myeloid cells in peripheral blood.

Mice were inoculated subcutaneously in the fourth mammary fat pad of female BALB/c mice with 1 x 10^6 4T1 mammary carcinoma cells. Frequency and cell density of granulocytic and monocytic subpopulations in $CD45^+$ peripheral blood leukocytes are shown. All values are means ± SEM of n = 10 mice per group per at each time point. Statistical analyses were compared with the pSMP control using Kruskal-Wallis test; *$p < 0.05$; **$p < 0.01$; ***$p < 0.001$.

3.3 Prognostic value of IL-17RA and A20 in cancer patients

Given the role of baseline IL-17R expression in maintaining A20 homeostasis in murine cells, I questioned whether my finding could be verified in human cancers. If yes, which cancer types are likely to adopt a regulatory mechanism that is controlled by the IL-17R/A20 axis, and can the IL-17RA/A20 axis be used as a prognostic and/or predictive marker for human cancers. To this end, I performed gene copy number and expression analyses on datasets from clinical studies and human cell lines, together with human tissue arrays, to establish a comprehensive picture of the relationship between IL-17/IL-17R and A20 expression in various human neoplasms.

3.3.1 IL-17RA is co-expressed with A20 and bi-directionally altered in a subset of human cancers

Given that IL-17RA and IL-17RC have differential tissue distribution (321), I first determined whether the somatic copy number levels of IL-17RA and IL-17RC are altered in human cancers. To this end, I queried publicly available TCGA datasets in cBioportal and conducted cross-cancer genome-wide analysis of somatic copy number alterations (CNA) for IL-17RA and IL-17RC. I found bi-directional CNA of IL-17RA and IL-17RC in 22 and 24 out of 32 human cancer types, respectively (Figure 28a). Besides amplification or gain of copies, many cancer types also showed deletions of IL-17RA and/or IL-17RC. Among all examined cancer types, IL-17RA exhibited higher frequencies of deletion compared to IL-17RC, especially in chronic inflammation associated cancers of the mucosal system, including esophageal cancer, lung cancer, stomach (gastric) cancer, CRC, cervical cancer, breast cancer and melanoma, suggesting a role for IL-17RA in cancer biology and a molecule with strong prognosis. Notably, while most cancer types are associated with both gain and deletion of IL-17RA and IL-17RC, a cohort of CRC patients (n = 633) showed a predominant IL-17RA and IL-17RC deletion profile. I sub-grouped these patients based on their IL-17R and A20 CNA profiles. While the majority of the CRC patients carried a normal diploid profile, patients with co-deletion of IL-17RA/A20 (n = 43), or IL-17RC/A20 (n = 21), were identified in this CRC-TCGA dataset (Figure 28b).

Figure 28. Somatic copy numbers of IL-17RA and IL-17RC are bi-directionally altered in a fraction of human cancers in a cancer-type-specific manner.

(a) Cross-cancer analyses of IL-17RA/RC copy number alteration (CNA) frequency in 32 TCGA studies from cBioportal. Blue indicates deep loss of gene copy number, possibly a homozygous deletion. Red indicates a high-level amplification of gene copy number. (b) CNA of A20 grouped by CNA of IL-17RA or IL-17RC in CRC-TCGA dataset from cBioportal. N = 633. Each dot represents 10 patients. ACC, adrenocortical carcinoma; AML, acute myeloid leukemia; GBM, glioblastoma multiforme; PCPG, pheochromocytoma and paraganglioma; ccRCC, clear cell renal cell carcinoma; chRCC, chromophobe renal cell carcinoma; pRCC, papillary renal cell carcinoma; Lung squ, lung squamous cell carcinoma; DLBC, diffuse large b-cell lymphoma; Uterine CS, uterine carcinosarcoma.

(a)

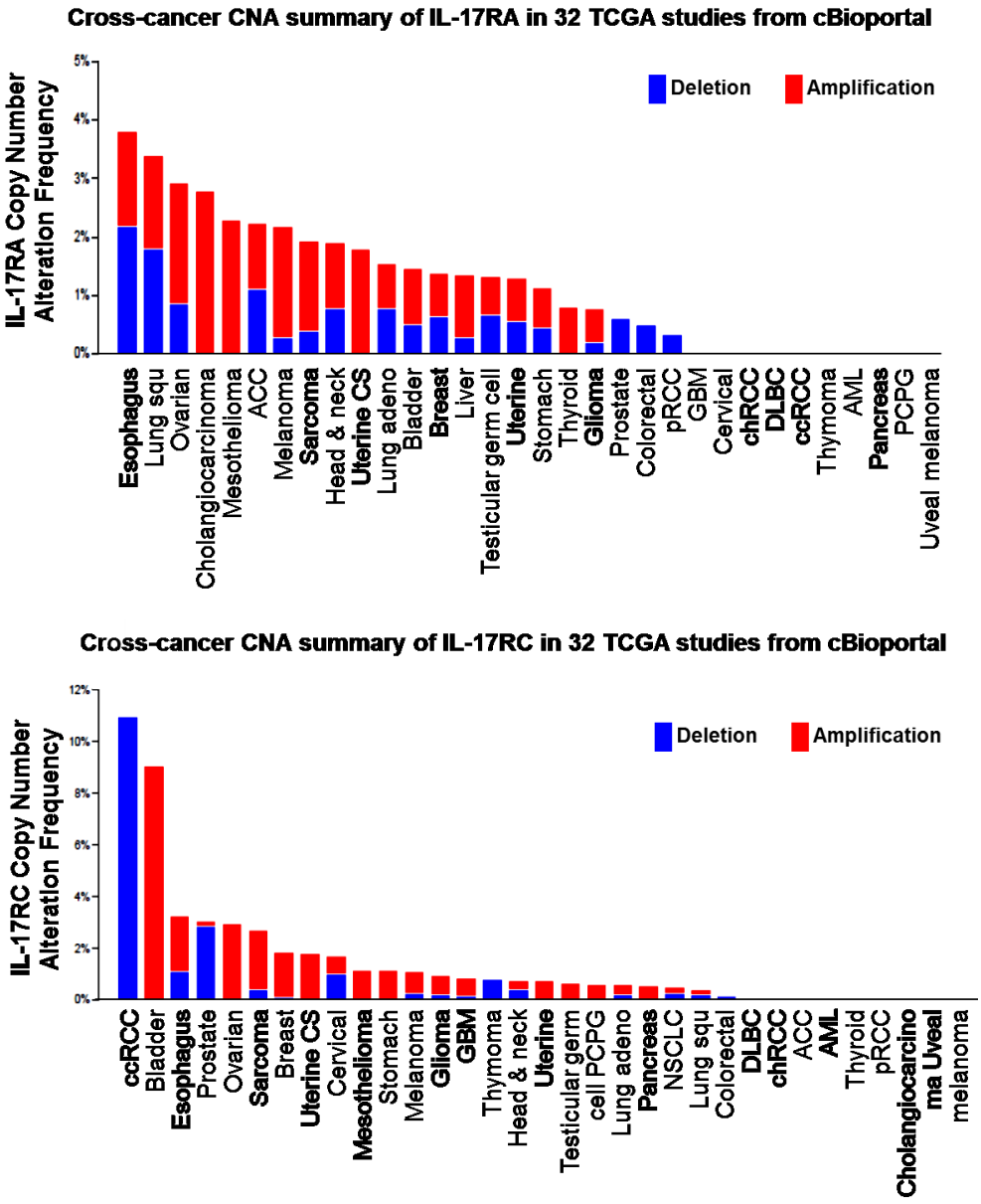
Cross-cancer CNA summary of IL-17RA in 32 TCGA studies from cBioportal
IL-17RA Copy Number Alteration Frequency
Deletion
Amplification
5%
4%
3%
2%
1%
0%
Esophagus
Lung squ
Ovarian
Cholangiocarcinoma
Mesothelioma
ACC
Melanoma
Sarcoma
Head & neck
Uterine CS
Lung adeno
Bladder
Breast
Liver
Testicular germ cell
Uterine
Stomach
Thyroid
Glioma
Prostate
Colorectal
pRCC
GBM
Cervical
chRCC
DLBC
ccRCC
Thymoma
AML
Pancreas
PCPG
Uveal melanoma

Cross-cancer CNA summary of IL-17RC in 32 TCGA studies from cBioportal
IL-17RC Copy Number Alteration Frequency
Deletion
Amplification
12%
10%
8%
6%
4%
2%
0%
ccRCC
Bladder
Esophagus
Prostate
Ovarian
Sarcoma
Breast
Uterine CS
Cervical
Mesothelioma
Stomach
Melanoma
Glioma
GBM
Thymoma
Head & neck
Uterine
Testicular germ cell
PCPG
Lung adeno
Pancreas
NSCLC
Lung squ
Colorectal
DLBC
chRCC
ACC
AML
Thyroid
pRCC
Cholangiocarcino ma
Uveal melanoma

(b)

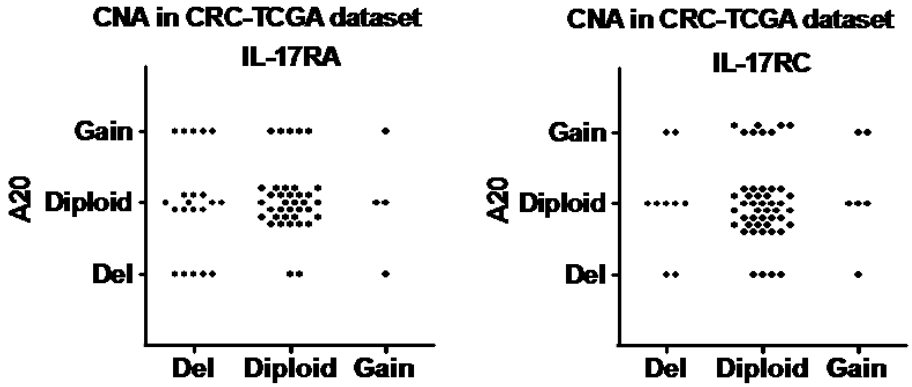
CNA in CRC-TCGA dataset
IL-17RA
A20
Gain
Diploid
Del
Del
Diploid
Gain
CNA in CRC-TCGA dataset
IL-17RC
A20
Gain
Diploid
Del
Del
Diploid
Gain

I downloaded and analyzed the mRNA gene expression data for IL-17RA and A20 from two additional searchable human cancer databases, Oncomine (Table 8) and GEO-NCBI (Table 9). A total of 59 datasets covering 20 types of cancer and normal tissues were identified based on my selection criteria (see Materials and Methods section). The two databases are highly complementary with only 5 overlapping datasets. In agreement with what I have in cBioportal datasets, IL-17RA mRNA expression also displayed bi-directional alterations in different cancer types (Table 8, 9). For example, melanoma samples exhibited a very broad range of IL-17RA expression (APPENDIX B) and no change observed in samples compared to normal counterparts (Table 8, 9). Breast and lung cancers were found to have decreased expression in some datasets, but significantly increased expression or no change in other datasets. Nevertheless, while IL-17RA expression is highly upregulated in pancreatic cancer to favor the IL-17R-dependent inflammatory responses, the downregulation of IL-17RA expression is consistently and significantly observed in all CRC datasets in both database systems (Table 8, 9).

Based on my novel finding that IL-17R expression is critically required for maintaining A20 homeostasis in cancer cells, I further examined the correlation of IL-17RA and A20 in different human cancers. Indeed, the mRNAs of IL-17RA and A20 were consistently co-expressed in many clinical samples, especially colorectal, gastric, lung and pancreatic cancers (Table 8, 9). Nevertheless, in some other cancer types, such as breast, adrenal, liver, thyroid, vulva cancers and melanoma, no significant co-expression pattern was consistently observed (Table 8, 9). Furthermore, IL-17RA and A20 are negatively correlated in prostate and head-neck cancers, suggesting the co-expression of IL-17RA and A20 is a tumour-specific phenomenon, which might be influenced by the IL-17R/A20 axis within the specific TME. Overall, the level of A20 was significantly correlated with IL-17RA expression in 17 out of 33 GEO-NCBI datasets (51.5%) and 11 out of 15 cancer types in Oncomine analyses (73.3%), which strongly supports my finding that IL-17R is critical in maintaining the homeostatic level of A20 in many human cancer types.

3.3.2 IL-17RA is significantly co-expressed with A20 and reduced in human CRC samples

Consistent with genome-wide CNA analysis presented above, CRC samples were repeatedly found to have significant co-expression between A20 and IL-17RA from

various datasets (Table 8, 9 and Figure 29), demonstrating that the IL-17R/A20 axis may play an important role in human CRC development.

The GEO-NCBI dataset GDS2947 contains 32 colorectal adenomas and 32 paired normal colorectal tissues, an ideal dataset for examining how the IL-17R and A20 may change during CRC development in an unbiased manner. Importantly, the overall levels of both IL-17RA and A20 were significantly reduced in CRC samples compared to their normal counterparts (Figure 29a), supporting a notion that the specific CRC tumor microenvironment reduces IL-17RA expression leading to attenuated baseline A20 production. Nevertheless, 7 and 4 out of 32 paired samples exhibited an increase in the IL-17RA and A20 levels in CRC, respectively, suggesting tumor-specific regulation of the IL-17RA/A20 axis. The Oncomine analysis which compiled all 5 available CRC studies exhibited a reduced overall IL-17RA level of CRC samples compared to normal colorectal tissues (Figure 29b), as well as a significant co-expression of IL-17RA and A20 (Pearson $R=0.4803$, $P<0.0001$; Spearman $R=0.4878$, $P<0.0001$). Importantly, the significant co-expression of IL-17RA and A20 was in agreement with the CRC-TCGA dataset from cBioportal (Pearson $R= 0.3655$, $p< 0.0001$; Spearman $R= 0.3398$, $p= 0.0001$) (Figure 29c). Together, CRC samples from all three databases consistently showed a clear co-reduction of IL-17RA and A20, highlighting a potential role of the IL-17RA/A20 axis in CRC development. Subsequently, I examined whether other pro-inflammatory signals, such as IL-1R1, TNFR1, MyD88 and TLR4 may also associate with the basal level of A20. My analyses indicated that IL-1R1, TNFR1 and MyD88 mRNA expression levels were significantly but relatively weakly correlated with A20 expression, whereas TLR4 appeared to be inversely correlated. Thus, my data strongly suggests that baseline IL-17RA level has a predominant role in maintaining basal A20 level in human CRC.

Figure 29. IL-17RA is significantly co-expressed with A20 and reduced in CRC patients.

(a) Relative mRNA expression of IL-17RA and A20 in normal and cancer tissues was quantified using the GEO-NCBI (GDS2947) database. (b) IL-17RA and A20 expression levels in a total of five CRC studies are quantified from Oncomine datasets and their co-expression was determined by Pearson and Spearman correlation analysis. (c) IL-17RA expression from the CRC-TCGA dataset were correlated with respective A20 expression levels. (d) Correlations of A20 with IL-17RA, IL-1R1, TNFR1, MyD88 and TLR4 mRNAs that are quantitated using the GEO-NCBI (GDS2947) dataset. Statistical analyses on relative expressions were compared with the respective normal tissue using an unpaired student t test for panel b, and paired student t test for panel a. *$p < 0.05$; ** $p < 0.01$; *** $p < 0.001$.

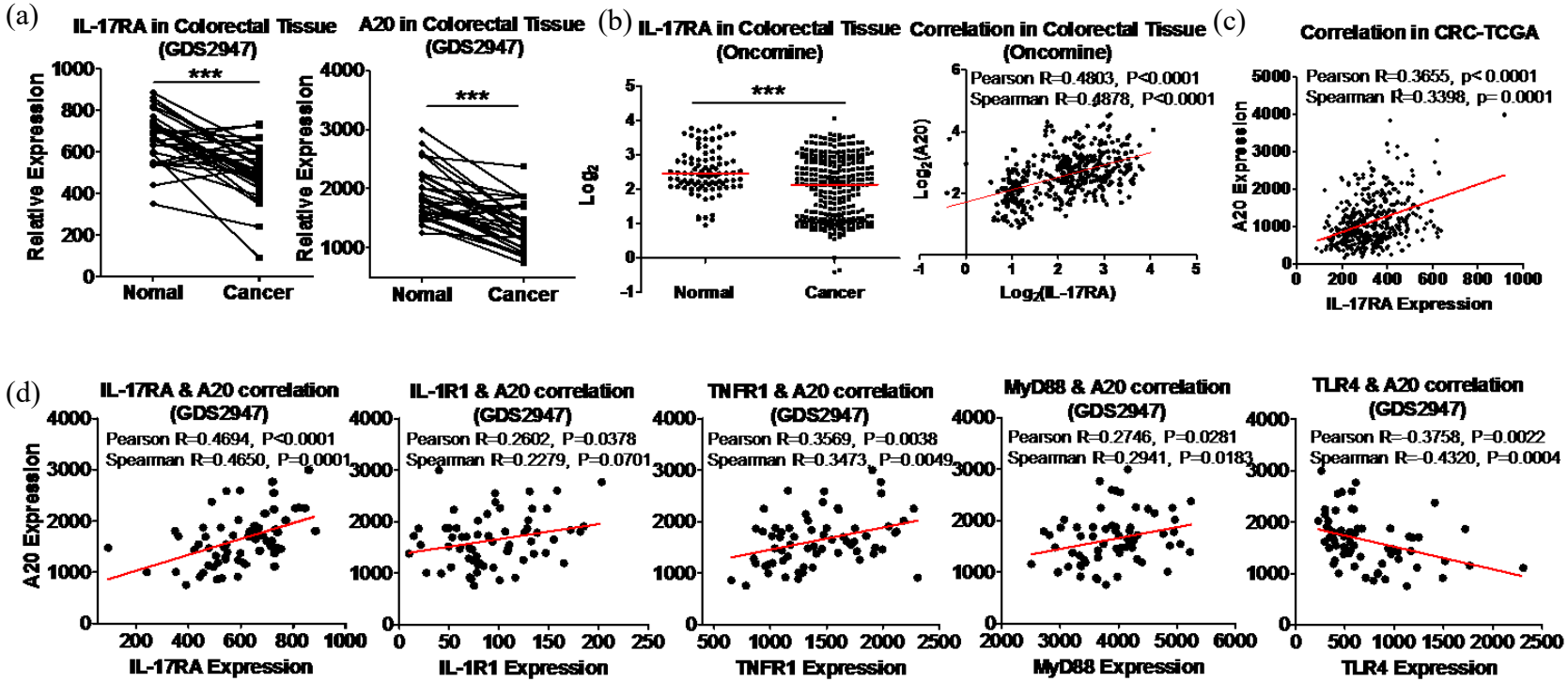
(a)
IL-17RA in Colorectal Tissue (GDS2947)
A20 in Colorectal Tissue (GDS2947)
Relative Expression
***
Nomal
Cancer
(b)
IL-17RA in Colorectal Tissue (Oncomine)
Correlation in Colorectal Tissue (Oncomine)
Log2
Pearson R=0.4803, P<0.0001
Spearman R=0.4878, P<0.0001
Log2(A20)
Log2(IL-17RA)
(c)
Correlation in CRC-TCGA
Pearson R=0.3655, p< 0.0001
Spearman R=0.3398, p= 0.0001
A20 Expression
IL-17RA Expression
(d)
IL-17RA & A20 correlation (GDS2947)
Pearson R=0.4694, P<0.0001
Spearman R=0.4650, P=0.0001
IL-1R1 & A20 correlation (GDS2947)
Pearson R=0.2602, P=0.0378
Spearman R=0.2279, P=0.0701
TNFR1 & A20 correlation (GDS2947)
Pearson R=0.3569, P=0.0038
Spearman R=0.3473, P=0.0049
MyD88 & A20 correlation (GDS2947)
Pearson R=0.2746, P=0.0281
Spearman R=0.2941, P=0.0183
TLR4 & A20 correlation (GDS2947)
Pearson R=-0.3758, P=0.0022
Spearman R=-0.4320, P=0.0004
A20 Expression
IL-17RA Expression
IL-1R1 Expression
TNFR1 Expression
MyD88 Expression
TLR4 Expression

Figure 29.

Table 8. Gene expression of Oncomine datasets used in this study

Sample Type	Dataset Count	Sample Count	P & R Values of IL-17RA & A20 Correlation Pearson	Spearman	IL-17RA Expression in Cancer	Dataset Source	References
All	30	4505	<0.0001, 0.3479	<0.0001, 0.3241	0.0001, ***, ↓	Oncomine	
Adrenal cancer	1	65	0.7956, 0.0328	0.9609, 0.0062	0.3140	Oncomine	(447)
Brain cancer	2	281	<0.0001, 0.2681	<0.0001, 0.3160	0.0099, **, ↑	Oncomine	(448, 449)
Breast cancer	3	99	0.2719, -0.1115	0.3397, -0.0970	0.2855	Oncomine	(450-452)
Colorectal cancer	5	396	<0.0001, 0.4803	<0.0001, 0.4878	<0.0001, ***, ↓	Oncomine	(424, 453-455)
Gastric cancer	2	96	<0.0001, 0.4507	<0.0001, 0.4876	0.0586	Oncomine	(456, 457)
Head-Neck cancer	2	79	<0.0001, -0.4389	<0.0001, -0.4334	0.6149	Oncomine	(458, 459)
Liver cancer	1	75	0.8157, -0.0274	0.8709, 0.0191	0.0988	Oncomine	(460)
Lung cancer	3	452	<0.0001, 0.8443	<0.0001, 0.7530	0.0220, *, ↑	Oncomine	(461-463)
Melanoma	1	86	0.0475, 0.2144	0.0607, 0.2031	0.2058	Oncomine	(464)
Multi-cancer	1	84	0.0516, 0.2131	0.0228, 0.2482	<0.0001, ***, ↑	Oncomine	(465)
Pancreatic cancer	2	130	<0.0001, 0.6079	<0.0001, 0.5390	<0.0001, ***, ↑	Oncomine	(466, 467)
Prostate cancer	2	40	0.0106, 0.3999	0.0083, 0.4114	0.9484	Oncomine	(468, 469)
Renal cancer	1	67	0.0053, 0.3369	0.0573, 0.2334	0.0166, *, ↑	Oncomine	(470)
Thyroid cancer	2	36	0.4105, 0.1415	0.2867, 0.1825	0.3846	Oncomine	(471, 472)
Uterus cancer	1	77	0.0077, 0.3015	0.0065, 0.3079	0.5508	Oncomine	(473)
Vulva cancer	1	19	0.0795, 0.4122	0.0726, 0.4211	0.1089	Oncomine	(474)

Note: N/A, not applicable. ↑, up-regulation. ↓, down-regulation.

Table 9. Gene expression of GEO-NCBI datasets used in this study

Dataset ID	Sample Type	Sample Count	Case Nationality	P value of IL-17RA in Cancer	Pearson P value of A20 Correlation					Ref
					IL-1R1	MyD88	TLR4	TNFR1	IL-17RA	
GDS4456	Bladder cancer	93	New York, USA	N/A	0.3166	0.0148, *	0.0121, *	0.623	0.0197, *	(475)
GDS3096	Breast cancer	47	Maryland, USA	N/A	0.1497	0.0728	0.9299	0.993	0.0016, **	(476)
GDS2250	Breast cancer	47	Boston, USA	0.0336, ↓	0.5278	0.0298, *	0.0657	0.0159, *	0.3412	(477)
GDS3139	Breast cancer	29	Boston, USA	0.0094, ↑	0.7707	0.0331, *	0.4868	0.7604	Reverse, 0.0249, *	(478)
GDS3716	Breast cancer	42	Boston, USA	N/A	0.6849	0.264	0.6541	0.0662	Reverse, 0.0017, **	(479)
GDS4761	Breast cancer	91	Sweden	N/A	0.0051, **	<0.0001, ***	<0.0001, ***	N/A	<0.0001, ***	(480)
GDS2416	Cervical cancer	33	Toronto, Canada	N/A	0.2545	0.5447	0.0002, ***	0.1797	0.8052	(481)
GDS3233	Cervical cancer	61	New York, USA	0.1872	0.1084	0.0002, ***	0.8936	0.4854	0.372	(482)
GDS3292	Cervical cancer	38	New York, USA	0.8600	0.8777	0.7782	0.8011	0.4694	0.0254, *	(483)
GDS4664	Cervical cancer	39	Groningen/Netherlands	N/A	0.0417, *	0.0139, *	0.7632	0.1089	0.404	(484)
GDS2947	Colorectal cancer	64	Viterbo, Italy	<0.0001, ↓, #	0.0378, *	0.0281, *	Reverse, 0.0022, **	0.0038, **	<0.0001, ***	(424)
GDS4379	Colorectal cancer	62	N/A	N/A	0.4354	0.6497	0.0221, *	0.0078, **	0.1205	(485)
GDS4381	Colorectal cancer	64	Durham, USA	N/A	<0.0001, ***	0.1124	0.1073	<0.0001, ***	<0.0001, ***	(486)
GDS4382	Colorectal cancer	34	Tokyo, Japan	0.0119, ↓, #	0.3806	0.679	0.1133	0.9014	0.4532	(487)
GDS4515	Colorectal cancer	49	Finland	0.0035, ↓	0.5376	0.9922	0.0518	0.5833	0.8321	(488)
GDS4516	Colorectal cancer	104	Tokyo, Japan	N/A	0.1745	0.4946	0.5437	0.0221, *	0.0005, ***	(489)
GDS4718	Colorectal cancer	44	Tokyo, Japan	N/A	0.0448, *	0.8147	0.467	0.2672	0.4341	(489)
GDS4513	Colon cancer	53	Berlin, Germany	N/A	0.0015, **	0.0111, *	0.8304	0.0008, ***	0.0104, *	(490)
GDS4589	Endometrial cancer	103	Durham, USA	0.0087, ↑	0.5648	0.0005, ***	0.5679	0.0002, ***	0.8085	(491)
GDS4198	Gastric cancer	70	Australia	N/A	0.052	0.0344, *	0.0248, *	0.0789	0.0231, *	(492)
GDS2771	Lung cancer	192	USA/Germany/Ireland	0.0072, ↓	<0.0001, ***	<0.0001, ***	0.1428	0.9848	0.3753	(493)

Table 9 (continued).

Dataset ID	Sample Type	Sample Count	Case Nationality	P value of IL-17RA in Cancer	Pearson P value of A20 Correlation					Ref
					IL-1R1	MyD88	TLR4	TNFR1	IL-17RA	
GDS3837	Lung cancer	120	Taiwan	0.0032, ↓, #	0.057	<0.0001, ***	0.0006, ***	<0.0001, ***	<0.0001, ***	(494)
GDS4794	Lung cancer	65	Japan	0.0046, ↓, #	0.0715	<0.0001, ***	<0.0001, ***	0.003, **	<0.0001, ***	(495)
GDS3966	Melanoma	83	Massachusetts, USA	N/A	0.7739	0.0004, ***	0.0303, *	0.1004	0.0928	(496)
GDS4281	Melanoma	29	Genoa, Italy	N/A	0.6841	0.0317, *	0.8614	0.0591	0.9232	(497)
GDS3341	Nasopharyngeal cancer	41	Taiwan	0.0388, ↑	Reverse, 0.0028, **	0.7148	0.6853	0.8856	0.5526	(498)
GDS3592	Ovarian cancer	24	Atlanta, USA	0.0010, ↑	0.1025	0.0183, *	0.768	0.9371	0.6502	(499)
GDS4102	Pancreatic cancer	52	Rochester, USA	0.7217	0.0617	0.0001, ***	0.0166, *	0.0072, **	0.0085, *	(467)
GDS4103	Pancreatic cancer	78	Romania/Germany	0.0453, ↑	<0.0001, ***	<0.0001, ***	<0.0001, ***	<0.0001, ***	<0.0001, ***	(466)
GDS4329	Pancreatic cancer	24	Belgium	0.1868, #	N/A	0.0029, **	0.1605	0.5389	0.0085, *	(500)
GDS4109	Prostate cancer	79	New York, USA	N/A	0.4338	0.1517	0.4025	0.218	0.6686	(501)
GDS4824	Prostate cancer	21	Boston, USA	0.0105, ↓	0.3425	0.7269	0.4938	0.0055, **	0.0826	(468)
GDS1096	Normal tissues	36	Japan	N/A	0.0005, ***	0.0035, **	0.3584	0.0383, *	0.0072, **	(502)

Note: N/A, not applicable. ↑, up-regulation. ↓, down-regulation. #, statistical analyses were compared with the respective normal tissue using paired *t* test.

3.3.3 IL-17RA protein is significantly reduced in high grade CRC tumors, correlating with a poor clinical outcome

To identify the clinical impact of alterations in the IL-17RA-A20 axis in CRC, I analyzed the CRC-TCGA dataset from cBioportal for Cancer Genomics (Figure 30). Importantly, CRC patients with either shallow heterozygous or homozygous copy number (CN) deletions of IL-17RA (n = 198) exhibited a significantly poorer overall 5-year survival rate ($p = 0.01$) compared to the patients with normal IL-17RA levels (n = 373) (Figure 30a). An absolute 5-year survival rate in this cohort of CRC patients with an IL-17RA-deletion or normal IL-17RA was calculated as 44% and 66%, respectively. Patients with an IL-17RA CN deletion had an estimated median survival of 51.45 months. Those patients without deletions did not reach 50% mortality by 60 months. In agreement with the CNA profile, CRC patients with downregulation of IL-17RA mRNA, albeit a small sample size (n = 12), also exhibited significantly decreased OS ($p = 0.0004$) compared to those without mRNA alterations (n = 597). Similar to IL-17RA, CRC patients with a CN deletion of A20 (n = 73) also displayed a poor overall 5-year survival rate compared to their normal counterparts ($p = 0.01$) (Figure 30b). Importantly, patients with a double-deletion of IL-17RA and A20 (n = 43) had a reduction in median survival of 45.37 months (Figure 30c), suggesting a synergistic value of IL-17RA and A20 in CRC prognosis. Finally, patients with CN deletion of IL-17RC alone (n = 84) or in combination with A20 (n = 21) displayed significantly worse clinical outcomes compared to their normal counterparts (Figure 30d). Notably, patients with CN amplification of IL-17RA, IL-17RC and/or A20 showed a trend, but no significance due to small number, toward worse overall survival compared to their counterparts with a normal CN profile.

Finally, I wanted to verify IL-17RA protein expression in human tissue arrays by IL-17RA immunohistochemical staining (Figure 31). Four different CRC tissue arrays with clear histological grading assessments were subjected to IL-17RA staining. Colon tissue derived from normal human colon or normal tissue adjacent to the tumor samples were included in all tissue arrays. These controls had comparable IL-17RA staining and were grouped together in my analyses. Notably, only marginal IL-17RA staining was detected on inflammatory cellular infiltrates. I found that IL-17RA staining was comparable between low grade (I and II) CRC samples and normal/adjacent samples. However, IL-

17RA staining was significantly decreased in high grade CRC tumors in both female and male patients (Figure 31a/b). Of note, IL-17RA staining level displayed an interesting distribution profile in different stages of CRC (Figure 31c/d). In normal/adjacent tissue samples, approximately 70% had a normal range (7-29%) of IL-17RA staining, and the remaining 30% of samples showed a low range of IL-17RA staining (0-7%). This distribution profile was highly maintained in stage I CRC samples, but bi-directionally altered in later stages of CRC samples. One one hand, samples with a high range of IL-17RA staining (>30%) were consistently observed in stage II, III and IV, as well as metastatic tumors. On the other hand, the fraction of low range IL-17RA staining in stage III samples was markedly increased, which accounted for at least 50% of stage III samples I examined. Of interest, there was no single stage IV sample or metastatic sample expressing a low range of IL-17RA. While the data may indicate a stage-dependent control of IL-17RA expression, it is possible that low sample size might be responsible for the observation.

The location of CRC tumors is recognized as a criteria for establishing prognosis in all stages of diseases (503, 504). To this end, I compared IL-17RA protein expression between right colonic (ascending colon) and left colonic (descending colon and sigmoid colon) samples (Figure 31e). In agreement with the clinical observation that left colon CRC patietns have poor clinical outcomes (505), tumor samples in left colon showed significantly reduced IL-17RA staining compared to tumors on the right colon. Collectively, IL-17RA expression was consistently demonstrated to be bi-directionally altered at the CN, mRNA and protein levels in CRC tumor samples. Given the deletion of IL-17RA is associated with high grade CRC tumors and poorer overall 5-year survival, IL-17RA/A20 status could be used as a potential prognostic biomarker in CRC.

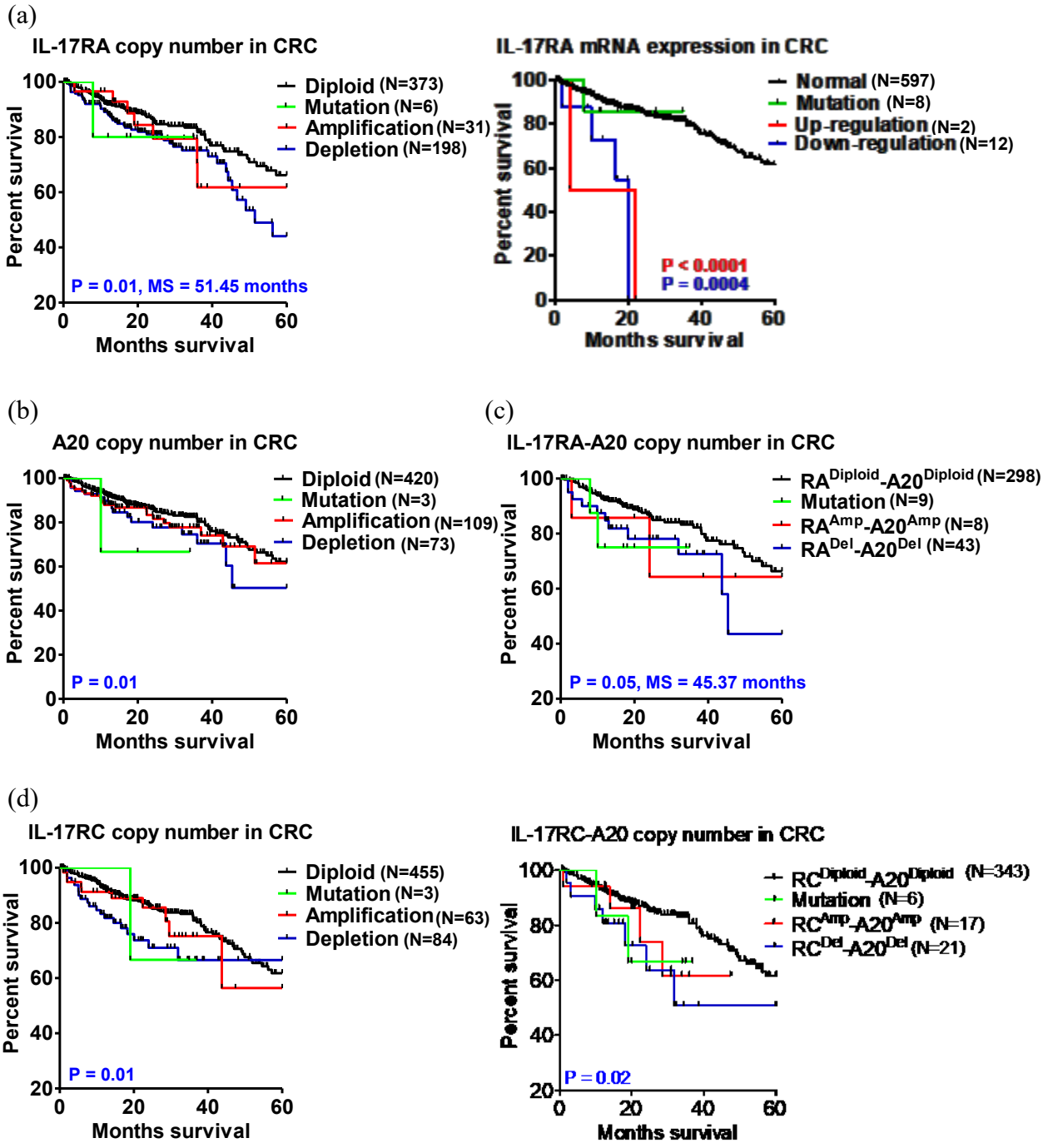

Figure 30. Altered IL-17R/A20 copy number level in CRC patients is associated with poor survival rate.

Five year overall survival of patients with CRC is analyzed with IL-17RA CNA, IL-17RA mRNA, A20 CNA, IL-17RA/A20 CNA, IL-17RC CNA, and IL-17RC/A20 CNA.

Figure 31. IL-17RA protein level is significantly reduced in high grade CRC tumors. (a-d) Quantitative results and representative images of IL-17RA protein levels observed in normal and cancerous colon tissues by immunohistochemistry. The solid red line indicates the median in panel b/c/e. Statistical analyses were compared using Kruskal-Wallis test for b/c or Mann Whitney test for (e). ND. no significant differences. *$p < 0.05$; ** $p < 0.01$.

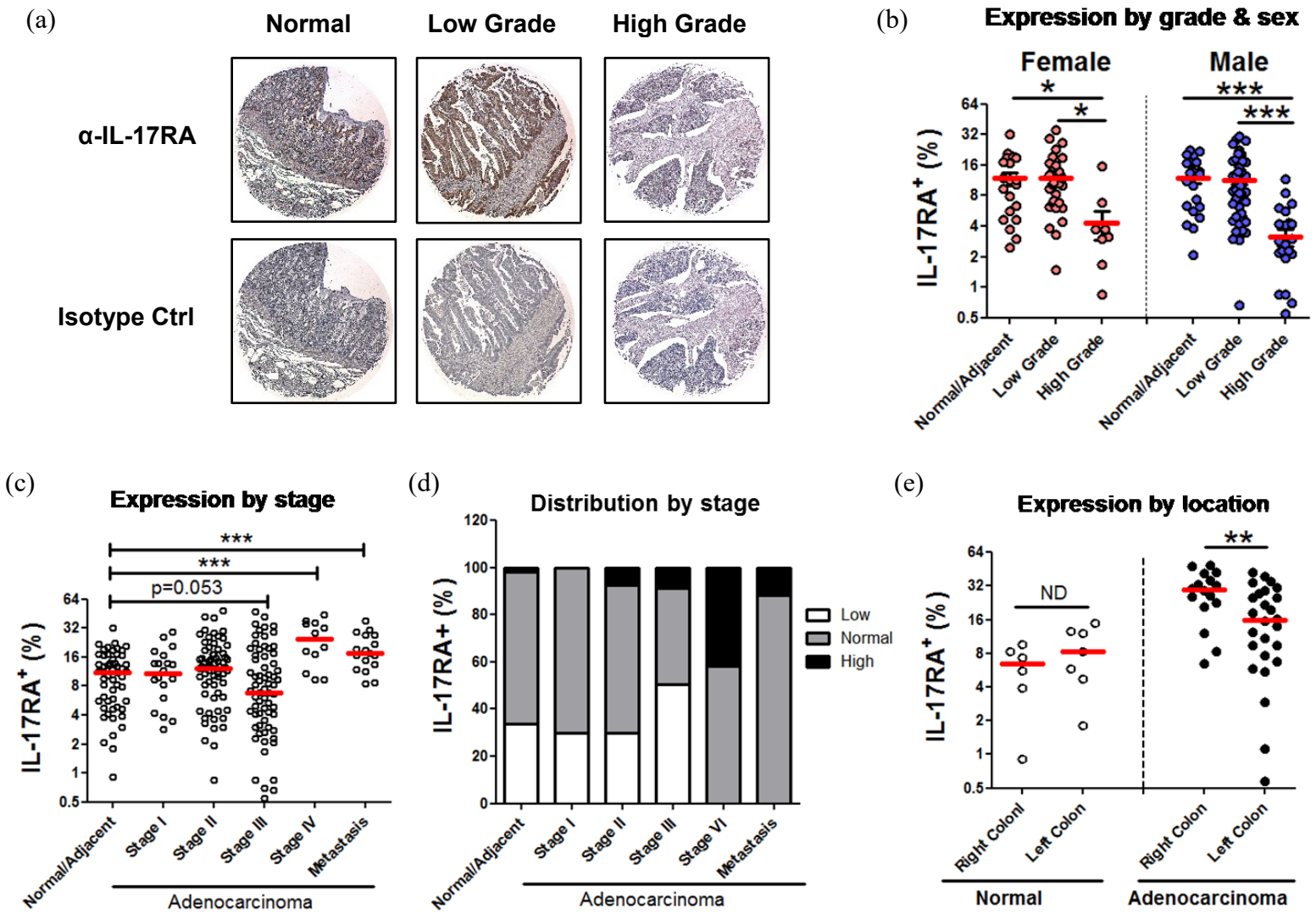
(a)
Normal
Low Grade
High Grade
α-IL-17RA
Isotype Ctrl
(b)
Expression by grade & sex
Female
Male
IL-17RA+ (%)
Normal/Adjacent
Low Grade
High Grade
(c)
Expression by stage
p=0.053
Normal/Adjacent
Stage I
Stage II
Stage III
Stage IV
Metastasis
Adenocarcinoma
(d)
Distribution by stage
IL-17RA+ (%)
Low
Normal
High
Stage VI
(e)
Expression by location
ND
Right Colonl
Left Colon
Right Colon
Normal
Adenocarcinoma

Figure 31.

CHAPTER 4 DISCUSSION

4.1 Summary of major findings

The current study offers important insights into the controversial role of the IL-17/IL-17R axis in tumorigenesis. In contrast to the classic IL-17A-induced proinflammatory responses, which are often implicated in inflammation and cancer development, I found that the loss of baseline IL-17/IL-17R signaling also favors disease progression. Using a model system implementing loss or gain of IL-17R expression in cancer cells, herein I have demonstrated that baseline IL-17R level maintains A20 homeostasis, which restrains JNK/c-Jun-dependent cellular proliferation and the inflammatory pathology of tumorigenesis. The role of IL-17R/A20 in controlling cell proliferation and proinflammatory cytokine/chemokine production also applied to primary BMDCs and MEFs.

Besides the direct regulation on cancer cells, I also demonstrated that the IL-17R/A20 axis may influence immunosuppression at the tumor sites. I discovered that B16 melanoma cells lacking IL-17R expression promote proinflammatory cytokine production *in vitro* and *in vivo*, which is associated with PD-L1^{+}/L2^{+} M2 polarization within the TME, along with attenuated accumulation of T cells, B cells and NK cells. Unique to the IL-17RA, but not IL-17RC signal, the inflamed TME also converted CD45^{-} host-derived cells into potentially immunosuppressive MHCII^{+}PD-L1^{+} cells.

Importantly, I have also provided clinical evidence for co-expression of IL-17RA and A20 in human neoplasms. Of note, I identified the down-regulation of the IL-17RA/A20 axis in a variety of human cancer types. In particular, high grade CRC samples have significantly attenuated IL-17RA expression which is associated with poor overall 5-year patient survival.

4.2 Implications and relevance of major findings

4.2.1 Baseline verses induced IL-17/IL-17R/A20 signaling

Constitutive activation of various transcription factors, including NF-κB and AP-1, is commonly observed in human malignancies (39, 506); however, the molecular mechanisms and consequences underlying deregulation of these transcription factors remain incompletely understood. In the present study, I have provided compelling *in vitro* and *in vivo* evidence to demonstrate a novel scenario in which aberrant activation of NF-

κB and JNK/c-Jun in cancer cells is triggered by the loss of baseline IL-17R expression, and an anti-inflammatory molecule—A20 (see Figure 32 for my model).

Using a shRNA knockdown approach, I have demonstrated in two different cancer cell lines that the biological impact of attenuating IL-17R expression is more than just losing conventional IL-17A-induced signaling pathways (e.g., reduced CXCL1 production). Tumor cells with IL-17RA silencing are hyper-proliferative due to aberrant JNK activation that promotes G1-to-S phase cell cycle transition. In addition to aberrant JNK activation, IL-17RC silencing in tumor cells further promotes constitutive NF-κB activation. My findings are in sharp contrast with the prevailing understanding that IL-17A induces NF-κB and JNK activation (291-293, 366, 409). I have identified that baseline IL-17R level is imperative in maintaining basal production of A20, a key signaling molecule that negatively controls NF-κB and JNK activity. Therefore, for the first time, my study has united two distinct signals (pro-inflammatory and anti-inflammatory) into a single regulatory system and revealed an elegant "yin-yang" collaborative mechanism for controlling aberrant activation of transcription factors. Notably, this "yin-yang" mechanism of proliferation control is not restricted to tumor cells, but was also evident in primary hematopoietic and non-hematopoietic cells. However, loss of this proliferation control in primary cells is not sufficient for early tumor initiation. As demonstrated in a recent study, IL-17RA-deficiency in enterocytes significantly reduced the incidence of adenoma, despite that increased crypt hyperplasia in IL-17RA-deficient gut compared to WT control (507). In this sense, my approach of blunting IL-17RA expression in already transformed tumor cell lines provides an excellent model system to accurately examine the impact of IL-17RA in regulating the invasiveness of tumor cells and disease progression.

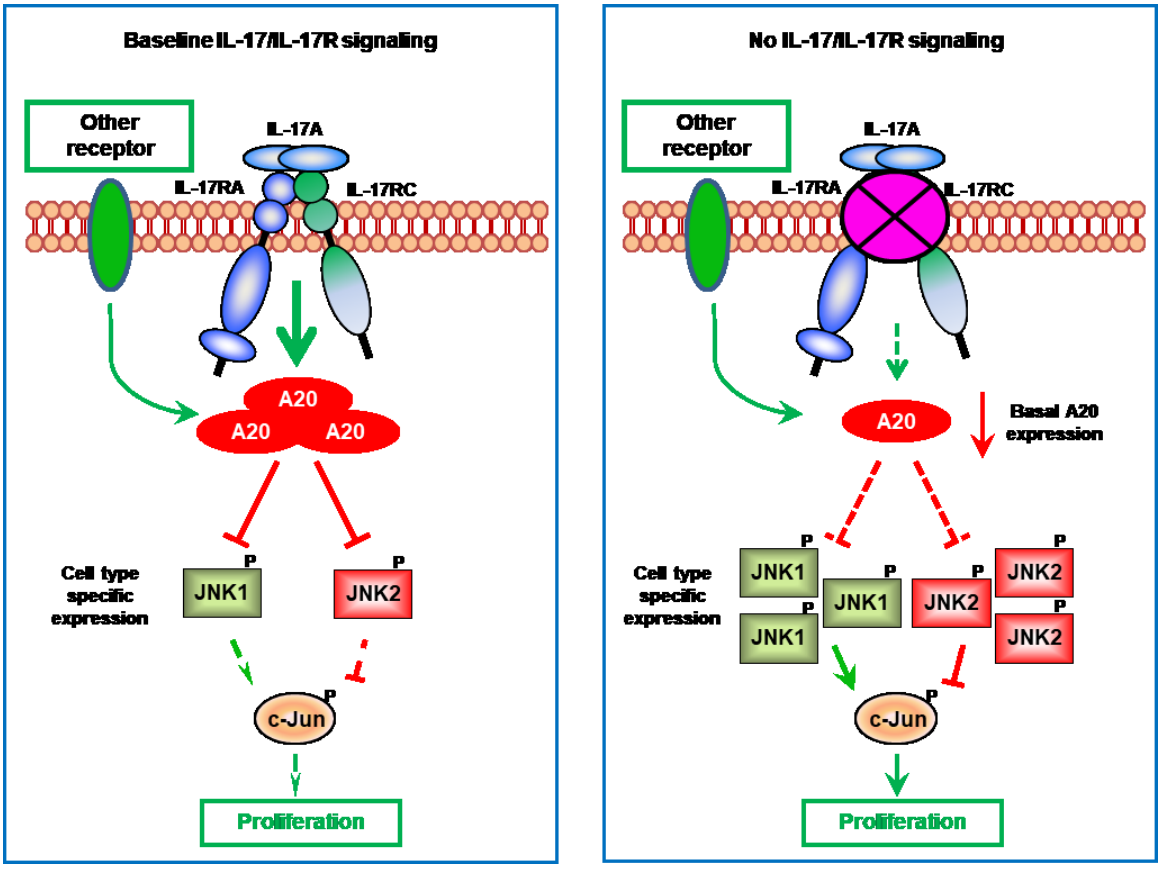

Figure 32. Proposed model for JNK1/JNK2 isoform-dependent tumor proliferation controlled by baseline IL-17/IL-17R level.

Under steady-state conditions, IL-17R-dependent signaling and, to a lesser extent, IL-17R-independent signaling are required for maintaining baseline A20 production, which serves as a negative regulator for restraining the activation of both JNK1 and JNK2. When baseline IL-17R level is severely diminished, basal A20 production is reduced, leading to aberrant production/stability and functional activities of JNK1 and/or JNK2 in a cell type-dependent manner. When JNK1 is present as the dominant isoform, JNK1 induces c-Jun phosphorylation and promotes c-Jun-dependent proliferation; conversely, when JNK2 is present as the dominant isoform, JNK2 degrades c-Jun and suppresses c-Jun-dependent cellular proliferation.

While A20 is widely recognized for its role in controlling inflammation and apoptosis (413, 415, 422), it is less appreciated that A20 also has a role in controlling homeostatic cell proliferation. Consistent with my finding, A20-deficient mice and mice with epidermis-specific A20-deficiency both exhibit thickening of epidermal and dermal layers as the result of uncontrolled proliferation of keratinocytes (418, 508). In 2014, Vereecke *et al.* reported that combining intestinal epithelial cell (IEC)- and myeloid-specific A20 deletion induces ileitis and severe colitis, associated with epithelial hyper-proliferation and continuous epithelial cell death *in vivo*; however, the molecular mechanism was still unclear (509). A two-phase model has been proposed to describe A20-mediated cytokine regulation. A20 expression is induced in the first phase by inflammatory stimuli like TNF-α, IL-1β, LPS and IL-17A and then acts as a feedback inhibitor of inflammatory pathways in the second phase (510). My study has extended this model to include basal IL-17R-dependent signaling controlling baseline A20 production and A20-dependent responses under steady-state conditions. Consistently, a recent study by Dr. Kolls's group has provided supporting evidence (319). They found that while conditional deletion of IL-17R in the mouse enteric epithelium caused reduced expression of α-defensins, Pigr, and Nox1, which are required to control gut commensal bacteria, other anti-microbial peptides, including members of regenerating-islet derived (Reg) 3 family (Reg3α/β/γ), were markedly increased in these mice, along with increased intestinal and systemic GM-CSF cytokine production and increased susceptibility to autoimmune responses (319). Although an increased load of enteric segmented filamentous bacteria is likely to be an important trigger for over-expression of Reg3α/β/γ and GM-CSF in the gut (319), I believe the loss of IL-17R-A20 regulation contributes to selective up-regulation of certain anti-microbial peptides and pro-inflammatory cytokines in this model.

Multiple intracellular molecules have been reported to directly or indirectly interact with IL-17R under resting conditions. Gaffen's group has identified interactions of both IL-17RA and IL-17RC with anaphase-promoting complex protein 5 and anaphase-promoting complex protein 7 under steady-state conditions, which also directly interacts with A20 (410). Of note, the anaphase-promoting complex/cyclosome is a multi-subunit E3 ubiquitin ligase that targets more than 30 proteins for ubiquitin-dependent proteasome degradation and has an essential role in controlling the cell cycle (511). anaphase-

promoting complex protein 5 and anaphase-promoting complex protein 7 also interact directly with the transcription co-activators CBP/p300, stimulating intrinsic CBP/p300 acetyltransferase activity to potentiate transcription of target genes, including A20 (512). Notably, the general transcription apparatus and the CBP/p300 coactivators are indeed constitutively associated with the core promoter of A20 under basal conditions, which allows basal production of A20 (415). Collectively, my results, in conjunction with other published studies, suggest that a basal level of A20 production may be maintained through a mechanism involving anaphase-promoting complex protein 5 and anaphase-promoting complex protein 7 and CBP/p300. Of importance, once A20 levels are maintained, IL-17R is unlikely to be required for the biological activities of A20 since reconstituted A20 was able to inhibit NF-κB and JNK activity in the absence of IL-17R. Furthermore, it is intriguing to speculate whether other non-IL-17R inflammatory receptors including TNFR, IL-1R and TLR may also control tumor-specific proliferation in the manner that I have demonstrated for IL-17R.

In addition to restraining homeostatic JNK activation, the basal levels of A20 may also control IL-17A-induced JNK activation. Existing evidence indicates that IL-17A-induced signaling pathways, including the JNK pathway, are subjected to regulation, and thus are only inducible in selective cell types (376-379). For example, IL-17A directly induces production of signaling molecules A20 and C/EBPβ at mRNA and protein levels and phosphorylation of C/EBPβ (18-22), which in turn negatively modify the magnitude of IL-17A-induced signaling. It is possible that the JNK activity in IL-17A-stimulated cells is controlled by the balance of stimulatory and inhibitory signals. In sharp contrast, JNK inhibition controlled by the baseline IL-17R-A20 axis is widely conserved in primary and neoplastic cells with distinct origins. Furthermore, baseline IL-17R has highly selective target molecules such as A20 but not C/EBP proteins, indicating that IL-17A likely utilizes different signaling pathways in stimulating versus maintaining basal A20 production. In my hands, although IL-17A was able to induce NF-κB activation and A20 production in both B16 and 4T1 cells, it only induced JNK activation in B16 but not 4T1 cells (Figure 33). The selective IL-17A-induced activation of JNK in B16 cells is likely due to the lower basal levels of A20 in B16 cells compared to 4T1 cells, since 4T1 and B16 cells exhibited comparable JNK activation upon TGFβ stimulation (Figure 33). Therefore, different from

A20-mediated regulation of the NF-κB pathway, which only restricts the second phase of classic NF-κB activation as predicted by a mathematical model (513), A20 is able to control both the first and second phases of JNK activation. Most importantly, while my data indicate that both homeostatic activation of JNK and NF-κB pathways are restrained by the IL-17R-A20 axis, it is the JNK pathway and not the NF-κB pathway that is responsible for controlling homeostatic tumor-dependent proliferation.

4.2.2 The role of JNK isoforms in the functional IL-17/IL-17R paradox in cancer

The role of different JNK isoforms and the JNK-c-Jun axis in controlling cell cycle progression, cell proliferation and cell apoptosis has been extensively studied. My data is highly consistent with the notion that JNK1 and JNK2 have opposing roles in controlling cell cycle progression and cell proliferation, with JNK1 and JNK2 being positive and negative regulators of these processes, respectively. Relevant to my study, specific gene knockdown of JNK1, but not JNK2, inhibits the growth of human melanoma cell lines (514). JNK2 inhibits oncogene-induced breast cancer development *in vivo* by preventing cell cycle progression and DNA repair in breast cancer cells (515). The opposing roles of JNK1 and JNK2 in regulating c-Jun dependent cell cycle progression was first observed in fibroblasts, erythroblasts and hepatocytes lacking JNK1 and/or JNK2 expression (279). However, the notion of JNK2 functioning as a negative regulator of c-Jun was challenged by the observation that JNK2 is fully able to phosphorylate c-Jun upon stimulation-induced activation (282). Notably, in addition to activation of their substrates, the JNKs cause degradation of various substrate proteins, including c-Jun, ATF2, and p53, under non-stimulatory conditions (516). The substrate degradation process is dependent on binding of the JNKs to the substrates and occurs in the absence of substrate phosphorylation (516). Biochemically, JNK2 has a 25-fold higher binding affinity for c-Jun than JNK1, which is the major JNK isoform that binds to and constitutively degrades c-Jun under steady-state conditions (279, 517). Upon stimulation, JNK1 becomes the major isoform to preferentially bind to c-Jun and induce c-Jun activation and c-Jun-dependent responses (279). Therefore, the specific role of JNK1 and JNK2 in regulating c-Jun-dependent cell proliferation is context-dependent and stimulation-dependent. The opposing roles of JNK1 and JNK2 in controlling tumor cell proliferation are mediated through distinct molecular

mechanisms and more applicable under steady-state conditions and, potentially, developing tumors during equilibrium phase.

4.2.3 IL-17R alteration and its prognostic value in human cancer management

CRC is caused by a successive accumulation of mutations in oncogenes, tumor suppressor genes and genes related to DNA repair mechanisms (518, 519). The three major pathogenic mechanisms leading to the disease are chromosomal instability, microsatellite instability (MSI), and epigenetic instability that is responsible for the CpG island methylator phenotype. Currently, the most widely used biomarkers in CRC are the determinations of MSI and KRAS mutations in tumor samples, which are used for diagnostic, classification and therapy management purposes (35). MSI is caused by a deficient mismatch repair system and occurs in approximately 15% of CRC. As a stage-dependent biomarker of CRC, MSI frequently occurs in early rather than late-stage disease. MSI-high CRCs exhibit a higher mutational load and are more immunogenic with a better prognosis (520). Nevertheless, in late-stage and metastatic CRC, MSI-high seems to confer a negative prognosis. Like MSI in CRC prognosis, KRAS mutation also exhibits certain prognostic limitations, since 40-60% of CRC patients with wild-type KRAS tumors do not respond to anti-EGFR antibody therapy (521). Given the drawbacks of the current clinical screening methods for CRC (e.g., colonoscopy), such as invasiveness, low specificity and sensitivity and high cost, the identification of novel molecular predictive and/or prognostic biomarkers with more specific, sensitive features and less invasiveness, has become an essential issue to improve cancer detection, treatment allocation and patient outcome.

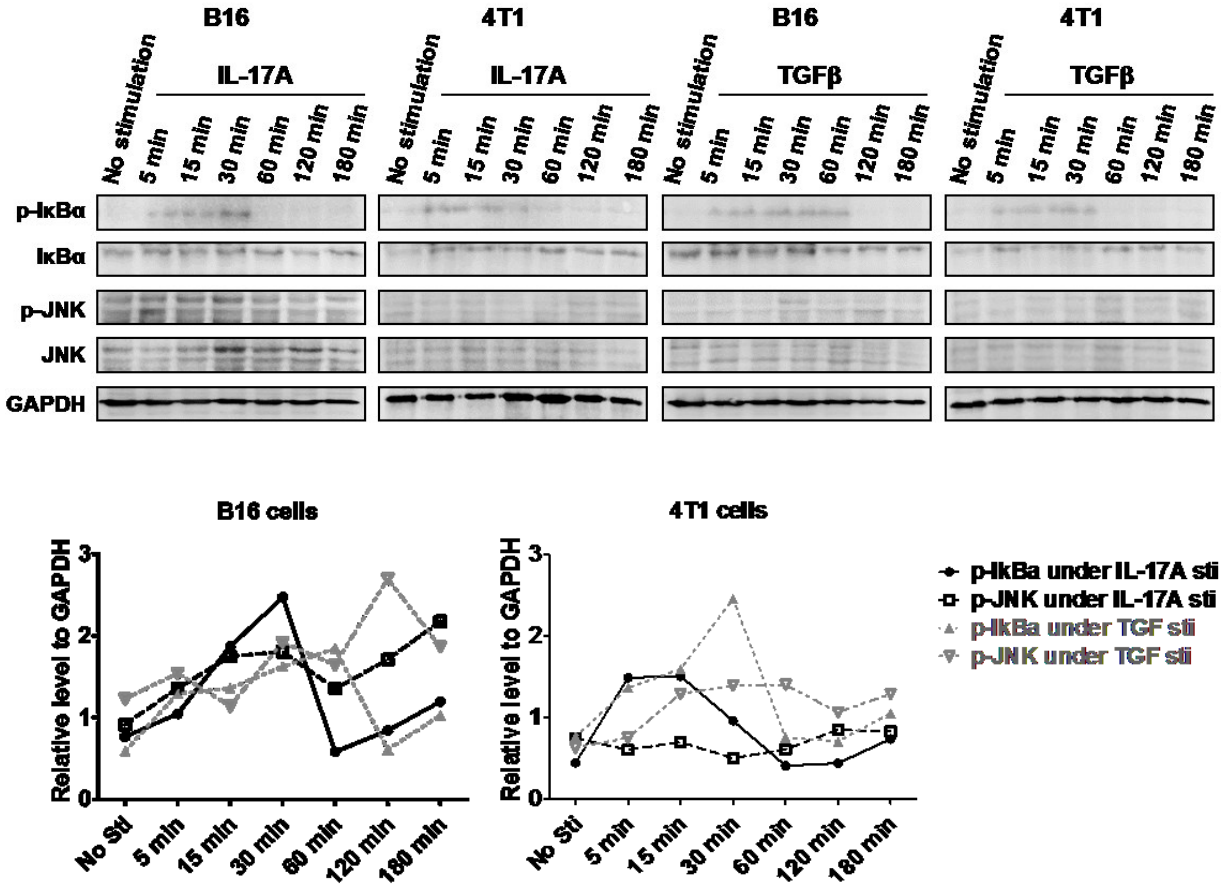

Figure 33. IL-17A triggers A20 and NF-κB induction and cell-type-dependent JNK activation.

B16 or 4T1 tumor cells were treated with or without 50 ng/ml IL-17A or 5 ng/ml TGF-β for the time indicated. Whole-cell extracts were harvested and immunoblotted to detect total or phosphorylated proteins as indicated. GAPDH was used as a loading control.

Chronic inflammatory conditions, such as inflammatory bowel disease (IBD), can drive the development of CRC (55). The axis of Th17 cells and their signature product proinflammatory cytokine IL-17, is highly increased and thought to contribute to the pathogenesis of IBD and CRC (522). Indeed, extensive mouse studies using either azoxymethane (AOM) and dextran sulfate sodium (DSS), with deliberately induces inflammation (523, 524), or spontaneous intestinal tumorigenesis in adenomatous polyposis coli Apc^{Min} mice confirmed this idea (507, 525). Furthermore, IL-17 neutralizing antibody prevented colitis and CRC initiation triggered by human enterotoxigenic *Bacteroides fragilis* bacteria(526). However, the pathogenic role of IL-17 is challenged by the most recent findings that IL-17 inhibits intestinal epithelial permeability during DSS-mediated injury (527) and colitis in mice deficient in the multiple drug resistance gene $Abcb1a^{-/-}$ (318). The inconsistent results in the mouse models highlight the need to examine the role of IL-17 in human CRC.

To examine the clinical relevance of IL-17R-downregulation in human cancers, I used a TCGA database to examine correlations between the genomic CNAs, transcriptomic mRNA levels and their associations with clinical and histopathological parameters in 633 CRC patients. In addition, we validated IL-17RA expression by immunohistochemical staining of human CRC tissue arrays. While confirming that excessive IL-17/IL-17R signaling promotes inflammatory responses associated with a trend towards poor clinical outcome, my work adds to the existing knowledge in two important ways: 1. Baseline IL-17R level is essential in maintaining anti-inflammatory A20 homeostasis in human CRC; 2. IL-17RA/A20-downregulation is a novel and potent prognostic signature associated with poor overall survival in CRC patients. My gene ontology enrichment analysis of gene targets either positively or negatively correlated with IL-17RA/A20 mRNA expression in CRC-TCGA database and clearly separated the IL-17R-dependent genes into two clusters. While the IL-17RA/A20 axis induces pro-inflammatory responses, inducing cytokine secretion, immune cell proliferation, activation and recruitment, it also negatively represses gene transcripts responsible for mitochondrial metabolism and protein synthesis (see Figure 34 for my model). Indeed, as a method to detect healthy mitochondrial activity in cells (528), the MTT assay has been used to show IL-17R-attenuation-induced cellular proliferation in my study. Altered energy metabolism is a hallmark of cancer (39). How

energy metabolism is regulated by baseline IL-17R level in cancer cells is intriguing and needs to be explored. Taken together, the gene transcriptional profile extended my proposed dual character of IL-17R signaling in cancer development as a "yin-yang" collaborative mechanism.

My human CRC tissue array suggested that the most aggressive stage IV and metastatic tumors didn't have IL-17RA-downregulation. This observation could be the result of the fatal effect of losing IL-17RA/A20 control during cancer growth and progression, or an increased IL-17RA level of early stage tumors to gain stem-cell like quiescent phenotypes. Given the potent inhibitory effect of A20 in restraining pro-survival signals, such as NF-κB and JNK (409, 416, 423), the down-regulation of IL-17RA/A20 in the dedifferentiation of CRC may allow the tumors to achieve an anti-apoptotic property and uncontrolled proliferation during disease development. Notably, hematopoietic stem cells that lack A20 display a loss of quiescence and hyperproliferation (529). Further studies with paired samples collected from early stage, e.g., stage II, and stage IV CRC patients would provide valuable insight regarding this question. In addition, future studies that aim to dissect the potential involvement of IL-17RA-A20 axis in stem cell biology would be valuable in understanding its role in proper maintenance of hematopoietic stem cell homeostasis. Together with my reported detrimental role of IL-17/A20 downregulation in murine cancer models and the current protective role of baseline IL-17RA/A20 axis in human cancers, my data draw caution on the utility of IL-17A neutralizing antibodies in cancer immunotherapy.

Figure 34. IL-17RA/A20 axis restrains mitochondrial metabolism and protein synthesis while inducing inflammation in CRC.

(a) Gene ontology enrichment analysis of gene targets either positively or negatively correlated with IL-17RA/A20 mRNA expression in CRC-TCGA database. (b) Revised model on the role of the IL-17R/A20 axis in predicting clinical outcomes in CRC patients. The intensity of IL-17A/IL-17R signaling can be divided into increased signaling (left), baseline signaling (middle), or reduced/no signaling (right). The increased signaling commonly occurs when exogenous or paracrine IL-17A is present, which stimulates NF-kB and MAPK pathways. However, IL-17A concurrently stimulates the production of signaling molecules including A20, which negatively regulate IL-17A-induced proinflammatory NF-κB and MAPK activation. The moderate IL-17A-induced inflammatory responses in CRC patients are associated with a trend towards poor overall survival. Under resting conditions, endogenous IL-17A/IL-17R level is required to specifically maintain basal production of A20 and restrains basal NF-κB and MAPK activities. When baseline IL-17A/IL-17R level is severely diminished, basal A20 production and A20-dependent suppression are markedly reduced. As such, IL-17R-independent signals trigger aberrant mitochondrial metabolism and protein synthesis in cancers, which are associated with poor overall survival of CRC patients.

Figure 34.

(a)

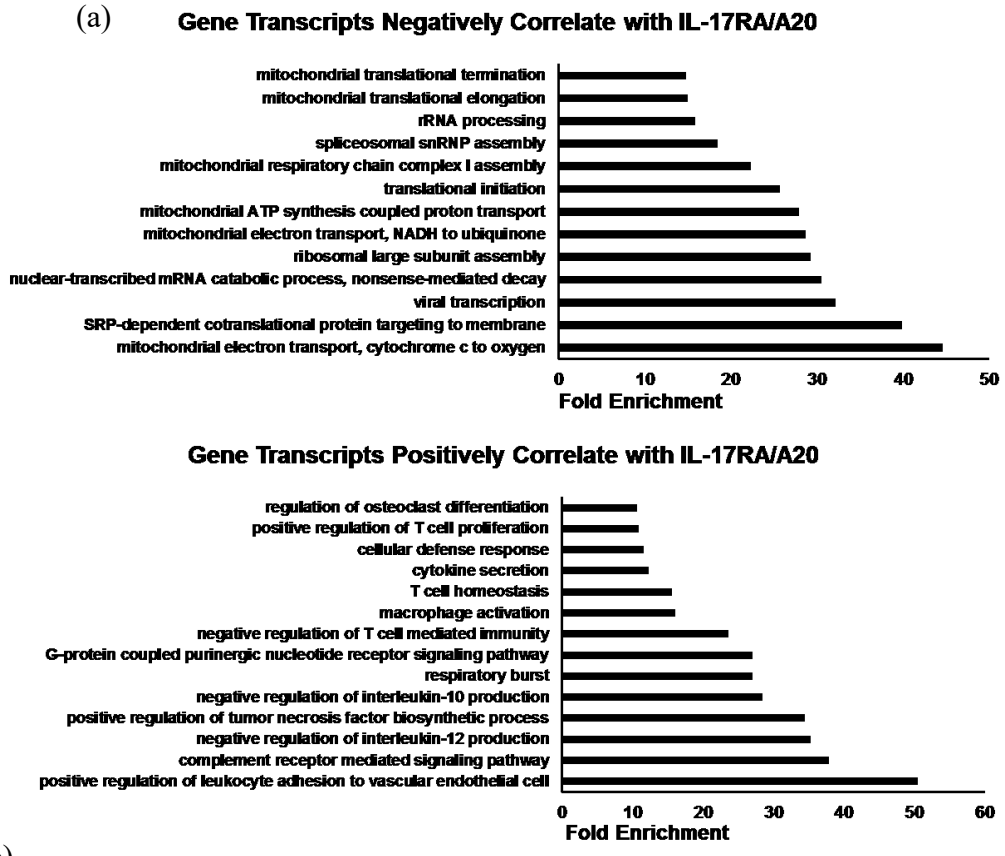
Gene Transcripts Negatively Correlate with IL-17RA/A20
mitochondrial translational termination
mitochondrial translational elongation
rRNA processing
spliceosomal snRNP assembly
mitochondrial respiratory chain complex I assembly
translational initiation
mitochondrial ATP synthesis coupled proton transport
mitochondrial electron transport, NADH to ubiquinone
ribosomal large subunit assembly
nuclear-transcribed mRNA catabolic process, nonsense-mediated decay
viral transcription
SRP-dependent cotranslational protein targeting to membrane
mitochondrial electron transport, cytochrome c to oxygen
0
10
20
30
40
50
Fold Enrichment
Gene Transcripts Positively Correlate with IL-17RA/A20
regulation of osteoclast differentiation
positive regulation of T cell proliferation
cellular defense response
cytokine secretion
T cell homeostasis
macrophage activation
negative regulation of T cell mediated immunity
G-protein coupled purinergic nucleotide receptor signaling pathway
respiratory burst
negative regulation of interleukin-10 production
positive regulation of tumor necrosis factor biosynthetic process
negative regulation of interleukin-12 production
complement receptor mediated signaling pathway
positive regulation of leukocyte adhesion to vascular endothelial cell
0
10
20
30
40
50
60
Fold Enrichment

(b)

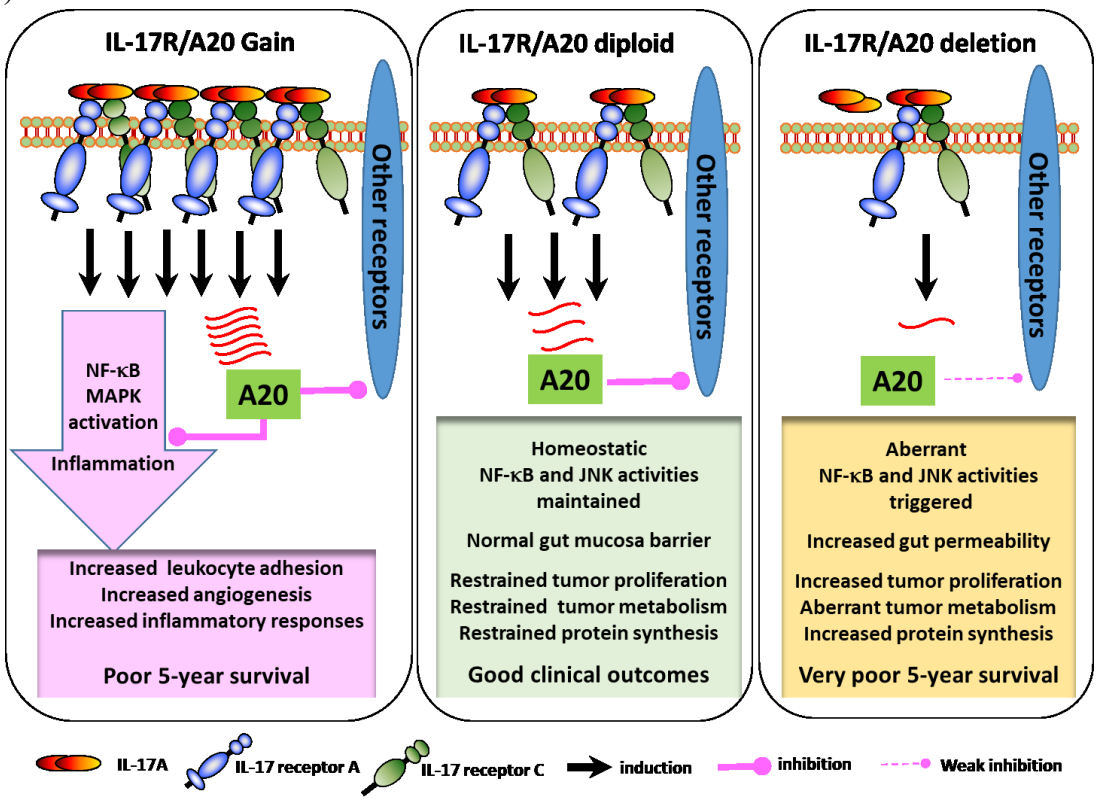
IL-17R/A20 Gain
Other receptors
NF-κB
MAPK
activation
A20
Inflammation
Increased leukocyte adhesion
Increased angiogenesis
Increased inflammatory responses
Poor 5-year survival
IL-17R/A20 diploid
Other receptors
A20
Homeostatic
NF-κB and JNK activities
maintained
Normal gut mucosa barrier
Restrained tumor proliferation
Restrained tumor metabolism
Restrained protein synthesis
Good clinical outcomes
IL-17R/A20 deletion
Other receptors
A20
Aberrant
NF-κB and JNK activities
triggered
Increased gut permeability
Increased tumor proliferation
Aberrant tumor metabolism
Increased protein synthesis
Very poor 5-year survival
IL-17A
IL-17 receptor A
IL-17 receptor C
induction
inhibition
Weak inhibition

The molecular mechanism of copy number deletion and downregulation of IL-17RA expression in CRC is unclear so far. Nevertheless, IL-17RA level alteration could result from multiple conditions dependent on the differentiation stage and cell type, as well as the tumor-specific microenvironment. For example, KRAS mutations in neoplastic epithelial cells directly induces IL-17RA expression and IL-17A production (245, 246). Under steady-state conditions, IL-17RA expression on tumor cells appears to be tightly regulated by an intrinsic mechanism since I was not able to over-express it. Members of γc-family of cytokines, IL-15 and IL-21, have been reported to increase IL-17RA expression in the murine HT-2 T cell line, whereas IL-2 is able to suppress IL-17RA expression (530). In addition, pro-inflammatory stimuli, including TNFα, poly(I:C) and LPS, induced IL-17RA/RC expression on synovial fibroblasts isolated from human arthritis patients (409, 412). Given the emerging role of the human microbiome in tumorigenesis (531), further investigation of the relationship and impact of the gut microbiome in regulating IL-17R-dependent immunologic dysregulation and cancer is clearly warranted. Moreover, vasoactive intestinal peptide, which ameliorates or prevents several inflammatory and autoimmune disorders in animal models (532-540), and IL-22 have been suggested to antagonize the pro-inflammatory stimuli signals and down-regulate IL-17RA/RC expression (541, 542). In conjunction with a recent finding that CRC patients have a significantly higher serum level of IL-22 and anti-IL-22 antibody markedly attenuated tumor growth in an animal model (541), it is reasonable to speculate that IL-22-induced down-regulation of IL-17RA might be involved in mediating IL-22-dependent CRC progression.

I found that IL-17RA is more prone to CNA in cancers than IL-17RC (Figure 28). Indeed, with limited alteration in IL-17RC expression, it failed to correlate with A20 levels in the CRC-TCGA dataset (Figure 35a). Furthermore, A20 mRNA is significantly co-expressed with IL-17A and IL-17F, but not IL-17C or IL-17E (IL-25), highlighting the critical role of IL-17A/IL-17R axis in maitaining A20 homeostasis in human CRC (Figure 35b). Consistent with the data from human samples, while 4T1 mouse breast cancer cells exhibited ~400 fold higher IL-17RA mRNA expression than B16 melanoma cells (Figure 35c), IL-17A and IL-17F markedly induced A20 expression in both 4T1 and B16 cell lines (Figure 18a). Nevertheless, IL-17C and IL-17E could only induce A20 in 4T1, but not B16

cells, suggesting the important role of the local cytokine milieu in controlling the tumor-type-specific IL-17R-induced reponses. I conducted ddPCR to examine the involvement of baseline IL-17 family ligands in repressing the IL-17R-suppressed signal (Figure 35d). I found that B16 cells secreted marginal IL-17C and IL-17F, with no detectable level of IL-17A and IL-17E. Furthermore, mRNA for IL-17 family ligands were not detected in the 4T1 cultures. Further ELISA experiments also failed to detect any ligand secretion in day 3 cell culture supernantants. Given the consistent observation that IL-17RA-attenuation induces cellular proliferation in both B16 and 4T1 models, it is more likely that the baseline IL-17 family ligands are dispensable for this phenotype. In future studies, however, it would be valuable to determine the impact of the functional domain of IL-17R in maintaining A20 using truncated IL-17R constructs. While an IL-17R mutant lacking the extracellular ligand-binding domain can validate the involvement of IL-17 family ligands, mutants with the deletion of different intracellullar domains will be required to further dissect the functional domain(s) of IL-17R in A20 homeostasis.

Figure 35. Significant association between IL-17A-F/IL-17R axis with A20 alteration. (a, b) mRNA expression levels were quantified from RNA-Seq data in the CRC-TCGA dataset from cBioportal. Correlation analyses of A20 mRNA expression with IL-17RA, IL-17RC, IL-17A, IL-17F, IL-17C and IL-17E (IL-25) mRNA levels. (c) Mouse cell lines were either untreated or starved in the serum-free DMEM for 14 hrs and recovered in complete DMEM medium with or without exogenous mouse recombinant IL-17 family ligands (200 ng/ml, 30 mins). Total RNA was extracted from approximately 3 x 10^6 cells of different mouse cell lines. RNA was reverse-transcribed into cDNA and amplified by quantitative real-time PCR and (d) digital droplet PCR. The gene expression was normalized to the expression of the housekeeping gene GAPDH. (c, d) All values are means ± SEM of 3 independent experiments. Statistical analyses were compared with the pSMP control for pannel (d) using one-way ANOVA.

Figure 35.

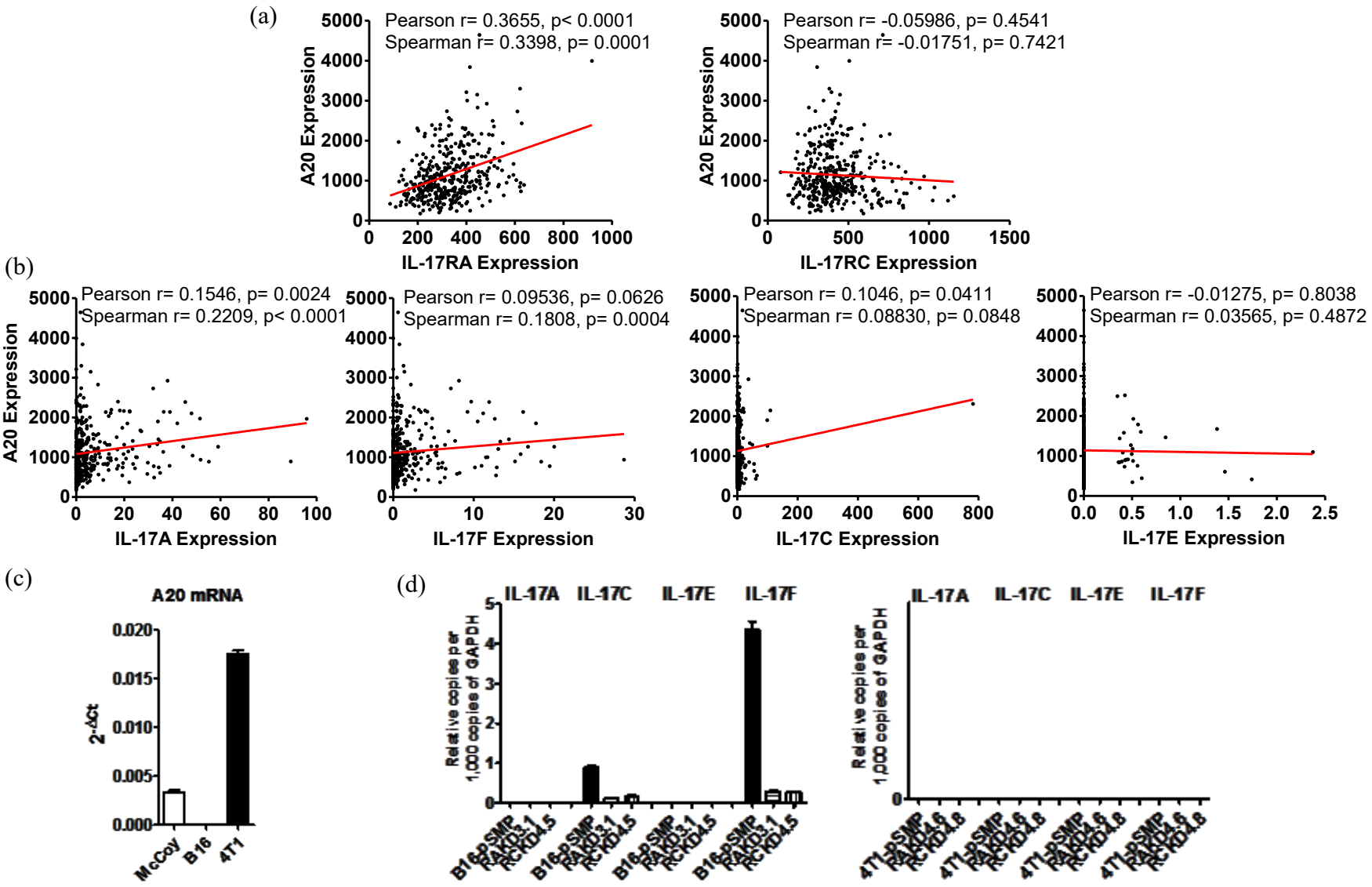
(a)
Pearson r= 0.3655, p< 0.0001
Spearman r= 0.3398, p= 0.0001
A20 Expression
IL-17RA Expression
Pearson r= -0.05986, p= 0.4541
Spearman r= -0.01751, p= 0.7421
IL-17RC Expression
(b)
Pearson r= 0.1546, p= 0.0024
Spearman r= 0.2209, p< 0.0001
IL-17A Expression
Pearson r= 0.09536, p= 0.0626
Spearman r= 0.1808, p= 0.0004
IL-17F Expression
Pearson r= 0.1046, p= 0.0411
Spearman r= 0.08830, p= 0.0848
IL-17C Expression
Pearson r= -0.01275, p= 0.8038
Spearman r= 0.03565, p= 0.4872
IL-17E Expression
(c)
A20 mRNA
2^-ΔCt
McCoy
B16
4T1
(d)
IL-17A
IL-17C
IL-17E
IL-17F
Relative copies per 1,000 copies of GAPDH
B16-P
SMP
RAKD3.1
RCKD4.5
4T1-P
RAKD4.6
RCKD4.8

I observed co-expression of IL-17RA and A20 in clinical tumor samples; however, the co-expression was not detected in two datasets of human cancer cell lines, i.e., the NCI-60 cancer cell line panel (GDS4296) in GEO-NCBI (Table 10) (543) and the Cancer Cell Line Encyclopedia (CCLE) from cBioportal (Table 11) (544). Specifically, NCI-60 covers human cancer cell lines from 9 different tissues of origin, including breast, central nervous system (CNS), colon, leukocytes, skin, non-small cell lung (NSCL), ovary, prostate, and kidney. In the NCI-60, while A20 expression is significantly correlated with IL-17RA in ovarian cancer and melanoma, A20 homeostasis is dependent on other pro-inflammatory signals in the other cancer types, such as IL-1 and TNF signals in breast cancer, TNF signals in renal and prostate cancer and TLR4 signals in NSCLC. Interestingly, TLR-MyD88 signals are negatively correlated with A20 expression in leukemia and prostate cancer. Notably, A20 didn't exhibit a clear co-expression with any signals examined in leukemia or CNS cancer; nevertheless, it is significantly correlated with IL-17RA level in all leukemia subsets (Pearson R=0.6226, P=0.0132; Spearman R=0.7143, P=0.0028), except acute promyelocytic leukemia HL-16.

The CCLE panel contains a massive parallel sequencing dataset covering 947 human cancer cell lines that compiling gene expression and chromosomal copy number. In the CCLE dataset, IL-17RA/A20 co-expression was observed in cancer cell lines originating from autonomic ganglia and the upper aerodigestive tract, but not from other tissues. Possible explanations of this inconsistency include the limitation that molecular signatures of cancer cell lines in culture may do not capture all aspects of cellular activity in the TME (545). The intratumor heterogeneity and molecular differences among cells within an individual tumor have clinical implications and highlight the need to use integrative samples and models to provide a greater predictive power. In addition, given that the co-expression pattern is disrupted in lung cancer patients from GDS2771 in GEO-NCBI, which were all collected from current and former smokers, patient lifestyle background (e.g., cigarette smoker) may be another factor that influences the intrinsic correlation of IL-17RA and A20 (546, 547). Moreover, limited sample size (e.g., GDS4824 of prostate cancer, n = 21 and GDS3592 of ovarian cancer, n = 24) (Table 9), and/or potential intrinsic stimuli, such as hormone receptor signaling in breast cancers (435), may alter the expressions of IL-17RA and/or A20 and also contribute to inconsistencies. Importantly,

the paired analyses of normal vs cancer samples obtained from the individual patients with CRC clearly exhibited down-regulation of IL-17/A20 as well as their intrinsic co-expression pattern, which strongly highlights the importance of this regulatory control mechanism in clinical settings.

Furthermore, I found that both IL-17RA and IL-17RC mRNA levels were significantly decreased in human colon cancer cell lines compared to primary HCEC (Figure 36). Nevertheless, while A20 expression is significantly attenuated in the human colon cancer line, HT29, compared to the primary HCEC, there is a 7-fold increase in the A20 mRNA level in another human colon cancer line, CaCo2 (Figure 36). Indeed, the high level of A20 in CaCo2 cells was associated with significantly weaker pro-inflammatory cytokine production of both IL-6 and IL-8 under IL-17A stimulation (Figure 36). Given that HT29 and CaCo2 have distinct gene mutation backgrounds with respect to BRAF, PIK3CA and TP53 (548), co-expression of IL-17RA and A20 may be biased by patient (cell line)-specific regulation.

Table 10. A20 correlation analysis grouped by cancer types in NCI-60 cancer cell line panel (GDS4296)

Cancer Type	Sample Count	Test Method	P and R values of A20 correlation				
			IL-1R1	MyD88	TLR4	TNFR1	IL-17RA
All	174	Pearson	0.8656; 0.0129	0.8265; 0.0167	0.2686; 0.0843	0.6028; 0.0397	**<0.0001; 0.3446**
		Spearman	0.4162; 0.0620	0.9770; -0.0022	0.0120; 0.1901	0.3564; 0.0703	**<0.0001; 0.3347**
Leukemia	18	Pearson	0.5482; 0.1516	0.1432; 0.3592	**0.0010; -0.7068**	0.5735; 0.1422	0.6840; 0.1031
		Spearman	0.5758; -0.1414	0.0504; 0.4675	**0.0088; -0.5975**	0.4888; 0.1744	0.3583; 0.2301
Leukemia	15	Pearson	0.7870; 0.0763	0.3462; 0.2616	0.0076; -0.6588	0.0870; 0.4567	**0.0132; 0.6226**
(excludes HL-16)		Spearman	0.4201; -0.2250	0.1641; 0.3786	0.1556; -0.3857	0.0839; 0.4607	**0.0028; 0.7143**
Breast cancer	15	Pearson	**0.0014; 0.7460**	0.6604; 0.1237	0.0221; 0.5845	**0.0001; 0.8294**	0.5947; -0.1496
		Spearman	**0.0037; 0.7000**	0.4910; 0.1929	0.1283; 0.4107	**0.0048; 0.6857**	0.6205; -0.1393
Ovarian cancer	21	Pearson	0.5339; -0.1438	0.4636; -0.1691	0.9677; -0.0094	0.3174; -0.2293	**0.0040; 0.6004**
		Spearman	0.5072; 0.1532	0.9554; -0.0130	0.9554; 0.0130	0.4856; -0.1610	**0.0010; 0.6636**
Melanoma	26	Pearson	0.6366; -0.0972	0.1806; -0.2710	0.8475; -0.0397	0.7023; 0.0787	**0.0120; 0.4851**
		Spearman	0.1815; -0.2704	0.3010; -0.2109	0.8048; 0.0509	0.4851; 0.1432	**0.0010; 0.6089**
CNS cancer	18	Pearson	0.1915; 0.3227	0.2571; -0.2819	0.1273; -0.3731	0.2195; 0.3043	0.6088; 0.1294
		Spearman	0.1279; 0.3725	0.3762; -0.2219	0.0778; -0.4262	0.1822; 0.3292	0.7048; 0.0960
Colon cancer	21	Pearson	0.5298; -0.1453	0.0821; -0.3881	0.6713; -0.0984	0.8658; 0.0392	0.0659; 0.4086
		Spearman	0.6827; -0.0948	0.0734; -0.3987	0.5670; -0.1325	0.5442; -0.1403	0.0510; 0.4312
Renal cancer	23	Pearson	0.3315; -0.2120	0.9666; 0.0092	0.0272; 0.4599	**0.0020; -0.6100**	0.8474; -0.0425
		Spearman	0.2132; -0.2698	0.5962; -0.1166	0.0750; 0.3785	**0.0053; -0.5613**	0.7301; -0.0761
NSCLC	26	Pearson	0.8680; 0.0342	0.5720; -0.1162	**0.0478; 0.3917**	0.8098; 0.0496	0.8991; -0.0261
		Spearman	0.5982; 0.1084	0.7337; -0.0701	**0.0121; 0.4844**	0.9063; 0.0243	0.4705; -0.1480
Prostate cancer	6	Pearson	0.8763; -0.0826	**0.0002; -0.9875**	0.0013; -0.9709	0.0109; 0.9134	0.0508; 0.8099
		Spearman	0.2132; -0.2698	**0.0167; -0.9429**	0.1028; -0.7714	0.0583; 0.8286	0.1028; 0.7714

Note: CNS, central nervous system. NSCLC, non-small cell lung cancer.

Table 11. Correlation analysis of Cancer Cell Line Encyclopedia in cBioPortal.

Sample Type	Sample Count	P & R Values of IL-17RA & A20 Correlation Pearson	Spearman
All	967	**0.0006, 0.1124**	**0.0009, 0.1081**
Autonomic Ganglia	17	**0.0892, 0.4248**	**0.0130, 0.5882**
Biliary Tract	7	0.2772, -0.4787	0.2000, -0.5714
Bone	25	0.7923, 0.05545	0.4696, 0.1515
Breast	58	0.7902, -0.03570	0.8533, 0.02482
Central Nervous System	52	0.9726, -0.004889	0.7116, -0.05251
Endometrium	24	0.5317, -0.1342	0.5572, -0.1261
Hematopoietic and lymphoid tissue	174	0.4928, -0.05233	0.5944, -0.04064
Kidney	21	0.1258, 0.3448	0.2158, 0.2818
Large Intestine	50	0.2246, 0.1748	0.3161, 0.1447
Liver	27	0.4949, -0.1372	0.3113, -0.2024
Lung	164	0.8595, -0.01393	0.8327, -0.01662
Oesophagus	24	0.2361, -0.2514	0.3016, -0.2200
Ovary	50	0.1134, -0.2267	0.3246, -0.1422
Pancreas	44	0.2313, 0.1842	0.4275, 0.1227
Pleura	10	0.2698, 0.3866	0.3487, 0.3333
Prostate	7	0.8592, -0.08324	0.4976, 0.3214
Skin	58	0.0816, 0.2306	0.0611, 0.2475
Soft Tissue	20	0.3269, -0.2311	0.5781, -0.1323
Stomach	37	0.1999, 0.2157	0.4002, 0.1425
Thyroid	12	0.2471, -0.3623	0.1309, -0.4615
Upper Aerodigestive Tract	30	**0.0223, -0.4158**	**0.0166, -0.4339**
Urinary Tract	23	0.3672, -0.1972	0.3057, -0.2233

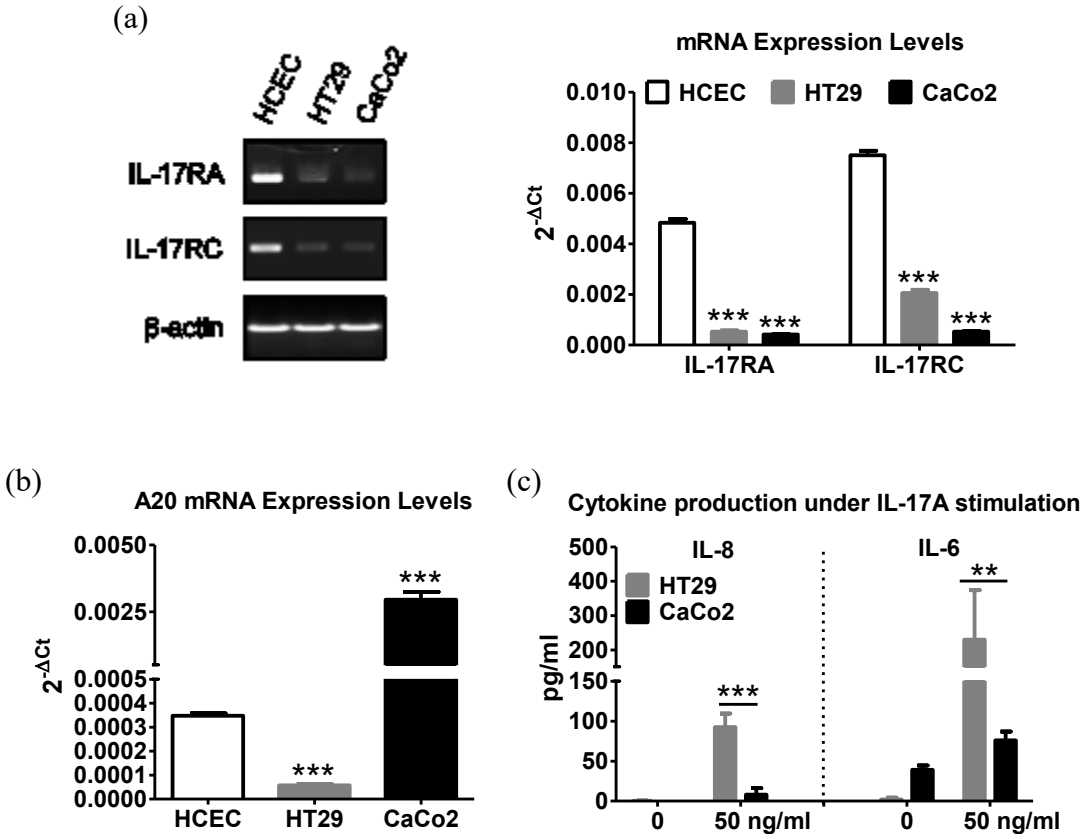

Figure 36. A20 restrains IL-17A-induced proinflammatory cytokine production in human colon cell lines.

(a,b) Total RNA was extracted from approximately 3 x 10^6 cells of different human cell lines. RNA was reverse-transcribed into cDNA and amplified by polymerase chain reaction (PCR) and quantitative real-time PCR. The gene expression was normalized to the expression of the housekeeping gene β-actin. HCEC: human colon epithelial cells; HT29 and CaCo2: human colon cancer cell line. (c) Human IL-8 and IL-6 production were determined by ELISA following stimulation with 50 ng/ml of recombinant mouse IL-17A. Values are means ± SEM of 6 replicates from two independent experiments. Statistical analyzes were compared with HCEC using Kruskal-Wallis test. *$p < 0.05$; ** $p < 0.01$; *** $p < 0.001$.

4.3 Limitations of experimental system

4.3.1 Apoptosis versus proliferation

The review by Hanahan and Weinberg entitled "The Hallmarks of Cancer" characterizes sustaining proliferation and resistance of apoptosis as two of the first six traits of cancer (38). As such, the design and development of cancer chemotherapies and other treatments have generally been evaluated based on their ability to inhibit proliferation and induce cell death. Nevertheless, these two hallmarks of cancer do not necessarily co-exist in cancer cells. In a large cohort of 791 breast cancer patients with long-term follow-up (range, 8.9-36.5 years), tumors exhibited high levels of apoptosis and increased cellular proliferation (549). Indeed, other clinical studies have suggested that other cancers exhibit increased frequency of proliferation and apoptosis, rather than evasion of apoptosis (273, 550). The harsh microenvironment of the tumor core, such as hypoxia, nutrient deprivation and low extracellular pH, is not a favorable condition for cancer cells to thrive (65). Nevertheless, cancer is not merely a mixture of neoplastic cells. The crosstalk among the cancer cells, stromal and immune cells, remodels the TME to favor an immune suppressive phenotype, which supports tumor cell proliferation over the rate of cell death, which in turn, leads to tumor growth and progression.

In my B16 and 4T1 cancer cell line models, the rate of cellular proliferation and apoptosis exhibited the same trend in alteration, which is consistent with clinical observations. I identified that cellular proliferation under IL-17R signaling is c-Jun-dependent and is alerted through entry modification at the G1-to-S phase of cell cycle. Indeed, it has been proposed that mutations of the Rb tumor suppressor lead to increased E2F family of DNA-binding transcription factors (E2F) activity, and this promotes both G1-to-S phase transition and apoptosis in cancer cells (551-553). Another new theory of increased cellular turnover of both proliferation and apoptosis in cancers proposed that the apoptosis of cancer tissues drives the surviving cancer cells to proliferate in an uncontrolled way through a process named "Compensatory Growth" (Figure 3) (273, 274). In the present study, the siRNA knockdown of either JNK1 or JNK2 altered cellular proliferation but not apoptosis (Figure 10f), suggesting the IL-17R-attenuation-induced JNK/c-Jun-dependent proliferation is independent of apoptosis. Further studies will be required to determine the

role for JNK isoforms in apoptosis under IL-17R-dependent versus IL-17R-independent signaling pathways.

4.3.2 Lentiviral-shRNA/siRNA delivery system

In the present study, I used a lentiviral-shRNA/siRNA delivery system to knockdown genes of interest. The main reason for choosing the lentivirus delivery system over other systems, such as plasmid DNA or adenovirus, is due to the ability of lentiviruses to infect both dividing and non-dividing cells and integrate into the host genome to achieve stable and sustained gene knockdowns (554). Nevertheless, the main drawback of the lentivirus-based delivery system is off-target effects. To confirm that my observation was not biased by any off-target effect, I examined IL-17R knockdown in multiple primary and cancer cells. Consistent results were observed and the full-length reconstitution of IL-17RA restored the proliferation rate, as well as JNK/c-Jun activities to the control level. To further validate my results, strategies to overcome or avoid the off-target effects using newly developed genome-editing systems, such as CRISPR/Cas9 (555), would be needed.

4.3.3 Online database and human tissue array analyses

In interpreting the results, some limitations of this study should be addressed. Firstly, the compiled analyses of multiple database and subgroup IHC analyses of CRC tissue array were performed based on a fraction of all the possible data to be pooled, so selection bias may have occurred and my results may be overinflated. Thus, additional large scale studies on IL-17RA/A20 interaction are needed to validate my findings. Secondly, in the pooled analyses of online datasets, different ethnicities were grouped in other population and the patient-specific regulation of gene expression profile may bring in some heterogeneity. Moreover, the gene-environment interactions including diet, microbiota, alcohol drinking, cigarette consumption, inflammation and other lifestyle factors, should also be considered in future studies.

4.4 Proposed future directions

While my study unmasked a role for repression of baseline IL-17R level in cancer progression and its clinical implication, there are many questions that remain to be answered. In my study, the endogenous level of A20 was maintained by baseline IL-17R level; however, the molecular mechanism is unclear. It would be interesting to determine

the functional domain of IL-17R, which are required for A20 homeostasis. Furthermore, while the expression levels of IL-17 family ligands are under the limit of detection by ddPCR, direct evidence to support the notion that IL-17 family ligands are dispensable for the IL-17R-repressing signal is missing. Further studies using truncated IL-17R lacking the extracellular domain for ligand binding will be required to validate this finding.

While I identified a critical role for IL-17R in A20 homeostasis, A20 can be induced by a variety of proinflammatory stimuli (409, 412). This may raise a question as to whether other pro-inflammatory signals are able to compensate for the IL-17R-A20 axis and override IL-17R silencing-induced A20 reduction and JNK-isoform-dependent cell proliferation *in vivo*. However, this may not be the case in my study. Although the loss of IL-17R triggered elevated production of proinflammatory cytokines, such as IL-6 and GM-CSF in B16 and 4T1 cells, IL-17R KD clones in both tumor models exhibited consistent invasiveness *in vitro* and *in vivo*. Nevertheless, this remains to be determined experimentally.

In my study, IL-17RC signaling in the two cancer cell line models, B16 and 4T1, exhibited opposing effects on proliferation via an unclear mechanism. This finding is novel in the context of recent literature suggesting a TME-specific role of IL-17 signaling in cancers (136). Nevertheless, the mechanism underlying this intrinsic phenotype of cells from various origins is intriguing. My preliminary work on the screening of IL-17RC isoform expression in B16, 4T1 and MEF cells suggested that these cells express both full-length IL-17RC and another isoform with a deletion of exon 7 and part of exon 8 (ΔExon7/8) (Figure 37). Notably, the truncated ΔExon7/8 isoform of IL-17RC fails to bind with either IL-17A or IL-17F (307), suggesting that the ΔExon7/8 isoform may serve as a decoy receptor to block downstream signaling. While the shRNA targets both isoforms of IL-17RC, the ratio of full length verses ΔExon7/8 is decreased in B16-RCKD compared to the pSMP control. In a sharp contrast, the ratio is increased in both 4T1 and MEF cells after the loss of IL-17RC. Given that the loss of IL-17RC exhibited decreased proliferation in B16 cells, but increased cell growth in 4T1 and MEF cells, these data enable us to hypothesize that the intrinsic proliferation control downstream of IL-17RC/A20 may be caused by the preferential expression pattern of full length versus ΔExon7/8 isoforms of IL-1RC in distinct cell types. Besides the identification of functional domain in IL-17R to

maintain A20 level, further studies will be required to reconstitute the two IL-17RC isoforms to examine this hypothesis.

Immunotherapy functions to overcome tumor suppression by (i) boosting the patient's immune system, (ii) increasing the immunogenicity of the tumor itself, and/or (iii) decreasing cancer-associated immunosuppression. There are a variety of approaches to eliciting an anti-tumor immune response, with advancements in techniques involving therapeutic cancer vaccines, adoptive T cell therapies, anti-tumor antibodies, and immune checkpoint blockade. The concept of utilizing beneficial immunosurveillance effects of acute inflammation in cancer treatment was applied by bone surgeon William Coley in the 1890s (556). "Coley's toxin" is a Gram-negative bacterial preparation that induces inflammation and was associated with some success in the treatment of sarcoma patients. Subsequently, researchers identified that "therapeutic inflammation" is conducted through the induction of TNF-α triggered by the LPS. More recently, using a wound-induced acute inflammation model in murine tumors, the authors found that the inflammation-induced secretion of IFN-γ interferes with the growth of early tumors. However, in the later stages of tumorigenesis, IFN-γ resistant tumors promote TGF-β against the IFN-γ effect in the restoration of tumor proliferation, invasion, and migration (557). Currently, in line with the "Coley's toxin" preparation, an attenuated *Mycobacterium bovis* strain (*Mycobacterium bovis* bacillus Calmette-Guerin—BCG)-derived therapeutic vaccine against tuberculosis is used in the treatment of squamous cancer of the bladder (558). The protective immune reaction primarily results from the induction of a variety of pro-inflammatory cytokines, including IL-1, TNF-α, IL-6, IL-8, IL-2, IL-12 , IL-5, IL-15, IL-18, GM-CSF and IFN-γ (558). The hypoxic and necrotic TME in the tumor mass is an attractive environment for anaerobic bacteria such as *Salmonella*, *Clostridium*, and *Listeria*. As such, the potential use of an engineered version of anaerobic bacteria to induce oncological therapy is promising. Indeed, a recent report by Min *et al.* (559) engineered *Salmonella typhimurium* to overexpress flagellin B, which stimulates a potent beneficial host immune response to inhibit cancer development and growth. However, there are several potential drawbacks regarding this acute inflammation-driven cancer therapy. Since it is difficult to balance the potency of the inflammation process, the induced anti-cancer responses are normally not cancer-specific. Host may not be able to clear bacteria due to impaired immune system,

and lastly, many pathogens themselves try to avoid immunosurveillance, which may lead to a chronic inflammatory condition that often accompanies cancer relapse with resistance to the same treatment.

Besides inducing acute inflammatory cytokine production to boost the immune system to combat cancer, immunomodulatory antibodies that directly enhance the function of T cells have recently been garnering significant attention. These agents, commonly called “checkpoint inhibitors” because they block negative regulators of T cell immunity, such as α-PD1/PD-L1 and α-CTLA4 have demonstrated meaningful results in terms of efficacy with a good safety profile in selected immunogenic cancers like melanoma and renal cell carcinomas (560, 561). Nevertheless, most patients (50% ~ 80%) do not respond to these therapies, and more concerningly, some patients who exhibit encouraging initial responses to the immunotherapy, can acquire resistance over time. In the present study, B16 tumors with attenuated IL-17RA expression induced PD-L1^{+} cells within the TME, including both CD45^{-}MHCII^{+} host cells and M2 infiltrates (Figure 25, 26), which are associated with a potent immunosuppression (Figure 23). Therefore, selectively targeting tumors with attenuated IL-17R expression may increase the α-PD-L1 response rate. Furthermore, since IL-17R-silencing may induce JNK1/c-Jun-dependent cell cycle progression and hyper-proliferation of tumor cells, JNK1-specific cell cycle inhibitors may potentially be used as a combination strategy with checkpoint inhibitors, possibly yielding better outcomes for patients.

Figure 37. IL-17RC isoform expression pattern is associated with IL-17R/A20-dependent proliferation control.

(a) Schematic diagram of mouse IL-17RC isoforms. (b) Total RNA was extracted from approximately 3 x 10^6 cells of different cells. RNA was reverse-transcribed into cDNA and IL-17RC isoforms were amplified by PCR. The gene expression was normalized to the expression of the housekeeping gene GAPDH. Gel image and quantitative densitometry analysis were shown. (c) The GOR method (http://gor.bb.iastate.edu/) of protein secondary structure prediction of the 24 amino acids deleted in the truncated IL-17RC isoform. (d) The IL-17RC isoform protein tertiary structure and function prediction through iterative threading assembly simulations by I-TASSER (http://zhanglab.ccmb.med.umich.edu/I-TASSER/).

(a) **Full Length IL-17RC Protein**

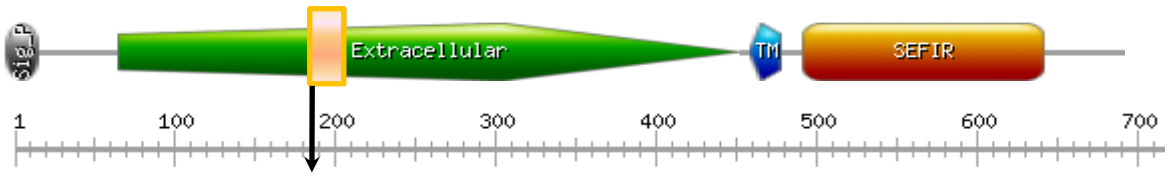

Exon△7,8: 24 amino acid (795-866bp) deletion. (Exon 7: 794-838bp; Exon 8: 839-978bp)

(b)

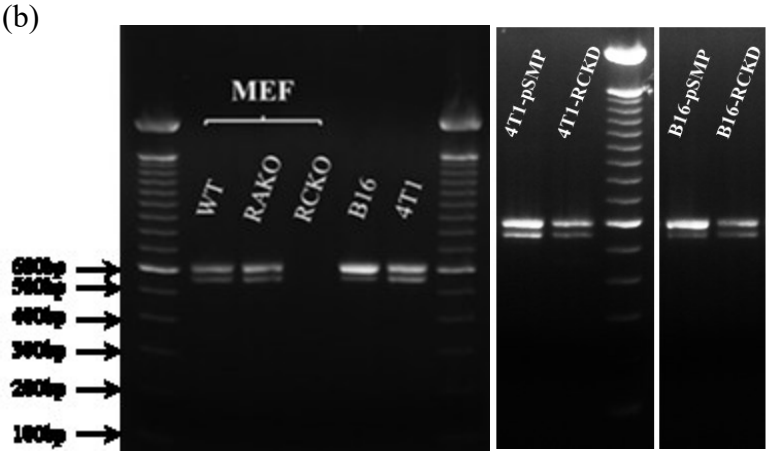

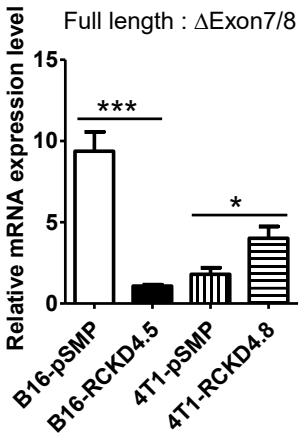

(c) **GOR method** (Garnier-Osguthorpe-Robson):

```
                    *     *     *     *
Query 181 LNLTQQLPDCRGLEVRDSIQSCWVLPWLNVSTDGD
Helix 181 ----->       <--------------->
Sheet 181 EEEEEE           EEEEEEEEEEEE
Turns 181     T           T   T          TT
```

+ ve residues: Arg (R), Lys (K);
- ve residues: Asp (D), Glu (E).

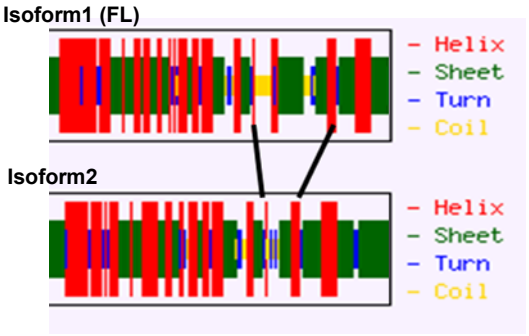

(d)

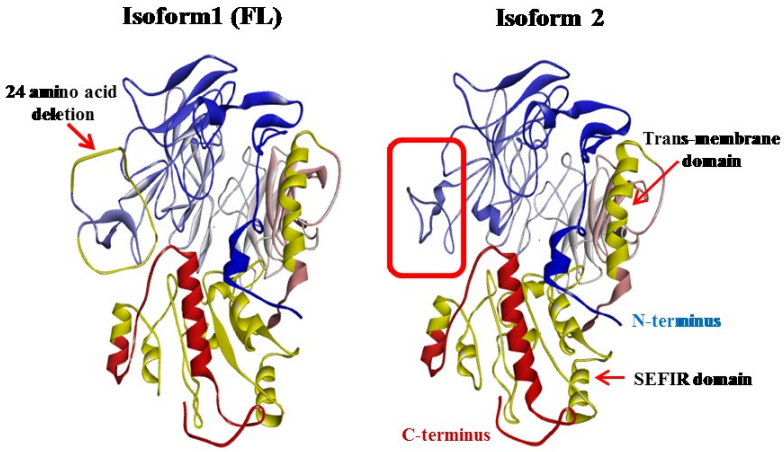

4.5 Concluding remarks

The role of the IL-17/IL-17R axis in cancer has been widely explored; however, conflicting results were reported without a satisfactory explanation. My findings highlight a previously unrecognized role of baseline IL-17R-A20 signaling in restraining JNK activation and tumor cell proliferation. My revised model emphasizes that both enhanced and severely reduced or blunted IL-17R-dependent signaling may lead to JNK activation. Depending on the endogenous activities of JNK1 and JNK2, IL-17R-dependent signaling may either positively or negatively regulate homeostatic proliferation and invasiveness of tumor cells. Furthermore, my study identifies a prognostic value of this novel tumor-suppression/evasion mechanism, whereby down-regulation of the IL-17R level in CRC tumors was associated with poor overall patient survival. Effective cancer therapies may be devised by manipulating this novel control mechanism. Future work based on the discoveries presented in this study could have significant implications for JNK isoform-specific inhibitors in cancer immunotherapies (253). At last, I would like to quote the wisdom of George Herbert, a Welsh poet, orator and Anglican priest (April 3rd, 1593 to March 1st, 1633): “Sometimes the best gain is to lose” (562). In the context of cancer, when the tumor cells lose the IL-17R/A20 expression, they can actually gain much more!

BIBLIOGRAPHY

1. Ryerson AB, Eheman CR, Altekruse SF, Ward JW, Jemal A, Sherman RL, et al. Annual report to the nation on the status of cancer, 1975-2012, featuring the increasing incidence of liver cancer. Cancer. 2016;122(9):1312-37.
2. Zugazagoitia J, Guedes C, Ponce S, Ferrer I, Molina-Pinelo S, Paz-Ares L. Current challenges in cancer treatment. Clinical therapeutics. 2016;38(7):1551-66.
3. Fearon ER, Vogelstein B. A genetic model for colorectal tumorigenesis. Cell. 1990;61(5):759-67.
4. Hansen MF, Cavenee WK. Tumor suppressors: recessive mutations that lead to cancer. Cell. 1988;53(2):173-4.
5. Yue X, Zhao Y, Xu Y, Zheng M, Feng Z, Hu W. Mutant p53 in cancer: accumulation, gain-of-function, and therapy. Journal of molecular biology. 2017;429(11):1595-606.
6. Fischer M. Census and evaluation of p53 target genes. Oncogene. 2017.
7. Azzam EI, de Toledo SM, Pykett MJ, Nagasawa H, Little JB. CDC2 is down-regulated by ionizing radiation in a p53-dependent manner. Cell growth & differentiation. 1997;8(11):1161-9.
8. Miyashita T, Reed JC. Tumor suppressor p53 is a direct transcriptional activator of the human bax gene. Cell. 1995;80(2):293-9.
9. Nakano K, Vousden KH. PUMA, a novel proapoptotic gene, is induced by p53. Molecular cell. 2001;7(3):683-94.
10. Liu G, Chen X. The ferredoxin reductase gene is regulated by the p53 family and sensitizes cells to oxidative stress-induced apoptosis. Oncogene. 2002;21(47):7195-204.
11. Crighton D, Wilkinson S, O'Prey J, Syed N, Smith P, Harrison PR, et al. DRAM, a p53-induced modulator of autophagy, is critical for apoptosis. Cell. 2006;126(1):121-34.
12. Budanov AV, Karin M. p53 target genes sestrin1 and sestrin2 connect genotoxic stress and mTOR signaling. Cell. 2008;134(3):451-60.
13. Xie J, Itzkowitz SH. Cancer in inflammatory bowel disease. World journal of gastroenterology. 2008;14(3):378-89.
14. Sherr CJ. Principles of tumor suppression. Cell. 2004;116(2):235-46.
15. Seemayer TA, Cavenee WK. Molecular mechanisms of oncogenesis. Laboratory investigation. 1989;60(5):585-99.
16. Croce CM. Oncogenes and cancer. The New England journal of medicine. 2008;358(5):502-11.
17. Kunz M. Oncogenes in melanoma: an update. European journal of cell biology. 2014;93(1-2):1-10.
18. McLaughlin-Drubin ME, Munger K. Viruses associated with human cancer. Biochimica et biophysica acta. 2008;1782(3):127-50.
19. Plummer M, de Martel C, Vignat J, Ferlay J, Bray F, Franceschi S. Global burden of cancers attributable to infections in 2012: a synthetic analysis. The lancet global health. 2016;4(9):e609-16.
20. Taylor AM, McConville CM, Byrd PJ. Cancer and DNA processing disorders. British medical bulletin. 1994;50(3):708-17.
21. Burnet FM. The concept of immunological surveillance. Progress in experimental tumor research. 1970;13:1-27.
22. Dunn GP, Old LJ, Schreiber RD. The immunobiology of cancer immunosurveillance and immunoediting. Immunity. 2004;21(2):137-48.
23. Mapara MY, Sykes M. Tolerance and cancer: mechanisms of tumor evasion and strategies for breaking tolerance. Journal of clinical oncology. 2004;22(6):1136-51.
24. Schietinger A, Philip M, Schreiber H. Specificity in cancer immunotherapy. Seminars in immunology. 2008;20(5):276-85.
25. Lennerz V, Fatho M, Gentilini C, Frye RA, Lifke A, Ferel D, et al. The response of autologous T cells to a human melanoma is dominated by mutated neoantigens. Proceedings of the national academy of sciences of the United States of America. 2005;102(44):16013-8.
26. Prior IA, Lewis PD, Mattos C. A comprehensive survey of Ras mutations in cancer. Cancer research. 2012;72(10):2457-67.
27. Witkiewicz AK, McMillan EA, Balaji U, Baek G, Lin WC, Mansour J, et al. Whole-exome sequencing of pancreatic cancer defines genetic diversity and therapeutic targets. Nature communications. 2015;6:6744.

28. Guerra C, Schuhmacher AJ, Canamero M, Grippo PJ, Verdaguer L, Perez-Gallego L, et al. Chronic pancreatitis is essential for induction of pancreatic ductal adenocarcinoma by K-Ras oncogenes in adult mice. Cancer cell. 2007;11(3):291-302.
29. Stuart D, Sellers WR. Linking somatic genetic alterations in cancer to therapeutics. Current opinion in cell biology. 2009;21(2):304-10.
30. Beroukhim R, Mermel CH, Porter D, Wei G, Raychaudhuri S, Donovan J, et al. The landscape of somatic copy-number alteration across human cancers. Nature. 2010;463(7283):899-905.
31. Ng CKY, Piscuoglio S, Geyer FC, Burke KA, Pareja F, Eberle CA, et al. The landscape of somatic genetic alterations in metaplastic breast carcinomas. Clinical cancer research. 2017.
32. Zitvogel L, Tesniere A, Kroemer G. Cancer despite immunosurveillance: immunoselection and immunosubversion. Nature reviews immunology. 2006;6(10):715-27.
33. Steeg PS. Tumor metastasis: mechanistic insights and clinical challenges. Nature medicine. 2006;12(8):895-904.
34. Edge SB BD, Carducci MA, Compton CC, editors. AJCC cancer staging manual. 7th ed. New York, NY: Springer. 2009.
35. Ludwig JA, Weinstein JN. Biomarkers in cancer staging, prognosis and treatment selection. Nature reviews cancer. 2005;5(11):845-56.
36. Compton CC. Prognostic factors in cancer. In: Gospodarowicz MK, O'Sullivan B, Sobin LH, eds. New York, NY: Wiley-Liss. 2006:133-7.
37. Tripathy D EL, Goodson, WH, et al. Breast. Ko, A. H., Dollinger, M., Rosenbaum, E. Everyone's guide to cancer therapy: how cancer is diagnosed, treated and managed day to day. (5th edition). Kansas City: Andrews McMeel Publishing. 2008:473-514.
38. Hanahan D, Weinberg RA. The hallmarks of cancer. Cell. 2000;100(1):57-70.
39. Hanahan D, Weinberg RA. Hallmarks of cancer: the next generation. Cell. 2011;144(5):646-74.
40. Colotta F, Allavena P, Sica A, Garlanda C, Mantovani A. Cancer-related inflammation, the seventh hallmark of cancer: links to genetic instability. Carcinogenesis. 2009;30(7):1073-81.
41. Grivennikov SI, Greten FR, Karin M. Immunity, inflammation, and cancer. Cell. 2010;140(6):883-99.
42. Nakamura K, Smyth MJ. Targeting cancer-related inflammation in the era of immunotherapy. Immunology and cell biology. 2017;95(4):325-32.
43. Kolaczkowska E. Acute inflammation as a beneficial process—history and recent developments. Kosmos. 2007;56:27-38.
44. Virchow R. Cellular pathology as based upon physiological and pathological histology. J B Lippincott, Philadelphia. 1863.
45. Korniluk A, Koper O, Kemona H, Dymicka-Piekarska V. From inflammation to cancer. Irish journal of medical science. 2017;186(1):57-62.
46. Kundu JK, Surh YJ. Inflammation: gearing the journey to cancer. Mutation research. 2008;659(1-2):15-30.
47. Landskron G, De la Fuente M, Thuwajit P, Thuwajit C, Hermoso MA. Chronic inflammation and cytokines in the tumor microenvironment. Journal of immunology research. 2014;2014:149185.
48. Correa P. Helicobacter pylori and gastric carcinogenesis. The American journal of surgical pathology. 1995;19(Suppl 1):S37-43.
49. Parsonnet J. Bacterial infection as a cause of cancer. Environmental health perspectives. 1995;103 Suppl 8:263-8.
50. Lowy DR, Schiller JT. Reducing HPV-associated cancer globally. Cancer prevention research. 2012;5(1):18-23.
51. Hayashi PH, Zeldis JB. Molecular biology of viral hepatitis and hepatocellular carcinoma. Comprehensive therapy. 1993;19(5):188-96.
52. Rosin MP, Anwar WA, Ward AJ. Inflammation, chromosomal instability, and cancer: the schistosomiasis model. Cancer research. 1994;54(7 Suppl):1929s-33s.
53. Pera M, Trastek VF, Pairolero PC, Cardesa A, Allen MS, Deschamps C. Barrett's disease: pathophysiology of metaplasia and adenocarcinoma. The annals of thoracic surgery. 1993;56(5):1191-7.
54. Hursting SD, Dunlap SM. Obesity, metabolic dysregulation, and cancer: a growing concern and an inflammatory (and microenvironmental) issue. Annals of the New York academy of sciences. 2012;1271:82-7.

55. Rubin DC, Shaker A, Levin MS. Chronic intestinal inflammation: inflammatory bowel disease and colitis-associated colon cancer. Frontiers in immunology. 2012;3:107.
56. Yan L, Anderson GM, DeWitte M, Nakada MT. Therapeutic potential of cytokine and chemokine antagonists in cancer therapy. European journal of cancer. 2006;42(6):793-802.
57. Todoric J, Antonucci L, Karin M. Targeting inflammation in cancer prevention and therapy. Cancer prevention research. 2016;9(12):895-905.
58. Rothwell PM, Fowkes FG, Belch JF, Ogawa H, Warlow CP, Meade TW. Effect of daily aspirin on long-term risk of death due to cancer: analysis of individual patient data from randomised trials. Lancet. 2011;377(9759):31-41.
59. Sorensen HT, Friis S, Norgard B, Mellemkjaer L, Blot WJ, McLaughlin JK, et al. Risk of cancer in a large cohort of nonaspirin NSAID users: a population-based study. British journal of cancer. 2003;88(11):1687-92.
60. Friis S, Thomassen L, Sorensen HT, Tjonneland A, Overvad K, Cronin-Fenton DP, et al. Nonsteroidal anti-inflammatory drug use and breast cancer risk: a Danish cohort study. European journal of cancer prevention. 2008;17(2):88-96.
61. Friis S, Riis AH, Erichsen R, Baron JA, Sorensen HT. Low-dose aspirin or nonsteroidal anti-inflammatory drug use and colorectal cancer risk: a population-based, case-control study. Annals of internal medicine. 2015;163(5):347-55.
62. Nickoloff BJ, Ben-Neriah Y, Pikarsky E. Inflammation and cancer: is the link as simple as we think? The journal of investigative dermatology. 2005;124(6):x-xiv.
63. Monjazeb AM, Zamora AE, Grossenbacher SK, Mirsoian A, Sckisel GD, Murphy WJ. Immunoediting and antigen loss: overcoming the achilles heel of immunotherapy with antigen non-specific therapies. Frontiers in oncology. 2013;3:197.
64. Mittal D, Gubin MM, Schreiber RD, Smyth MJ. New insights into cancer immunoediting and its three component phases--elimination, equilibrium and escape. Current opinion in immunology. 2014;27:16-25.
65. Kharaishvili G, Simkova D, Bouchalova K, Gachechiladze M, Narsia N, Bouchal J. The role of cancer-associated fibroblasts, solid stress and other microenvironmental factors in tumor progression and therapy resistance. Cancer cell international. 2014;14:41.
66. Veglia F, Gabrilovich DI. Dendritic cells in cancer: the role revisited. Current opinion in immunology. 2017;45:43-51.
67. Kim R, Emi M, Tanabe K. Functional roles of immature dendritic cells in impaired immunity of solid tumour and their targeted strategies for provoking tumour immunity. Clinical and experimental immunology. 2006;146(2):189-96.
68. Naik SH, Sathe P, Park HY, Metcalf D, Proietto AI, Dakic A, et al. Development of plasmacytoid and conventional dendritic cell subtypes from single precursor cells derived *in vitro* and *in vivo*. Nature immunology. 2007;8(11):1217-26.
69. Lombardi VC, Khaiboullina SF, Rizvanov AA. Plasmacytoid dendritic cells, a role in neoplastic prevention and progression. European journal of clinical investigation. 2015;45(Suppl 1):1-8.
70. Swiecki M, Colonna M. The multifaceted biology of plasmacytoid dendritic cells. Nature reviews immunology. 2015;15(8):471-85.
71. Liu W, Almo SC, Zang X. Co-stimulate or co-inhibit regulatory T cells, which side to go? Immunological investigations. 2016;45(8):813-31.
72. Munn DH, Sharma MD, Lee JR, Jhaver KG, Johnson TS, Keskin DB, et al. Potential regulatory function of human dendritic cells expressing indoleamine 2,3-dioxygenase. Science. 2002;297(5588):1867-70.
73. Franca CN, Izar MCO, Hortencio MNS, do Amaral JB, Ferreira CES, Tuleta ID, et al. Monocyte subtypes and the CCR2 chemokine receptor in cardiovascular disease. Clinical science. 2017;131(12):1215-24.
74. Italiani P, Boraschi D. From monocytes to M1/M2 macrophages: phenotypical vs. functional differentiation. Frontiers in immunology. 2014;5:514.
75. Gordon S. Phagocytosis: the legacy of metchnikoff. Cell. 2016;166(5):1065-8.
76. Pucci F, Venneri MA, Biziato D, Nonis A, Moi D, Sica A, et al. A distinguishing gene signature shared by tumor-infiltrating Tie2-expressing monocytes, blood "resident" monocytes, and embryonic macrophages suggests common functions and developmental relationships. Blood. 2009;114(4):901-14.

77. Santin AD, Hermonat PL, Ravaggi A, Chiriva-Internati M, Cannon MJ, Hiserodt JC, et al. Expression of surface antigens during the differentiation of human dendritic cells vs macrophages from blood monocytes *in vitro*. Immunobiology. 1999;200(2):187-204.
78. Geissmann F, Jung S, Littman DR. Blood monocytes consist of two principal subsets with distinct migratory properties. Immunity. 2003;19(1):71-82.
79. Goubran HA, Kotb RR, Stakiw J, Emara ME, Burnouf T. Regulation of tumor growth and metastasis: the role of tumor microenvironment. Cancer growth and metastasis. 2014;7:9-18.
80. Szebeni GJ, Vizler C, Kitajka K, Puskas LG. Inflammation and cancer: Extra- and intracellular determinants of tumor-associated macrophages as tumor promoters. Mediators of inflammation. 2017;2017:9294018.
81. Solinas G, Germano G, Mantovani A, Allavena P. Tumor-associated macrophages (TAM) as major players of the cancer-related inflammation. Journal of leukocyte biology. 2009;86(5):1065-73.
82. Noonan DM, De Lerma Barbaro A, Vannini N, Mortara L, Albini A. Inflammation, inflammatory cells and angiogenesis: decisions and indecisions. Cancer metastasis reviews. 2008;27(1):31-40.
83. Franklin RA, Li MO. Ontogeny of tumor-associated macrophages and its implication in cancer regulation. Trends in cancer. 2016;2(1):20-34.
84. Sunderkotter C, Nikolic T, Dillon MJ, Van Rooijen N, Stehling M, Drevets DA, et al. Subpopulations of mouse blood monocytes differ in maturation stage and inflammatory response. Journal of immunology. 2004;172(7):4410-7.
85. Nahrendorf M, Swirski FK, Aikawa E, Stangenberg L, Wurdinger T, Figueiredo JL, et al. The healing myocardium sequentially mobilizes two monocyte subsets with divergent and complementary functions. The journal of experimental medicine. 2007;204(12):3037-47.
86. Duluc D, Delneste Y, Tan F, Moles MP, Grimaud L, Lenoir J, et al. Tumor-associated leukemia inhibitory factor and IL-6 skew monocyte differentiation into tumor-associated macrophage-like cells. Blood. 2007;110(13):4319-30.
87. Roszer T. Understanding the mysterious M2 macrophage through activation markers and effector mechanisms. Mediators of inflammation. 2015;2015:816460.
88. Martinez FO, Helming L, Milde R, Varin A, Melgert BN, Draijer C, et al. Genetic programs expressed in resting and IL-4 alternatively activated mouse and human macrophages: similarities and differences. Blood. 2013;121(9):e57-69.
89. Biswas SK, Mantovani A. Macrophage plasticity and interaction with lymphocyte subsets: cancer as a paradigm. Nature immunology. 2010;11(10):889-96.
90. Murdoch C, Muthana M, Coffelt SB, Lewis CE. The role of myeloid cells in the promotion of tumour angiogenesis. Nature reviews cancer. 2008;8(8):618-31.
91. Guo F, Wang Y, Liu J, Mok SC, Xue F, Zhang W. CXCL12/CXCR4: a symbiotic bridge linking cancer cells and their stromal neighbors in oncogenic communication networks. Oncogene. 2016;35(7):816-26.
92. Kamper P, Bendix K, Hamilton-Dutoit S, Honore B, Nyengaard JR, d'Amore F. Tumor-infiltrating macrophages correlate with adverse prognosis and Epstein-Barr virus status in classical Hodgkin's lymphoma. Haematologica. 2011;96(2):269-76.
93. Coffelt SB, Kersten K, Doornebal CW, Weiden J, Vrijland K, Hau CS, et al. IL-17-producing gammadelta T cells and neutrophils conspire to promote breast cancer metastasis. Nature. 2015;522(7556):345-8.
94. Fossiez F, Djossou O, Chomarat P, Flores-Romo L, Ait-Yahia S, Maat C, et al. T cell interleukin-17 induces stromal cells to produce proinflammatory and hematopoietic cytokines. The journal of experimental medicine. 1996;183(6):2593-603.
95. Mantovani A, Cassatella MA, Costantini C, Jaillon S. Neutrophils in the activation and regulation of innate and adaptive immunity. Nature reviews immunology. 2011;11(8):519-31.
96. Tazzyman S, Lewis CE, Murdoch C. Neutrophils: key mediators of tumour angiogenesis. International journal of experimental pathology. 2009;90(3):222-31.
97. Nicolas-Avila JA, Adrover JM, Hidalgo A. Neutrophils in homeostasis, immunity, and cancer. Immunity. 2017;46(1):15-28.
98. Ley K, Laudanna C, Cybulsky MI, Nourshargh S. Getting to the site of inflammation: the leukocyte adhesion cascade updated. Nature reviews immunology. 2007;7(9):678-89.
99. Kolaczkowska E, Kubes P. Neutrophil recruitment and function in health and inflammation. Nature reviews immunology. 2013;13(3):159-75.

100. Kunz M, Hartmann A, Flory E, Toksoy A, Koczan D, Thiesen HJ, et al. Anoxia-induced up-regulation of interleukin-8 in human malignant melanoma. A potential mechanism for high tumor aggressiveness. The American journal of pathology. 1999;155(3):753-63.
101. Shi Q, Abbruzzese JL, Huang S, Fidler IJ, Xiong Q, Xie K. Constitutive and inducible interleukin 8 expression by hypoxia and acidosis renders human pancreatic cancer cells more tumorigenic and metastatic. Clinical cancer research. 1999;5(11):3711-21.
102. Fridlender ZG, Sun J, Kim S, Kapoor V, Cheng G, Ling L, et al. Polarization of tumor-associated neutrophil phenotype by TGF-beta: "N1" versus "N2" TAN. Cancer cell. 2009;16(3):183-94.
103. Fridlender ZG, Albelda SM. Tumor-associated neutrophils: friend or foe? Carcinogenesis. 2012;33(5):949-55.
104. Scapini P, Morini M, Tecchio C, Minghelli S, Di Carlo E, Tanghetti E, et al. CXCL1/macrophage inflammatory protein-2-induced angiogenesis in vivo is mediated by neutrophil-derived vascular endothelial growth factor-A. Journal of immunology. 2004;172(8):5034-40.
105. Benelli R, Morini M, Carrozzino F, Ferrari N, Minghelli S, Santi L, et al. Neutrophils as a key cellular target for angiostatin: implications for regulation of angiogenesis and inflammation. FASEB journal. 2002;16(2):267-9.
106. Cools-Lartigue J, Spicer J, McDonald B, Gowing S, Chow S, Giannias B, et al. Neutrophil extracellular traps sequester circulating tumor cells and promote metastasis. The journal of clinical investigation. 2013;123(8):3446–3458.
107. Gabrilovich DI, Nagaraj S. Myeloid-derived suppressor cells as regulators of the immune system. Nature reviews immunology. 2009;9(3):162-74.
108. Ostrand-Rosenberg S. Myeloid-derived suppressor cells: more mechanisms for inhibiting antitumor immunity. Cancer immunology, immunotherapy. 2010;59(10):1593-600.
109. Liu C, Yu S, Kappes J, Wang J, Grizzle WE, Zinn KR, et al. Expansion of spleen myeloid suppressor cells represses NK cell cytotoxicity in tumor-bearing host. Blood. 2007;109(10):4336-42.
110. Sinha P, Clements VK, Ostrand-Rosenberg S. Interleukin-13-regulated M2 macrophages in combination with myeloid suppressor cells block immune surveillance against metastasis. Cancer research. 2005;65(24):11743-51.
111. Serafini P, Mgebroff S, Noonan K, Borrello I. Myeloid-derived suppressor cells promote cross-tolerance in B-cell lymphoma by expanding regulatory T cells. Cancer research. 2008;68(13):5439-49.
112. Movahedi K, Guilliams M, Van den Bossche J, Van den Bergh R, Gysemans C, Beschin A, et al. Identification of discrete tumor-induced myeloid-derived suppressor cell subpopulations with distinct T cell-suppressive activity. Blood. 2008;111(8):4233-44.
113. Youn JI, Nagaraj S, Collazo M, Gabrilovich DI. Subsets of myeloid-derived suppressor cells in tumor-bearing mice. Journal of immunology. 2008;181(8):5791-802.
114. Fink T, Ebbesen P, Koppelhus U, Zachar V. Natural killer cell-mediated basal and interferon-enhanced cytotoxicity against liver cancer cells is significantly impaired under *in vivo* oxygen conditions. Scandinavian journal of immunology. 2003;58(6):607-12.
115. Loeffler DA, Juneau PL, Heppner GH. Natural killer-cell activity under conditions reflective of tumor micro-environment. International journal of cancer. 1991;48(6):895-9.
116. Tu MM, Mahmoud AB, Makrigiannis AP. Licensed and unlicensed NK cells: differential roles in cancer and viral control. Frontiers in immunology. 2016;7:166.
117. Takahashi E, Kuranaga N, Satoh K, Habu Y, Shinomiya N, Asano T, et al. Induction of $CD16^{+}$ $CD56^{bright}$ NK cells with antitumour cytotoxicity not only from $CD16^{-}CD56^{bright}$ NK Cells but also from $CD16^{-}CD56^{dim}$ NK cells. Scandinavian journal of immunology. 2007;65(2):126-38.
118. Robertson FC, Berzofsky JA, Terabe M. NKT cell networks in the regulation of tumor immunity. Frontiers in immunology. 2014;5:543.
119. Gebremeskel S, Clattenburg DR, Slauenwhite D, Lobert L, Johnston B. Natural killer T cell activation overcomes immunosuppression to enhance clearance of postsurgical breast cancer metastasis in mice. Oncoimmunology. 2015;4(3):e995562.
120. Ambrosino E, Terabe M, Halder RC, Peng J, Takaku S, Miyake S, et al. Cross-regulation between type I and type II NKT cells in regulating tumor immunity: a new immunoregulatory axis. Journal of immunology. 2007;179(8):5126-36.
121. Kanamori M, Tasumi Y, Iyoda T, Ushida M, Inaba K. Sulfatide inhibits alpha-galactosylceramide presentation by dendritic cells. International immunology. 2012;24(2):129-36.

122. Zhu J, Yamane H, Paul WE. Differentiation of effector CD4 T cell populations (*). Annual review of immunology. 2010;28:445-89.
123. Chen L, Flies DB. Molecular mechanisms of T cell co-stimulation and co-inhibition. Nature reviews immunology. 2013;13(4):227-42.
124. Zhu J, Paul WE. CD4 T cells: fates, functions, and faults. Blood. 2008;112(5):1557-69.
125. DuPage M, Bluestone JA. Harnessing the plasticity of CD4(+) T cells to treat immune-mediated disease. Nature reviews immunology. 2016;16(3):149-63.
126. Szabo SJ, Sullivan BM, Peng SL, Glimcher LH. Molecular mechanisms regulating Th1 immune responses. Annual review of immunology. 2003;21:713-58.
127. Ansel KM, Djuretic I, Tanasa B, Rao A. Regulation of Th2 differentiation and Il4 locus accessibility. Annual review of immunology. 2006;24:607-56.
128. Zou W, Restifo NP. Th17 cells in tumour immunity and immunotherapy. Nature reviews immunology. 2010;10(4):248-56.
129. Kolls JK, Linden A. Interleukin-17 family members and inflammation. Immunity. 2004;21(4):467-76.
130. Harrington LE, Hatton RD, Mangan PR, Turner H, Murphy TL, Murphy KM, et al. Interleukin 17-producing $CD4^+$ effector T cells develop via a lineage distinct from the T helper type 1 and 2 lineages. Nature immunology. 2005;6(11):1123-32.
131. Park H, Li Z, Yang XO, Chang SH, Nurieva R, Wang YH, et al. A distinct lineage of CD4 T cells regulates tissue inflammation by producing interleukin 17. Nature immunology. 2005;6(11):1133-41.
132. Korn T, Bettelli E, Oukka M, Kuchroo VK. IL-17 and Th17 Cells. Annual review of immunology. 2009;27:485-517.
133. Ivanov, II, McKenzie BS, Zhou L, Tadokoro CE, Lepelley A, Lafaille JJ, et al. The orphan nuclear receptor RORgammat directs the differentiation program of proinflammatory IL-17^+ T helper cells. Cell. 2006;126(6):1121-33.
134. Bailey SR, Nelson MH, Himes RA, Li Z, Mehrotra S, Paulos CM. Th17 cells in cancer: the ultimate identity crisis. Frontiers in immunology. 2014;5:276.
135. Peck A, Mellins ED. Precarious balance: Th17 cells in host defense. Infection and immunity. 2010;78(1):32-8.
136. Punt S, Langenhoff JM, Putter H, Fleuren GJ, Gorter A, Jordanova ES. The correlations between IL-17 vs. Th17 cells and cancer patient survival: a systematic review. Oncoimmunology. 2015;4(2):e984547.
137. Zheng Y, Rudensky AY. Foxp3 in control of the regulatory T cell lineage. Nature immunology. 2007;8(5):457-62.
138. Miyara M, Sakaguchi S. Natural regulatory T cells: mechanisms of suppression. Trends in molecular medicine. 2007;13(3):108-16.
139. Chaudhary B, Elkord E. Regulatory T Cells in the Tumor Microenvironment and Cancer Progression: Role and Therapeutic Targeting. Vaccines. 2016;4(3):28.
140. Anikeeva N, Sykulev Y. Mechanisms controlling granule-mediated cytolytic activity of cytotoxic T lymphocytes. Immunologic research. 2011;51(2-3):183-94.
141. Weigelin B, Krause M, Friedl P. Cytotoxic T lymphocyte migration and effector function in the tumor microenvironment. Immunology letters. 2011;138(1):19-21.
142. Sharma RK, Chheda ZS, Jala VR, Haribabu B. Regulation of cytotoxic T lymphocyte trafficking to tumors by chemoattractants: implications for immunotherapy. Expert review of vaccines. 2015;14(4):537-49.
143. Qin Z, Schwartzkopff J, Pradera F, Kammertoens T, Seliger B, Pircher H, et al. A critical requirement of interferon gamma-mediated angiostasis for tumor rejection by CD8+ T cells. Cancer research. 2003;63(14):4095-100.
144. Zarour HM. Reversing T-cell dysfunction and exhaustion in cancer. Clinical cancer research. 2016;22(8):1856-64.
145. Fourcade J, Sun Z, Benallaoua M, Guillaume P, Luescher IF, Sander C, et al. Upregulation of Tim-3 and PD-1 expression is associated with tumor antigen-specific $CD8^+$ T cell dysfunction in melanoma patients. The journal of experimental medicine. 2010;207(10):2175-86.
146. Kindt JT GA, Osborne AB, Kuby J. Kuby immunology. New York: WH Freeman. 2007.
147. Nelson BH. $CD20^+$ B cells: the other tumor-infiltrating lymphocytes. Journal of immunology. 2010;185(9):4977-82.

148. Zhang H, Lake DF, Barbuto JA, Bernstein RM, Grimes WJ, Hersh EM. A human monoclonal antimelanoma single-chain Fv antibody derived from tumor-infiltrating lymphocytes. Cancer research. 1995;55(16):3584-91.
149. Imahayashi S, Ichiyoshi Y, Yoshino I, Eifuku R, Takenoyama M, Yasumoto K. Tumor-infiltrating B-cell-derived IgG recognizes tumor components in human lung cancer. Cancer investigation. 2000;18(6):530-6.
150. Tsou P, Katayama H, Ostrin EJ, Hanash SM. The emerging role of B cells in tumor immunity. Cancer research. 2016;76(19):5597-601.
151. Li Q, Teitz-Tennenbaum S, Donald EJ, Li M, Chang AE. *In vivo* sensitized and *in vitro* activated B cells mediate tumor regression in cancer adoptive immunotherapy. Journal of immunology. 2009;183(5):3195-203.
152. Hagn M, Jahrsdorfer B. Why do human B cells secrete granzyme B? Insights into a novel B-cell differentiation pathway. Oncoimmunology. 2012;1(8):1368-75.
153. Andreu P, Johansson M, Affara NI, Pucci F, Tan T, Junankar S, et al. FcRgamma activation regulates inflammation-associated squamous carcinogenesis. Cancer cell. 2010;17(2):121-34.
154. Rauch PJ, Chudnovskiy A, Robbins CS, Weber GF, Etzrodt M, Hilgendorf I, et al. Innate response activator B cells protect against microbial sepsis. Science. 2012;335(6068):597-601.
155. Zhong X, Gao W, Degauque N, Bai C, Lu Y, Kenny J, et al. Reciprocal generation of Th1/Th17 and Treg cells by B1 and B2 B cells. European journal of immunology. 2007;37(9):2400-4.
156. Mizoguchi A, Mizoguchi E, Takedatsu H, Blumberg RS, Bhan AK. Chronic intestinal inflammatory condition generates IL-10-producing regulatory B cell subset characterized by CD1d upregulation. Immunity. 2002;16(2):219-30.
157. Shalapour S, Karin M. Immunity, inflammation, and cancer: an eternal fight between good and evil. The journal of clinical investigation. 2015;125(9):3347-55.
158. Lazennec G, Richmond A. Chemokines and chemokine receptors: new insights into cancer-related inflammation. Trends in molecular medicine. 2010;16(3):133-44.
159. Dudley AC, Shih SC, Cliffe AR, Hida K, Klagsbrun M. Attenuated p53 activation in tumour-associated stromal cells accompanies decreased sensitivity to etoposide and vincristine. British journal of cancer. 2008;99(1):118-25.
160. Barcellos-Hoff MH, Ravani SA. Irradiated mammary gland stroma promotes the expression of tumorigenic potential by unirradiated epithelial cells. Cancer research. 2000;60(5):1254-60.
161. Joyce JA, Pollard JW. Microenvironmental regulation of metastasis. Nature reviews cancer. 2009;9(4):239-52.
162. Quail DF, Joyce JA. Microenvironmental regulation of tumor progression and metastasis. Nature medicine. 2013;19(11):1423-37.
163. Lowy CM, Oskarsson T. Tenascin C in metastasis: a view from the invasive front. Cell adhesion & migration. 2015;9(1-2):112-24.
164. Richmond A, Thomas HG. Purification of melanoma growth stimulatory activity. Journal of cellular physiology. 1986;129(3):375-84.
165. Torisu H, Ono M, Kiryu H, Furue M, Ohmoto Y, Nakayama J, et al. Macrophage infiltration correlates with tumor stage and angiogenesis in human malignant melanoma: possible involvement of TNFalpha and IL-1alpha. International journal of cancer. 2000;85(2):182-8.
166. Schoppmann SF, Birner P, Stockl J, Kalt R, Ullrich R, Caucig C, et al. Tumor-associated macrophages express lymphatic endothelial growth factors and are related to peritumoral lymphangiogenesis. The American journal of pathology. 2002;161(3):947-56.
167. de Visser KE, Eichten A, Coussens LM. Paradoxical roles of the immune system during cancer development. Nature reviews cancer. 2006;6(1):24-37.
168. Langowski JL, Zhang X, Wu L, Mattson JD, Chen T, Smith K, et al. IL-23 promotes tumour incidence and growth. Nature. 2006;442(7101):461-5.
169. Kumari N, Dwarakanath BS, Das A, Bhatt AN. Role of interleukin-6 in cancer progression and therapeutic resistance. Tumour biology. 2016;37(9):11553-72.
170. Zhen Y, Guanghui L, Xiefu Z. Knockdown of EGFR inhibits growth and invasion of gastric cancer cells. Cancer gene therapy. 2014;21(11):491-7.
171. Deep G, Jain AK, Ramteke A, Ting H, Vijendra KC, Gangar SC, et al. SNAI1 is critical for the aggressiveness of prostate cancer cells with low E-cadherin. Molecular cancer. 2014;13:37.

172. Kim S, Gwak H, Kim HS, Kim B, Dhanasekaran DN, Song YS. Malignant ascites enhances migratory and invasive properties of ovarian cancer cells with membrane bound IL-6R *in vitro*. Oncotarget. 2016;7(50):83148-59.
173. Li D, Jin Y, Sun Y, Lei J, Liu C. Knockdown of toll-like receptor 4 inhibits human NSCLC cancer cell growth and inflammatory cytokine secretion *in vitro* and *in vivo*. International journal of oncology. 2014;45(2):813-21.
174. Balkwill F. Tumour necrosis factor and cancer. Nature reviews cancer. 2009;9(5):361-71.
175. Carey A, Edwards DKt, Eide CA, Newell L, Traer E, Medeiros BC, et al. Identification of interleukin-1 by functional screening as a key mediator of cellular expansion and disease progression in acute myeloid leukemia. Cell reports. 2017;18(13):3204-18.
176. Fu HJ, Jia LT, Bao W, Zhao J, Meng YL, Wang CJ, et al. Stable knockdown of estrogen receptor alpha by vector-based RNA interference suppresses proliferation and enhances apoptosis in breast cancer cells. Cancer biology & therapy. 2006;5(7):842-7.
177. Moasser MM. The oncogene HER2: its signaling and transforming functions and its role in human cancer pathogenesis. Oncogene. 2007;26(45):6469-87.
178. Daniel AR, Gaviglio AL, Knutson TP, Ostrander JH, D'Assoro AB, Ravindranathan P, et al. Progesterone receptor-B enhances estrogen responsiveness of breast cancer cells via scaffolding PELP1- and estrogen receptor-containing transcription complexes. Oncogene. 2015;34(4):506-15.
179. Lee YJ, Shin KJ, Park SA, Park KS, Park S, Heo K, et al. G-protein-coupled receptor 81 promotes a malignant phenotype in breast cancer through angiogenic factor secretion. Oncotarget. 2016;7(43):70898-911.
180. Grudzien P, Lo S, Albain KS, Robinson P, Rajan P, Strack PR, et al. Inhibition of Notch signaling reduces the stem-like population of breast cancer cells and prevents mammosphere formation. Anticancer research. 2010;30(10):3853-67.
181. Ueno K, Hirata H, Hinoda Y, Dahiya R. Frizzled homolog proteins, microRNAs and Wnt signaling in cancer. International journal of cancer. 2013;132(8):1731-40.
182. Sutmuller RP, van Duivenvoorde LM, van Elsas A, Schumacher TN, Wildenberg ME, Allison JP, et al. Synergism of cytotoxic T lymphocyte-associated antigen 4 blockade and depletion of $CD25^+$ regulatory T cells in antitumor therapy reveals alternative pathways for suppression of autoreactive cytotoxic T lymphocyte responses. The journal of experimental medicine. 2001;194(6):823-32.
183. Wang D, DuBois RN. Immunosuppression associated with chronic inflammation in the tumor microenvironment. Carcinogenesis. 2015;36(10):1085-93.
184. Gerlini G, Tun-Kyi A, Dudli C, Burg G, Pimpinelli N, Nestle FO. Metastatic melanoma secreted IL-10 down-regulates CD1 molecules on dendritic cells in metastatic tumor lesions. The American journal of pathology. 2004;165(6):1853-63.
185. Yue FY, Dummer R, Geertsen R, Hofbauer G, Laine E, Manolio S, et al. Interleukin-10 is a growth factor for human melanoma cells and down-regulates HLA class-I, HLA class-II and ICAM-1 molecules. International journal of cancer. 1997;71(4):630-7.
186. Ostrand-Rosenberg S, Sinha P. Myeloid-derived suppressor cells: linking inflammation and cancer. Journal of immunology. 2009;182(8):4499-506.
187. Dawod B. The role of the IL-17/IL-17R axis in breast tumor growth and metastasis (master's thesis). Retrieved from Faculty of Graduate Studies Online Theses databases of Dalhousie University. 2014;http://hdl.handle.net/10222/72247.
188. Uyttenhove C, Pilotte L, Theate I, Stroobant V, Colau D, Parmentier N, et al. Evidence for a tumoral immune resistance mechanism based on tryptophan degradation by indoleamine 2,3-dioxygenase. Nature medicine. 2003;9(10):1269-74.
189. Shin MS, Park WS, Kim SY, Kim HS, Kang SJ, Song KY, et al. Alterations of Fas (Apo-1/CD95) gene in cutaneous malignant melanoma. The American journal of pathology. 1999;154(6):1785-91.
190. Hersey P, Zhang XD. How melanoma cells evade trail-induced apoptosis. Nature reviews cancer. 2001;1(2):142-50.
191. Algarra I, Collado A, Garrido F. Altered MHC class I antigens in tumors. International journal of clinical & laboratory research. 1997;27(2):95-102.
192. de Vries TJ, Fourkour A, Wobbes T, Verkroost G, Ruiter DJ, van Muijen GN. Heterogeneous expression of immunotherapy candidate proteins gp100, MART-1, and tyrosinase in human melanoma cell lines and in human melanocytic lesions. Cancer research. 1997;57(15):3223-9.

193. Schwartz RH. A cell culture model for T lymphocyte clonal anergy. Science. 1990;248(4961):1349-56.
194. Blank C, Gajewski TF, Mackensen A. Interaction of PD-L1 on tumor cells with PD-1 on tumor-specific T cells as a mechanism of immune evasion: implications for tumor immunotherapy. Cancer immunology, immunotherapy. 2005;54(4):307-14.
195. Kahan SM, Wherry EJ, Zajac AJ. T cell exhaustion during persistent viral infections. Virology. 2015;479-480:180-93.
196. Dong H, Strome SE, Salomao DR, Tamura H, Hirano F, Flies DB, et al. Tumor-associated B7-H1 promotes T-cell apoptosis: a potential mechanism of immune evasion. Nature medicine. 2002;8(8):793-800.
197. Rosenwald A, Wright G, Leroy K, Yu X, Gaulard P, Gascoyne RD, et al. Molecular diagnosis of primary mediastinal B cell lymphoma identifies a clinically favorable subgroup of diffuse large B cell lymphoma related to Hodgkin lymphoma. The journal of experimental medicine. 2003;198(6):851-62.
198. Petrovas C, Casazza JP, Brenchley JM, Price DA, Gostick E, Adams WC, et al. PD-1 is a regulator of virus-specific $CD8^+$ T cell survival in HIV infection. The journal of experimental medicine. 2006;203(10):2281-92.
199. Cho HY, Lee SW, Seo SK, Choi IW, Choi I, Lee SW. Interferon-sensitive response element (ISRE) is mainly responsible for IFN-alpha-induced upregulation of programmed death-1 (PD-1) in macrophages. Biochimica et biophysica acta. 2008;1779(12):811-9.
200. Yamazaki T, Akiba H, Iwai H, Matsuda H, Aoki M, Tanno Y, et al. Expression of programmed death 1 ligands by murine T cells and APC. Journal of immunology. 2002;169(10):5538-45.
201. Flies DB, Chen L. Modulation of immune response by B7 family molecules in tumor microenvironments. Immunological investigations. 2006;35(3-4):395-418.
202. Seliger B, Quandt D. The expression, function, and clinical relevance of B7 family members in cancer. Cancer immunology, immunotherapy. 2012;61(8):1327-41.
203. Bardhan K, Anagnostou T, Boussiotis VA. The PD1:PD-L1/2 Pathway from Discovery to Clinical Implementation. Frontiers in immunology. 2016;7:550.
204. Ohaegbulam KC, Assal A, Lazar-Molnar E, Yao Y, Zang X. Human cancer immunotherapy with antibodies to the PD-1 and PD-L1 pathway. Trends in molecular medicine. 2015;21(1):24-33.
205. Prasad DV, Nguyen T, Li Z, Yang Y, Duong J, Wang Y, et al. Murine B7-H3 is a negative regulator of T cells. Journal of immunology. 2004;173(4):2500-6.
206. Dong Y, Sun Q, Zhang X. PD-1 and its ligands are important immune checkpoints in cancer. Oncotarget. 2017;8(2):2171-86.
207. Hui E, Cheung J, Zhu J, Su X, Taylor MJ, Wallweber HA, et al. T cell costimulatory receptor CD28 is a primary target for PD-1-mediated inhibition. Science. 2017;355(6332):1428-33.
208. Yokosuka T, Takamatsu M, Kobayashi-Imanishi W, Hashimoto-Tane A, Azuma M, Saito T. Programmed cell death 1 forms negative costimulatory microclusters that directly inhibit T cell receptor signaling by recruiting phosphatase SHP2. The journal of experimental medicine. 2012;209(6):1201-17.
209. Ahmadzadeh M, Johnson LA, Heemskerk B, Wunderlich JR, Dudley ME, White DE, et al. Tumor antigen-specific CD8 T cells infiltrating the tumor express high levels of PD-1 and are functionally impaired. Blood. 2009;114(8):1537-44.
210. Zou W, Chen L. Inhibitory B7-family molecules in the tumour microenvironment. Nature reviews immunology. 2008;8(6):467-77.
211. Borch TH, Donia M, Andersen MH, Svane IM. Reorienting the immune system in the treatment of cancer by using anti-PD-1 and anti-PD-L1 antibodies. Drug discovery today. 2015;20(9):1127-34.
212. Terawaki S, Chikuma S, Shibayama S, Hayashi T, Yoshida T, Okazaki T, et al. IFN-alpha directly promotes programmed cell death-1 transcription and limits the duration of T cell-mediated immunity. Journal of immunology. 2011;186(5):2772-9.
213. Chen N, Fang W, Zhan J, Hong S, Tang Y, Kang S, et al. Upregulation of PD-L1 by EGFR activation mediates the immune escape in EGFR-driven NSCLC: implication for optional immune targeted therapy for NSCLC patients with EGFR mutation. Journal of thoracic oncology. 2015;10(6):910-23.
214. Parsa AT, Waldron JS, Panner A, Crane CA, Parney IF, Barry JJ, et al. Loss of tumor suppressor PTEN function increases B7-H1 expression and immunoresistance in glioma. Nature medicine. 2007;13(1):84-8.
215. Noman MZ, Desantis G, Janji B, Hasmim M, Karray S, Dessen P, et al. PD-L1 is a novel direct target of HIF-1alpha, and its blockade under hypoxia enhanced MDSC-mediated T cell activation. The journal of experimental medicine. 2014;211(5):781-90.

216. Latchman Y, Wood CR, Chernova T, Chaudhary D, Borde M, Chernova I, et al. PD-L2 is a second ligand for PD-1 and inhibits T cell activation. Nature immunology. 2001;2(3):261-8.
217. Xiao Y, Yu S, Zhu B, Bedoret D, Bu X, Francisco LM, et al. RGMb is a novel binding partner for PD-L2 and its engagement with PD-L2 promotes respiratory tolerance. The journal of experimental medicine. 2014;211(5):943-59.
218. Garcia-Diaz A, Shin DS, Moreno BH, Saco J, Escuin-Ordinas H, Rodriguez GA, et al. Interferon receptor signaling pathways regulating PD-L1 and PD-L2 expression. Cell reports. 2017;19(6):1189-201.
219. Kundu JK, Surh YJ. Emerging avenues linking inflammation and cancer. Free radical biology & medicine. 2012;52(9):2013-37.
220. Vendramini-Costa DB, Carvalho JE. Molecular link mechanisms between inflammation and cancer. Current pharmaceutical design. 2012;18(26):3831-52.
221. Gilmore TD. Introduction to NF-kappaB: players, pathways, perspectives. Oncogene. 2006;25(51):6680-4.
222. Gupta SC, Kim JH, Kannappan R, Reuter S, Dougherty PM, Aggarwal BB. Role of nuclear factor kappaB-mediated inflammatory pathways in cancer-related symptoms and their regulation by nutritional agents. Experimental biology and medicine. 2011;236(6):658-71.
223. Xie QW, Kashiwabara Y, Nathan C. Role of transcription factor NF-kappa B/Rel in induction of nitric oxide synthase. The journal of biological chemistry. 1994;269(7):4705-8.
224. Newton R, Kuitert LM, Bergmann M, Adcock IM, Barnes PJ. Evidence for involvement of NF-kappaB in the transcriptional control of COX-2 gene expression by IL-1beta. Biochemical and biophysical research communications. 1997;237(1):28-32.
225. Sun SC. The non-canonical NF-kappaB pathway in immunity and inflammation. Nature reviews immunology. 2017;doi:10.1038/nri.2017.52.
226. Perkins ND. Regulation of NF-kappaB by atypical activators and tumour suppressors. Biochemical society transactions. 2004;32(Pt 6):936-9.
227. Karin M, Cao Y, Greten FR, Li ZW. NF-kappaB in cancer: from innocent bystander to major culprit. Nature reviews cancer. 2002;2(4):301-10.
228. Richmond A. Nf-kappa B, chemokine gene transcription and tumour growth. Nature reviews immunology. 2002;2(9):664-74.
229. Kaser A, Zeissig S, Blumberg RS. Inflammatory bowel disease. Annual review of immunology. 2010;28:573-621.
230. Ben-Neriah Y, Karin M. Inflammation meets cancer, with NF-kappaB as the matchmaker. Nature immunology. 2011;12(8):715-23.
231. Sohur US, Dixit MN, Chen CL, Byrom MW, Kerr LA. Rel/NF-kappaB represses bcl-2 transcription in pro-B lymphocytes. Gene expression. 1999;8(4):219-29.
232. Chilov D, Kukk E, Taira S, Jeltsch M, Kaukonen J, Palotie A, et al. Genomic organization of human and mouse genes for vascular endothelial growth factor C. The journal of biological chemistry. 1997;272(40):25176-83.
233. Huang S, DeGuzman A, Bucana CD, Fidler IJ. Nuclear factor-kappaB activity correlates with growth, angiogenesis, and metastasis of human melanoma cells in nude mice. Clinical cancer research. 2000;6(6):2573-81.
234. Hsia CY, Cheng S, Owyang AM, Dowdy SF, Liou HC. c-Rel regulation of the cell cycle in primary mouse B lymphocytes. International immunology. 2002;14(8):905-16.
235. Muz B, de la Puente P, Azab F, Azab AK. The role of hypoxia in cancer progression, angiogenesis, metastasis, and resistance to therapy. Hypoxia. 2015;3:83-92.
236. Katz M, Amit I, Yarden Y. Regulation of MAPKs by growth factors and receptor tyrosine kinases. Biochimica et biophysica acta. 2007;1773(8):1161-76.
237. Brown MD, Sacks DB. Protein scaffolds in MAP kinase signalling. Cellular signalling. 2009;21(4):462-9.
238. Pritchard AL, Hayward NK. Molecular pathways: mitogen-activated protein kinase pathway mutations and drug resistance. Clinical cancer research. 2013;19(9):2301-9.
239. Geest CR, Coffer PJ. MAPK signaling pathways in the regulation of hematopoiesis. Journal of leukocyte biology. 2009;86(2):237-50.
240. Davies H, Bignell GR, Cox C, Stephens P, Edkins S, Clegg S, et al. Mutations of the BRAF gene in human cancer. Nature. 2002;417(6892):949-54.

241. Marks JL, Gong Y, Chitale D, Golas B, McLellan MD, Kasai Y, et al. Novel MEK1 mutation identified by mutational analysis of epidermal growth factor receptor signaling pathway genes in lung adenocarcinoma. Cancer research. 2008;68(14):5524-8.
242. Bos JL, Verlaan-de Vries M, van der Eb AJ, Janssen JW, Delwel R, Lowenberg B, et al. Mutations in N-ras predominate in acute myeloid leukemia. Blood. 1987;69(4):1237-41.
243. Farr CJ, Saiki RK, Erlich HA, McCormick F, Marshall CJ. Analysis of RAS gene mutations in acute myeloid leukemia by polymerase chain reaction and oligonucleotide probes. Proceedings of the national academy of sciences of the United States of America. 1988;85(5):1629-33.
244. Reuter CW, Morgan MA, Bergmann L. Targeting the Ras signaling pathway: a rational, mechanism-based treatment for hematologic malignancies? Blood. 2000;96(5):1655-69.
245. Petanidis S, Anestakis D, Argyraki M, Hadzopoulou-Cladaras M, Salifoglou A. Differential expression of IL-17, 22 and 23 in the progression of colorectal cancer in patients with K-ras mutation: Ras signal inhibition and crosstalk with GM-CSF and IFN-gamma. PloS one. 2013;8(9):e73616.
246. McAllister F, Bailey JM, Alsina J, Nirschl CJ, Sharma R, Fan H, et al. Oncogenic Kras activates a hematopoietic-to-epithelial IL-17 signaling axis in preinvasive pancreatic neoplasia. Cancer cell. 2014;25(5):621-37.
247. Hui L, Zatloukal K, Scheuch H, Stepniak E, Wagner EF. Proliferation of human HCC cells and chemically induced mouse liver cancers requires JNK1-dependent p21 downregulation. The journal of clinical investigation. 2008;118(12):3943-53.
248. Chang Q, Chen J, Beezhold KJ, Castranova V, Shi X, Chen F. JNK1 activation predicts the prognostic outcome of the human hepatocellular carcinoma. Molecular cancer. 2009;8:64.
249. Barbarulo A, Iansante V, Chaidos A, Naresh K, Rahemtulla A, Franzoso G, et al. Poly(ADP-ribose) polymerase family member 14 (PARP14) is a novel effector of the JNK2-dependent pro-survival signal in multiple myeloma. Oncogene. 2013;32(36):4231-42.
250. Ha JH, Yan M, Gomathinayagam R, Jayaraman M, Husain S, Liu J, et al. Aberrant expression of JNK-associated leucine-zipper protein, JLP, promotes accelerated growth of ovarian cancer. Oncotarget. 2016;7(45):72845-59.
251. Nateri AS, Spencer-Dene B, Behrens A. Interaction of phosphorylated c-Jun with TCF4 regulates intestinal cancer development. Nature. 2005;437(7056):281-5.
252. Weston CR, Davis RJ. The JNK signal transduction pathway. Current opinion in genetics & development. 2002;12(1):14-21.
253. Bubici C, Papa S. JNK signalling in cancer: in need of new, smarter therapeutic targets. British journal of pharmacology. 2014;171(1):24-37.
254. Wang X, Destrument A, Tournier C. Physiological roles of MKK4 and MKK7: insights from animal models. Biochimica et biophysica acta. 2007;1773(8):1349-57.
255. Kan Z, Jaiswal BS, Stinson J, Janakiraman V, Bhatt D, Stern HM, et al. Diverse somatic mutation patterns and pathway alterations in human cancers. Nature. 2010;466(7308):869-73.
256. Krauthammer M, Kong Y, Ha BH, Evans P, Bacchiocchi A, McCusker JP, et al. Exome sequencing identifies recurrent somatic RAC1 mutations in melanoma. Nature genetics. 2012;44(9):1006-14.
257. Su GH, Hilgers W, Shekher MC, Tang DJ, Yeo CJ, Hruban RH, et al. Alterations in pancreatic, biliary, and breast carcinomas support MKK4 as a genetically targeted tumor suppressor gene. Cancer research. 1998;58(11):2339-42.
258. Royuela M, Arenas MI, Bethencourt FR, Sanchez-Chapado M, Fraile B, Paniagua R. Regulation of proliferation/apoptosis equilibrium by mitogen-activated protein kinases in normal, hyperplastic, and carcinomatous human prostate. Human pathology. 2002;33(3):299-306.
259. Mechta F, Lallemand D, Pfarr CM, Yaniv M. Transformation by ras modifies AP1 composition and activity. Oncogene. 1997;14(7):837-47.
260. Shaulian E. AP-1--The Jun proteins: oncogenes or tumor suppressors in disguise? Cellular signalling. 2010;22(6):894-9.
261. Papoudou-Bai A, Hatzimichael E, Barbouti A, Kanavaros P. Expression patterns of the activator protein-1 (AP-1) family members in lymphoid neoplasms. Clinical and experimental medicine. 2017; 17(3):291-304.
262. Hess J, Angel P, Schorpp-Kistner M. AP-1 subunits: quarrel and harmony among siblings. Journal of cell science. 2004;117(Pt 25):5965-73.
263. Piechaczyk M, Farras R. Regulation and function of JunB in cell proliferation. Biochemical society transactions. 2008;36(Pt 5):864-7.

264. Behrens A, Sibilia M, Wagner EF. Amino-terminal phosphorylation of c-Jun regulates stress-induced apoptosis and cellular proliferation. Nature genetics. 1999;21(3):326-9.
265. Wei W, Jin J, Schlisio S, Harper JW, Kaelin WG, Jr. The v-Jun point mutation allows c-Jun to escape GSK3-dependent recognition and destruction by the Fbw7 ubiquitin ligase. Cancer cell. 2005;8(1):25-33.
266. Hilberg F, Aguzzi A, Howells N, Wagner EF. c-jun is essential for normal mouse development and hepatogenesis. Nature. 1993;365(6442):179-81.
267. Johnson RS, van Lingen B, Papaioannou VE, Spiegelman BM. A null mutation at the c-jun locus causes embryonic lethality and retarded cell growth in culture. Genes & development. 1993;7(7B):1309-17.
268. Dhanasekaran DN, Reddy EP. JNK signaling in apoptosis. Oncogene. 2008;27(48):6245-51.
269. Yu C, Minemoto Y, Zhang J, Liu J, Tang F, Bui TN, et al. JNK suppresses apoptosis via phosphorylation of the proapoptotic Bcl-2 family protein BAD. Molecular cell. 2004;13(3):329-40.
270. Mocellin S, Nitti D. TNF and cancer: the two sides of the coin. Frontiers in bioscience. 2008;13:2774-83.
271. Karin M, Lin A. NF-kappaB at the crossroads of life and death. Nature immunology. 2002;3(3):221-7.
272. Liu J, Lin A. Role of JNK activation in apoptosis: a double-edged sword. Cell research. 2005;15(1):36-42.
273. Wang RA, Li QL, Li ZS, Zheng PJ, Zhang HZ, Huang XF, et al. Apoptosis drives cancer cells proliferate and metastasize. Journal of cellular and molecular medicine. 2013;17(1):205-11.
274. Ryoo HD, Bergmann A. The role of apoptosis-induced proliferation for regeneration and cancer. Cold Spring Harbor perspectives in biology. 2012;4(8):a008797.
275. Chen F. JNK-induced apoptosis, compensatory growth, and cancer stem cells. Cancer research. 2012;72(2):379-86.
276. Davis RJ. Signal transduction by the JNK group of MAP kinases. Cell. 2000;103(2):239-52.
277. Yang DD, Kuan CY, Whitmarsh AJ, Rincon M, Zheng TS, Davis RJ, et al. Absence of excitotoxicity-induced apoptosis in the hippocampus of mice lacking the JNK3 gene. Nature. 1997;389(6653):865-70.
278. Kuan CY, Whitmarsh AJ, Yang DD, Liao G, Schloemer AJ, Dong C, et al. A critical role of neural-specific JNK3 for ischemic apoptosis. Proceedings of the national academy of sciences of the United States of America. 2003;100(25):15184-9.
279. Sabapathy K, Hochedlinger K, Nam SY, Bauer A, Karin M, Wagner EF. Distinct roles for JNK1 and JNK2 in regulating JNK activity and c-Jun-dependent cell proliferation. Molecular cell. 2004;15(5):713-25.
280. Weston CR, Wong A, Hall JP, Goad ME, Flavell RA, Davis RJ. The c-Jun NH2-terminal kinase is essential for epidermal growth factor expression during epidermal morphogenesis. Proceedings of the national academy of sciences of the United States of America. 2004;101(39):14114-9.
281. Fuchs SY, Dolan L, Davis RJ, Ronai Z. Phosphorylation-dependent targeting of c-Jun ubiquitination by Jun N-kinase. Oncogene. 1996;13(7):1531-5.
282. Jaeschke A, Karasarides M, Ventura JJ, Ehrhardt A, Zhang C, Flavell RA, et al. JNK2 is a positive regulator of the cJun transcription factor. Molecular cell. 2006;23(6):899-911.
283. Choi HS, Bode AM, Shim JH, Lee SY, Dong Z. c-Jun N-terminal kinase 1 phosphorylates Myt1 to prevent UVA-induced skin cancer. Molecular and cellular biology. 2009;29(8):2168-80.
284. Liu J, Minemoto Y, Lin A. c-Jun N-terminal protein kinase 1 (JNK1), but not JNK2, is essential for tumor necrosis factor alpha-induced c-Jun kinase activation and apoptosis. Molecular and cellular biology. 2004;24(24):10844-56.
285. Tournier C, Hess P, Yang DD, Xu J, Turner TK, Nimnual A, et al. Requirement of JNK for stress-induced activation of the cytochrome c-mediated death pathway. Science. 2000;288(5467):870-4.
286. Chen N, Nomura M, She QB, Ma WY, Bode AM, Wang L, et al. Suppression of skin tumorigenesis in c-Jun NH(2)-terminal kinase-2-deficient mice. Cancer research. 2001;61(10):3908-12.
287. She QB, Chen N, Bode AM, Flavell RA, Dong Z. Deficiency of c-Jun-NH2-terminal kinase-1 in mice enhances skin tumor development by 12-O-tetradecanoylphorbol-13-acetate. Cancer research. 2002;62(5):1343-8.
288. Tong C, Yin Z, Song Z, Dockendorff A, Huang C, Mariadason J, et al. c-Jun NH2-terminal kinase 1 plays a critical role in intestinal homeostasis and tumor suppression. The American journal of pathology. 2007;171(1):297-303.

289. Wellbrock C, Arozarena I. The complexity of the ERK/MAP-kinase pathway and the treatment of melanoma skin cancer. Frontiers in cell and developmental biology. 2016;4:33.
290. Nakagawa I, Kamimura D, Atsumi T, Arima Y, Murakami M. Role of inflammation amplifier-induced growth factor expression in the development of inflammatory diseases. Critical reviews in immunology. 2015;35(5):365-78.
291. Amatya N, Garg AV, Gaffen SL. IL-17 signaling: the yin and the yang. Trends in immunology. 2017;38(5):310-322.
292. Gaffen SL. Structure and signalling in the IL-17 receptor family. Nature reviews immunology. 2009;9(8):556-67.
293. Gu C, Wu L, Li X. IL-17 family: cytokines, receptors and signaling. Cytokine. 2013;64(2):477-85.
294. Noack M, Ndongo-Thiam N, Miossec P. Interaction among activated lymphocytes and mesenchymal cells through podoplanin is critical for a high IL-17 secretion. Arthritis research & therapy. 2016;18:148.
295. Chabaud M, Page G, Miossec P. Enhancing effect of IL-1, IL-17, and TNF-alpha on macrophage inflammatory protein-3alpha production in rheumatoid arthritis: regulation by soluble receptors and Th2 cytokines. Journal of immunology. 2001;167(10):6015-20.
296. Zrioual S, Ecochard R, Tournadre A, Lenief V, Cazalis MA, Miossec P. Genome-wide comparison between IL-17A- and IL-17F-induced effects in human rheumatoid arthritis synoviocytes. Journal of immunology. 2009;182(5):3112-20.
297. Yao Z, Fanslow WC, Seldin MF, Rousseau AM, Painter SL, Comeau MR, et al. Herpesvirus Saimiri encodes a new cytokine, IL-17, which binds to a novel cytokine receptor. Immunity. 1995;3(6):811-21.
298. Ishigame H, Kakuta S, Nagai T, Kadoki M, Nambu A, Komiyama Y, et al. Differential roles of interleukin-17A and -17F in host defense against mucoepithelial bacterial infection and allergic responses. Immunity. 2009;30(1):108-19.
299. Onishi RM, Park SJ, Hanel W, Ho AW, Maitra A, Gaffen SL. SEF/IL-17R (SEFIR) is not enough: an extended SEFIR domain is required for IL-17RA-mediated signal transduction. The journal of biological chemistry. 2010;285(43):32751-9.
300. Haudenschild D, Moseley T, Rose L, Reddi AH. Soluble and transmembrane isoforms of novel interleukin-17 receptor-like protein by RNA splicing and expression in prostate cancer. The journal of biological chemistry. 2002;277(6):4309-16.
301. Moseley TA, Haudenschild DR, Rose L, Reddi AH. Interleukin-17 family and IL-17 receptors. Cytokine & growth factor reviews. 2003;14(2):155-74.
302. Wright JF, Bennett F, Li B, Brooks J, Luxenberg DP, Whitters MJ, et al. The human IL-17F/IL-17A heterodimeric cytokine signals through the IL-17RA/IL-17RC receptor complex. Journal of immunology. 2008;181(4):2799-805.
303. Alinejad V, Dolati S, Motallebnezhad M, Yousefi M. The role of IL17B-IL17RB signaling pathway in breast cancer. Biomedicine & pharmacotherapy = Biomedecine & pharmacotherapie. 2017;88:795-803.
304. Onishi RM, Gaffen SL. Interleukin-17 and its target genes: mechanisms of interleukin-17 function in disease. Immunology. 2010;129(3):311-21.
305. Fujino S, Andoh A, Bamba S, Ogawa A, Hata K, Araki Y, et al. Increased expression of interleukin 17 in inflammatory bowel disease. Gut. 2003;52(1):65-70.
306. Hueber W, Patel DD, Dryja T, Wright AM, Koroleva I, Bruin G, et al. Effects of AIN457, a fully human antibody to interleukin-17A, on psoriasis, rheumatoid arthritis, and uveitis. Science translational medicine. 2010;2(52):52ra72.
307. Kuestner RE, Taft DW, Haran A, Brandt CS, Brender T, Lum K, et al. Identification of the IL-17 receptor related molecule IL-17RC as the receptor for IL-17F. Journal of immunology. 2007;179(8):5462-73.
308. Huang CK, Yang CY, Jeng YM, Chen CL, Wu HH, Chang YC, et al. Autocrine/paracrine mechanism of interleukin-17B receptor promotes breast tumorigenesis through NF-kappaB-mediated antiapoptotic pathway. Oncogene. 2014;33(23):2968-77.
309. Song X, Gao H, Lin Y, Yao Y, Zhu S, Wang J, et al. Alterations in the microbiota drive interleukin-17C production from intestinal epithelial cells to promote tumorigenesis. Immunity. 2014;40(1):140-52.
310. O'Sullivan T, Saddawi-Konefka R, Gross E, Tran M, Mayfield SP, Ikeda H, et al. Interleukin-17D mediates tumor rejection through recruitment of natural killer cells. Cell reports. 2014;7(4):989-98.
311. Xu S, Cao X. Interleukin-17 and its expanding biological functions. Cellular & molecular immunology. 2010;7(3):164-74.

312. Wong CK, Ho CY, Ko FW, Chan CH, Ho AS, Hui DS, et al. Proinflammatory cytokines (IL-17, IL-6, IL-18 and IL-12) and Th cytokines (IFN-gamma, IL-4, IL-10 and IL-13) in patients with allergic asthma. Clinical and experimental immunology. 2001;125(2):177-83.
313. Novatchkova M, Leibbrandt A, Werzowa J, Neubuser A, Eisenhaber F. The STIR-domain superfamily in signal transduction, development and immunity. Trends in biochemical sciences. 2003;28(5):226-9.
314. Tesmer LA, Lundy SK, Sarkar S, Fox DA. Th17 cells in human disease. Immunological reviews. 2008;223:87-113.
315. Lin Y, Ritchea S, Logar A, Slight S, Messmer M, Rangel-Moreno J, et al. Interleukin-17 is required for T helper 1 cell immunity and host resistance to the intracellular pathogen *Francisella tularensis*. Immunity. 2009;31(5):799-810.
316. Qian X, Chen H, Wu X, Hu L, Huang Q, Jin Y. Interleukin-17 acts as double-edged sword in anti-tumor immunity and tumorigenesis. Cytokine. 2017;89:34-44.
317. Curtis MM, Way SS. Interleukin-17 in host defence against bacterial, mycobacterial and fungal pathogens. Immunology. 2009;126(2):177-85.
318. Maxwell JR, Zhang Y, Brown WA, Smith CL, Byrne FR, Fiorino M, et al. Differential roles for interleukin-23 and interleukin-17 in intestinal immunoregulation. Immunity. 2015;43(4):739-50.
319. Kumar P, Monin L, Castillo P, Elsegeiny W, Horne W, Eddens T, et al. Intestinal interleukin-17 receptor signaling mediates reciprocal control of the gut microbiota and autoimmune inflammation. Immunity. 2016;44(3):659-71.
320. Ho AW, Shen F, Conti HR, Patel N, Childs EE, Peterson AC, et al. IL-17RC is required for immune signaling via an extended SEF/IL-17R signaling domain in the cytoplasmic tail. Journal of immunology. 2010;185(2):1063-70.
321. Ely LK, Fischer S, Garcia KC. Structural basis of receptor sharing by interleukin 17 cytokines. Nature immunology. 2009;10(12):1245-51.
322. Bazan JF. Structural design and molecular evolution of a cytokine receptor superfamily. Proceedings of the national academy of sciences of the United States of America. 1990;87(18):6934-8.
323. Yao Z, Painter SL, Fanslow WC, Ulrich D, Macduff BM, Spriggs MK, et al. Human IL-17: a novel cytokine derived from T cells. Journal of immunology. 1995;155(12):5483-6.
324. Miossec P, Kolls JK. Targeting IL-17 and Th17 cells in chronic inflammation. Nature reviews drug discovery. 2012;11(10):763-76.
325. Yang XO, Chang SH, Park H, Nurieva R, Shah B, Acero L, et al. Regulation of inflammatory responses by IL-17F. The journal of experimental medicine. 2008;205(5):1063-75.
326. Hueber W, Sands BE, Lewitzky S, Vandemeulebroecke M, Reinisch W, Higgins PD, et al. Secukinumab, a human anti-IL-17A monoclonal antibody, for moderate to severe Crohn's disease: unexpected results of a randomised, double-blind placebo-controlled trial. Gut. 2012;61(12):1693-700.
327. Targan SR, Feagan B, Vermeire S, Panaccione R, Melmed GY, Landers C, et al. A randomized, double-blind, placebo-controlled phase 2 study of brodalumab in patients with moderate-to-severe Crohn's disease. The American journal of gastroenterology. 2016;111(11):1599-607.
328. Haudenschild DR, Curtiss SB, Moseley TA, Reddi AH. Generation of interleukin-17 receptor-like protein (IL-17RL) in prostate by alternative splicing of RNA. The prostate. 2006;66(12):1268-74.
329. Ramirez-Carrozzi V, Sambandam A, Luis E, Lin Z, Jeet S, Lesch J, et al. IL-17C regulates the innate immune function of epithelial cells in an autocrine manner. Nature immunology. 2011;12(12):1159-66.
330. Nirula A, Nilsen J, Klekotka P, Kricorian G, Erondu N, Towne JE, et al. Effect of IL-17 receptor A blockade with brodalumab in inflammatory diseases. Rheumatology. 2016;55(suppl 2):ii43-ii55.
331. Starnes T, Broxmeyer HE, Robertson MJ, Hromas R. Cutting edge: IL-17D, a novel member of the IL-17 family, stimulates cytokine production and inhibits hemopoiesis. Journal of immunology. 2002;169(2):642-6.
332. Saddawi-Konefka R, Seelige R, Gross ET, Levy E, Searles SC, Washington A, Jr., et al. Nrf2 induces IL-17D to mediate tumor and virus surveillance. Cell reports. 2016;16(9):2348-58.
333. Owyang AM, Zaph C, Wilson EH, Guild KJ, McClanahan T, Miller HR, et al. Interleukin 25 regulates type 2 cytokine-dependent immunity and limits chronic inflammation in the gastrointestinal tract. The journal of experimental medicine. 2006;203(4):843-9.
334. Fort MM, Cheung J, Yen D, Li J, Zurawski SM, Lo S, et al. IL-25 induces IL-4, IL-5, and IL-13 and Th2-associated pathologies *in vivo*. Immunity. 2001;15(6):985-95.

335. Tamachi T, Maezawa Y, Ikeda K, Iwamoto I, Nakajima H. Interleukin 25 in allergic airway inflammation. International archives of allergy and immunology. 2006;140(Suppl 1):59-62.
336. Furuta S, Jeng YM, Zhou L, Huang L, Kuhn I, Bissell MJ, et al. IL-25 causes apoptosis of IL-25R-expressing breast cancer cells without toxicity to nonmalignant cells. Science translational medicine. 2011;3(78):78ra31.
337. Wilson NJ, Boniface K, Chan JR, McKenzie BS, Blumenschein WM, Mattson JD, et al. Development, cytokine profile and function of human interleukin 17-producing helper T cells. Nature immunology. 2007;8(9):950-7.
338. Korn T, Oukka M, Kuchroo V, Bettelli E. Th17 cells: effector T cells with inflammatory properties. Seminars in immunology. 2007;19(6):362-71.
339. Cua DJ, Tato CM. Innate IL-17-producing cells: the sentinels of the immune system. Nature reviews immunology. 2010;10(7):479-89.
340. Takahashi N, Vanlaere I, de Rycke R, Cauwels A, Joosten LA, Lubberts E, et al. IL-17 produced by Paneth cells drives TNF-induced shock. The journal of experimental medicine. 2008;205(8):1755-61.
341. Hu Y, Ota N, Peng I, Refino CJ, Danilenko DM, Caplazi P, et al. IL-17RC is required for IL-17A- and IL-17F-dependent signaling and the pathogenesis of experimental autoimmune encephalomyelitis. Journal of immunology. 2010;184(8):4307-16.
342. Su X, Ye J, Hsueh EC, Zhang Y, Hoft DF, Peng G. Tumor microenvironments direct the recruitment and expansion of human Th17 cells. Journal of immunology. 2010;184(3):1630-41.
343. Meng XY, Zhou CH, Ma J, Jiang C, Ji P. Expression of interleukin-17 and its clinical significance in gastric cancer patients. Medical oncology. 2012;29(5):3024-8.
344. Xu C, Hao K, Yu L, Zhang X. Serum interleukin-17 as a diagnostic and prognostic marker for non-small cell lung cancer. Biomarkers. 2014;19(4):287-90.
345. Kryczek I, Banerjee M, Cheng P, Vatan L, Szeliga W, Wei S, et al. Phenotype, distribution, generation, and functional and clinical relevance of Th17 cells in the human tumor environments. Blood. 2009;114(6):1141-9.
346. Ghadjar P, Rubie C, Aebersold DM, Keilholz U. The chemokine CCL20 and its receptor CCR6 in human malignancy with focus on colorectal cancer. International journal of cancer. 2009;125(4):741-5.
347. Muranski P, Boni A, Antony PA, Cassard L, Irvine KR, Kaiser A, et al. Tumor-specific Th17-polarized cells eradicate large established melanoma. Blood. 2008;112(2):362-73.
348. Zhou L, Ivanov, II, Spolski R, Min R, Shenderov K, Egawa T, et al. IL-6 programs Th17 cell differentiation by promoting sequential engagement of the IL-21 and IL-23 pathways. Nature immunology. 2007;8(9):967-74.
349. Numasaki M, Fukushi J, Ono M, Narula SK, Zavodny PJ, Kudo T, et al. Interleukin-17 promotes angiogenesis and tumor growth. Blood. 2003;101(7):2620-7.
350. Numasaki M, Watanabe M, Suzuki T, Takahashi H, Nakamura A, McAllister F, et al. IL-17 enhances the net angiogenic activity and in vivo growth of human non-small cell lung cancer in SCID mice through promoting CXCR-2-dependent angiogenesis. Journal of immunology. 2005;175(9):6177-89.
351. Wakita D, Sumida K, Iwakura Y, Nishikawa H, Ohkuri T, Chamoto K, et al. Tumor-infiltrating IL-17-producing gammadelta T cells support the progression of tumor by promoting angiogenesis. European journal of immunology. 2010;40(7):1927-37.
352. Chung AS, Wu X, Zhuang G, Ngu H, Kasman I, Zhang J, et al. An interleukin-17-mediated paracrine network promotes tumor resistance to anti-angiogenic therapy. Nature medicine. 2013;19(9):1114-23.
353. Wang L, Yi T, Kortylewski M, Pardoll DM, Zeng D, Yu H. IL-17 can promote tumor growth through an IL-6-STAT3 signaling pathway. The journal of experimental medicine. 2009;206(7):1457-64.
354. He D, Li H, Yusuf N, Elmets CA, Li J, Mountz JD, et al. IL-17 promotes tumor development through the induction of tumor promoting microenvironments at tumor sites and myeloid-derived suppressor cells. Journal of immunology. 2010;184(5):2281-8.
355. Benchetrit F, Ciree A, Vives V, Warnier G, Gey A, Sautes-Fridman C, et al. Interleukin-17 inhibits tumor cell growth by means of a T-cell-dependent mechanism. Blood. 2002;99(6):2114-21.
356. Kryczek I, Wei S, Szeliga W, Vatan L, Zou W. Endogenous IL-17 contributes to reduced tumor growth and metastasis. Blood. 2009;114(2):357-9.
357. Tartour E, Fossiez F, Joyeux I, Galinha A, Gey A, Claret E, et al. Interleukin 17, a T-cell-derived cytokine, promotes tumorigenicity of human cervical tumors in nude mice. Cancer research. 1999;59(15):3698-704.

358. Schwartz S, Beaulieu JF, Ruemmele FM. Interleukin-17 is a potent immuno-modulator and regulator of normal human intestinal epithelial cell growth. Biochemical and biophysical research communications. 2005;337(2):505-9.
359. You Z, Ge D, Liu S, Zhang Q, Borowsky AD, Melamed J. Interleukin-17 induces expression of chemokines and cytokines in prostatic epithelial cells but does not stimulate cell growth in vitro. International journal of medical and biological frontiers. 2012;18(8):629-44.
360. Li Z, Li K, Zhu L, Kan Q, Yan Y, Kumar P, et al. Inhibitory effect of IL-17 on neural stem cell proliferation and neural cell differentiation. BMC immunology. 2013;14:20.
361. Zhang Q, Liu S, Ge D, Zhang Q, Xue Y, Xiong Z, et al. Interleukin-17 promotes formation and growth of prostate adenocarcinoma in mouse models. Cancer research. 2012;72(10):2589-99.
362. Zhang Q, Liu S, Zhang Q, Xiong Z, Wang AR, Myers L, et al. Interleukin-17 promotes development of castration-resistant prostate cancer potentially through creating an immunotolerant and pro-angiogenic tumor microenvironment. The prostate. 2014;74(8):869-79.
363. You Z, Shi XB, DuRaine G, Haudenschild D, Tepper CG, Lo SH, et al. Interleukin-17 receptor-like gene is a novel antiapoptotic gene highly expressed in androgen-independent prostate cancer. Cancer research. 2006;66(1):175-83.
364. Nam JS, Terabe M, Kang MJ, Chae H, Voong N, Yang YA, et al. Transforming growth factor beta subverts the immune system into directly promoting tumor growth through interleukin-17. Cancer research. 2008;68(10):3915-23.
365. Chang Y, Al-Alwan L, Risse PA, Halayko AJ, Martin JG, Baglole CJ, et al. Th17-associated cytokines promote human airway smooth muscle cell proliferation. FASEB journal. 2012;26(12):5152-60.
366. Kim G, Khanal P, Lim SC, Yun HJ, Ahn SG, Ki SH, et al. Interleukin-17 induces AP-1 activity and cellular transformation via upregulation of tumor progression locus 2 activity. Carcinogenesis. 2013;34(2):341-50.
367. Lee SY, Kwok SK, Son HJ, Ryu JG, Kim EK, Oh HJ, et al. IL-17-mediated Bcl-2 expression regulates survival of fibroblast-like synoviocytes in rheumatoid arthritis through STAT3 activation. Arthritis research & therapy. 2013;15(1):R31.
368. Wu X, Zeng Z, Xu L, Yu J, Cao Q, Chen M, et al. Increased expression of IL17A in human gastric cancer and its potential roles in gastric carcinogenesis. Tumour biology. 2014;35(6):5347-56.
369. Sun Y, Pan J, Mao S, Jin J. IL-17/miR-192/IL-17Rs regulatory feedback loop facilitates multiple myeloma progression. PloS one. 2014;9(12):e114647.
370. Wu L, Chen X, Zhao J, Martin B, Zepp JA, Ko JS, et al. A novel IL-17 signaling pathway controlling keratinocyte proliferation and tumorigenesis via the TRAF4-ERK5 axis. The journal of experimental medicine. 2015;212(10):1571-87.
371. Mombelli S, Cochaud S, Merrouche Y, Garbar C, Antonicelli F, Laprevotte E, et al. IL-17A and its homologs IL-25/IL-17E recruit the c-RAF/S6 kinase pathway and the generation of pro-oncogenic LMW-E in breast cancer cells. Scientific reports. 2015;5:11874.
372. Bi L, Wu J, Ye A, Wu J, Yu K, Zhang S, et al. Increased Th17 cells and IL-17A exist in patients with B cell acute lymphoblastic leukemia and promote proliferation and resistance to daunorubicin through activation of Akt signaling. Journal of translational medicine. 2016;14(1):132.
373. Chang SH, Park H, Dong C. Act1 adaptor protein is an immediate and essential signaling component of interleukin-17 receptor. The journal of biological chemistry. 2006;281(47):35603-7.
374. Sonder SU, Saret S, Tang W, Sturdevant DE, Porcella SF, Siebenlist U. IL-17-induced NF-kappaB activation via CIKS/Act1: physiologic significance and signaling mechanisms. The journal of biological chemistry. 2011;286(15):12881-90.
375. Wang C, Deng L, Hong M, Akkaraju GR, Inoue J, Chen ZJ. TAK1 is a ubiquitin-dependent kinase of MKK and IKK. Nature. 2001;412(6844):346-51.
376. Zhou Y, Toh ML, Zrioual S, Miossec P. IL-17A versus IL-17F induced intracellular signal transduction pathways and modulation by IL-17RA and IL-17RC RNA interference in AGS gastric adenocarcinoma cells. Cytokine. 2007;38(3):157-64.
377. Iyoda M, Shibata T, Kawaguchi M, Hizawa N, Yamaoka T, Kokubu F, et al. IL-17A and IL-17F stimulate chemokines via MAPK pathways (ERK1/2 and p38 but not JNK) in mouse cultured mesangial cells: synergy with TNF-alpha and IL-1beta. American journal of physiology renal physiology. 2010;298(3):F779-87.
378. Lin D, Li L, Sun Y, Wang W, Wang X, Ye Y, et al. IL-17 regulates the expressions of RANKL and OPG in human periodontal ligament cells via TRAF6/TBK1-JNK/NF-kappaB pathways. Immunology. 2014.

379. Li JK, Nie L, Zhao YP, Zhang YQ, Wang X, Wang SS, et al. IL-17 mediates inflammatory reactions via p38/c-Fos and JNK/c-Jun activation in an AP-1-dependent manner in human nucleus pulposus cells. Journal of translational medicine. 2016;14:77.
380. Ruddy MJ, Wong GC, Liu XK, Yamamoto H, Kasayama S, Kirkwood KL, et al. Functional cooperation between interleukin-17 and tumor necrosis factor-alpha is mediated by CCAAT/enhancer-binding protein family members. The journal of biological chemistry. 2004;279(4):2559-67.
381. Cortez DM, Feldman MD, Mummidi S, Valente AJ, Steffensen B, Vincenti M, et al. IL-17 stimulates MMP-1 expression in primary human cardiac fibroblasts via p38 MAPK- and ERK1/2-dependent C/EBP-beta , NF-kappaB, and AP-1 activation. American journal of physiology heart and circulatory physiology. 2007;293(6):H3356-65.
382. Patel DN, King CA, Bailey SR, Holt JW, Venkatachalam K, Agrawal A, et al. Interleukin-17 stimulates C-reactive protein expression in hepatocytes and smooth muscle cells via p38 MAPK and ERK1/2-dependent NF-kappaB and C/EBPbeta activation. The journal of biological chemistry. 2007;282(37):27229-38.
383. Huang F, Kao CY, Wachi S, Thai P, Ryu J, Wu R. Requirement for both JAK-mediated PI3K signaling and ACT1/TRAF6/TAK1-dependent NF-kappaB activation by IL-17A in enhancing cytokine expression in human airway epithelial cells. Journal of immunology. 2007;179(10):6504-13.
384. Guo X, Jiang X, Xiao Y, Zhou T, Guo Y, Wang R, et al. IL-17A signaling in colonic epithelial cells inhibits pro-inflammatory cytokine production by enhancing the activity of ERK and PI3K. PloS one. 2014;9(2):e89714.
385. Sun D, Novotny M, Bulek K, Liu C, Li X, Hamilton T. Treatment with IL-17 prolongs the half-life of chemokine CXCL1 mRNA via the adaptor TRAF5 and the splicing-regulatory factor SF2 (ASF). Nature immunology. 2011;12(9):853-60.
386. Hartupee J, Liu C, Novotny M, Li X, Hamilton T. IL-17 enhances chemokine gene expression through mRNA stabilization. Journal of immunology. 2007;179(6):4135-41.
387. Bakheet T, Williams BR, Khabar KS. ARED 3.0: the large and diverse AU-rich transcriptome. Nucleic acids research. 2006;34:D111-4.
388. Garneau NL, Wilusz J, Wilusz CJ. The highways and byways of mRNA decay. Nature reviews molecular cell biology. 2007;8(2):113-26.
389. Cobb MH, Goldsmith EJ. How MAP kinases are regulated. The journal of biological chemistry. 1995;270(25):14843-6.
390. Shen F, Gaffen SL. Structure-function relationships in the IL-17 receptor: implications for signal transduction and therapy. Cytokine. 2008;41(2):92-104.
391. van den Berg A, Kuiper M, Snoek M, Timens W, Postma DS, Jansen HM, et al. Interleukin-17 induces hyperresponsive interleukin-8 and interleukin-6 production to tumor necrosis factor-alpha in structural lung cells. American journal of respiratory cell and molecular biology. 2005;33(1):97-104.
392. Ruddy MJ, Shen F, Smith JB, Sharma A, Gaffen SL. Interleukin-17 regulates expression of the CXC chemokine LIX/CXCL5 in osteoblasts: implications for inflammation and neutrophil recruitment. Journal of leukocyte biology. 2004;76(1):135-44.
393. Karlsen JR, Borregaard N, Cowland JB. Induction of neutrophil gelatinase-associated lipocalin expression by co-stimulation with interleukin-17 and tumor necrosis factor-alpha is controlled by IkappaB-zeta but neither by C/EBP-beta nor C/EBP-delta. The journal of biological chemistry. 2010;285(19):14088-100.
394. Sonder SU, Paun A, Ha HL, Johnson PF, Siebenlist U. CIKS/Act1-mediated signaling by IL-17 cytokines in context: implications for how a CIKS gene variant may predispose to psoriasis. Journal of immunology. 2012;188(12):5906-14.
395. Annemann M, Wang Z, Plaza-Sirvent C, Glauben R, Schuster M, Ewald Sander F, et al. IkappaBNS regulates murine Th17 differentiation during gut inflammation and infection. Journal of immunology. 2015;194(6):2888-98.
396. Garg AV, Amatya N, Chen K, Cruz JA, Grover P, Whibley N, et al. MCPIP1 endoribonuclease activity negatively regulates interleukin-17-mediated signaling and inflammation. Immunity. 2015;43(3):475-87.
397. Okamoto K, Iwai Y, Oh-Hora M, Yamamoto M, Morio T, Aoki K, et al. IkappaBzeta regulates Th17 development by cooperating with ROR nuclear receptors. Nature. 2010;464(7293):1381-5.

398. Zhu S, Pan W, Song X, Liu Y, Shao X, Tang Y, et al. The microRNA miR-23b suppresses IL-17-associated autoimmune inflammation by targeting TAB2, TAB3 and IKK-alpha. Nature medicine. 2012;18(7):1077-86.
399. Mellett M, Atzei P, Horgan A, Hams E, Floss T, Wurst W, et al. Orphan receptor IL-17RD tunes IL-17A signalling and is required for neutrophilia. Nature communications. 2012;3:1119.
400. Maitra A, Shen F, Hanel W, Mossman K, Tocker J, Swart D, et al. Distinct functional motifs within the IL-17 receptor regulate signal transduction and target gene expression. Proceedings of the national academy of sciences of the United States of America. 2007;104(18):7506-11.
401. Shen F, Li N, Gade P, Kalvakolanu DV, Weibley T, Doble B, et al. IL-17 receptor signaling inhibits C/EBPbeta by sequential phosphorylation of the regulatory 2 domain. Science signaling. 2009;2(59):ra8.
402. Yamada T, Tsuchiya T, Osada S, Nishihara T, Imagawa M. CCAAT/enhancer-binding protein delta gene expression is mediated by autoregulation through downstream binding sites. Biochemical and biophysical research communications. 1998;242(1):88-92.
403. Ramji DP, Foka P. CCAAT/enhancer-binding proteins: structure, function and regulation. The biochemical journal. 2002;365(Pt 3):561-75.
404. Zhu S, Pan W, Shi P, Gao H, Zhao F, Song X, et al. Modulation of experimental autoimmune encephalomyelitis through TRAF3-mediated suppression of interleukin 17 receptor signaling. The journal of experimental medicine. 2010;207(12):2647-62.
405. Zepp JA, Liu C, Qian W, Wu L, Gulen MF, Kang Z, et al. Cutting edge: TNF receptor-associated factor 4 restricts IL-17-mediated pathology and signaling processes. Journal of immunology. 2012;189(1):33-7.
406. Wan Q, Zhou Z, Ding S, He J. The miR-30a negatively regulates IL-17-mediated signal transduction by targeting Traf3ip2. Journal of interferon & cytokine research. 2015;35(11):917-23.
407. Jeltsch KM, Hu D, Brenner S, Zoller J, Heinz GA, Nagel D, et al. Cleavage of roquin and regnase-1 by the paracaspase MALT1 releases their cooperatively repressed targets to promote Th17 differentiation. Nature immunology. 2014;15(11):1079-89.
408. Zhong B, Liu X, Wang X, Chang SH, Liu X, Wang A, et al. Negative regulation of IL-17-mediated signaling and inflammation by the ubiquitin-specific protease USP25. Nature immunology. 2012;13(11):1110-7.
409. Garg AV, Ahmed M, Vallejo AN, Ma A, Gaffen SL. The deubiquitinase A20 mediates feedback inhibition of interleukin-17 receptor signaling. Science signaling. 2013;6(278):ra44.
410. Ho AW, Garg AV, Monin L, Simpson-Abelson MR, Kinner L, Gaffen SL. The anaphase-promoting complex protein 5 (AnapC5) associates with A20 and inhibits IL-17-mediated signal transduction. PloS one. 2013;8(7):e70168.
411. Yamaguchi N, Oyama M, Kozuka-Hata H, Inoue J. Involvement of A20 in the molecular switch that activates the non-canonical NF-kappaB pathway. Scientific reports. 2013;3:2568.
412. Vereecke L, Beyaert R, van Loo G. The ubiquitin-editing enzyme A20 (TNFAIP3) is a central regulator of immunopathology. Trends in immunology. 2009;30(8):383-91.
413. Ma A, Malynn BA. A20: linking a complex regulator of ubiquitylation to immunity and human disease. Nature reviews immunology. 2012;12(11):774-85.
414. Boone DL, Turer EE, Lee EG, Ahmad RC, Wheeler MT, Tsui C, et al. The ubiquitin-modifying enzyme A20 is required for termination of Toll-like receptor responses. Nature immunology. 2004;5(10):1052-60.
415. Verstrepen L, Verhelst K, van Loo G, Carpentier I, Ley SC, Beyaert R. Expression, biological activities and mechanisms of action of A20 (TNFAIP3). Biochemical pharmacology. 2010;80(12):2009-20.
416. Srinivasula SM, Ashwell JD. A20: more than one way to skin a cat. Molecular cell. 2011;44(4):511-2.
417. Zhang M, Peng LL, Wang Y, Wang JS, Liu J, Liu MM, et al. Roles of A20 in autoimmune diseases. Immunologic research. 2016;64(2):337-44.
418. Lee EG, Boone DL, Chai S, Libby SL, Chien M, Lodolce JP, et al. Failure to regulate TNF-induced NF-kappaB and cell death responses in A20-deficient mice. Science. 2000;289(5488):2350-4.
419. Turer EE, Tavares RM, Mortier E, Hitotsumatsu O, Advincula R, Lee B, et al. Homeostatic MyD88-dependent signals cause lethal inflammation in the absence of A20. The journal of experimental medicine. 2008;205(2):451-64.

420. Mele A, Cervantes JR, Chien V, Friedman D, Ferran C. Single nucleotide polymorphisms at the TNFAIP3/A20 locus and susceptibility/resistance to inflammatory and autoimmune diseases. Advances in experimental medicine and biology. 2014;809:163-83.
421. Zhou Q, Wang H, Schwartz DM, Stoffels M, Park YH, Zhang Y, et al. Loss-of-function mutations in TNFAIP3 leading to A20 haploinsufficiency cause an early-onset autoinflammatory disease. Nature genetics. 2016;48(1):67-73.
422. Hymowitz SG, Wertz IE. A20: from ubiquitin editing to tumour suppression. Nature reviews cancer. 2010;10(5):332-41.
423. Won M, Park KA, Byun HS, Sohn KC, Kim YR, Jeon J, et al. Novel anti-apoptotic mechanism of A20 through targeting ASK1 to suppress TNF-induced JNK activation. Cell death and differentiation. 2010;17(12):1830-41.
424. Sabates-Bellver J, Van der Flier LG, de Palo M, Cattaneo E, Maake C, Rehrauer H, et al. Transcriptome profile of human colorectal adenomas. Molecular cancer research. 2007;5(12):1263-75.
425. Shao L, Oshima S, Duong B, Advincula R, Barrera J, Malynn BA, et al. A20 restricts wnt signaling in intestinal epithelial cells and suppresses colon carcinogenesis. PloS one. 2013;8(5):e62223.
426. Malynn BA, Ma A. A20 takes on tumors: tumor suppression by an ubiquitin-editing enzyme. The journal of experimental medicine. 2009;206(5):977-80.
427. Schmitz R, Hansmann ML, Bohle V, Martin-Subero JI, Hartmann S, Mechtersheimer G, et al. TNFAIP3 (A20) is a tumor suppressor gene in Hodgkin lymphoma and primary mediastinal B cell lymphoma. The journal of experimental medicine. 2009;206(5):981-9.
428. Troppan K, Hofer S, Wenzl K, Lassnig M, Pursche B, Steinbauer E, et al. Frequent down regulation of the tumor suppressor gene A20 in multiple myeloma. PloS one. 2015;10(4):e0123922.
429. Wenzl K, Hofer S, Troppan K, Lassnig M, Steinbauer E, Wiltgen M, et al. Higher incidence of the SNP Met 788 Ile in the coding region of A20 in diffuse large B cell lymphomas. Tumour biology. 2016;37(4):4785-9.
430. Xu Y, Hu J, Wang X, Xuan L, Lai J, Xu L, et al. Overexpression of MALT1-A20-NF-kappaB in adult B-cell acute lymphoblastic leukemia. Cancer cell international. 2015;15:73.
431. Johansson P, Bergmann A, Rahmann S, Wohlers I, Scholtysik R, Przekopowitz M, et al. Recurrent alterations of TNFAIP3 (A20) in T-cell large granular lymphocytic leukemia. International journal of cancer. 2016;138(1):121-4.
432. Chen S, Xing H, Li S, Yu J, Li H, Liu S, et al. Up-regulated A20 promotes proliferation, regulates cell cycle progression and induces chemotherapy resistance of acute lymphoblastic leukemia cells. Leukemia research. 2015;39(9):976-83.
433. Chen H, Hu L, Luo Z, Zhang J, Zhang C, Qiu B, et al. A20 suppresses hepatocellular carcinoma proliferation and metastasis through inhibition of Twist1 expression. Molecular cancer. 2015;14(1):186.
434. Codd JD, Salisbury JR, Packham G, Nicholson LJ. A20 RNA expression is associated with undifferentiated nasopharyngeal carcinoma and poorly differentiated head and neck squamous cell carcinoma. The journal of pathology. 1999;187(5):549-55.
435. Vendrell JA, Ghayad S, Ben-Larbi S, Dumontet C, Mechti N, Cohen PA. A20/TNFAIP3, a new estrogen-regulated gene that confers tamoxifen resistance in breast cancer cells. Oncogene. 2007;26(32):4656-67.
436. Tang YJ, Khalaf AT, Liu XM, Xu CX, Zhao W, Cheng S, et al. Zinc finger A20 and NF-kappaB correlate with high-risk human papillomavirus of squamous cell carcinoma patients. Tumour biology. 2014;35(12):11855-60.
437. da Silva CG, Minussi DC, Ferran C, Bredel M. A20 expressing tumors and anticancer drug resistance. Advances in experimental medicine and biology. 2014;809:65-81.
438. Frisan T, Levitsky V, Masucci M. Limiting dilution assay. Methods in molecular biology. 2001;174:213-6.
439. Laemmli UK. Cleavage of structural proteins during the assembly of the head of bacteriophage T4. Nature. 1970;227(5259):680-5.
440. Junkins RD, MacNeil AJ, Wu Z, McCormick C, Lin TJ. Regulator of calcineurin 1 suppresses inflammation during respiratory tract infections. Journal of immunology. 2013;190(10):5178-86.
441. Geft D, Schwartzenberg S, Rogowsky O, Finkelstein A, Ablin J, Maysel-Auslender S, et al. Circulating apoptotic progenitor cells in patients with congestive heart failure. PloS one. 2008;3(9):e3238.

442. Faustino-Rocha A, Oliveira PA, Pinho-Oliveira J, Teixeira-Guedes C, Soares-Maia R, da Costa RG, et al. Estimation of rat mammary tumor volume using caliper and ultrasonography measurements. Lab animal. 2013;42(6):217-24.
443. Cerami E, Gao J, Dogrusoz U, Gross BE, Sumer SO, Aksoy BA, et al. The cBio cancer genomics portal: an open platform for exploring multidimensional cancer genomics data. Cancer discovery. 2012;2(5):401-4.
444. Gao J, Aksoy BA, Dogrusoz U, Dresdner G, Gross B, Sumer SO, et al. Integrative analysis of complex cancer genomics and clinical profiles using the cBioPortal. Science signaling. 2013;6(269):pl1.
445. Yan C, Lei Y, Lin TJ, Hoskin DW, Ma A, Wang J. IL-17RC is critically required to maintain baseline A20 production to repress JNK isoform-dependent tumor-specific proliferation. Oncotarget. 2017;8(26):43153-68.
446. Moghaddam A, Zhang HT, Fan TP, Hu DE, Lees VC, Turley H, et al. Thymidine phosphorylase is angiogenic and promotes tumor growth. Proceedings of the national academy of sciences of the United States of America. 1995;92(4):998-1002.
447. Giordano TJ, Kuick R, Else T, Gauger PG, Vinco M, Bauersfeld J, et al. Molecular classification and prognostication of adrenocortical tumors by transcriptome profiling. Clinical cancer research. 2009;15(2):668-76.
448. Sun L, Hui AM, Su Q, Vortmeyer A, Kotliarov Y, Pastorino S, et al. Neuronal and glioma-derived stem cell factor induces angiogenesis within the brain. Cancer cell. 2006;9(4):287-300.
449. Lee J, Kotliarova S, Kotliarov Y, Li A, Su Q, Donin NM, et al. Tumor stem cells derived from glioblastomas cultured in bFGF and EGF more closely mirror the phenotype and genotype of primary tumors than do serum-cultured cell lines. Cancer cell. 2006;9(5):391-403.
450. Karnoub AE, Dash AB, Vo AP, Sullivan A, Brooks MW, Bell GW, et al. Mesenchymal stem cells within tumour stroma promote breast cancer metastasis. Nature. 2007;449(7162):557-63.
451. Turashvili G, Bouchal J, Baumforth K, Wei W, Dziechciarkova M, Ehrmann J, et al. Novel markers for differentiation of lobular and ductal invasive breast carcinomas by laser microdissection and microarray analysis. BMC cancer. 2007;7:55.
452. Richardson AL, Wang ZC, De Nicolo A, Lu X, Brown M, Miron A, et al. X chromosomal abnormalities in basal-like human breast cancer. Cancer cell. 2006;9(2):121-32.
453. Hong Y, Downey T, Eu KW, Koh PK, Cheah PY. A 'metastasis-prone' signature for early-stage mismatch-repair proficient sporadic colorectal cancer patients and its implications for possible therapeutics. Clinical & experimental metastasis. 2010;27(2):83-90.
454. Skrzypczak M, Goryca K, Rubel T, Paziewska A, Mikula M, Jarosz D, et al. Modeling oncogenic signaling in colon tumors by multidirectional analyses of microarray data directed for maximization of analytical reliability. PloS one. 2010;5(10):e13091.
455. Kaiser S, Park YK, Franklin JL, Halberg RB, Yu M, Jessen WJ, et al. Transcriptional recapitulation and subversion of embryonic colon development by mouse colon tumor models and human colon cancer. Genome biology. 2007;8(7):R131.
456. Wang Q, Wen YG, Li DP, Xia J, Zhou CZ, Yan DW, et al. Upregulated INHBA expression is associated with poor survival in gastric cancer. Medical oncology. 2012;29(1):77-83.
457. D'Errico M, de Rinaldis E, Blasi MF, Viti V, Falchetti M, Calcagnile A, et al. Genome-wide expression profile of sporadic gastric cancers with microsatellite instability. European journal of cancer. 2009;45(3):461-9.
458. Ye H, Yu T, Temam S, Ziober BL, Wang J, Schwartz JL, et al. Transcriptomic dissection of tongue squamous cell carcinoma. BMC genomics. 2008;9:69.
459. Sengupta S, den Boon JA, Chen IH, Newton MA, Dahl DB, Chen M, et al. Genome-wide expression profiling reveals EBV-associated inhibition of MHC class I expression in nasopharyngeal carcinoma. Cancer research. 2006;66(16):7999-8006.
460. Wurmbach E, Chen YB, Khitrov G, Zhang W, Roayaie S, Schwartz M, et al. Genome-wide molecular profiles of HCV-induced dysplasia and hepatocellular carcinoma. Hepatology. 2007;45(4):938-47.
461. Hou J, Aerts J, den Hamer B, van Ijcken W, den Bakker M, Riegman P, et al. Gene expression-based classification of non-small cell lung carcinomas and survival prediction. PloS one. 2010;5(4):e10312.
462. Okayama H, Kohno T, Ishii Y, Shimada Y, Shiraishi K, Iwakawa R, et al. Identification of genes upregulated in ALK-positive and EGFR/KRAS/ALK-negative lung adenocarcinomas. Cancer research. 2012;72(1):100-11.

463. Wei TY, Juan CC, Hisa JY, Su LJ, Lee YC, Chou HY, et al. Protein arginine methyltransferase 5 is a potential oncoprotein that upregulates G1 cyclins/cyclin-dependent kinases and the phosphoinositide 3-kinase/AKT signaling cascade. Cancer science. 2012;103(9):1640-50.
464. Riker AI, Enkemann SA, Fodstad O, Liu S, Ren S, Morris C, et al. The gene expression profiles of primary and metastatic melanoma yields a transition point of tumor progression and metastasis. BMC medical genomics. 2008;1:13.
465. Pyeon D, Newton MA, Lambert PF, den Boon JA, Sengupta S, Marsit CJ, et al. Fundamental differences in cell cycle deregulation in human papillomavirus-positive and human papillomavirus-negative head/neck and cervical cancers. Cancer research. 2007;67(10):4605-19.
466. Badea L, Herlea V, Dima SO, Dumitrascu T, Popescu I. Combined gene expression analysis of whole-tissue and microdissected pancreatic ductal adenocarcinoma identifies genes specifically overexpressed in tumor epithelia. Hepato-gastroenterology. 2008;55(88):2016-27.
467. Pei H, Li L, Fridley BL, Jenkins GD, Kalari KR, Lingle W, et al. FKBP51 affects cancer cell response to chemotherapy by negatively regulating Akt. Cancer cell. 2009;16(3):259-66.
468. Arredouani MS, Lu B, Bhasin M, Eljanne M, Yue W, Mosquera JM, et al. Identification of the transcription factor single-minded homologue 2 as a potential biomarker and immunotherapy target in prostate cancer. Clinical cancer research. 2009;15(18):5794-802.
469. Varambally S, Yu J, Laxman B, Rhodes DR, Mehra R, Tomlins SA, et al. Integrative genomic and proteomic analysis of prostate cancer reveals signatures of metastatic progression. Cancer cell. 2005;8(5):393-406.
470. Yusenko MV, Kuiper RP, Boethe T, Ljungberg B, van Kessel AG, Kovacs G. High-resolution DNA copy number and gene expression analyses distinguish chromophobe renal cell carcinomas and renal oncocytomas. BMC cancer. 2009;9:152.
471. Vasko V, Espinosa AV, Scouten W, He H, Auer H, Liyanarachchi S, et al. Gene expression and functional evidence of epithelial-to-mesenchymal transition in papillary thyroid carcinoma invasion. Proceedings of the national academy of sciences of the United States of America. 2007;104(8):2803-8.
472. He H, Jazdzewski K, Li W, Liyanarachchi S, Nagy R, Volinia S, et al. The role of microRNA genes in papillary thyroid carcinoma. Proceedings of the national academy of sciences of the United States of America. 2005;102(52):19075-80.
473. Crabtree JS, Jelinsky SA, Harris HA, Choe SE, Cotreau MM, Kimberland ML, et al. Comparison of human and rat uterine leiomyomata: identification of a dysregulated mammalian target of rapamycin pathway. Cancer research. 2009;69(15):6171-8.
474. Santegoets LA, Seters M, Helmerhorst TJ, Heijmans-Antonissen C, Hanifi-Moghaddam P, Ewing PC, et al. HPV related VIN: highly proliferative and diminished responsiveness to extracellular signals. International journal of cancer. 2007;121(4):759-66.
475. Riester M, Taylor JM, Feifer A, Koppie T, Rosenberg JE, Downey RJ, et al. Combination of a novel gene expression signature with a clinical nomogram improves the prediction of survival in high-risk bladder cancer. Clinical cancer research. 2012;18(5):1323-33.
476. Boersma BJ, Reimers M, Yi M, Ludwig JA, Luke BT, Stephens RM, et al. A stromal gene signature associated with inflammatory breast cancer. International journal of cancer. 2008;122(6):1324-32.
477. Martin-Orozco N, Muranski P, Chung Y, Yang XO, Yamazaki T, Lu S, et al. T helper 17 cells promote cytotoxic T cell activation in tumor immunity. Immunity. 2009;31(5):787-98.
478. Tripathi A, King C, de la Morenas A, Perry VK, Burke B, Antoine GA, et al. Gene expression abnormalities in histologically normal breast epithelium of breast cancer patients. International journal of cancer. 2008;122(7):1557-66.
479. Graham K, de las Morenas A, Tripathi A, King C, Kavanah M, Mendez J, et al. Gene expression in histologically normal epithelium from breast cancer patients and from cancer-free prophylactic mastectomy patients shares a similar profile. British journal of cancer. 2010;102(8):1284-93.
480. Kimbung S, Kovacs A, Bendahl PO, Malmstrom P, Ferno M, Hatschek T, et al. Claudin-2 is an independent negative prognostic factor in breast cancer and specifically predicts early liver recurrences. Molecular oncology. 2014;8(1):119-28.
481. Bachtiary B, Boutros PC, Pintilie M, Shi W, Bastianutto C, Li JH, et al. Gene expression profiling in cervical cancer: an exploration of intratumor heterogeneity. Clinical cancer research. 2006;12(19):5632-40.
482. Scotto L, Narayan G, Nandula SV, Arias-Pulido H, Subramaniyam S, Schneider A, et al. Identification of copy number gain and overexpressed genes on chromosome arm 20q by an integrative

genomic approach in cervical cancer: potential role in progression. Genes, chromosomes & cancer. 2008;47(9):755-65.
483. Zhai Y, Kuick R, Nan B, Ota I, Weiss SJ, Trimble CL, et al. Gene expression analysis of preinvasive and invasive cervical squamous cell carcinomas identifies HOXC10 as a key mediator of invasion. Cancer research. 2007;67(21):10163-72.
484. Noordhuis MG, Fehrmann RS, Wisman GB, Nijhuis ER, van Zanden JJ, Moerland PD, et al. Involvement of the TGF-beta and beta-catenin pathways in pelvic lymph node metastasis in early-stage cervical cancer. Clinical cancer research. 2011;17(6):1317-30.
485. Schlicker A, Beran G, Chresta CM, McWalter G, Pritchard A, Weston S, et al. Subtypes of primary colorectal tumors correlate with response to targeted treatment in colorectal cell lines. BMC medical genomics. 2012;5:66.
486. Uronis JM, Osada T, McCall S, Yang XY, Mantyh C, Morse MA, et al. Histological and molecular evaluation of patient-derived colorectal cancer explants. PloS one. 2012;7(6):e38422.
487. Khamas A, Ishikawa T, Shimokawa K, Mogushi K, Iida S, Ishiguro M, et al. Screening for epigenetically masked genes in colorectal cancer Using 5-Aza-2'-deoxycytidine, microarray and gene expression profile. Cancer genomics & proteomics. 2012;9(2):67-75.
488. Alhopuro P, Sammalkorpi H, Niittymaki I, Bistrom M, Raitila A, Saharinen J, et al. Candidate driver genes in microsatellite-unstable colorectal cancer. International journal of cancer. 2012;130(7):1558-66.
489. Tsukamoto S, Ishikawa T, Iida S, Ishiguro M, Mogushi K, Mizushima H, et al. Clinical significance of osteoprotegerin expression in human colorectal cancer. Clinical cancer research. 2011;17(8):2444-50.
490. Grone J, Lenze D, Jurinovic V, Hummel M, Seidel H, Leder G, et al. Molecular profiles and clinical outcome of stage UICC II colon cancer patients. International journal of colorectal disease. 2011;26(7):847-58.
491. Day RS, McDade KK, Chandran UR, Lisovich A, Conrads TP, Hood BL, et al. Identifier mapping performance for integrating transcriptomics and proteomics experimental results. BMC bioinformatics. 2011;12:213.
492. Wu Y, Grabsch H, Ivanova T, Tan IB, Murray J, Ooi CH, et al. Comprehensive genomic meta-analysis identifies intra-tumoural stroma as a predictor of survival in patients with gastric cancer. Gut. 2013;62(8):1100-11.
493. Spira A, Beane JE, Shah V, Steiling K, Liu G, Schembri F, et al. Airway epithelial gene expression in the diagnostic evaluation of smokers with suspect lung cancer. Nature medicine. 2007;13(3):361-6.
494. Lu TP, Tsai MH, Lee JM, Hsu CP, Chen PC, Lin CW, et al. Identification of a novel biomarker, SEMA5A, for non-small cell lung carcinoma in nonsmoking women. Cancer epidemiology, biomarkers & prevention. 2010;19(10):2590-7.
495. Sato T, Kaneda A, Tsuji S, Isagawa T, Yamamoto S, Fujita T, et al. PRC2 overexpression and PRC2-target gene repression relating to poorer prognosis in small cell lung cancer. Scientific reports. 2013;3:1911.
496. Xu L, Shen SS, Hoshida Y, Subramanian A, Ross K, Brunet JP, et al. Gene expression changes in an animal melanoma model correlate with aggressiveness of human melanoma metastases. Molecular cancer research. 2008;6(5):760-9.
497. Gangemi R, Mirisola V, Barisione G, Fabbi M, Brizzolara A, Lanza F, et al. Mda-9/syntenin is expressed in uveal melanoma and correlates with metastatic progression. PloS one. 2012;7(1):e29989.
498. Dodd LE, Sengupta S, Chen IH, den Boon JA, Cheng YJ, Westra W, et al. Genes involved in DNA repair and nitrosamine metabolism and those located on chromosome 14q32 are dysregulated in nasopharyngeal carcinoma. Cancer epidemiology, biomarkers & prevention. 2006;15(11):2216-25.
499. Bowen NJ, Walker LD, Matyunina LV, Logani S, Totten KA, Benigno BB, et al. Gene expression profiling supports the hypothesis that human ovarian surface epithelia are multipotent and capable of serving as ovarian cancer initiating cells. BMC medical genomics. 2009;2:71.
500. Sergeant G, van Eijsden R, Roskams T, Van Duppen V, Topal B. Pancreatic cancer circulating tumour cells express a cell motility gene signature that predicts survival after surgery. BMC cancer. 2012;12:527.
501. Sun Y, Goodison S. Optimizing molecular signatures for predicting prostate cancer recurrence. The prostate. 2009;69(10):1119-27.
502. Ge X, Yamamoto S, Tsutsumi S, Midorikawa Y, Ihara S, Wang SM, et al. Interpreting expression profiles of cancers by genome-wide survey of breadth of expression in normal tissues. Genomics. 2005;86(2):127-41.

503. Saidi HS, Karuri D, Nyaim EO. Correlation of clinical data, anatomical site and disease stage in colorectal cancer. East African medical journal. 2008;85(6):259-62.
504. Shen H, Yang J, Huang Q, Jiang MJ, Tan YN, Fu JF, et al. Different treatment strategies and molecular features between right-sided and left-sided colon cancers. World journal of gastroenterology. 2015;21(21):6470-8.
505. Petrelli F, Tomasello G, Borgonovo K, Ghidini M, Turati L, Dallera P, et al. Prognostic survival associated with left-sided vs right-sided colon cancer: a systematic review and meta-analysis. JAMA oncology. 2017;3(2):211-219.
506. Nebert DW. Transcription factors and cancer: an overview. Toxicology. 2002;181-182:131-41.
507. Wang K, Kim MK, Di Caro G, Wong J, Shalapour S, Wan J, et al. Interleukin-17 receptor a signaling in transformed enterocytes promotes early colorectal tumorigenesis. Immunity. 2014;41(6):1052-63.
508. Lippens S, Lefebvre S, Gilbert B, Sze M, Devos M, Verhelst K, et al. Keratinocyte-specific ablation of the NF-kappaB regulatory protein A20 (TNFAIP3) reveals a role in the control of epidermal homeostasis. Cell death and differentiation. 2011;18(12):1845-53.
509. Vereecke L, Vieira-Silva S, Billiet T, van Es JH, Mc Guire C, Slowicka K, et al. A20 controls intestinal homeostasis through cell-specific activities. Nature communications. 2014;5:5103.
510. Garg AV, Gaffen SL. IL-17 signaling and A20: a balancing act. Cell cycle. 2013;12(22):3459-60.
511. Peters JM. The anaphase promoting complex/cyclosome: a machine designed to destroy. Nature reviews molecular cell biology. 2006;7(9):644-56.
512. Turnell AS, Stewart GS, Grand RJ, Rookes SM, Martin A, Yamano H, et al. The APC/C and CBP/p300 cooperate to regulate transcription and cell-cycle progression. Nature. 2005;438(7068):690-5.
513. Basak S, Behar M, Hoffmann A. Lessons from mathematically modeling the NF-kappaB pathway. Immunological reviews. 2012;246(1):221-38.
514. Alexaki VI, Javelaud D, Mauviel A. JNK supports survival in melanoma cells by controlling cell cycle arrest and apoptosis. Pigment cell & melanoma research. 2008;21(4):429-38.
515. Chen P, O'Neal JF, Ebelt ND, Cantrell MA, Mitra S, Nasrazadani A, et al. JNK2 effects on tumor development, genetic instability and replicative stress in an oncogene-driven mouse mammary tumor model. PloS one. 2010;5(5):e10443.
516. Fuchs SY, Fried VA, Ronai Z. Stress-activated kinases regulate protein stability. Oncogene. 1998;17(11):1483-90.
517. Kallunki T, Su B, Tsigelny I, Sluss HK, Derijard B, Moore G, et al. JNK2 contains a specificity-determining region responsible for efficient c-Jun binding and phosphorylation. Genes & development. 1994;8(24):2996-3007.
518. Kinzler KW, Vogelstein B. Lessons from hereditary colorectal cancer. Cell. 1996;87(2):159-70.
519. Marmol I, Sanchez-de-Diego C, Pradilla Dieste A, Cerrada E, Rodriguez Yoldi MJ. Colorectal carcinoma: a general overview and future perspectives in colorectal cancer. International journal of molecular sciences. 2017;18(1).
520. Gelsomino F, Barbolini M, Spallanzani A, Pugliese G, Cascinu S. The evolving role of microsatellite instability in colorectal cancer: A review. Cancer treatment reviews. 2016;51:19-26.
521. Wilson PM, Labonte MJ, Lenz HJ. Molecular markers in the treatment of metastatic colorectal cancer. Cancer journal. 2010;16(3):262-72.
522. Catana CS, Berindan Neagoe I, Cozma V, Magdas C, Tabaran F, Dumitrascu DL. Contribution of the IL-17/IL-23 axis to the pathogenesis of inflammatory bowel disease. World journal of gastroenterology. 2015;21(19):5823-30.
523. Hyun YS, Han DS, Lee AR, Eun CS, Youn J, Kim HY. Role of IL-17A in the development of colitis-associated cancer. Carcinogenesis. 2012;33(4):931-6.
524. Tong Z, Yang XO, Yan H, Liu W, Niu X, Shi Y, et al. A protective role by interleukin-17F in colon tumorigenesis. PloS one. 2012;7(4):e34959.
525. Chae WJ, Gibson TF, Zelterman D, Hao L, Henegariu O, Bothwell AL. Ablation of IL-17A abrogates progression of spontaneous intestinal tumorigenesis. Proceedings of the national academy of sciences of the United States of America. 2010;107(12):5540-4.
526. Wu S, Rhee KJ, Albesiano E, Rabizadeh S, Wu X, Yen HR, et al. A human colonic commensal promotes colon tumorigenesis via activation of T helper type 17 T cell responses. Nature medicine. 2009;15(9):1016-22.
527. Lee JS, Tato CM, Joyce-Shaikh B, Gulen MF, Cayatte C, Chen Y, et al. Interleukin-23-independent IL-17 production regulates intestinal epithelial permeability. Immunity. 2015;43(4):727-38.

528. Berridge MV, Herst PM, Tan AS. Tetrazolium dyes as tools in cell biology: new insights into their cellular reduction. Biotechnology annual review. 2005;11:127-52.
529. Nakagawa MM, Thummar K, Mandelbaum J, Pasqualucci L, Rathinam CV. Lack of the ubiquitin-editing enzyme A20 results in loss of hematopoietic stem cell quiescence. The journal of experimental medicine. 2015;212(2):203-16.
530. Lindemann MJ, Hu Z, Benczik M, Liu KD, Gaffen SL. Differential regulation of the IL-17 receptor by gammac cytokines: inhibitory signaling by the phosphatidylinositol 3-kinase pathway. The journal of biological chemistry. 2008;283(20):14100-8.
531. Dzutsev A, Badger JH, Perez-Chanona E, Roy S, Salcedo R, Smith CK, et al. Microbes and cancer. Annual review of immunology. 2017;35:199-228.
532. Lodde BM, Mineshiba F, Wang J, Cotrim AP, Afione S, Tak PP, et al. Effect of human vasoactive intestinal peptide gene transfer in a murine model of Sjogren's syndrome. Annals of the rheumatic diseases. 2006;65(2):195-200.
533. Jonsson M, Norrgard O, Forsgren S. Epithelial expression of vasoactive intestinal peptide in ulcerative colitis: down-regulation in markedly inflamed colon. Digestive diseases and sciences. 2012;57(2):303-10.
534. Said SI, Hamidi SA, Dickman KG, Szema AM, Lyubsky S, Lin RZ, et al. Moderate pulmonary arterial hypertension in male mice lacking the vasoactive intestinal peptide gene. Circulation. 2007;115(10):1260-8.
535. Jimeno R, Gomariz RP, Gutierrez-Canas I, Martinez C, Juarranz Y, Leceta J. New insights into the role of VIP on the ratio of T-cell subsets during the development of autoimmune diabetes. Immunology and cell biology. 2010;88(7):734-45.
536. Abad C, Martinez C, Juarranz MG, Arranz A, Leceta J, Delgado M, et al. Therapeutic effects of vasoactive intestinal peptide in the trinitrobenzene sulfonic acid mice model of Crohn's disease. Gastroenterology. 2003;124(4):961-71.
537. Delgado M, Abad C, Martinez C, Juarranz MG, Arranz A, Gomariz RP, et al. Vasoactive intestinal peptide in the immune system: potential therapeutic role in inflammatory and autoimmune diseases. Journal of molecular medicine. 2002;80(1):16-24.
538. Juarranz MG, Santiago B, Torroba M, Gutierrez-Canas I, Palao G, Galindo M, et al. Vasoactive intestinal peptide modulates proinflammatory mediator synthesis in osteoarthritic and rheumatoid synovial cells. Rheumatology. 2004;43(4):416-22.
539. Delgado M, Abad C, Martinez C, Leceta J, Gomariz RP. Vasoactive intestinal peptide prevents experimental arthritis by downregulating both autoimmune and inflammatory components of the disease. Nature medicine. 2001;7(5):563-8.
540. Li H, Mei Y, Wang Y, Xu L. Vasoactive intestinal polypeptide suppressed experimental autoimmune encephalomyelitis by inhibiting T helper 1 responses. Journal of clinical immunology. 2006;26(5):430-7.
541. Carrion M, Juarranz Y, Martinez C, Gonzalez-Alvaro I, Pablos JL, Gutierrez-Canas I, et al. IL-22/IL-22R1 axis and S100A8/A9 alarmins in human osteoarthritic and rheumatoid arthritis synovial fibroblasts. Rheumatology. 2013;52(12):2177-86.
542. Carrion M, Perez-Garcia S, Jimeno R, Juarranz Y, Gonzalez-Alvaro I, Pablos JL, et al. Inflammatory mediators alter interleukin-17 receptor, interleukin-12 and -23 expression in human osteoarthritic and rheumatoid arthritis synovial fibroblasts: immunomodulation by vasoactive intestinal Peptide. Neuroimmunomodulation. 2013;20(5):274-84.
543. Pfister TD, Reinhold WC, Agama K, Gupta S, Khin SA, Kinders RJ, et al. Topoisomerase I levels in the NCI-60 cancer cell line panel determined by validated ELISA and microarray analysis and correlation with indenoisoquinoline sensitivity. Molecular cancer therapeutics. 2009;8(7):1878-84.
544. Barretina J, Caponigro G, Stransky N, Venkatesan K, Margolin AA, Kim S, et al. The Cancer Cell Line Encyclopedia enables predictive modelling of anticancer drug sensitivity. Nature. 2012;483(7391):603-7.
545. Goodspeed A, Heiser LM, Gray JW, Costello JC. Tumor-derived cell lines as molecular models of cancer pharmacogenomics. Molecular cancer research : MCR. 2016;14(1):3-13.
546. Mattes W, Yang X, Orr MS, Richter P, Mendrick DL. Biomarkers of tobacco smoke exposure. Advances in clinical chemistry. 2014;67:1-45.

547. Montalbano AM, Riccobono L, Siena L, Chiappara G, Di Sano C, Anzalone G, et al. Cigarette smoke affects IL-17A, IL-17F and IL-17 receptor expression in the lung tissue: *ex vivo* and *in vitro* studies. Cytokine. 2015;76(2):391-402.
548. Khan S, Cameron S, Blaschke M, Moriconi F, Naz N, Amanzada A, et al. Differential gene expression of chemokines in KRAS and BRAF mutated colorectal cell lines: role of cytokines. World journal of gastroenterology. 2014;20(11):2979-94.
549. Liu S, Edgerton SM, Moore DH, 2nd, Thor AD. Measures of cell turnover (proliferation and apoptosis) and their association with survival in breast cancer. Clinical cancer research. 2001;7(6):1716-23.
550. Parton M, Dowsett M, Smith I. Studies of apoptosis in breast cancer. British medical journal. 2001;322(7301):1528-32.
551. Qin XQ, Livingston DM, Kaelin WG, Jr., Adams PD. Deregulated transcription factor E2F-1 expression leads to S-phase entry and p53-mediated apoptosis. Proceedings of the national academy of sciences of the United States of America. 1994;91(23):10918-22.
552. Shan B, Lee WH. Deregulated expression of E2F-1 induces S-phase entry and leads to apoptosis. Molecular and cellular biology. 1994;14(12):8166-73.
553. Wu X, Levine AJ. p53 and E2F-1 cooperate to mediate apoptosis. Proceedings of the national academy of sciences of the United States of America. 1994;91(9):3602-6.
554. Walther W, Stein U. Viral vectors for gene transfer: a review of their use in the treatment of human diseases. Drugs. 2000;60(2):249-71.
555. Hsu PD, Lander ES, Zhang F. Development and applications of CRISPR-Cas9 for genome engineering. Cell. 2014;157(6):1262-78.
556. Aggarwal BB, Sung B. The relationship between inflammation and cancer is analogous to that between fuel and fire. Oncology. 2011;25(5):414-8.
557. Ma YM, Sun T, Liu YX, Zhao N, Gu Q, Zhang DF, et al. A pilot study on acute inflammation and cancer: a new balance between IFN-gamma and TGF-beta in melanoma. Journal of experimental & clinical cancer research. 2009;28:23.
558. Askeland EJ, Newton MR, O'Donnell MA, Luo Y. Bladder cancer immunotherapy: BCG and beyond. Advances in urology. 2012;2012:181987.
559. Zheng JH, Nguyen VH, Jiang SN, Park SH, Tan W, Hong SH, et al. Two-step enhanced cancer immunotherapy with engineered *Salmonella typhimurium* secreting heterologous flagellin. Science translational medicine. 2017;9(376):eaak9537.
560. Hamid O, Robert C, Daud A, Hodi FS, Hwu WJ, Kefford R, et al. Safety and tumor responses with lambrolizumab (anti-PD-1) in melanoma. The new England journal of medicine. 2013;369(2):134-44.
561. O'Donnell JS, Long GV, Scolyer RA, Teng MW, Smyth MJ. Resistance to PD1/PDL1 checkpoint inhibition. Cancer treatment reviews. 2017;52:71-81.
562. Herbert G. Sometimes the best gain is to lose. Retrieved from BrainyQuote.com. Xplore Inc. 2017. https://www.brainyquote.com/quotes/quotes/g/georgeherb379990.html.

APPENDICES

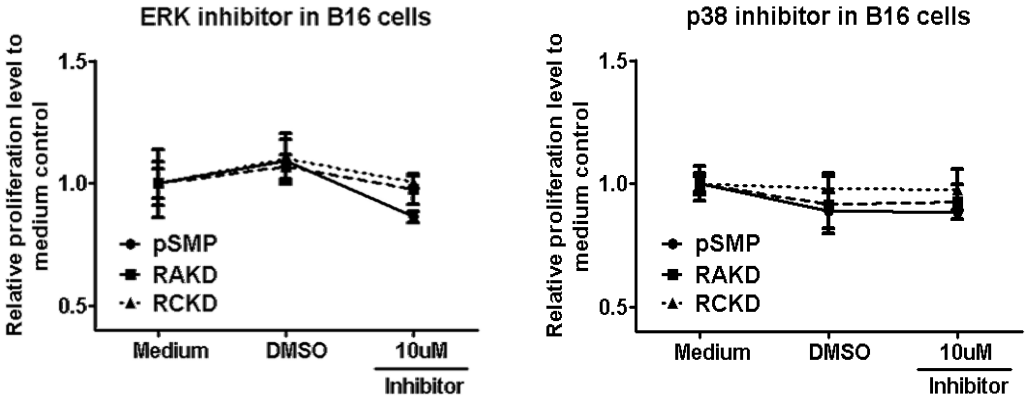

APPENDIX A IL-17R silencing alters the proliferation of B16 cells independent of ERK or p38 pathways

B16 melanoma cells were treated with DMSO or one of the inhibitors indicated for 48 hrs. Cell proliferation was then measured by MTT assay. *p ≤ 0.05; **p ≤ 0.01; ***p ≤ 0.001; statistical analysis was compared with the DMSO control. ##p ≤ 0.01; ###p ≤ 0.001; statistical analysis was compared with the pSMP control line. All values are means ± SEM of 4-6 replicates in two independent experiments.

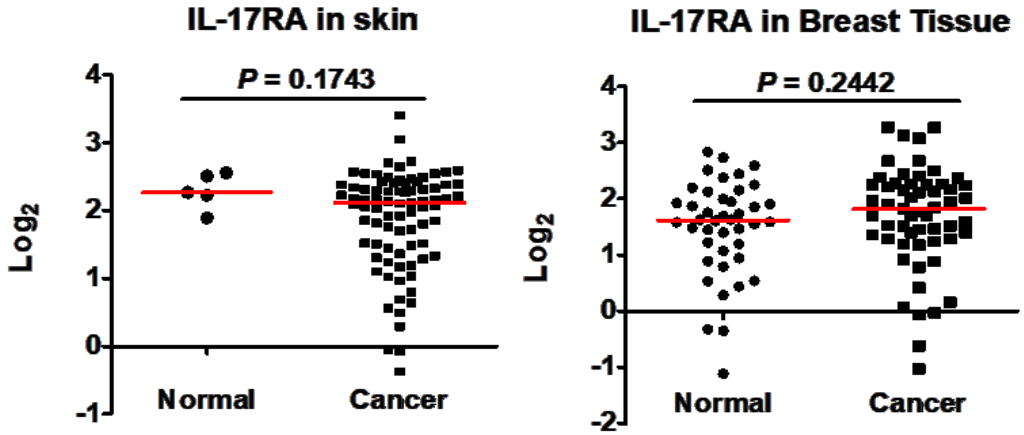

APPENDIX B No change of IL-17RA level in melanoma and breast carcinoma samples compared to normal counterparts

IL-17RA mRNA expression levels in one melanoma and three breast cancer studies are quantified from Oncomine datasets. Statistical analyses were compared with respective normal tissues using nonparametric Mann Whitney test.